Forschungszentrum Jülich
in der Helmholtz-Gemeinschaft

Biological Principles Applied to Technical Asymmetric Catalysis

Andreas Liese

Lebenswissenschaften
Life Sciences

Schriften des Forschungszentrums Jülich
Reihe Lebenswissenschaften / Life Sciences Band / Volume 7

Forschungszentrum Jülich GmbH
Institut für Biotechnologie

Biological Principles Applied to Technical Asymmetric Catalysis

Andreas Liese

Schriften des Forschungszentrums Jülich
Reihe Lebenswissenschaften / Life Sciences Band / Volume 7

ISSN 1433-5549 ISBN 3-89336-344-0

Bibliographic information published by Die Deutsche Bibliothek.
Die Deutsche Bibliothek lists this publication in the Deutsche Nationalbibliografie; detailed bibliographic data are available in the Internet <http://dnb.ddb.de>.

Publisher and Distributor:	Forschungszentrum Jülich GmbH Zentralbibliothek 52425 Jülich Phone +49 (0) 24 61 61 53 68 · Fax +49 (0) 24 61 61 61 03 e-mail: zb-publikation@fz-juelich.de Internet: http://www.fz-juelich.de/zb
Cover Design:	Grafische Betriebe, Forschungszentrum Jülich GmbH
Printer:	Grafische Betriebe, Forschungszentrum Jülich GmbH
Copyright:	Forschungszentrum Jülich 2003

Printed on environmentally friendly paper.

Schriften des Forschungszentrums Jülich
Reihe Lebenswissenschaften/Life Sciences Band/Volume 7

D 98 (Habil.-Schr., Bonn, Univ. 2003)

ISSN 1433-5549
ISBN 3-89336-344-0

For Gesine, Caroline & Johanna

Preface / Acknowledgements

This book was written as postdoctoral lecture qualification (German: Habilitationsschrift) *Biological Principles Applied to Technical Asymmetric Catalysis*. The investigations were carried out at the Institute of Biotechnology 2 of the Research Center Jülich and at the Department of Biotechnology of the Rheinisch Friedrich-Wilhelms University of Bonn.

I would like to especially thank Prof. Dr. Christian Wandrey for all of the many inspiring scientific discussions and giving me perfect working conditions. Without his trust in me as a group leader and in my supervising diploma and PhD theses, this thesis would not have been possible.

Furthermore, I would like to especially acknowledge all present and past members of the enzyme group, especially the (former) diploma and PhD students as well as Post-Docs (Dr. Beliczey, Dr. Brinkmann, Dr. Greiner, Dr. Haberland, Dipl.-Chem. Hoh, Dipl.-Chem. Kihumbu, Dipl.-Chem. Kriegesmann, Dr. Laue, Dipl.-Chem. Lütz, Dipl.-Chem. Mertens, Dipl.-Chem. Rentmeister, Dr. Schröder, Dr. Schuster, Dipl.-Chem. Stillger, Dipl.-Chem. Tan, Dr. Villela Filho, Dr. Vuorilehto, Dr. Wöltinger), who are cited in the according chapters. The many "dedicated and helping hands" in the laboratories were a great asset during my work, namely: Ms. Härter, Ms. Hahn, Ms. Herzog, Ms. Mackfeld, Ms. Müller, Ms. Offermann, Ms. Pickart and Mr. Reimers.

All here not mentioned employees of the Institute of Biotechnology, especially those in all of the workshops, as well as all of those who are aware or unaware of having helped me, I owe my thank you. Ms. Hess and Ms. Lauer made my life at the institute a lot easier, for which I would like to especially thank them.

The interdisciplinary field of biotechnology lives from scientific discussion and cooperation with colleges in various fields. I would also like to show my appreciation to: Prof. Dr. Kragl, PD Dr. Müller, Dr. Noll, Dr. Sprenger and Dr. Takos at the Institute of Biotechnology; Prof. Dr. Kula, PD Dr. Hummel, Dr. Lingen, and PD Dr. Pohl at the neighbouring Institute for Enzymetechnology of the Heinrich-Heine University of Düsseldorf. Furthermore, I would like to thank my cooperation partners Prof. Dr. Elling, RWTH Aachen, Prof. Dr. Kunz, University of Mainz, and in the Netherlands Prof. Dr. Hagen and Dr. Straathoff, both at the University of Delft; Prof. Dr. de Bont and Dr. Haaker, both at the University Wageningen. In remembrance of Prof. Dr. Steckhan, University of Bonn, I would like to acknowledge him for helping initiate the electroenzymatic research carried out in this professorial dissertation.

Financial assistance was made possible by the State of Nordrhein-Westfalen (Katalyseverbund NRW), the Deutsche Forschungsgemeinschaft (SFB 380, project-part C1), the Federal Ministry for Education and Research (BMBF-Project number 3A835140398 and 0312639B), as well as the companies BASF AG, BAYER AG, Degussa and Jülich Fine Chemicals. I also thank these cooperation partners for their productive discussions during the projects. Some of these projects are still being continued in current R&D projects.

Finally, I would like to appreciate the support and understanding my wife Gesine and my daughters Caroline and Johanna have given me during my work, especially for the small, nice distractions from my work every now and then.

Contents:

List of abbreviations and symbols

Abbreviations

(*S*), (*R*)	absolute configuration
2-HPP	2-hydroxy-1-phenylpropanone
AA	2-acetoamido cinnamic acid
AC	acetone
AD/DA	analog-digital/digital-analog converter
ADH	alcohol dehydrogenase
AP	acetophenone
ATP	adenosine triphosphate
BAL	benzaldehyde lyase
BFD	benzoylformate decarboxylase
BINAP	2,2-bis(diphenylphosphino)-1,1-binaphthyl
BMBF	Ministry of Science and Technology
BPE	1,2-bis(phospholano)ethane
BPPM	ethyl4-diphenylphosphanyl-2-[(diphenylphosphanyl)-methyl]-pyrrolidine-1-carboxylate
BuLi	butyl lithium
cat	catalyst
cdw	cell dry weight
CE	capillary electrophoresis
CIAP	Calf intestine alkaline phosphatase
CMR	chemzyme membrane reactor
COD	1,5-cyclooctadiene
*CP*CR	*Candida parapsilosis* carbonyl reductase
CPO	chloroperoxidase
cstr	continuously operated stirred tank reactor
cwm	cell wet mass
DASGIP	DASGIP Company (Jülich, Germany)
DIBAL	diisobutylaluminium hydridw
DIMEB	hepta-(2,6-di-O-methyl)-β-cyclodextrin
DIOP	2-dimethyl-4,5-bis-(diphenylphosphanyl)-pyrrolidine
DMSO	dimethylsulfoxide
DSM	Dutch States Mines
DuPhos	1,2-bis(2,5-dimethylphospholanyl)-benzene
EMR	enzyme membrane reactor

EPR	electron spin resonance
Et	ethyl
F&E	Research and Development
FAD	flavine adenine dinucleotide
FDA	American Food and Drug Administration
FDH	formate dehydrogenase
Fmoc	9-Fluorenylmethoxycarbonyl protective group
FZ Jülich	Research Center Jülich
GALOP	genetic algorithm for the optimization of processes
GAs	genetic algorithms
GC	gas chromatograph
GDH	glycerol dehydrogenase
GlcNAcT	N-acetylglucosamine transferase
GPC	gel permeation chromatography
HPLC	high pressure liquid chromatography
HPP	hydroxy-1-phenyl-propanone
IBT	Institute of Biotechnology
IP	2-propanol
LDH	lactate dehydrogenase
L-dopa	3,4-dihydroxyphenylalanine
MFM	mass flow meter
MTBE	methyl *tert*-butyl ether
MWCO	molecular weight cut-off
NADH/NAD^+	nicotinamid adenine dinucleotide, reduced and oxidized form
NMR	nuclear magnetic resonance
NRW	North-Rhein-Westfalia
OLGA	online glucose analyzer
PDC	pyruvate decarboxylase
PEEK	poly(ether-ether ketone)
PEG	polyethylene glycol
PEI	polyetherimide
PF H	hydrogenase from *Pyrococcus furiosus*
PFA	perfluoroalkoxy
pfr	plug flow reactor
PTFE	polytetrafluoroethylene
PyrPhos	1-phenyl-3,4-bis-(diphenylphosphanyl)-pyrrolidine
rec*Lb*-ADH	recombinant *Lactobacillus brevis* alcohol dehydrogenase
RWTH	Technical University of Aachen

SFB	Sonderforschungsbereich of German Research Foundation
str	stirred tank reactor or 'batch'
TBDMSCl	*tert*-butyltrimethylsilylchloride
TEA	triethylamine
Tefzel	ethylene tetrafluoro-ethylene
Th.sp.-ADH	*Thermoanaerobium species* alcohol dehydrogenase
TH-chemzyme	transfer hydrogenation chemzyme
ThDP	thiamine diphosphate
UDP	uridine-5'-diphosphate
UV	ultra-violet

Symbols

δ	g cm^{-3}	density
η	Pa s = kg m^{-1} s^{-1}	dynamic viscosity
κ	mol s^{-1} m^{-1} bar^{-1}	material-specific transport coefficient
ν	-	number of redox electrons
ρ	kg L^{-1}	density
$\sum'_{<OH>}$	mmol	sum of the hydroxy functions
σ	-, %	selectivity
σ_{para}, σ_{meta}	-	*Hammett* parameters for *para* and m*eta* substitution
τ	h, min	residence time
υ	m s^{-1}	liquid velocity
υ	mmol L^{-1} min^{-1}	reaction rate
[A]	mol L^{-1}	concentration of component A
A_Q	m^2	cross section of flow area
C/C$_0$	-, %	residual fraction
de	-, %	diastereomeric excess
d_h	m	hydraulic diameter
d_i	m	inner diameter
d'_i	m	inner diameter of outer tubing
d_o	m	outer diameter
E	-, %	degree of extraction
E^0	V	standard redox potential
ee	-, %	enantiomeric excess
F	9.64846 10^4 C mol^{-1}	*Faraday* constant
F	kg h^{-1} m^{-2}	membrane specific fluxe

F	$m^3\ s^{-1}$	flow rate
$[H_2]_{eq}$	mM	equilibrium concentration
H_{H_2}	bar mM^{-1}	specific *Henry* coefficient for H_2
k_{act}	h^{-1}	activation constant
K_{AP}, K_{IP}, K_S, K_R, K_{AC}	mM	five dissociation constants
K_D	-	partition coefficient
K_M	mM	*Michaelis-Menten* constant
k_{de}	h^{-1}	deactivation constant
K_{eq}	-	equilibrium constant
K_i	mM	inhibiton constant
k_l		mass transport coefficient
$\vec{k}_S$, $\overleftarrow{k}_S$, $\vec{k}_R$, $\overleftarrow{k}_R$,	$time^{-1}$	four rate constants
l	m	tubing length
M_n	g/mol	average molecular weight
MR	$cm^3\ mol^{-1}$	molar refractivity
MV	$cm^3\ mol^{-1}$	molar volume
MW	$g\ mol^{-1}$	molecular weight
n	-	refractive index
$\dot{n}$	$mol\ s^{-1}$	mass transport
$n \cdot \tau$	-, %	number of residence times
Ø	mm, cm	diameter
p	bar	pressure
Δp	bar	differential pressure
p_g	bar	partial pressure for the gas phase
p_{H_2}	bar	hydrogen pressure in gas phase
p_l	bar	partial pressure for the liquid phase
R	-, %	retention
R	$8.31441\ J\ K^{-1}\ mol^{-1}$	ideal gas constant
Re	-	*Reynolds* number
r_0	-	excess ratio
(S/R)	-	molar ratio of enantiomers
sty	$g_{product}\ L^{-1}_{reactor\ volume}\ d^{-1}$	space-time yield
T	K	temperature
tof	h^{-1}, min^{-1}	turnover frequencies
ttn	-	total turnover number
v	$\mu mol\ min^{-1}$	reaction rate
V_{max}	U/g	maximal rate
X_{eq}	-, %	equilibrium conversion

"... mimicry of biological functions and processes
means learning chemistry from biology
with chemical means."

G. v. Kiedrowski, ChemBioChem **2001**, *2*, 597-598

1 Introduction[1]

1.1 Biological principles

The American Heritage Dictionary defines a *principle* as "a rule or law concerning the functioning of natural phenomena or mechanical processes" *[1992]*. In other words, a principle is a statement of fact that has a wide general applicability and has already been tested by many workers over long periods of time. *Biological principles* are those principles that are developed and applied by nature over thousands of years. In the course of time they are even optimized by evolution. Some examples are:

1. Living systems obey physical and chemical laws.
2. All organisms capture, store and transmit energy.
3. All organisms are adapted to their habitat.
4. Evolution is irreversible.
5. Growth is a fundamental characteristic of life.
6. Energy fixation in plants is carried out via photosynthesis.

The transfer of biological principles and concepts to technical applications leads to astonishingly successful results. Often, even if no transfer was planned in the first place, the solutions developed for a given problem look surprisingly similar. One example is the development of highly specialized tools for drilling hard materials. In the top picture of Figure 1.1 the drill of the yellow-headed giant wasp of North America is shown. Several thousands years later the same principle of a drill was developed by engineers for drilling holes into hard materials.

[1] **Parts of this chapter are published in:**

1. A. Liese, M. Villela Filho: *Production of fine chemicals using biocatalysis*; Current Opinion in Biotechnology 10 (6) (1999) 595-603
2. C. Wandrey, A. Liese, D. Kihumbu: *Industrial biocatalysis: Past, present and future*; Organic Process Research & Development 4 (2000) 286-290
3. A. Liese, K. Seelbach und C. Wandrey: *Industrial Biotransformations*; VCH-Wiley, Weinheim, 2000
4. A. Liese: *Industrial applications and processes using biocatalysis*; in: Enzyme Catalysis in Organic Synthesis, 2nd edition, (K. Drauz, H. Waldmann, S.M. Roberts, eds.), VCH-Wiley, Weinheim (2002) 1419-1460
5. A. Liese: *53 Keywords* in Catalysis from A to Z (B. Cornils, W. Hermann, R. Schlögl, C.-H. Wong eds), Wiley-VCH, 2003

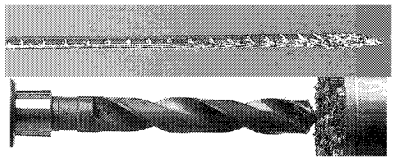

Figure 1.1: Original and copy: Drill of the yellow-headed giant wasp of North America made out of chitin, trademark nature, and a high performance drill, trademark man-made engineering *[Nachtigall 1991].*

Leonardo da Vinci (1452-1519) used nature as a source of inspiration. Based on his observations of how birds fly, he planned the first machines, enabling man to fly. Both examples demonstrate that bio-inspired design and development consistently has provided and always will point to solutions of given technological problems. But what other principles from nature can be transferred to chemical synthesis and chemical technology, besides these before mentioned, more engineering-type examples? This question we will explore in the following.

As the word 'biotechnology' already implies, different disciplines of natural sciences are united in this field. Aside from biology and the discipline-specific technology, also chemistry, physics, and engineering are of fundamental importance. This fact becomes especially obvious, if one considers a whole cell as a microfabrication unit (Figure 1.2): *Anton* from DuPont has pointed out before[2]: "You are looking at living organisms as tiny chemical factories in their own right - multiple 2-micron-sized reactors".

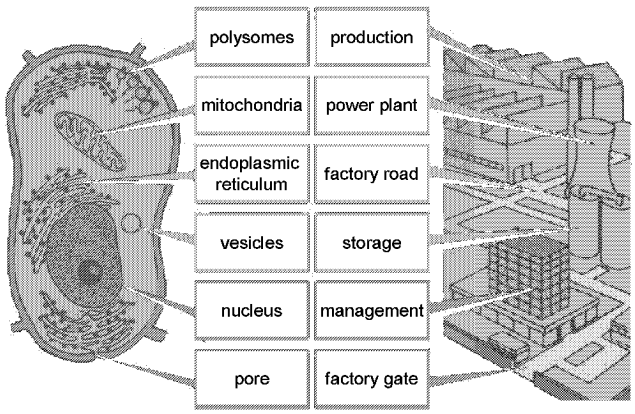

Figure 1.2: The whole cell as a microfabrication unit *[Folienserie 1985].*

Nature had to find ways to synthesize complex compounds, often in a highly stereoselective manner, from primitive starting materials, e.g. CO_2 or glucose. Setting up multi-step reactions in sequences or cycles solves this task. Enantio- or regioselectivity is introduced by using highly selective catalysts, the enzymes. These biological catalysts are in general of high

[2] David L. Anton, DuPont's research manager for bioprocess development, C&EN 22.6.1998, 15

molecular weight and either homogeneously solubilized within the cells or alternatively bound to membranes. Nature had to solve the problem that different reaction steps have to occur spatially separated in order to prevent cross-reactions or inhibitions. Therefore, different compartments in the cell exist, forming independent reaction volumes. The macromolecular biocatalysts are either retained there in by membranes, if they are solubilized, or alternatively, they are coupled to membranes. Starting materials need to be transported into the cell and products out of the cell. Besides this, also intermediates need to be transported between different compartments of the cell. For this purpose, different procedures are established, e.g. diffusive and active transport. Side products are being removed by separation or even by reactive workup, whereby they become integrated as starting materials into subsequent reaction sequences. To keep these little micron-sized factories running, energy needs to be supplied, either by photosynthesis or respiration. Energy is stored in chemical compounds, e.g. as adenosine triphosphate (ATP), and is being transported coupled to a mass-transfer action. Furthermore, the biological factories are very well adapted to their function and to their surroundings. A two-foot long neuron, a two pounds ostrich egg, and a 0.2 μm bacteria all represent a single cell. Bacteria can be found in the Antarctica much below 0°C, as well as in boiling fountains in the Yellowstone National Park in the USA. In other words, even if it is quite simplified: A cell is nothing more than a biological factory producing chemicals that was optimized over thousands of years. Nevertheless, as different as the shape and the functions of different cells are, they all follow the same biological principles as far as biosynthesis is concerned:

Biological Principles of biosynthesis:

1. Complex chemicals are synthesized in reaction sequences.
2. Biological catalysts are macromolecular and in general homogeneously soluble.
3. Membranes retain macromolecular, homogeneously solubilized catalysts.
4. Coupling to membranes heterogenizes catalysts.
5. Key steps of reaction sequences are catalyzed.
6. Energy and mass transport are coupled.

For sure there exist more biological principles of biosynthesis, but those listed above seem to be the fundamental ones, as will be outlined in this habilitation (postdoctoral lecture qualification). In the following, the focus is on technical asymmetric catalysis. Subsequently, the transfer and applicability of biological principles to technical asymmetric chemistry will be investigated.

1.2 Technical asymmetric catalysis

The term "catalysis" was first coined by *Berzelius* in 1836 and stems from the Greek meaning "down" or "loosen" *[Kieboom, et al. 1999]*. Up until then, only affinity, as a chemical driving force, was known. *Berzelius* stated that reactions occur by "catalytic contact". *Ostwald* developed a more detailed understanding of catalysis in 1883 *[Engels, et al. 1989]*. He described catalysis as the phenomenon, in which a small quantity of a certain substance, the catalyst, increases the rate of a chemical reaction or the rate of approaching the equilibrium of a chemical reaction, without being itself substantially consumed. Only thermodynamically feasible reactions can be accelerated by catalysts *[Cornils, et al. 1999]*.

Biological catalysts were already used by man long before *Berzelius* and *Ostwald* conducted their investigations, without anybody even being aware of their existence in the production of food and beverages. Sumerians and Babylonians practiced beer brewing before 6000 B.C., references to wine making can be found in the Book of Genesis, and Egyptians used yeast for baking bread. However, the knowledge of the production of chemicals such as alcohols and organic acids by fermentation is relatively recent, and the first reports in the literature appeared only in the second half of the 19th century. In 1921, *Chapman* reviewed a number of early industrial fermentation processes for the production of organic chemicals *[Turner 1998]*. In the course of time, it was discovered that microorganisms could modify certain compounds by simple, chemically well-defined reactions, which are further catalyzed by enzymes. Nowadays, these processes are called "biotransformations". The essential difference between fermentation and biotransformation is that there are several catalytic steps between substrate and product in fermentation while there are only one or two in biotransformation. The distinction is also that the chemical structures of the substrate and the product resemble one another in a biotransformation, but not necessarily so in fermentation.

Table 1.1: The first industrial chemical catalyzed processes *[Kieboom, et al. 1999]*.

Year	Process		Catalyst
1750	H_2SO_4 lead chamber process	*homogeneous catalyst system*	NO/NO_2
1870	SO_2 oxidation		Pt
1880	Deacon process (Cl_2 from HCl)		$ZnCl_2/CuCl_2$
1885	Claus Process (H_2S and SO_2 to S)		Bauxite
1900	Methane from synthesis gas		Ni
1910	Haber-Bosch ammonia synthesis		Fe/K
1920	Methanol synthesis (high pressure process)		Zn, Cr oxide
	Fischer-Tropsch synthesis		Promoted Fe, Co
	Acetaldehyde from acetylene	*homogeneous catalyst system*	Hg^{2+}/H_2SO_4

The early industrial catalytic processes used inorganic compounds as catalysts. To these belong the so-called "Deacon process", i.e., the oxidation of HCl into Cl_2, as well as the production of sulphuric acid (Table 1.1). Already in the mid-18th century, the production of sulphuric acid was commercialized *[Kieboom, et al. 1999]*. It should be especially mentioned that in the first industrially applied catalytic process a homogeneous catalyst was used.

Asymmetric catalysis is a special discipline in the field of catalysis that enables the selective synthesis of just one single enantiomer of a racemate *[Enders, Hoffmann 1985]*. In the chemical industry, this field of research has increasingly become more and more important over the past 20 to 30 years. This is due to the fact that many compounds associated with living organisms are chiral[3], for example the DNA, enzymes, antibodies, and hormones. Typically, different enantiomers of one and the same compound have different biological activity. Prominent examples are limonene and propanolol. (*S*)-Limonene smells like lemons and the enantio-complementary (*R*)-enantiomer smells like oranges. (*S*)-Propanolol is used as a drug against high blood pressure, whereas the (*R*)-enantiomer is contraceptive. In the past, almost all - and still today some - drugs were marketed as racemic 1:1 mixtures of both enantiomers. This leads sometimes to severe complications, as it has been in the sad case of thalidomide, an anti-inflammatory and sedative drug. In the nineties the American Food and Drug Administration (FDA) decided that a racemic drug could be patented again in its enantiopure form, if it is unequivocally proved that the enantiomer to be patented is solely responsible for the origin of the pharmaceutical effect *[Stinson 1999]*. Besides this, there is also an economical - if not also an environmental - consideration, because if 50% of the compound yield no effect, 50% of the production costs are spent on waste.

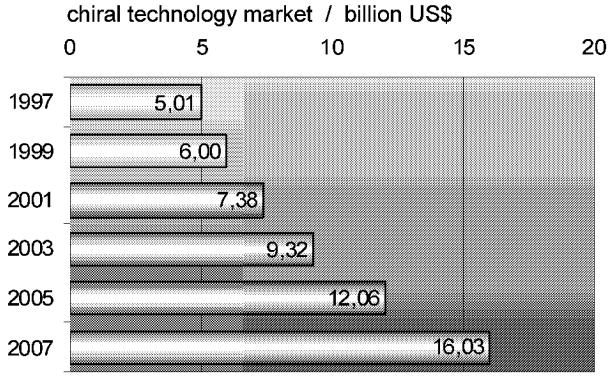

Figure 1.3: Chiral technologies, world market in billion US$ (A. Widmer, Chem. Rundschau 16.2.2001, p. 13).

[3] from Greek ξειρ meaning hand

As one can see from the aforementioned points, there is also a huge economical potential hidden in the so-called "chiral switches", compounds that where formerly introduced as racemates, but which now can be reregistered anew with the FDA as single enantiomer. In Figure 1.3 the expectations of exponential growth of the world market for chiral technology are presented.

And once again, here as well, nature is first. Nature is practicing asymmetric catalysis since thousands of years in its micron-sized reactors, namely the whole cells. In 1858, *Pasteur [Pasteur 1858]* was the first to demonstrate the microbial resolution of tartaric acid. He performed fermentation of the ammonium salt of racemic tartaric acid, mediated by the mold *Penicillium glaucum.* The fermentation yielded (-)-tartrate. Even if this is a resolution process and no asymmetric synthesis, it was the first time that nature's enantioselectivity has been demonstrated. L-Lactic acid was probably the first optically active compound to be produced industrially by fermentation. Its asymmetric synthesis via biochemistry was first accomplished in the USA in 1880 *[Sheldon 1993]. Neuberg* and *Hirsch [Neuberg, Ohle 1921]* discovered in 1921 that the condensation of benzaldehyde with acetaldehyde in the presence of yeast forms optically active (1*R*)-hydroxy-1-phenyl-2-propanone. This compound was converted further chemically into L-(-)-ephedrine (Figure 1.4) by Knoll A.G., Ludwigshafen, in Germany (1930) *[Hildebrandt, Klavehn 1932].*

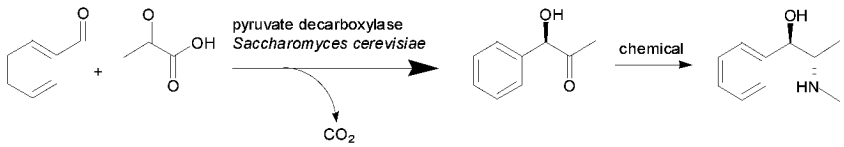

Figure 1.4: Synthesis of L-ephedrine.

Numerous authors have given overviews over biotransformations used in the industry *[Collins, et al. 1992; Sheldon 1993; Tanaka, et al. 1993; Peters 1998b; Liese, Villela Filho 1999; Bornscheuer 2000; Patel 2000, 2001; Schmid, et al. 2001a; Straathof, et al. 2002; Thomas, et al. 2002].* A very recent monograph is summarizing almost 100 processes including many details on reaction conditions, screening of the biocatalyst, or the application of the product *[Liese, et al. 2000].* The use of biocatalysis from the viewpoint of a chemist in the lab is summarized in several books as well. Recent ones are *[Faber 2000; Griengl 2000; Drauz, Waldmann 2002].* Some selected examples of technical asymmetric biotransformations as applied in industry are given in Table 1.2. Late in 2002 *M.-R. Kula* and *M. Pohl* received the German Future Prize 2002 – awarded by the President of the Federal Republic of Germany for Technology and Innovation – for their project: "Soft Chemistry with Biological Catalysts".

Table 1.2: Examples of technical asymmetric biosyntheses applied in industry *[Kieboom, et al. 1999; Liese, et al. 2000]*.

Year	Process	Catalyst
1880	L-lactic acid formation by fermentation of glucose or lactose	Lactobacillus
1930	L-ephedrine intermediate through asymmetric C-C bond formation	Yeast
	sorbitol to L-sorbose oxidation in vitamin C production	*Gluconobacter suboxydans*
1950	L-amino acids through fermentation	Brevi-, Corynebacterium species
1970	L-aspartic acid by ammonia addition to fumaric acid	aspartase (*E. coli*)
1980	L-dopa from ammonia, pyruvate and catechol	bacterial enzymes
	L-malic acid by water addition of to fumaric acid	fumarase (Brevibacterium)
2000	(1*S*)-hydroxy-(3-phenoxy-phenyl)-acetonitrile by hydrocyanation	oxynitrilase

Likewise, man has been - and still - is developing chiral catalysts. These achievements have been acknowledged by several Nobel Prizes in the field of chirality (Table 1.3). The latest one in this field has been awarded to *W. Knowles*, *R. Noyori,* and *K. Sharpless* in 2001 for their work on asymmetric catalysis.

Table 1.3: Nobel Prizes in the field of chirality.

Year	Who	Nobel Prize in chemistry for
1902	*Hermann E. Fischer*	recognition of the extraordinary services he has rendered by his work on sugar and purine syntheses
1975	*John W. Cornforth,*	work on the stereochemistry of enzyme- catalyzed reactions
	Vladimir Prelog	research into the stereochemistry of organic molecules and reactions
1990	*Elias J. Corey*	development of the theory and methodology of organic synthesis
2001	*William S. Knowles, Ryoji Noyori,*	work on chirally catalyzed hydrogenation reactions
	K. Barry Sharpless	work on chirally catalyzed oxidation reactions

The first asymmetric synthesis developed by man is the cyanohydrin synthesis, which was the focus of *E. Fischer's* seminal work on asymmetric induction *[Sheldon 1993]*. Subsequently, following *Bredig's* results that quinine catalyzes the enantioselective hydrocyanation of aldehydes *[Bredig, Fiske 1912]*, several cinchona alkaloid bases were investigated in enantioselective processes *[Wynberg 1986]*. Today most of the synthetic chiral catalysts are based on transition metals, modified by optically active additives, or by transition metal complexes, containing optically active ligands *[Cornils, et al. 1999]*. The milestones of man-made asymmetric catalysis are summarized in Table 1.4. For detailed discussion of asymmetric hydrogenations see (➲ chapter 4.1, page 103).

Table 1.4: Milestones in chemical asymmetric catalysis.

Year	Process	Literature
1912	enantioselective hydrocyanation	*[Bredig, Fiske 1912]*
1932	support of metallic catalysts in asymmetric (de)hydrogenations on quartz	*[Schwab, Rudolph 1932]*
1939	modification of a *heterogeneous* Pt hydrogenation catalyst by a chinchona alkaloid	*[Lipkin, Stewart 1939]*
1966	homogeneous asymmetric (cyclopropanation of styrene) catalysis by a soluble chiral metal complex 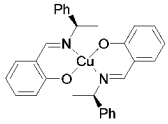	*[Nozaki, et al. 1966]*
1968	hydrogenation of olefines with modified *Wilkinson* catalyst	*[Horner, et al. 1968; Knowles, Sabacky 1968]*
1971	synthesis of L-dopa catalyzed by Rh-DIPAMP complex 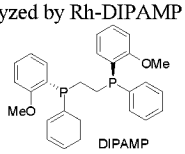	*[Izumi 1971; Knowles 1983]*
1980	asymmetric epoxidation of allylic alcohols with Ti^{IV}-tartrate complex	*[Katsuki, Sharpless 1980]*
1981	reduction of ketones catalyzed by oxazaborolidines 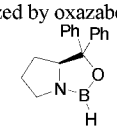	*[Itsuno, et al. 1985; Corey, et al. 1987]*
1984	$ZnEt_2$ addition to aldehydes catalyzed by β-amino alcohols 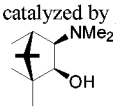	*[Oguni, Omi 1984]*
1988	asymmetric dihydroxylation via ligand-accelerated catalysis with chinchona alkaloid 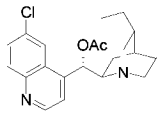	*[Jacobsen, et al. 1988]*
1991	epoxidation of unfunctionalized olefines catalzed by Mn^{III} salene complex 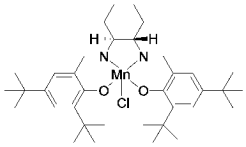	*[Jacobsen, et al. 1991]*
1993	L-menthol synthesis with (*S*)-BINAP 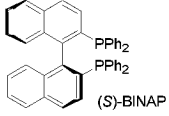	*[Wan, Davis 1983; Noyori, Hashigushi 1996]*

1.3 Transfer of biological principles to technical asymmetric catalysis

As has been outlined in ➲ chapter 1.1, page 1, nature is applying highly advanced technologies in microfabrication units, the whole cells. Nature's way represents the art of carrying out asymmetric catalysis to the highest degree, and this has been the case already since thousands of years. It is using enantio- and regioselective catalysts, the enzymes, preventing by this means the need for introducing and subsequently cleaving off protecting groups, a concept that by contrast is common to general chemistry. As has already been pointed out when discussing the history of technical asymmetric catalysis, the first asymmetric compounds were produced industrially using biotransformations (➲ Table 1.2, page 7). The biological catalysts have been optimized by evolution during the course of time. Since in general these biocatalysts are compatible regarding their reaction conditions, they are applied by nature in reaction sequences and cycles *[Cane 1990]*, as for example in the citric acid cycle. This represents the peviously named *1st biological principle: complex chemicals are synthesized in reaction sequences* (➲ box page 3). Furthermore, using biocatalysts, an intermediate separation and purification, as is common for ***classical*** organic syntheses, because of incompatibility of the reaction steps, in general is not needed (Figure 1.5). In ***modern*** organic synthesis, however, these additional separation and purification steps are frequently not needed anymore.

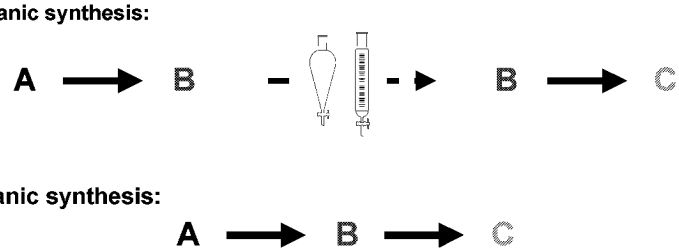

Figure 1.5: Comparison of classical and modern organic synthesis.

In the chemical literature, several names are being used to describe reaction sequences: cascade, consecutive, domino, iterative, one-pot (one-flask), sequential, tandem, and zipper reactions *[Bunce 1995]*. Listed below are two main reaction types to be differentiated. One is the so-called domino (or -'cascade') reaction, where the reaction sequence is initiated (or -'triggered') by the first step. The other one is the tandem (or sequence) reaction, i.e., two-step reactions in a consecutive fashion *[Mayer, et al. 2001]*. The first type is especially important, if the intermediates are unstable. For a recent review on enzyme-initiated domino reactions see *[Mayer, et al. 2001]*. In the last decade, more and more biocatalyzed reaction sequences

have been published. Examples are the synthesis of L-amino acids by the sequential usage of a hydantoinase and a carbamoylase *[Ragnitz, et al. 2001; Wiese, et al. 2001]*, the two-step enzymatic synthesis of cephalexin from D-phenylglycine nitrile *[Wegman, et al. 2002]*, the two-step enzymatic synthesis of L-lactic acid from acetaldehyde *[Miyazaki, et al. 2002]*, and the four-step enzymatic synthesis of non-natural carbohydrates from glycerol *[Schoevaart, et al. 2000, 2001]*. Multicatalyst systems are already established for *in situ* cofactor regeneration for several decades. Examples are the regeneration of the precious nicotinamide cofactors *[Jones, et al. 1972; Wichmann, et al. 1981; Wong, Whitesides 1982]* or the regeneration of the expensive nucleotide sugars *[Herrmann, et al. 1993; Wong, et al. 1995a, 1995b; Zervosen, Elling 1996]*. Besides the application of isolated enzymes, also whole cells are applied utilizing their *in vivo* reaction sequences for the synthesis of fine chemicals. The most popular microorganism for biocatalysis is baker's yeast (*Saccharomyces cerevisiae*) *[Hoffmann 1996]*. However, utilizing whole cells as 'bags of enzymes' has some drawbacks: 1) low enzymatic activities, 2) often low permeability for substrate and product, 3) inhibition of cell growth by reactants, 4) degradation of substrate or product by cellular activity, and 6) difficulties in the isolation and purification from the reaction mixture *[Endo, Koizumi 2001]*. Nevertheless, many approaches for whole cell conversions have been investigated and are applied to industrial scale *[Liese, et al. 2000]*. These limitations can be partly overcome by reaction engineering, as has also been pointed out in this work (➲ chapter 3.1.1, page 21). Furthermore, new strains are constructed by means of recent genetic engineering technologies, whereby the desired enzymes are cloned and overexpressed *[Rodriguez, et al. 2000; Stewart 2000]*. A very prominent example is the asymmetric reduction of ethyl 4-chloro-3-oxobutanoate to ethyl (*S*)-4-chloro-3-hydroxy-butanoate. In this case *Escherichia coli* cells expressing both the carbonyl reductase gene from *Candida magnoliae* and the glucose dehydrogenase gene from *Bacillus megaterium* are used as the catalyst. In a two-phase system consisting of an organic solvent and an aqueous phase, ethyl (*S*)-4-chloro-3-hydroxy-butanoate is being formed in the aqueous phase and reextracted into the organic phase. Reportedly, the final concentration of the product amounted to 2.58 M (430 g L^{-1}), the molar yield being 85%. *[Kataoka, et al. 1997; Kataoka, et al. 1998; Kataoka, et al. 1999; Kizaki, et al. 2001; Yasohara, et al. 2001]*. A new way to carry out a reaction sequence was introduced by the *Kyowa Hakko* company. Recombinant *E. coli* and *C. ammoniagenes* could be applied for the industrial manufacture of oligosaccharides, e.g. Lewsi X *[Endo, Koizumi 2000; Endo, et al. 2000; Koizumi, et al. 2000; Endo, Koizumi 2001; Endo, et al. 2001; Tabata, et al. 2002]*. Hereby different enzyme activities are located in different recombinant *E. coli* cells that are added as a function of time to the batch process, thereby circumventing feed back inhibitions. This points out the importance of reaction engineering and of technical chemistry, if biological principles are to be transferred to technically useful forms of asymmetric catalysis. If different catalysts are combined in a one-pot synthesis, often

problems of feedback inhibition and of concurring reactions occur. Therefore, it is often important to separate individual reaction chambers. Likewise, nature too had to solve this problem and introduced already long ago the separation of reaction chambers, as for example in the Golgi apparatus. Therefore, separation of reaction chambers is a further biological principle.

Since for nature as well the syntheses of its catalysts, the enzymes, are laborious, nature needed to develop principles for the recyclization of enzymes. As the solution, nature uses either coupling the catalyst to a heterogeneous support or retaining the catalyst by membranes. Still in contrast to the majority of chemical catalysts, enzymes are macromolecular and in general homogeneously soluble. This is the previously named *2nd biological principle: Biological catalysts are macromolecular and in general homogeneously soluble* (➲ box page 3). By this means it is easy for nature to recycle its catalysts by either retaining it with or coupling it to membranes (*3rd and 4th biological principle*).
Heterogenization of catalysts is one of the oldest technologies to retain and to recycle catalyst in technical asymmetric catalysis *[Fodor 1999; De Vos, et al. 2000; Smet, et al. 2001]*. Such hetereogenized catalysts are then applied in slurry or plug flow reactors. However, quite frequently, heterogenized or immobilized enantioselective homogeneous catalysts often perform only rather dissapointingly. Their reduced enantioselectivity may be caused by the heterogeneous support iself *[Blaser 1991; De Vos, et al. 2000]*, or - and perhaps additionally, - mass transport limitations may be the reason. An alternative approach is the application of homogeneously soluble catalysts in two-phase systems, where the catalyst is only soluble in one phase and by this means recycled. The respective example is the hydroformylation process of the former Ruhrchemie/Rhone-Poulenc companies *[Cornils, Herrmann 2000]*. The water-soluble homogeneous catalyst is separated from the reactants in the organic phase. However, it is very difficult to transfer this very interesting concept to asymmetric synthesis, since the different polarities of the two-phase system disturb the stereochemical processes at the catalyst *[Cornils, Herrmann 2000]*.
In contrast to immobilization on a carrier, the catalytic properties are generally conserved, if the homogeneously soluble catalyst is retained by membranes. In this technology, nature is already a perfectionist (*3rd biological principle*). Enzymes typically are macromolecular (20,000 to 200,000 g mol^{-1}), but still homogeneously soluble. The synthetic pendant of an enzyme is called *chemzyme* or also sometimes *synzyme* (Figure 1.6, left). In contrast to enzymes, which posses in general one active site, it is possible to couple a number of active sites, - often via a spacer unit - to a polymeric backbone *[Kragl, Dwars 2001; Wöltinger, et al. 2001b]*. The idea behind synthesizing such an artificial biomimetic catalyst is, to obtain a catalyst exhibiting the same attractive properties as an enzyme: namely to be macromolecular and still homogeneously soluble. In contrast to enzymes, the chemzymes should be homogeneously soluble in the organic phase. By this means the high solubility of the

reactants increases the chance to reach a high *space-time yield* (*sty*)[4].
One crucial factor for the successful application of chemzymes is the *retention* (*R*)[5]. As can be seen from Figure 1.6, right, retention of $R > 0.999$ is required to render the application of the chemzyme feasible in a continuously operated process. If for example a retention of $R = 0.98$ is given, then this means that 2% of catalyst are lost per residence time; in other words, after 37 residence times, already half of the catalyst is gone. This is the case with a BINAP-ruthenium hydrogenation catalyst as outlined in the literature *[Smet, et al. 2001]*.

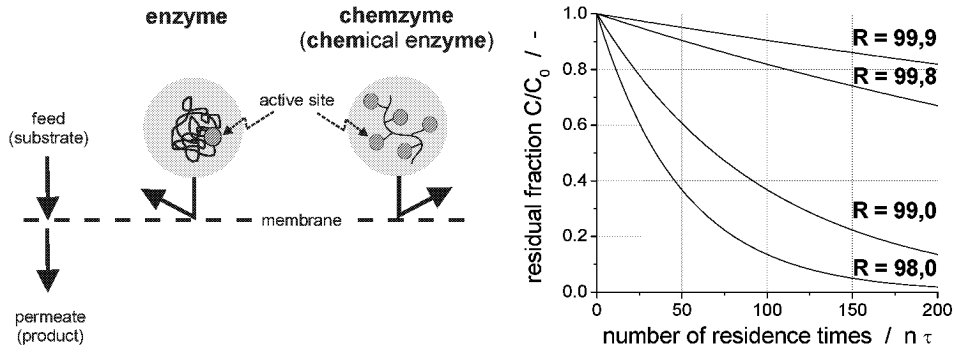

Figure 1.6: **Left: comparison between an enzyme and a chemzyme; right: retention as function of the number of residence times n τ.**

The field of the synthesis and application of chemzymes is very new and just started in the last decade. New reactors needed to be developed to provide for the application of the newly synthesized chemzymes. The transfer of the second biological principle, namely that of of a soluble, macromolecular catalyst to technical asymmetric catalysis offers a very high potential for the chemical industry. Therefore, different reviews have been published regarding this topic within the last two years *[Kragl, Dwars 2001; Wöltinger, et al. 2001b; Bergbreiter 2002; Leadbeater, Marco 2002]*. The reader is also referred to ➲ chapter 4, page 99.

Beyond the aspects discussed so far, transferring the biological principles to technical asymmetric synthesis also allows for the development of new methods that could not be established by nature. For example, in homogeneous hydrogenation catalysts most often ruthenium or rhodium are found as the central atoms, whereas in natural enzymes mainly zinc, copper, iron, nickel, and magnesium occur. This might be due to the lack of availability of precious metals in nature. But then in turn this opens up a huge potential for modifying enzymes accordingly and applying the resulting chemzymes for enantioselective reductions. In nature reduction equivalents are generally supplied via nicotinamide cofactors that need to

[4] *space-time yield* (*sty*) = $g_{product}\ L^{-1}_{reactor\ volume}\ d^{-1}$
[5] retention (*R*) = $1 - C_{permeate}/C_{retentate}$

be recycled. When utilizing chemzymes, it is possible to carry out enantioselective reductions with either formate, 2-propanol, or even molecular hydrogen as a low cost supply of the reduction equivalents (➲ chapter 4, page 99). Another cheap source of redox equivalents are electrons. But where to obtain them from? Nature also uses electrons as redox equivalents. Here the transport of electrons is generally coupled to mass transport as for example in respiration or in photosynthesis *[Stryer 1990]*. This is the *6th biological principle: energy and mass transport are coupled.* In contrast to nature it is possible to separate energy and mass transport *in vitro*. A very attractive artificial source of electrons is provided by electrochemistry. This cheap source for reduction equivalents combined with biocatalytical steps offers a wide range of new possibilities. This concept, namely combining electrochemical and biocatalytical steps has been termed 'electroenzymatic synthesis'.

The feasibility of supplying redox equivalents directly via an electrode was demonstrated on some selected examples (for reviews see *[Steckhan 1994; Schmid, et al. 2002a]*). So far no electroenzymatic synthesis has been scaled up to an industrial process. The reason for this might be the still missing link between electroenzymatic synthesis and reaction engineering with the aim to design an efficient production process. First promising results will be demonstrated here within this report (➲ chapter 3.3, page 87).

Currently, in technical asymmetric synthesis different biological principles are already being applied without the scientific community at large being aware of it. In those examples namely, where additionally reaction engineering has been integrated, very efficient production processes were designed. This gives rise to high expectations for the future of a sustainable, technical asymmetric catalysis.

It is not unusual for strikingly new concepts to require 'incubation periods' of more than a decade or even a few thereof, to really become accepted and successful. The transistor, the laser, or conducting organic polymers may serve as characteristic examples for this dilemma: In all of these cases the most attractive applications did not become commonplace until decades after their initial discoveries, i.e., at times, when the original patents had expired long before.

2 Scope and objectives

The objective of this habilitation is to understand selected biological principles as well as processes in chemical terms, to transfer, apply them to and combine them with the traditional concepts of chemical, i.e., homogeneous catalysis. Simultaneously, the aim is to design and to develop novel reactors, i.e., engineered systems based on these biological principles. The two following fundamental biological principles, as formulated in the introduction on page 3, are used to subdivide this work into two parts:

1. Complex chemicals are synthesized in reaction sequences.
2. Biological catalysts are macromolecular and in general homogeneously soluble.

The dotted oval in Figure 2.1, top, represents a whole cell that is converting a starting material **A** in a reaction sequence via the intermediate **B** to the product **C**. Each step is catalyzed by a homogeneously soluble, macromolecular biocatalyst.

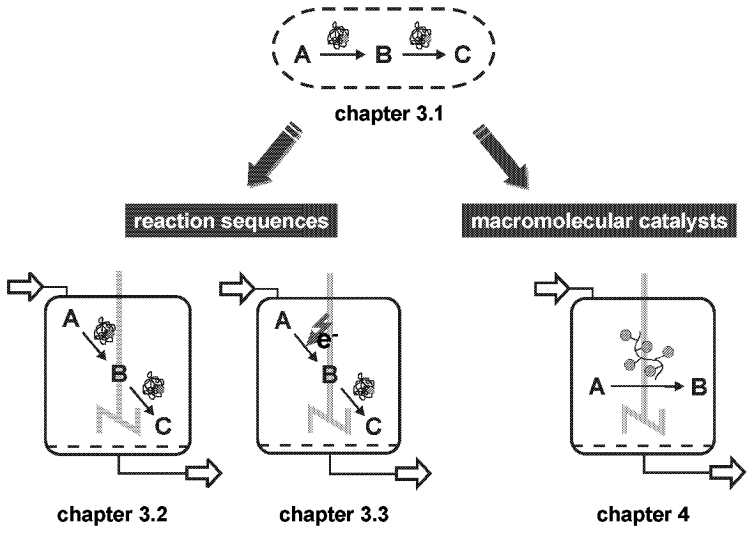

Figure 2.1: Biological principles applied to technical asymmetric catalysis.

The first part of this treatise (chapter 3) deals with the application of reaction sequences to technical asymmetric catalysis. Besides utilizing whole cells as the natural reference system, different isolated enzymes are also applied in reaction sequences to synthesize complex products **C** starting up from e.g. bulk chemicals **A**. Here the control of the selectivity between

B and **C** is of major importance. In addition to concepts of nature, electrochemical steps are also exploited and combined with biocatalytical ones in reaction sequences. The advantages of enzymes as enantioselective catalysts are combined here with the waste-free electrochemical *in situ* generation or regeneration of reagents.

The second part (chapter 4) deals with the application of macromolecular catalysts. New chemzymes have been synthesized and compared to the performance of their natural pendants, catalyzing the same reactions. In the focus of our investigations have chiefly been hydrogenations with molecular hydrogen and transfer hydrogenations with 2-propanol as reduction equivalent. A new hydrogenation reactor has been developed enabling the application of chemzymes as well as of enzymes.
The common basis of all the systems investigated is reaction engineering (Figure 2.2). By characterizing the catalysts in view of activity, stability, and selectivity as well as the reaction itself in view of kinetics, thermodynamics, and possible side reactions, operating points are identified that enable the production of the respective fine chemicals. With this knowledge dedicated reactors are developed that allow an easy up scaling of the process. At this stage of process development also downstream processing becomes of major importance.

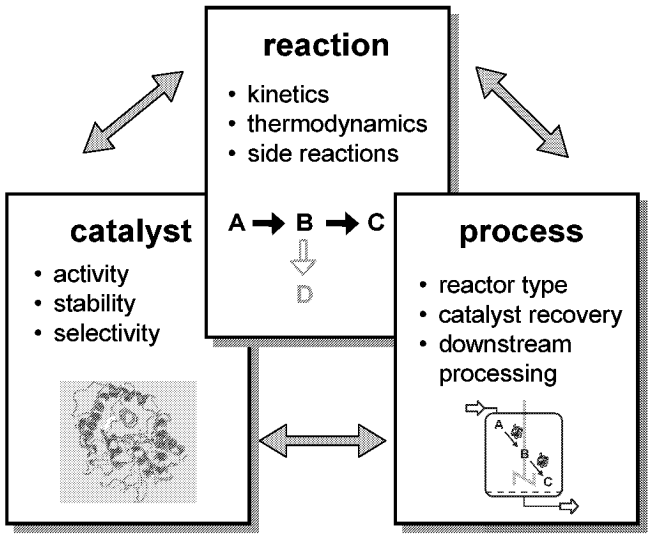

Figure 2.2: Interaction of different process relevant parameters.

2.1 Graphical abstract of investigated systems

Chapter 3: First biological principle: Reaction sequences

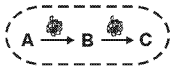

3.1 ***in vivo*** **reaction sequences**

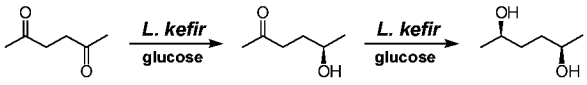

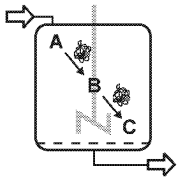

3.2 ***in vitro*** **reaction sequences by combination of biocatalytical steps**

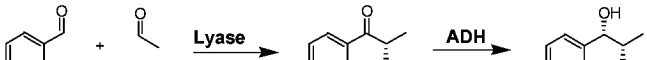

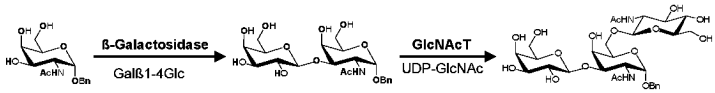

core1-Bn core2-Bn

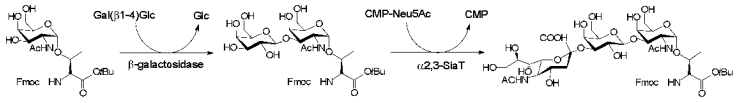

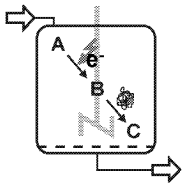

3.3 ***in vitro*** **reaction sequences by combination of electrochemical with biocatalytical steps**

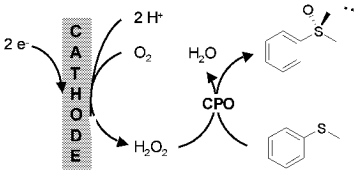

Chapter 4: Second biological principle: Macromolecular catalysts

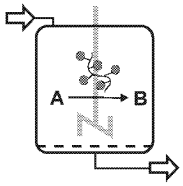

direct hydrogenation

4.1 with chemzymes

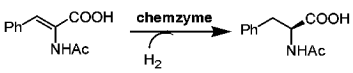

4.2 with enzymes

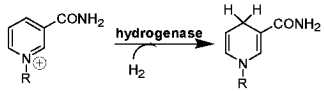

transfer hydrogenation

4.3 with chemzymes

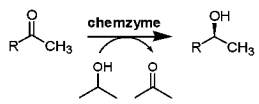

4.4 with enzymes

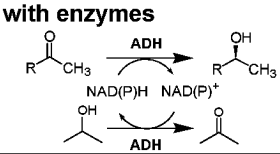

There are three answers to the question
"Why use enzymes?":
necessity, convenience and opportunity.

C.-H. Wong, G. M. Whitesides, 1995

3 First biological principle: Reaction sequences

In nature, the most complex chemical molecules with a high number of stereochemical centers can be found (e.g. peptides, pheromones, and oligosaccharides). To synthesize these molecules nature employs reaction sequences that are catalyzed by highly selective enzymes. For a kinetic analysis multiple reactions can be reduced to combinations of two primary types (Figure 3.1):

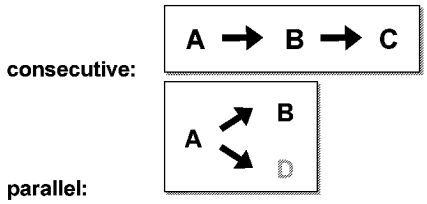

Figure 3.1: Comparison of sequential and parallel reaction pathways.

The distinction between a single reaction and multiple reactions is that the latter ones require more than one rate equations to describe their kinetic behavior, which is a prerequisite for setting up a simulation model for the purpose of optimization. Often, additional feed back inhibitions and/or other cross inhibitions occur, making it very difficult to determine the exact kinetics of the whole reaction system. In these cases it might be helpful to use a non-model based optimization method like for example the genetic algorithm (➲ chapter 3.2.2.2, page 72). By help of this mathematical optimization method, it is possible to optimize a reaction sequence for the investigated reactor configuration.

Depending on the connection of the catalysts different challenges are arising:

- Control of selectivity depending on the product of an individual reaction step being either an intermediate or the final product in a reaction sequence (➲ chapter 3.1.1, page 21).
- Influence of selectivity by choice of the reactor type (➲ chapter 3.1.1, page 21 and ➲ chapter 3.2.1, page 45).
- Influence of selectivity by the properties of the substrate (➲ chapter 3.2.1, page 45).

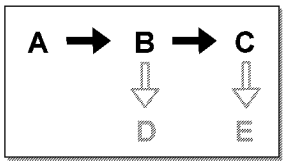

- Optimization of multicatalyst systems either based on the kinetic and thermodynamic models or as a black box system by means of the genetic algorithm. The choice of the optimization methods hereby depends on the complexity of the system investigated (➲ chapter 3.2.2, page 70).
- Circumvention of feed back inhibitions (➲chapter 3.2.2, page 70).
- Shifting of the reaction equilibrium by removal of side products (➲ chapter 4.4.1, page 164).

The central challenge in technical asymmetric catalysis via reaction sequences is selectivity. This is especially important, if fine chemicals for the subsequent synthesis of pharmaceuticals are produced. Here the request for purity is very high. Likewise, in the field of food additives the regulatory authorities require an extraordinary purity. To select the appropriate synthesis scheme associated with high selectivity to achieve unique products the two industrial key factors yield and costs have to be considered.

You are looking at living organisms
as tiny chemical factories in their own right
- multiple 2-micron-sized reactors.

David L. Anton,
DuPont's research manager for bioprocess development,
C&EN 22.6.1998, 15

3.1 *In vivo* reaction sequences

3.1.1 Diastereoselective production of diols with resting cells[6]

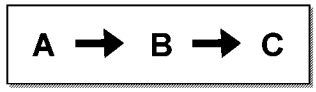

In vivo reaction sequences are explored using the diastereoselective production of (2*R*,5*R*)-hexanediol as a characteristic example (**C**). Resting whole cells of *Lactobacillus kefir* DSM 20587 are used as black box catalyst system to reduce 2,5-hexanedione (**A**) to (2*R*,5*R*)-hexanediol (**C**) enantio- as well as diastereoselectively (Figure 3.2) in a reaction sequence via (2*R*)-hydroxy-5-hexanone as an intermediate (**B**). The respective enantio[7]- and diastereoselectivities[8] of **C** were > 99%. The reduction equivalents are supplied via glucose. As side products (metabolites of *Lactobacillus kefir*) lactate, acetate, ethanol and CO_2 are produced.

[6] **Parts of this chapter are published in:**

1. A. Kriegesmann: *Ganzzellbiotransformationen mit Saccharomyces cerevisiae und Lactobacillus kefir zur Darstellung enantiomerenreiner 2,5-Hexandiole – Reaktionstechnische Untersuchungen*, diploma thesis, University of Bonn, 1999
2. J. Haberland: *Verfahrensentwicklung zur Darstellung von (2R,5R)-Hexandiol mit Lactobacillus kefir DSM20587*, PhD-thesis, University of Bonn, 2003
3. W. Hummel, A. Liese, C. Wandrey: *Verfahren zur Reduktion von Ketogruppen enthaltenden Verbindungen*, German Patent Application DE 199 32 040.3 (09.07.1999); *process for reducing keto-group containing compounds*, European Patent Application EP 00113127.51-2110 (29.06.2000)
4. J. Haberland, A. Kriegesmann, E. Wolfram, W. Hummel, A. Liese: *Diastereoselective synthesis of optically active (2R,5R)-hexanediol*; Applied Microbiology & Biotechnology 58 (2002) 595-599
5. J. Haberland, W. Hummel, T. Dausmann, A. Liese: *New continuous production process for enantiopure (2R,5R)-hexanediol*; Organic Process Research & Development 6 (2002) 458-462
6. I. Chin-Joe, J. Haberland, A. Straathof, J. Jongejan, A. Liese, J. Heijnen: *Reduction of ethyl 3-oxobutanoate using non-growing baker's yeast in a continuously operated reactor with cell retention*; Enzyme Microbial Technology 31 (2002) 665-672

[7] *ee* (enantiomeric excess) = $[(R) - (S)]/[(R) + (S)]$
[8] *de* (diastereomeric excess) = $[(R,R) - (S,S)]/[(R,R) + (S,S)]$

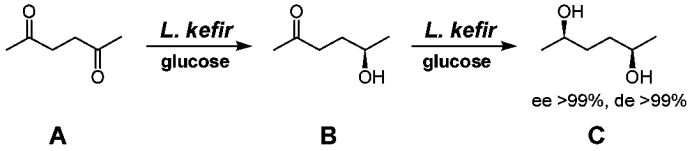

Figure 3.2: Synthesis of (2*R*,5*R*)-hexanediol (C) with whole cells of *Lactobacillus kefir*.

Lactobacillus kefir itself was discovered by *Kandler* and *Kunath* in 1983 *[Kandler, Kunath 1983]* from kefir grain. *Hummel et. al* isolated a number of enzymes, mainly oxidoreductases, from different sub-types of Lactobacilli. In 1990 the alcohol dehydrogenase from *Lactobacillus kefir* DSM20587 was isolated and characterized for the first time *[Hummel 1990]*. The alcohol dehydrogenase converts a broad range of prochiral oxo-compounds into chiral alcohols *[Bradshaw, et al. 1992]*. However, NADPH is required as a cofactor for the reduction, and the enzyme showed no activity in the case of NADH as a cofactor. Due to this dependence on NADPH the use of whole cells as a biocatalyst offers the advantage of using the available cell-internal cofactor regeneration cycles.

(2*R*,5*R*)-Hexanediol (**C**) is a versatile and important chiral building block for the syntheses of various chiral phosphine ligands (e.g. DuPhos[9] or BPE[10]) *[Burk, et al. 1990; Burk 1991a; Burk, et al. 1991]*, see Figure 3.3. Both ligands are used for the syntheses of transition metal catalysts that are applied for enantioselective hydrogenations of unsaturated α- and β-amino acids (Figure 3.4). In these hydrogenations enantiomeric excesses (*ee*) of up to > 98% are reached *[Caron, Kazlauskas 1994; Burk, et al. 1995b]*.

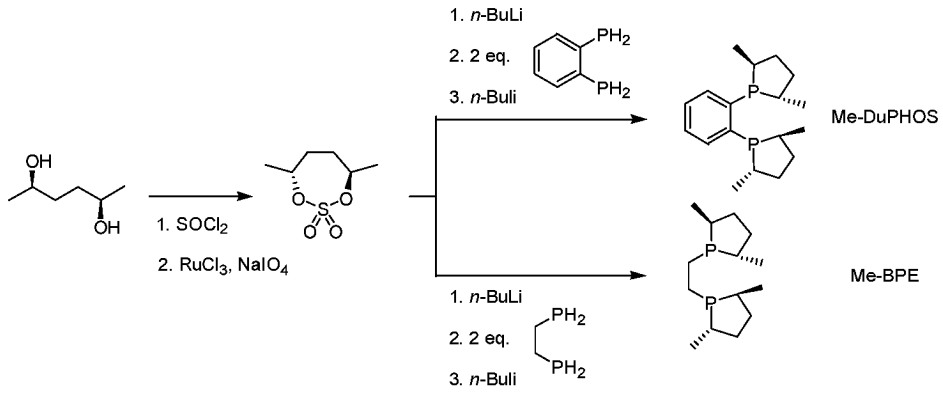

Figure 3.3: Application of (2*R*,5*R*)-hexanediol (C) for the synthesis of Me-DuPhos and Me-BPE *[Burk 1991a]*.

[9] 1,2-bis(phospholano)benzene
[10] 1,2-bis(phospholano)ethane

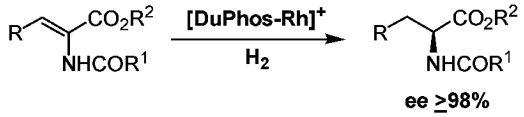

Figure 3.4: Synthesis of α-amino acids catalyzed by DuPhos.

In addition to these prominent applications (2*R*,5*R*)-hexanediol is also used as an intermediate in the synthesis of (2*S*,5*S*)-dimethylpyrrolidone and (2*S*,5*S*)-dimethylborane. Both compounds are used as chiral auxiliaries for asymmetric induction of enantioselective reactions *[Whitesell 1989; Kim, Lee 1993; Chong, et al. 1995; Pichon, Figadere 1996]*. Examples are the alkylation of enamines *[Whitesell, Felman 1977]*, aldol condensations *[Masamune, et al. 1986]*, Claisen rearrangements *[Yamazaki, et al. 1991]*, intramolecular cycloadditions *[Chen, Ghosez 1991]* as well as the reduction of ketones *[Imai, et al. 1986]* and of azides *[Wilson, Pasternak 1990]*.

Up until now, there were two established technical processes described in literature for the production of (2*R*,5*R*)-hexanediol on a multi kg scale: The first one was a chemical process that was substituted later by a biocatalytical one.
The chemical process was developed and patented by the DuPont company (Wilmington, USA) *[Cumbo 1981, 1982; Burk 1991b, 1992]*. In the first step methyl 2-oxobutyrate is reduced in an enantioselectively catalyzed reaction by Ru(*R*)-BINAP[11] to methyl 2*R*-hydroxybutyrate, which is subsequently hydrolyzed. In a subsequent step an electrochemical anodic dimerization (*Kolbe* coupling) is carried out to yield (2*R*,5*R*)-hexanediol (*ee* and *de* > 98%). The key problem of this synthesis is uncontrolled polymerization during large-scale syntheses, leading to a coating of the electrodes with non-conducting polymers. As a consequence the reaction ceases.

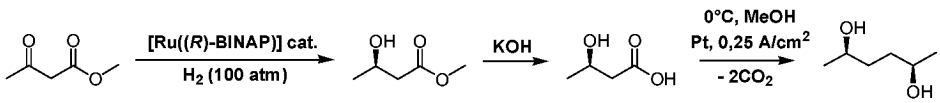

Figure 3.5: Former chemical synthesis of (2*R*,5*R*)-hexanediol as carried out by DuPont.

Besides this large scale chemical process, other chemical pathways have also been described in the literature leading to (2*R*,5*R*)-hexanediol, which are summarized in Table 3.1. Furthermore, chiral pool substances, e.g. D-mannitol, have been used as starting compounds. For example, (2*R*,5*R*)-hexanediol with high optical purity can be produced in a three-step reaction sequence, but the yield is only 30%.

[11] BINAP = 2,2-bis(diphenylphosphino)-1,1-binaphthyl

Table 3.1: Chemical methods for the synthesis of (2*R*,5*R*)-hexanediol.

catalyst	substrate	ee / %	meso/(*R,R* + *S,S*)	yield / %	Literature
-	D-mannose	99	1/100	30	*[Saravanan, et al. 1997]*
DIBAL	diketosulfoxide	95	5/100	75	*[Solladie, et al. 1994]*
Kolbe coupling	(3*R*)-hydroxy butyrate	98	1/100	55-70	*[Cumbo 1981, 1982; Burk 1991b, 1992]*
Raney-Ni / L-(+)-tartrate	(2,5)-hexanedione	10	1/7	10	*[Brunner, et al. 1991]*
Sharpless hydroxylation	1,5-hexadiene	n.g.	1/4	32	*[Maier, Reuter 1997]*

The most recent production process of (2*R*,5*R*)-hexanediol has been introduced by Chirotech (Cambridge, UK): Starting from the racemic/meso 2,5-hexanediol mixture a lipase catalyzed kinetic resolution is carried out as shown in Figure 3.6 *[Nagai, et al. 1994; Taylor, et al. 2000]*. The multi-step synthesis starts with enantioselective acylation of the (*R*)-hydroxy function catalyzed by lipase. Subsequently, the non-acylated (*S*)-hydroxy function of the meso-(*R,S*)-diol is inverted by chemical transformation with methane sulfonyl chloride leading to the (*R,R*)-diol. Additional reagents used in the production process are triethylamine, methane sulfonyl chloride, dichloromethane, dimethyl formamide, cesium acetate, methanol, and acidic resins (Amberlite IR 120). The maximum theoretical yield of this process is 75% yielding an *ee* of 99% and a diastereomeric excess (*de*) of 99% after recrystallization. However, no information has been published about the real yields achieved in this process.

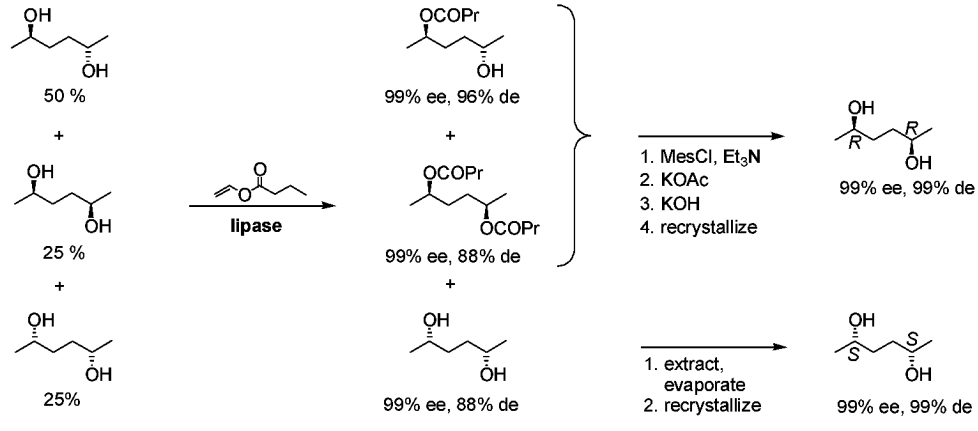

Figure 3.6: Biocatalytical production process of (2*R*,5*R*)-hexanediol at ChiroTech.

Another microbial approach using resting whole cells to produce (2*R*,5*R*)-hexanediol was published by *Ohta* et al. in 1996 *[Ikeda, et al. 1996]*. *Pichia farinosa* is used as a biocatalyst to reduce (2,5)-hexanedione to (2*R*,5*R*)-hexanediol. In batch experiments yields of about 83% are achieved. The *ee* is > 99%, but the de is only > 95%. The productivity is very low in this process (0.13 $g_{product}/g_{wet\ weight}$).

3.1.1.1 Production of *Lactobacillus kefir*

Cells of *Lactobacillus kefir* have been produced by several fermentations on a 200 L scale following a protocol published by *de Man [DeMan, et al. 1960]* as outlined in Figure 3.7. The cell mass is obtained by application of a continuously operated separator and stored at -20°C. Fermentation was stopped, when an optical density $OD_{660\ nm}$ = 4.5 was reached. The yield of biomass is between 0.9 and 1.2 kg of cell wet mass. The medium costs are 632 € kg^{-1}_{cwm}.

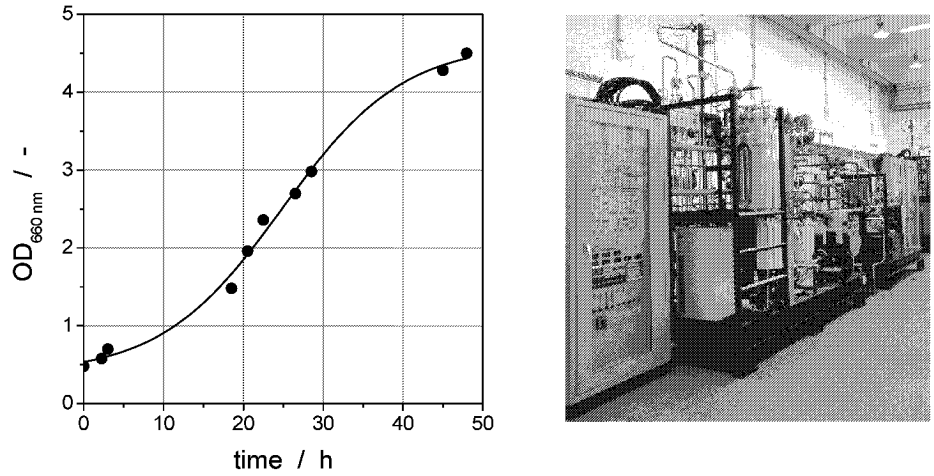

Figure 3.7: Fermentation on 200 L scale; left: $OD_{660\ nm}$ as a function of time (MRS-medium: 10 g L^{-1} casein peptone, 5 g L^{-1} sodium acetate, 10 g L^{-1} meat extract, 2 g L^{-1} K_2HPO_4, 5 g L^{-1} yeast extract, 22 g L^{-1} glucose*H_2O, 1 g L^{-1} Tween 80, 2 g L^{-1} diammonium hydrogencitrate, 0.2 g L^{-1} $MgSO_4$*7 H_2O, 0.05 g L^{-1} $MnSO_4$*H_2O at a starting pH of 6.5, 30°C, 300 rpm); right: photo of the 300 L fermenter, IBT at FZ Jülich.

Alcohol dehydrogenases within the cells of *Lactobacillus kefir* catalyze the enantioselective as well as diastereoselective reduction of 2,5-hexanedione. Reduction equivalents are supplied via glucose. Without adding the co-substrate glucose, no reaction was observed. The co-substrate is necessary to drive the internal cofactor regeneration cycles in the cell for the NADPH-dependent ADH *[Hummel 1990; Bradshaw, et al. 1992]*. *L. kefir* is known from the literature to be hetero-fermentative *[Kandler, Kunath 1983]*, meaning that 1 mole of lactic acid is formed per mol of glucose. Because of this, the pH shift during the course of the

reaction is very large. To circumvent the use of huge amounts of buffer salts, which would have to be removed during downstream processing, the pH is titrated with an autotitrator (4 N NaOH). The optimal pH was determined to be 6 *[Haberland 2003]*. At this pH value, the selectivity towards (2*R*,5*R*)-hexanediol reached 100% after 2 h in batch experiments.

3.1.1.2 Batch synthesis

The course of a batch reaction as shown in Figure 3.8 is typical for a successive reaction. Because of the different reaction rates of the two subsequent reduction steps, an interim accumulation of the intermediate (5*R*)-hydroxyhexane-2-one (**B**) is observed. Plotting the selectivity[12] of the intermediate (**B**) and the final product (**C**) as function of the conversion yields an almost ideal profile of a successive reaction (Figure 3.8).

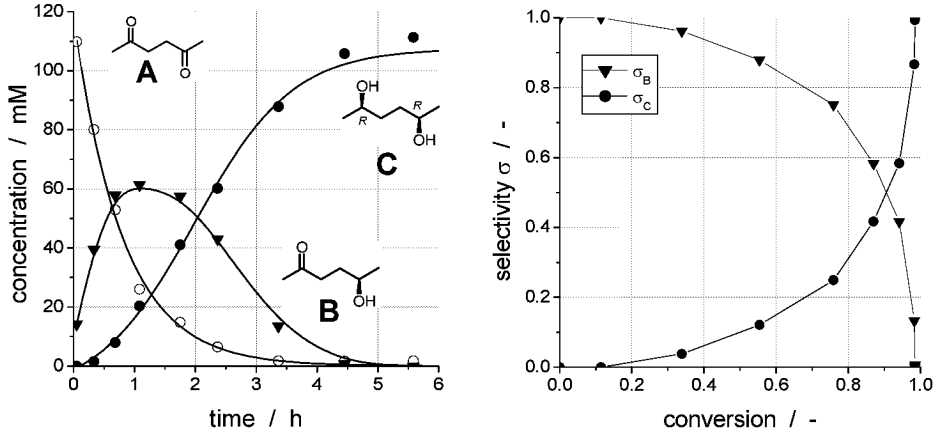

Figure 3.8: **Course of a standard batch reaction (141 mM glucose, 110 mM (2,5)–hexanedione (A), 22 g_{cdw} L^{-1} *L. kefir*, 30°C, titrated to pH 6 with 4N NaOH). Left: Concentrations as function of time; right: Selectivity as function of conversion.**

Nevertheless, considering an almost ideal successive reaction with enantio- and diastereoselectivities of > 99%, this batch process would be economically unattractive for the production of (2*R*,5*R*)-hexanediol (**C**). The drawback of this method is the low productivity of only 0.5 $g_{product}$ g_{cdw}^{-1} per batch. To increase the productivity of the cells and thereby reducing the biocatalyst[13] consumption only an reaction engineering approach will be successful, since so far no genetically engineered cells with cloned and over-expressed alcohol dehydrogenase from *L. kefir* are available.

[12] Here selectivity is defined as σ_B = [**B**]/([**B**]+[**C**]) and σ_C = [**C**]/([**B**]+[**C**]).
[13] Here whole cells of *L. kefir* are addressed as 'biocatalyst'.

Standard procedures for decreasing the catalyst consumption are the utilization of reactors that either allow for cell retention or addition of starting material *[Kragl, Liese 1999]*; in batch mode these are the repetitive or fed-batch reactors. For continuous mode operation, either plug flow reactors (pfr), requiring prior immobilization of the catalyst, or continuously operated stirred tank reactors (cstr) can be applied. Repetitive operation using whole cells would require additional filtration steps to recycle the cells. In view of an economic production the fed-batch operation was chosen in this study for exploratory investigations.

3.1.1.3 System investigations

The optimum ratio of the co-substrate, glucose, to the substrate, (2,5)-hexanedione, was determined. The final conversion and the final yield of (2*R*,5*R*)-hexanediol was investigated upon changing the initial ratio of both compounds. The ratios tested ranged from an excess of glucose (2.8) to a slight excess of the substrate (0.92) *[Haberland, et al. 2002]*. In the case of a ratio of 0.92, the reaction already stopped at a conversion of 83% due to the lack of further reduction equivalents. In all cases with an excess of glucose over (2,5)-hexanedione, quantitative conversion and yields were reached. A ratio of 1:1 was chosen for further experiments. Varying the ratio of glucose to (2,5)-hexanedione had no influence on the diastereoselectivity. By investigating the reaction conditions, it could be shown that the selectivity towards the diol reached its maximum at a pH of 6 *[Haberland 2003]*. At this pH, a maximum reaction rate for the second reaction from the hydroxyketone to the diol was achieved. All subsequent experiments were carried out at pH 6, because the main product of interest was (2*R*,5*R*)-hexanediol (**C**).

A detailed kinetic study of this whole-cell biotransformation is yet not possible. So far, namely, no methodology is established to measure the intracellular concentration of the relevant reactants and metabolites (2,5)-hexanedione (**A**), (5*R*)-hydroxyhexane-2-one (**B**), (2*R*,5*R*)-hexanediol (**C**), NADPH, $NADP^+$, lactate, acetate, and ethanol at the same time. The key challenge is a fast cell disruption preventing deactivation of the nicotinamide cofactors and quantitative analysis thereof. Nevertheless, the macroscopic kinetics of the whole cell as a black box system was carried out.

In respect to the starting material **A,** a substrate surplus inhibition is observed (Figure 3.9). Using a *Michaelis-Menten* approach for the kinetics (eq. 3-1) a substrate surplus inhibition was determined. The *Michaelis-Menten* approach to the kinetics is only valid to use, if no equilibrium reaction occurs. In the case of this whole-cell biotransformation an equilibrium is observed, as can be seen, if the initial activity as a function of the (5*R*)-hydroxyhexane-2-one **B** concentration is studied (Figure 3.10).

$$V = \frac{V_{max} \cdot [A]}{K_{M,A} + [A] + \frac{[A]^2}{K_{i,A}}} \qquad \text{eq. 3-1}$$

$V_{max} = 225.8 \pm 28.9$ U/g_{cdw}

$K_{M,A} = 25.7 \pm 5.1$ mM

$K_{i,A} = 52.8 \pm 10.4$ mM

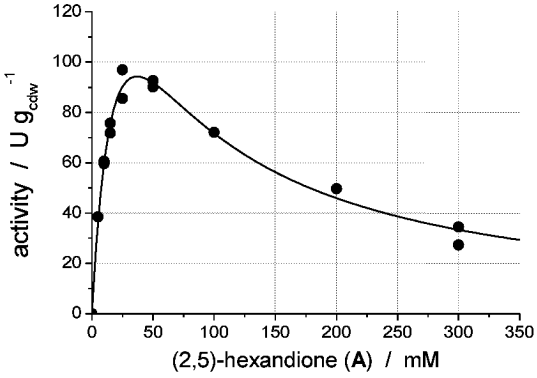

Figure 3.9: **Initial activity as function of A (400 mM glucose, 20 g_{cdw} L^{-1} *L. kefir*, 50 mM phosphate buffer pH 6, 30°C).**

The intermediate **B** can be reduced to the diol **C** and is oxidized to the starting material **A** at the same time. Surprisingly, this is possible, since it was not expected that such high amounts of oxidized cofactor $NADP^+$ are available during the start-up period within the cells, especially in presence of reduction equivalents supplied via glucose. Because of the aforementioned points, the *Michaelis-Menten* approach cannot be used here for detailed studies of the kinetics, rather the results thereof give a hint pertaining to the limiting parameters, e.g. $K_{i,A}$.

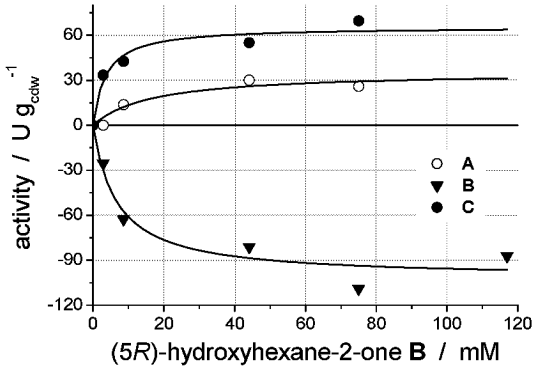

Figure 3.10: **Initial activity as function of B (400 mM glucose, 20 g_{cdw} L^{-1} *L. kefir*, 50 mM phosphate buffer pH 6, 30°C).**

Similar conclusions become also evident, if the influence of the product **C** is investigated. By addition of 100 mM (2*R*,5*R*)-hexanediol for start-up, a decrease of the diol concentration is initially observed, followed by a subsequent increase leading to 100% conversion (Figure 3.11). Once again this behavior points to an equilibrium reaction.

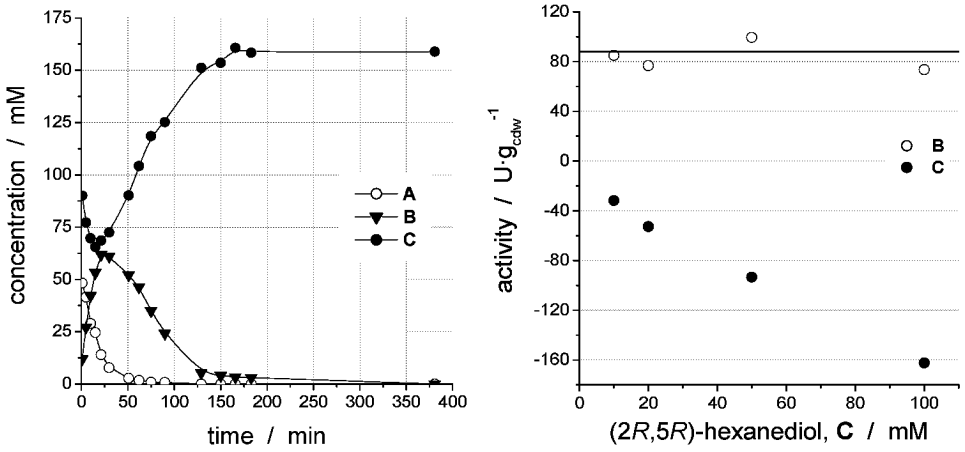

Figure 3.11: Left: Batch mode with addition of C for start-up (100 mM (2*R*,5*R*)-hexanediol, 400 mM glucose, 20 g_{cdw} L^{-1} *L. kefir*, 50 mM phosphate buffer pH 6, 30°C); right: Activity as function of C. The degradation of C (reverse reaction) is expressed in negative rate values.

These observations stress the fact that for detailed kinetic investigations of this system the intracellular reactants and metabolites need to be analyzed. This would render the determination of detailed kinetic parameters possible, even of the successive reaction based on an equilibrium model.

A detailed model of the metabolism of *Lactobacillus kefir* is not known yet. To gain some more insight, an experiment with a constant feed regarding glucose and a pulse addition regarding 2,5-hexanedione (**A**) after 3 h was performed (Figure 3.12). The batch could be separated into three different phases:

1. phase: fed-batch regarding glucose
2. phase: fed-batch regarding glucose and pulse of 2,5-hexanedione at 3 h
3. phase: fed-batch regarding glucose

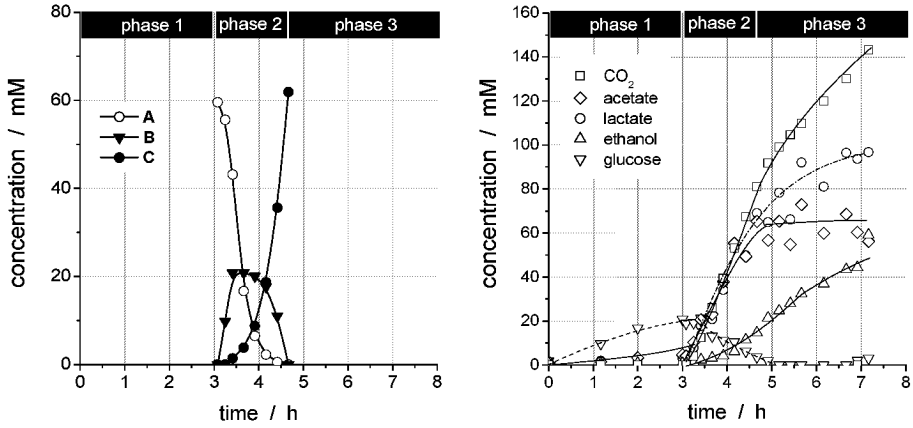

Figure 3.12: Results of the pulse experiment regarding 2,5-hexanedione and fed batch regarding glucose (60 mM 2,5-hexanedione pulse at 3 h, 1,19 mmol g_{cdw}^{-1} h^{-1} glucose, 12.6 g_{cdw} L^{-1} *L. kefir*, 50 mM phosphate buffer pH 6, 30°C, 4 vvm N_2). Left: Biotransformation in phase 2; right: Course of extra-cellular metabolites during the phases 1-3.

Prior to start of phase 2, almost no metabolites can be observed. By injecting the 2,5-hexanedione pulse the biotransformation is started. At the same time, also all other metabolites can be detected extra-cellularly. One possible explanation might be that NADPH, as shown in Figure 3.13, inhibits the metabolism. This might also be the reason, why there seems to be a high intracellular concentration of $NADP^+$ available during start up and enabling a reverse reaction as shown in Figure 3.11. This assumption is also supported by the fact that after reaching complete conversion in the biotransformation, (start of phase 3), and the metabolism is still continuing. Nevertheless, during the course of phase 3 the metabolism overall is slowing down again. Striking is the fact that the rate of product formation, namely of ethanol, is even increased in phase 3. A possible explanation might be regeneration of the cofactor $NADP^+$ during the production of ethanol. Since during the biotransformation most of the NADPH is consumed by the reduction of **A** to **C** the formation rate of ethanol is lower during phase 2 compared to that in phase 3.

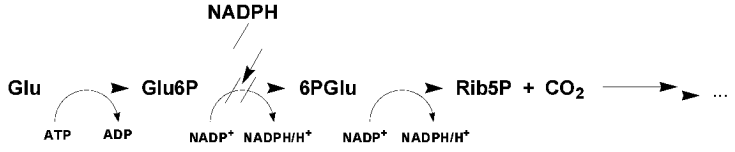

Figure 3.13: Inhibition of metabolism by NADPH.

3.1.1.4 Fed-batch operation

In this following section the possibility for the production of small amounts of (2*R*,5*R*)-hexanediol (**C**) in a fed-batch process is evaluated. Hereby important parameters will be productivity per experiment, expressed as $g_{product}/g_{cell\ dry\ weight}$ and selectivity. As fed-batch reactor the fedbatch-pro® from the DASGIP Company (Jülich, Germany) was used (Figure 3.14). This machine allows for the parallel execution of different batches with independent feed profiles. The pH is measured per batch vessel and titrated with 4 N NaOH to the set point of pH 6.

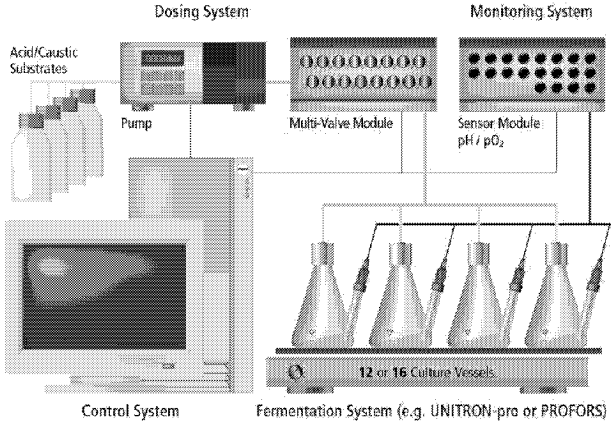

Figure 3.14: Fedbatch-pro® from DASGIP ***[Altenbach-Rehm, Weuster-Botz 1996; Altenbach-Rehm, et al. 1996].***

The results of a series of fed-batch experiments with different feed rates of (2,5)-hexanedione (**A**) are shown in Figure 3.15. All fed-batch experiments were carried out in 500 mL shake flasks with a starting volume of 100 mL and 22 $g_{cdw}\ L^{-1}$ cells of *L. kefir* (10% wet cells). The first set of experiments showed the influence of different feed rates. The concentrations of the glucose and (2,5)-hexanedione solutions were both 2 M. By reducing both feed rates from 24 mmol h^{-1} to 2.4 mmol h^{-1}, an increase of selectivity for (2*R*,5*R*)-hexanediol (**C**) to 93% was achieved. However, with decreasing feed rate the activity of the cells as well as the productivity is reduced.

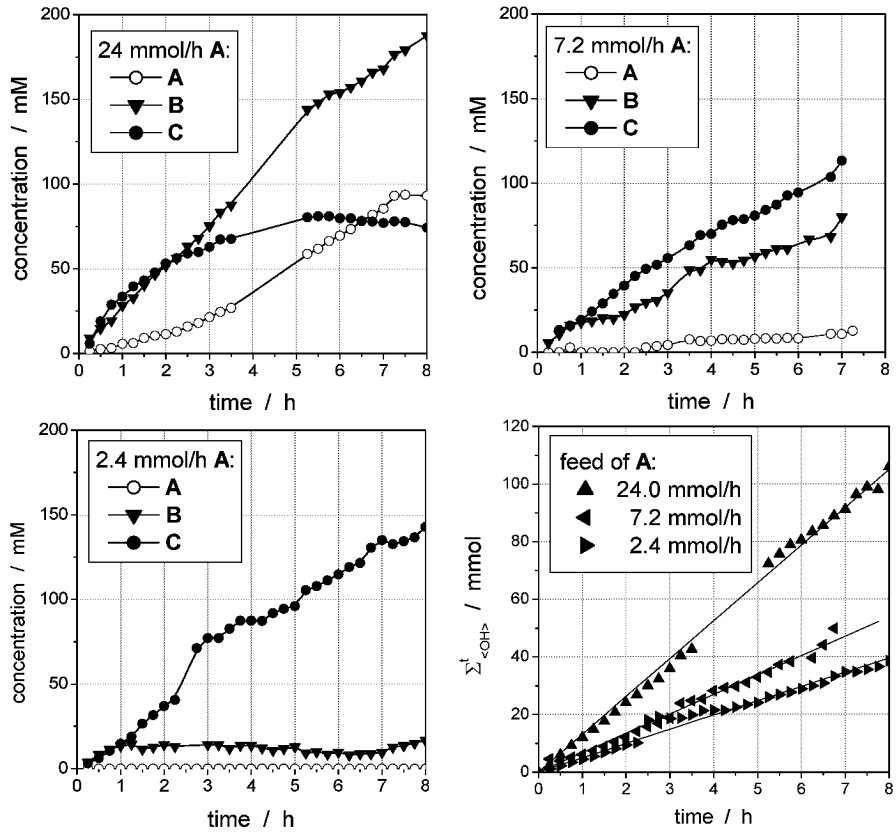

Figure 3.15: **Influence of different feed rates in fed-batch experiments (22 g_{cdw} L^{-1} *L. kefir*, 30°C, titrated to pH 6 with 4N NaOH, 2 M glucose and 2 M (2,5)–hexanedione (A) feed: top left: 24 mmol h^{-1}; top right: 7.2 mmol h^{-1}, bottom left: 2.4 mmol h^{-1}) and specific activities regarding reduction formation of oxo-functions (bottom right).**

As can be seen from Figure 3.15 the selectivity in the fed-batch experiments is influenced by two main parameters: The activity of the catalyst applied (relates to the catalyst concentration) and the feed rate of the starting materials. The accumulation of (2,5)-hexanedione (**A**) in the first experiment (Figure 3.15, top left) was a result of the high feed rate (24 mmol h^{-1}), because the total activity of the cell mass used was not high enough to convert all the starting material provided. By reducing the feed rates of **A** and of glucose, the residual concentration of (2,5)-hexanedione is also reduced, and the conversion increased (Figure 3.15, top right and bottom left). While decreasing the feed rates of glucose and (2,5)-hexanedione at a constant ratio, the selectivity increases significantly. In other words, the selectivity is governed by the ratio of feed rate to the activity of the biocatalyst. The mass-specific activity of the biocatalyst per fed-batch can be determined from Figure 3.15 (bottom right). Plotted is the sum of the hydroxy functions $\Sigma^{t}_{<OH>}$ reduced as a function of reaction time:

$$\sum_{<OH>}^{t} = n_t \mathbf{B} + 2\,n_t \mathbf{C} \qquad [mmol] \qquad \textbf{eq. 3-2}$$

With this simplification the mass-specific reaction rate of whole cells from *L. kefir* in the fed-batch mode can be determined:

$$v_{L.kefir} = \frac{d\sum_{<OH>}^{t} / m_{cdw}}{dt} \qquad \left[\frac{mmol}{g_{cdw}\,h}\right] \qquad \textbf{eq. 3-3}$$

For a generally applicable correlation between selectivity of **C**, feed rate, and catalyst concentration the following ration was defined:

$$\frac{feed\ rate}{mass\ of\ catalyst} \qquad \left[\frac{mmol}{g_{cdw}\,h}\right] \qquad \textbf{eq. 3-4}$$

Plotting the selectivity of **C**, σ_C, achieved at the end of each experiment outlined in Figure 3.15 as function of this ratio (Figure 3.16) reveals that decreasing the substrate feed or increasing the catalyst concentration results in higher selectivity. This information could be used for control of σ_C in fed-batch experiments. The parameters feed concentration and biomass concentration can be directly correlated with the selectivity. This is an easy tool to optimize different fed-batch experiments towards selectivity of (2*R*,5*R*)-hexanediol formation. The ratio of feed rate to mass of catalyst is rather a practical parameter.

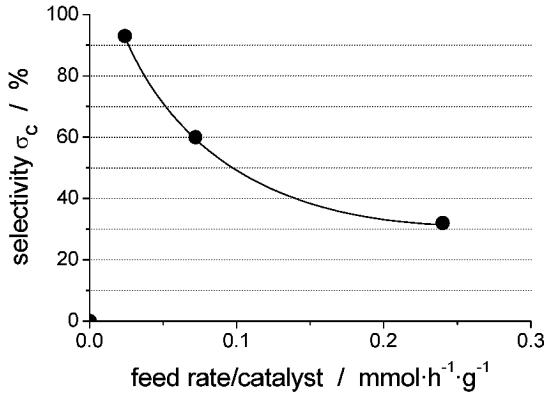

Figure 3.16: Selectivity of C as function of the ratio of feed rate to mass of catalyst.

However, the ratio in eq. 3-4 cannot be used to determine the operation point of highest selectivity of **B** (5*R*-hydroxy hexane-2-one) in a fed-batch reactor for production purposes. As can be seen in Figure 3.17 the highest selectivity regarding **B** is only reached at rather low points of conversion. For the efficient production of 5*R*-hydroxy hexane-2-one (**B**), however, the reaction conditions need to be changed, especially the pH, as has already been demonstrated before *[Haberland, et al. 2002]*. In the fed-batch experiment reaching 93% selectivity of **C,** the productivity per experiment is doubled to 1 $g_{product}/g_{cdw}$ compared to the simple batch mode.

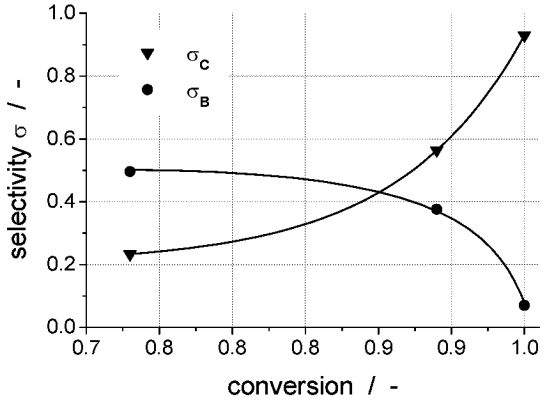

Figure 3.17: Conversion and selectivity of B and C as function of conversion (lines are only visual aids).

3.1.1.5 Development of a continuously operated process

Since the increase in productivity per experiment to 1 $g_{product}/g_{cdw}$ in the fed-batch mode is not high enough for a production process, a continuously operated process is to be developed, enabling recycling of the whole cells. By this means, the residence times of the catalyst and the reactants become decoupled resulting in a significant increase in productivity. The setup used for the continuously operated reactor is shown in Figure 3.18 and the corresponding photos are depicted in Figure 3.19.

The continuous reductions were carried out on a 2-L scale under anaerobic conditions (3-L Labfors bioreactor with a 2-L working volume; *H* 38 cm, *D* 11.6 cm, Infors, Basel, Switzerland). For the retention of the cells an ultrafiltration module (KrosFlow, Ø fibers 0.5 mm, A 1.7 m^2, Membrapure, Bodenheim, Germany) with a membrane area of 1.7 m^2 and a molecular weight cutoff of 400 kD was integrated into an external loop (dead volume of the loop approximately 200 mL, flux 60 L h^{-1}, permeate flux 0.5 L h^{-1}). The ultrafiltration module was chosen over a microfiltration module, because herein membrane fouling introduced by adsorption of whole cells in the pores of the membranes is much lower. The filtration module was sterilized each time before and after operating the reactor by rinsing with 1 M NaOH

solution. The stirrer speed was 1200 rpm, the fermenter temperature was set at 30 °C, and the condenser temperature was maintained at 4 °C, using a water bath and a cryostat. Nitrogen gas was applied at 6 L min^{-1} (6 vvm) to maintain anaerobic conditions and to increase the gas flow of carbon dioxide for off-gas analysis. The carbon dioxide concentration was measured using a Fisher-Rosemount carbon dioxide analyzer, type Binos 100, range 0-2%. LABVIEW 6.01 software (National Instruments, Munich, Germany) was used for online data acquisition. The pH was kept at 6 (0.05 with 4 M NaOH via a pH-stat; Metrohm, Herisau, Switzerland). The reactor was sterilized (121 °C for 20 min) prior to use; glucose solution was sterilized by filtration in a pre-sterilized vessel autoclavable sterile capsule 0.45 and 0.2 mm pores, Sartorius AG, Goettingen, Germany). A buffered glucose solution was the main feed to the reactor. The substrate itself was provided in a pure form at a very low flow rate. This set-up enabled easy variation of the substrate-to-glucose ratio. Variations of the substrate concentration and also a change to a different starting material can be realized conveniently. The residence time in the reactor was kept constant at 4 h for all experiments.

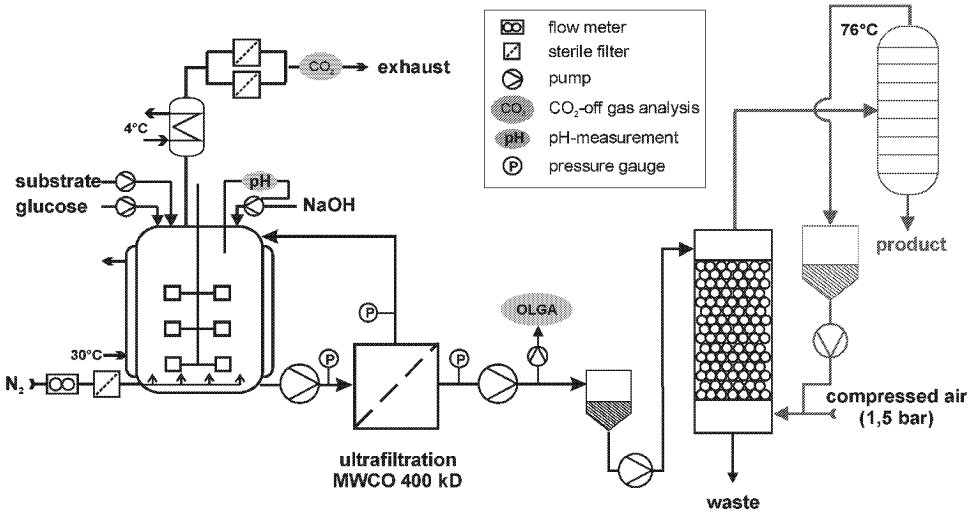

Figure 3.18: Flow scheme of the continuously operated membrane reactor with in-line product separation.

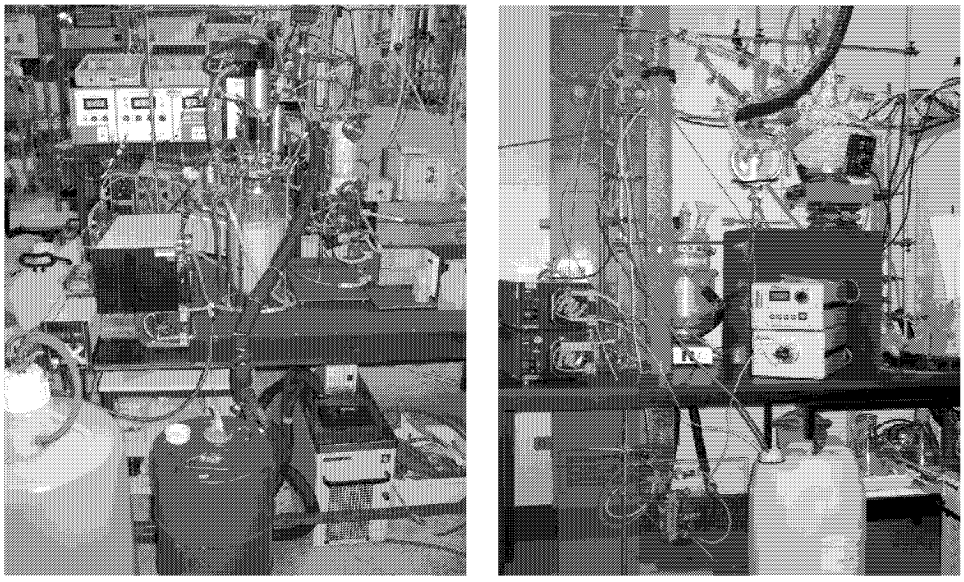

Figure 3.19: Photos of the continuously operated membrane reactor with in-line product separation.

Connected to the outflow of the membrane reactor is an in-line product separation unit, consisting of a continuously operated countercurrent extraction of the aqueous product solution with ethyl acetate as the eluent. The extraction is facilitated in a packed column (1.3 m height, 1.6 L volume, Ø 4.5 cm) that is thermostated to 50°C. The aqueous solution enters the column at the top, ethyl acetate at the bottom. The two phases are separated at the bottom of the packed column, where ethyl acetate is also fed in. To establish a steady inter-phase between aqueous and organic phase a level control device was integrated based upon a conductivity measurement utilizing three wolfram wires (Figure 3.20). If the aqueous phase reaches the top wire (max) and the electrical circuit is closed with the mass wire, the pump of the aqueous outflow is started. The organic solvent is recycled via an online distillation and the reaction product (2*R*,5*R*)-hexanediol **C** is collected at the bottom of the distillation unit.

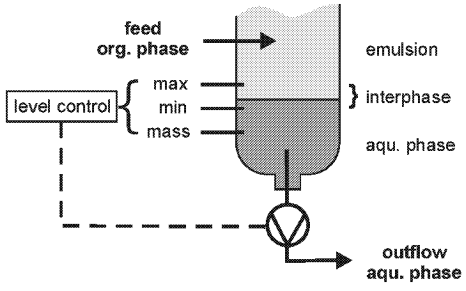

Figure 3.20: Level control of the inter-phase in the bottom of the packed column.

The characteristics of a continuously operated reactor run are shown in Figure 3.21. By changing the feed rate of (2,5)-hexanedione during continuous reduction different points of conversion and selectivity are reached. The feed ratio of glucose to (2,5)-hexanedione was changed between the steady states (0-54 h: glucose feed 75 mmol h^{-1}, (2,5)-hexanedione feed 38 mmol h^{-1}; 55-95 h: glucose feed 75 mmol h^{-1}, (2,5)-hexanedione feed 60 mmol h^{-1}). As can be seen in Figure 3.21, with the first set of operating conditions a steady state was reached. Here **C** is produced at a space-time yield of 46 g L^{-1} d^{-1}. Increasing the feed rate of 2,5-hexanedione (**A**) leads to an unstable operating point, which might be due to instability of the biocatalyst.

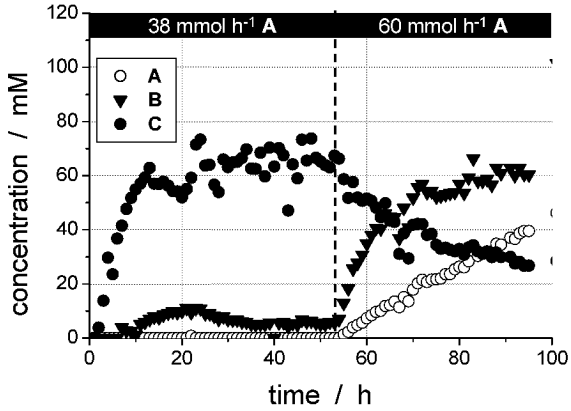

Figure 3.21: Concentration time course for different steady states during the continuous reduction of (2,5)-hexanedione. (152 mM glucose, 0-54 h: 76 mM (2,5)–hexanedione (A), 55-95 h: 120 mM (2,5)–hexanedione (A), 21 g_{cdw} L^{-1} *L. kefir*, 50 mM phosphate buffer, titrated to pH 6 with 4N NaOH, 30°C, τ = 4h).

A typical continuously operated production process of **C** is shown in (Figure 3.22, left). Glucose was fed with 76 mmol h^{-1} and a flow rate of 460 mL h^{-1}. Undiluted (2,5)-hexanedione **A** was fed out of the drum with 56 mmol h^{-1} and a flow rate of 7 mL h^{-1}. After the start-up phase of 20 h, a steady-state was reached with a (2*R*,5*R*)-hexanediol **C** concentration of 90 mM. The optical purity of the product was very high (*de*, *ee* > 99%). The residual concentration for the intermediate **B** was 30 mM and for **A** around 2 mM. The conversion is nearly quantitative over a range of 120 h. A space-time yield of 63.8 g L^{-1} d^{-1} and a selectivity of 78% for (2*R*,5*R*)-hexanediol **C** was achieved. In Figure 3.22, right, conversion and selectivity are plotted as function of time. Selectivity is an important parameter for downstream processing because crystallization of **C** is not possible, if the selectivity is lower than 60%. The conversion decreased rapidly after 120 h (not shown in Figure 3.22). A reason for this decrease is not known yet. Parallel to the biotransformation a macromolecule is excreted into the reaction medium that could not be identified up until now. Standard tests for alcohol dehydrogenases as well as proteases did not show any activity. A

SDS-Page revealed a molecular weight of approx. 66 kDa. Also sequencing the *N*-terminus did not reveal any information since no high homology with any protein sequence stored in databases could be identified.

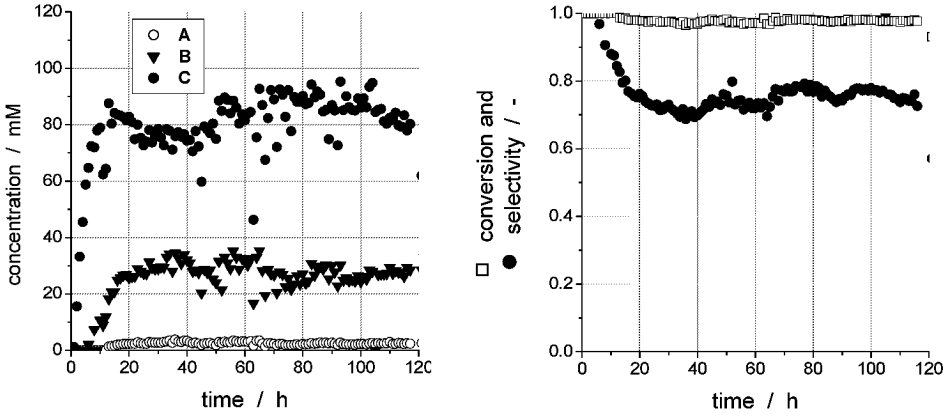

Figure 3.22: Concentration time course for the continuous production of (2*R*,5*R*)-hexanediol C with *L. kefir* (left) and selectivity of C as well as conversion as function of time (152 mM glucose, 112 mM (2,5)–hexanedione (A), 21 g_{cdw} L^{-1} *L. kefir*, 50 mM phosphate buffer, titrated to pH 6 with 4N NaOH, 30°C, τ = 4 h).

The productivity per experiment, however, of the cells in the continuously operated reactor (15 $g_{product}/g_{cdw}$) was increased significantly in comparison to previously used production methods such as batch or fed-batch. Because biomass is the cost-limiting factor, the improvement of the ratio of $g_{product}/g_{cdw}$ is the key step towards a low-priced enantiopure product. This ratio has now has been increased by factor of 30.

In Figure 3.23 it can be seen that the reproducibility between different continuous-mode experiments is very high. The selectivity of **C** increases with increasing conversion. Surprisingly, also the batch and fed-batch data show the same profile. Since we are dealing with a successive reaction, (**A** → **B** → **C**), a differentiation would be expected depending on the type of reactor applied. This points to a limiting factor that is independent on the reactor type. A possible explanation might be the ratio of $NADP^+$ to NADPH. This ratio should be constant independent of the reactor type. Additionally, this graph shows that at least a conversion of 95% is required to reach a selectivity of 60% for **C**, to enable crystallization of **C**.

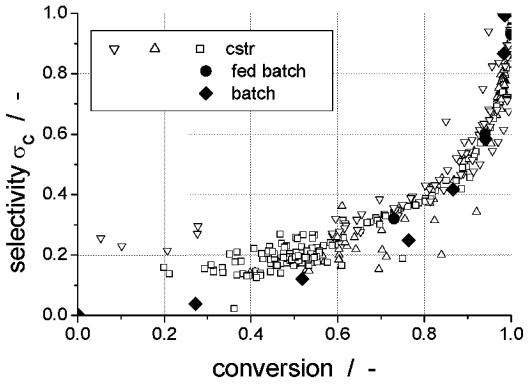

Figure 3.23: Selectivity of C as function of conversion for different reactors.

One important part of process development in this case is the downstream processing, which will be discussed in detail in the following. The state of the art at the company *Jülich Fine Chemicals* (Jülich, Germany) was a batch process with suspended cells. The procedure for downstream processing of an aqueous solution containing the product (2*R*,5*R*)-hexanediol **C** consisted of 4 steps:

1. Centrifugation of the cell suspension to separate whole cells.
2. Concentration of the aqueous solution using a rotary evaporator.
3. Batchwise extraction of the concentrated aqueous phase by means of separatory funnels.
4. Crystallization.

The application of this strategy leads to product losses of 30-40% during the downstream processing (➲ page 42). Therefore, a new strategy was to be developed to crease the yield of product separation. In addition, it should be possible to integrate this process into the continuous-production process. As already shown in Figure 3.18, an in-line counter current liquid-liquid extraction procedure was developed. There are two important values that can be used to judge the efficiency of the extraction: During equilibrium the *Nernst* distribution law (eq. 3-5) describes the distribution of the compound to be extracted between two phases of the same volume, in this case called the *extract* and the *raffinate* (K_D *distribution coefficient*). This law is only valid for diluted non-miscible solutions *[Treybal 1963]*.

$$K_D = \frac{c_{extract}}{c_{raffinate}} \qquad \textbf{eq. 3-5}$$

Of rather practical value is the *degree of extraction E* (eq. 3-6). To determine this degree of extraction during the continuously operated extraction process the difference of the inlet

concentration of the aqueous phase to the residual concentration in the raffinate is determined (eq. 3-6).

$$E = \frac{c_{extract}}{c_0} = \frac{c_0 - c_{raffinate}}{c_0} \qquad \textbf{eq. 3-6}$$

In Figure 3.24 the degree of extraction for **C** is given for different organic solvent/water mixtures. Ethyl acetate was chosen as the solvent of choice for the extraction, since in comparison to the ethers it is exhibits almost the same degree and efficiency of extraction, but by contrast to the ethers, it is not carcinogen. The partition of **C** between the ethyl acetate phase and water is increasing with temperature.

solvent	degree of extraction
MTBE	0.13
ethyl acetate	0.13
diethyl ether	0.15
iso-octane	insoluble
iso-hexane	insoluble

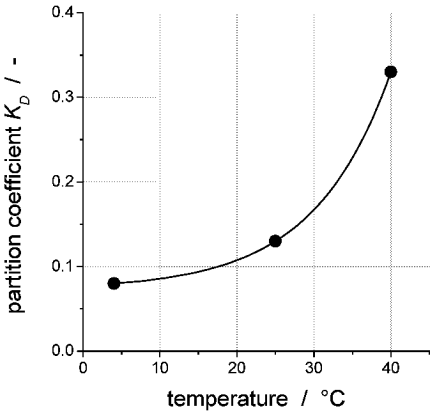

Figure 3.24: Degree of extraction for different organic solvents (left) and partition coefficient K_D as function of temperature for C between ethyl acetate and water (50 mM (2*R*,5*R*)-hexanediol C in water, 1:1 mixture with respective organic solvent).

To establish an effective phase contact within the extraction column, three different packing materials were tested:

- glass beads (Ø 5 mm)
- Sulzer SMV DN 40 mixers (l 48 mm, $Ø_a$ 43 mm)
- Raschig rings (l 10 mm, $Ø_a$ 10 mm, $Ø_i$ 5 mm)

At 4 h residence time the continuously operated membrane reactor produces an outflow of 0.5 L h^{-1} of aqueous phase. The installed distillation capacity limits the ethyl acetate recirculation rate to 1.7 L h^{-1}. An increase in the ethyl acetate flux would require a scale-up of the distillation unit.

The glass beads showed the lowest degree of extraction; therefore, they were omitted in

subsequent investigations. With the Sulzer packing material, a degree of extraction is yielded up to 75% at an aqueous flux of 0.25 L h^{-1}, as can be seen from Figure 3.25, left. With increasing flow rates of the aqueous phase the degree of extraction is decreasing again. At 0.5 L h^{-1} the degree of extraction is already reduced to 40%. On the other hand, a minimal flux needs to be established using the Sulzer packing to reach high extraction efficiency. Best results yielded the Raschig rings. At a flux of 0.5 L h^{-1} for the aqueous phase and 1.7 L h^{-1} for the organic phase a degree of extraction of 62% has been reached. Decreasing the aqueous flux to 0.1 L h^{-1} yields up to E = 90%. Decreasing the organic flux results in significantly lower degrees of extraction. The reason is that the aqueous phase, - fed to the extraction column on top, - is falling down the column due to gravity according to its density difference to the organic phase. As a consequence, the organic phase becomes loaded with the maximal concentration of **C** corresponding to the *Nernst* distribution. Therefore, a lower efficiency in the extraction results.

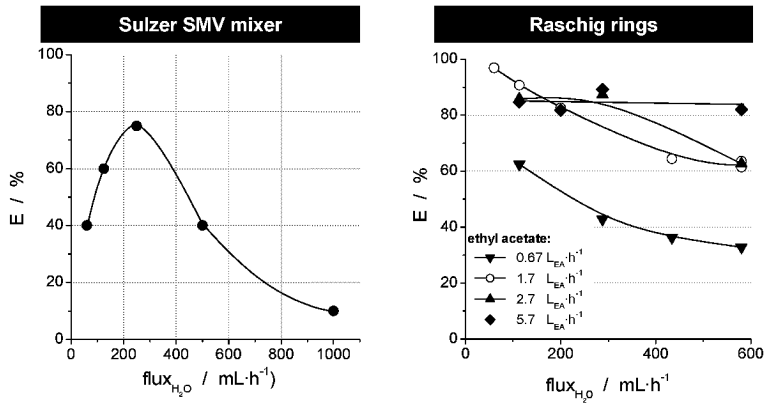

Figure 3.25: Characterization of different packings: Degree of extraction as function of the aqueous flux for Sulzer SMV mixers (left, 1.7 L h^{-1} ethyl acetate) and Raschig rings (right).

Since the product **C** accumulates at the bottom of the ethyl acetate re-distillation unit, a thorough characterization of the distillation step was carried out. Here one important question is, whether together with ethyl acetate **C** is re-distilled as well. To answer this question, investigations were carried out, utilizing the Gillespie apparatus to determine the relevant parameters of the liquid-vapor equilibrium. The principle of this dynamic method is the following: It is assumed that the vapor generated by a boiling liquid is totally condensed in a separate condenser and subsequently returned to the boiling liquid (circulation of vapor respectively of the condensate). After a certain time, a steady state is reached, in which the composition of boiling liquid and vapor, respectively the condensate, is not changing any more. This can then be used to determine the distribution of **C** between the liquid and gas phase in different solvents at equilibrium state. The concentration of **C** in the vapor phase

increases linearly with the respective concentration in the boiling liquid phase (Figure 3.26). This effect is approximately 17 times bigger with water as compared to ethyl acetate. This is also the reason, why there is such a high loss of **C**, if the supernatant of fermentation broths is concentrated by evaporation.

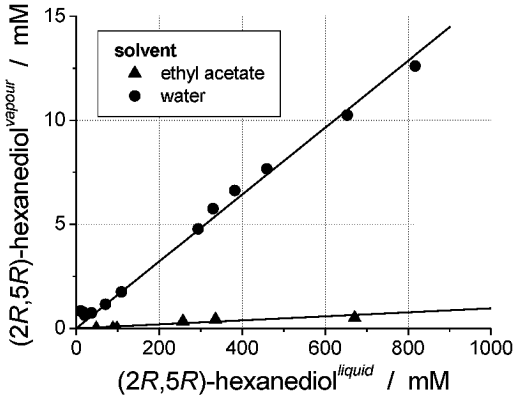

Figure 3.26: Distribution of C between vapor and liquid for different solvents.

After evaporation of the ethyl acetate, isooctane is added to start the crystallization of the product. Likewise, the product can be recrystallized from ethyl acetate, if needed. Beside the final product **C**, also the intermediate **B**, 2*R*-hydroxy-5-hexanone, can be easily isolated from the product solution of the continuous process. The selectivity regarding **B** is approximately 20%. By filtering off the crystallized **C**, the intermediate **B** can be isolated by column chromatography with a purity of 95% and an *ee* > 99%.

3.1.1.6 Summary

A new continuous process for the diastereomeric production of (2*R*,5*R*)-hexanediol (*ee* > 99%, *de* > 99%) has been developed on the basis of a reaction sequence carried out within a whole cell (**A** → **B** → **C**). To increase the attractiveness of this continuous process for industrial application, the productivity and the stability of the biocatalyst still needs to be improved. However, by changing over from batch to a continuously operated process the ratio of $g_{product}/g_{cdw}$ has already been increased by factor 30 to 15 g/g (Figure 3.27, left) or even by factor 250 in comparison to the synthesis as published by *Ohta [Ohta, et al. 1986]*. A typical space-time yield for the continuous process carried out over 5 days is 64 g L^{-1} d^{-1}. By contrast to the lipase process as developed by Chirotech (➲ Figure 3.6, page 24), here the catalyst costs are the biggest portion of the costs (Figure 3.27, right). Following our procedure, the costs for the production of 1 kg (2*R*,5*R*)-hexanediol **C** are reduced to by factor 10, utilizing the new whole cell process with *Lactobacillus kefir*. There is still a high potential to further decrease the production costs, because in the whole cell process the dominating fraction of the

over-all costs is that for the catalyst. Further optimizing the process will allow to further decrease the catalyst consumption. This will not be easily achieved in the lipase process, since here the dominating costs are those of the reagents, which are mostly required stoichiometrically.

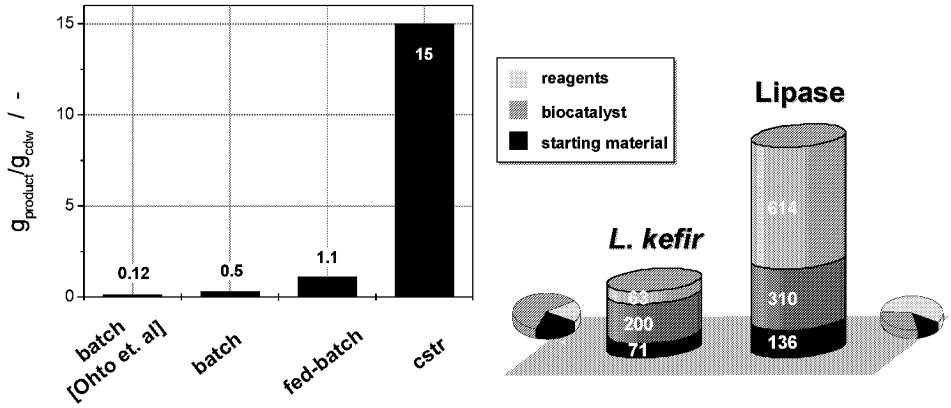

Figure 3.27: **Increase of productivity from batch to cstr (left); portion of costs in € of the established Chirotech lipase process compared to the process utilizing *Lactobacillus kefir* for the production of 1 kg (2*R*,5*R*)-hexanediol C (evaluation of costs on basis of Fluka prices 2002).**

The general view is
that asymmetric chemistry is the best route
to compounds with single chiral centers,
but compounds with multiple chiral centers
start to favour a biocatalytic route.

Taylor, Zeneca

3.2 *In vitro* reaction sequences by combination of biocatalytical steps

3.2.1 Diastereoselective production of diols with *in vitro* reaction sequences[14]

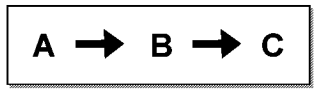

In contrast to chapter 3.1 here an *in vitro* reaction sequence is used for the diastereoselective synthesis of 1,2-diols starting from bulk chemicals. Optically active vicinal diols are interesting building blocks in asymmetric synthesis, especially for the synthesis of chiral phosphine ligands. Chemical routes towards *vic*-diols (Figure 3.28) in terms of stereospecificity and enantioselectivity include the catalytic *cis*-dihydroxylation of olefins by OsO_4 *[Kolb, et al. 1994; Choudary, et al. 2001]*, and the catalytic asymmetric transfer hydrogenation of diketones *[Koike, et al. 2000]*. Amongst the biocatalytic methods for the synthesis of *vic*-diols are the hydrolysis of epoxides with epoxide hydrolases *[Pedragosa-*

[14] **Parts of this chapter are published in:**

1. L. Greiner: *Reaktionstechnik der Benzoylformiatdecarboxylase*, diploma thesis, University of Bonn, 1999
2. D. Kihumbu: *Stereoselektive Synthese von 1-Phenlypropan-1,2-diol Isomeren mit Lyasen und Oxidoreductasen, Entwicklung eines kontinuierlichen Verfahrens, PhD-thesis*, University of Bonn, in progress
3. T. Stillger: *Reaktionstechnik der Benzaldehydlyase*, PhD-thesis, University of Bonn, in progress
4. D. Kihumbu, T. Stillger, W. Hummel, A. Liese: *Enzymatic synthesis of all stereoisomers of 1-phenylpropane-1,2-diol*, Tetrahedron Asymmetry 13 (2002) 1069-1072
5. H. Iding, P. Siegert, T. Dünnwald, M. Müller, L. Greiner, A. Liese, J. Grötzinger, A. Demir, M. Pohl: *Benzoylformate decarboxylase from Pseudomonas putida as stable catalyst for the synthesis of chiral 2-hydroxy ketones*; Chemistry – a European Journal 6 (8) (2000) 1483-14955.
6. D. Kihumbu, T. Dünnwald, J. Bargon, A. Liese: *Substituent effects on the enantioselectivity of the benzoylformate decarboxylase catalyzed (S)-2-hydroxy-1-phenyl-propanone formation*, (submitted)
7. B. Lingen, A. Liese, Michael Müller: *Enantioselective synthesis of hydroxy ketones via benzaldehyde lyase- and benzoylformate decarboxylase-catalyzed C-C bond formation*; in: Thiamine: Catalytic Mechanisms and Role in Normal and Disease States (M. S. Patel and. F. Jordan, eds.), Marcel Dekker, New York (in press)
8. T. Dünnwald, L. Greiner, H. Iding, A. Liese, M. Müller, M. Pohl: *Stereoselektive Synthese chiraler 2-Hydroxyketone mittels Benzoylformiatdecarboxylase*, German Patent Application DE 199 18 935.8 (26.04.1999); *Stereoselective synthesis of 2-hydroxyketones*, European Patent Application EP 00108709.7-2110 (22.04.2000)

Moreau, et al. 1996; Weijers 1997], the kinetic resolution of racemic *vic*-diols achieved by enzymatic oxidation *[Bortolini, et al. 1998]*, and the enzymatic and microbial reduction of 1,2-diketones and α–hydroxy ketones *[Mochizuki, et al. 1995; Bortolini, et al. 1997]*. Drawbacks of the methods mentioned above are the following:

- The starting material is in general an already advanced chemical.
- Only one or two diol stereoisomers are accessible in good optical purity from the same starting material.

In contrast to the above-mentioned methods, all four possible stereoisomers of 1-phenylpropane-1,2-diol can be synthesized separately by employing a combination of enantioselective lyases and diastereoselective alcohol dehydrogenases (ADH) in succession. Moreover, bulk chemicals like benzaldehyde (**A_1**) and acetaldehyde (**A_2**) are used as starting materials. In the first reaction step an enantioselective C-C bond formation is catalyzed by a lyase leading to e.g. (*S*)-2-hydroxy-1-phenylpropanone (2-HPP, **B**). This intermediate is reduced enantioselectively to the corresponding *vic*-diol e.g. (1*S*,2*S*)-1-phenylpropane-1,2-diol (**C**), catalyzed by an alcohol dehydrogenase (ADH).

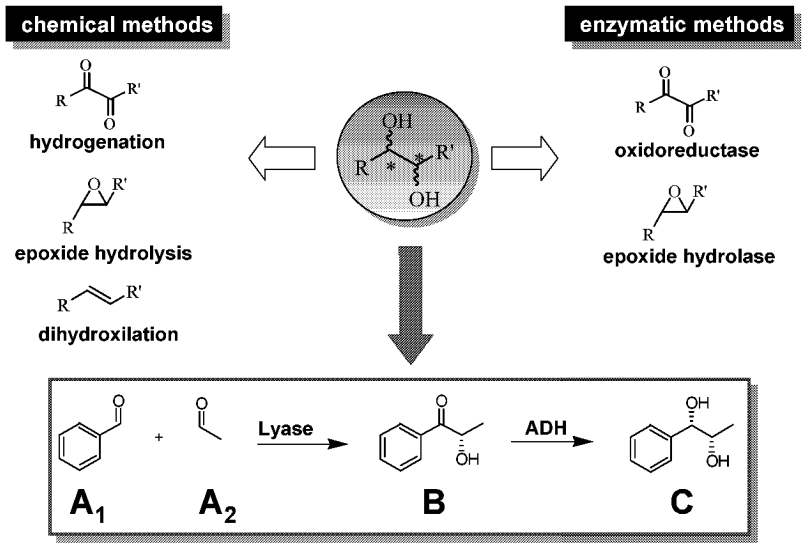

Figure 3.28: Chemo- and biocatalytic routes towards *vic*-diols starting from bulk chemicals like benzaldehyde and acetaldehyde (ADH = alcohol dehydrogenase).

Lyases are not yet applied that often by chemists as hydrolases or oxidoreductases. The main reason might be their limited commercial availability up until now. Only approximately 9% of all reported enzymes are lyases *[Faber 1995]*. Nevertheless, there are several industrial biotransformations that are catalyzed by lyases, either as whole cells or as isolated enzymes

[Liese, et al. 2000; Schmid, et al. 2001a; Zaks 2001]. The most prominent ones are the production of L-dopa (3,4-dihydroxyphenylalanine), acrylamide, and ephedrine.
Ajinomoto produces L-dopa, which is used for the treatment of Parkinson's disease, by a lyase-catalyzed C-C bond formation (Figure 3.29) with suspended whole cells in a fed batch reactor on a scale of 250 t a^{-1} *[Tsuchida, et al. 1993; Yamada 1998; Ager 1999]*. Already much earlier, Monsanto had successfully scaled up the chemical synthesis of L-dopa (➲ Figure 4.4, page 104).

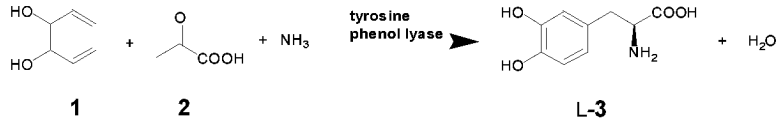

1 = catechol
2 = pyruvic acid
3 = dopa
tyrosine phenol lyase, whole cells from *Erwinia herbicola*

Figure 3.29: Industrial production of L-dopa with whole cells from *Erwinina herbicola*.

Acrylamide is an important commodity monomer used in coagulators, soil conditioners, and stock additives for paper treatment and paper sizing, and for adhesives, paints, and petroleum recovering agents *[Yamada, Kobayashi 1996]*. The biotransformation is started with an acrylonitrile concentration of 0.11 M and is stopped at an acrylamide concentration of 5.6 M (Figure 3.30). The process is operated at a capacity of 30,000 t a^{-1} *[Yamada, et al. 1986; Nagasawa, et al. 1993]*. This biotransformation has as advantages over the classical chemical process that no recovering of unreacted nitrile is necessary since the conversion is 100 % and that no copper catalyst removal is needed. This is the first case of a biocatalytic conversion of a bulk fiber monomer.

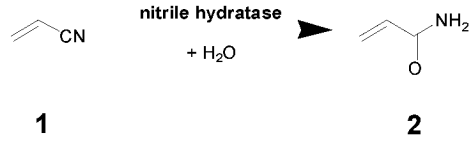

1 = acrylonitrile
2 = acrylamide
nitrile hydratase, whole cells from *Rhodococcus erythropolis*

Figure 3.30: Industrial production of acrylamide with whole cells from *Rhodococcus erythropolis*.

A special class of lyases represents the thiamine diphosphate (ThDP) – dependent group. Even if ThDP-dependent enzymes were already applied in 1921 for the production of chiral 2-hydroxyketones *[Neuberg, Ohle 1921]*, their structure was first elucidated in 1937 *[Lohmann, Schuster 1937]*. BASF, for example, is producing (*R*)-phenylacetyl carbinol (120 t a^{-1}) as an

intermediate for the synthesis of ephedrine (Figure 3.31), a bronchodilating agent and decongestant, via a whole-cell biotransformation utilizing pyruvate decarboxylase (PDC) as the ThDP-dependent lyase *[Pohl 1997; Schmid, et al. 2001a; Schmid, et al. 2002b]*. PDC, present in different organisms *[Pohl 1997]*, is one of the key enzymes in the anaerobic fermentation of glucose to ethanol and carbon dioxide *[McGill, Dawes 1971]*. The respective enzyme from *Zymomonas mobilis* exhibits a very high specific activity regarding the decarboxylation of pyruvate. For the carboligation of acetaldehyde and benzaldehyde leading to (*R*)-phenylacetyl carbinol the PDC has been genetically engineered *[Bruhn, et al. 1995; Pohl, et al. 1997]*.

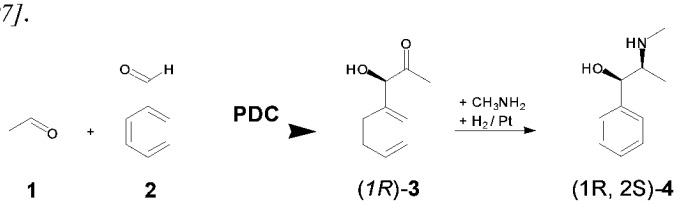

1 = acetaldehyde
2 = benzaldehyd
3 = phenylacetylcarbinol = PAC
4 = ephedrine

Figure 3.31: Industrial production of ephedrine with whole cells from *Saccharomyces cerevisiae*. The biotransformation is catalyzed by pyruvate decarboxylase (PDC).

Benzoylformate decarboxylase (BFD, E.C. 4.1.1.7) is the third enzyme in the mandelate catabolism *[Gunsalus, et al. 1953; Hegeman 1966]*, where (*R*)-mandelic acid is transformed to benzoic acid. *Wilcocks* and *Ward* describe (2*S*)-hydroxy-1-phenylpropanone as the reaction product of benzoylformate decarboxylation in presence of acetaldehyde and whole cells of *Pseudomonas putida*, respectively raw extracts of these cells *[Wilcocks, Ward 1991; Wilcocks, et al. 1992]*. BFD from *Pseudomonas putida* was cloned *[Wilcocks, Ward 1991]* and its three-dimensional structure has been published recently *[Hasson, et al. 1995; Hasson, et al. 1998]*. BFD is recombinant available as a hexahistidine fusion protein in *E.coli*. The synthetic potential of this enzyme has been investigated recently in detail by *Müller [Demir, et al. 1999; Dünnwald, et al. 2000; Dünnwald, Müller 2000]*. The main reaction of BFD is decarboxylation and the minor one carboligation (Table 3.2).

Benzaldehyde lyase (BAL, E.C. 4.1.2.38) from *Pseudomonas fluorescens* Biovar I does not catalyze decarboxylations by contrast to PDC and BFD. The main reaction of BAL is the kinetic resolution of benzoines. Contrary to the reports of *Gonzalés* and *Vicuña [Gonzáles, R. Vicuña 1989; Hinrichsen, et al. 1994]*, who stated an irreversible cleavage of 2-hydroxyketones by BAL, it could be demonstrated by *Müller et al. [Demir, et al. 2001; Demir, et al. 2002]* that BAL does also catalyze the carboligation in presence of DMSO. The enzymatic synthesis of (2*R*)-hydroxy-1-phenylpropanone is of high interest, since this enantiomer is only accessible via chemical methods with moderate enantiomeric excess *[Adam, et al. 1996; Curci, et al. 1996; Adam, et al. 1998a]*.

Table 3.2: Major and minor reaction activities of PDC, BFD and BAL.

	PDC	BFD	BAL
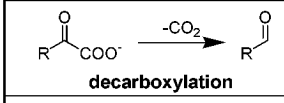 decarboxylation	major	major	-
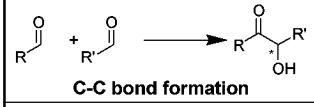 C-C bond formation	minor	minor	major (minor)
 C-C bond cleavage	-	-	major (minor)

α-Hydroxyketones, the reactions products of the carboligation of aldehydes, are ingredientsof several natural products *[Bewley, Faulkner 1998]*, and frequently they are pharmacologically active *[Mutschler 1997]*. The enantioselective syntheses of such compounds are in the focus of recent research *[Davis, Chen 1992; Gala, et al. 1995; Nakamura, et al. 1996; Adam, et al. 1998b; Corey, Helal 1998; Corrie 1998; Enders, Kallfass 2002]*. Most of the chemical syntheses start from the ketone, which becomes hydroxylated in the α-position to the α-hydroxyketone. With all three enzymes PDC, BFD, and BAL a direct highly enantioselective carboligation under formation of a secondary alcohol is possible.

3.2.1.1 BFD catalyzed enantioselective carboligation to (*S*)-2-hydroxy-1-phenylpropanone

The reaction system selected for investigation in this study is at the same time the first step (**A → B,** Figure 3.32) of the reaction sequence leading to vicinal diols (Figure 3.28). The main catalytic activity of BFD is the decarboxylation of benzoylformate, which is approximately 40 times higher than that of the carboligation. Since benzoylformate is much more expensive than benzaldehyde the reaction sequence starts with benzaldehyde. BFD is cloned and overexpressed; therefore, it does not impose any increase of the costs.

A → (*S*)-B

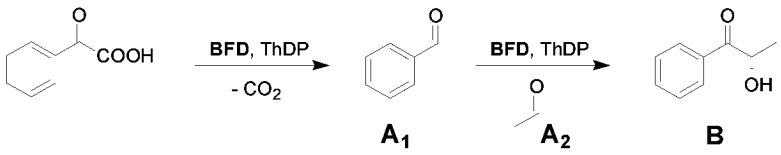

Figure 3.32: BFD-catalyzed decarboxylation of benzoylformate followed by carboligation in presence of the acceptor acetaldehyde (A_1) to (*S*)-2-hydroxy-1-phenylpropanone ((*S*)-2-HPP, B).

The ThDP-cofactor is not required stoichiometrically as is the case with NAD(P)H and oxidoreductases. The reaction mechanism is depicted in Figure 3.33. The thiazole residue of ThDP is actively involved in the catalytic cycle for binding and activation of benzaldehyde. The BFD-mediated carboligation of benzaldehyde (**A_1**) with acetaldehyde (**A_2**) leading to the (*S*)-2-hydroxy ketone (**B**) is started by a nucleophilic attack of the ylid-form of ThDP (**1**). The addition product (**2**) is rearranged to the enamine-carbanion intermediate (**3**). This transition state is probably coplanar, enabling a delocalization of the negative charge. In the presence of the acceptor acetaldehyde (**A_2**) a carboligation is catalyzed, followed by the rearrangement of the addition product (**4**) and simultaneous liberation of the (*S*)-2-hydroxy ketone (**B**) and regenerated ThDP (**1**). Therefore, only a low concentration of ThDP is required, since the cofactor is not covalently bound *[Pohl 1997]*. Besides ThDP, small amounts of Mg^{2+} are also needed.

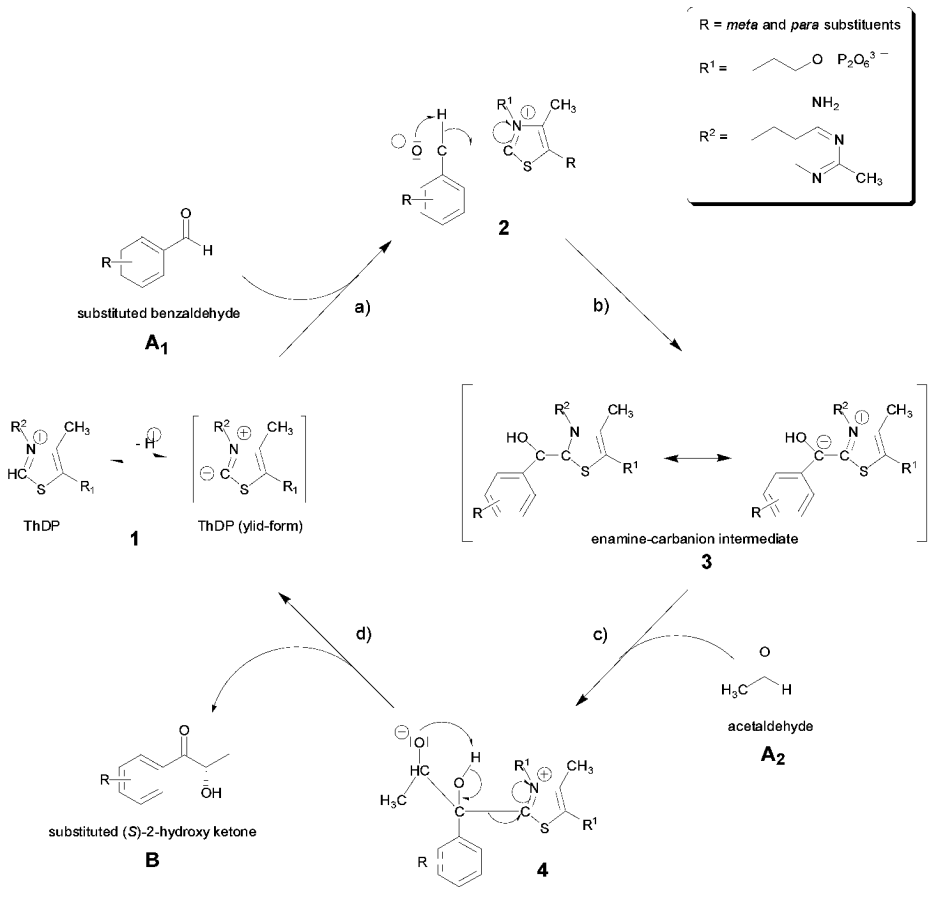

Figure 3.33: Reaction mechanism of the BFD-catalyzed carboligation.

System investigations

The results of kinetic investigations of the (*S*)-2-HPP (**B**) formation using aldehydes as substrates are shown in Figure 3.34. The enzyme activity as a function of the benzaldehyde concentration is in accord with a Michaelis-Menten-type kinetics, restricted by the solubility of benzaldehyde in aqueous solution (~50 mM). For acetaldehyde the initial rates were fit by the Michaelis-Menten double substrate kinetics (eq. 3-7) up to the maximum rate at a concentration of about 750 mM. Higher acetaldehyde concentrations lead to a decrease of the initial reaction rate, which might be interpreted in terms of substrate surplus inhibition or, more likely, by a rapid inactivation of the enzyme. The inhibition by surplus substrate of acetaldehyde ($\mathbf{A_1}$) was not taken into consideration, since concentrations of acetaldehyde ($\mathbf{A_1}$) no higher than 500 mM were applied. The kinetic parameters of the following double substrate Michaelis-Menten model were fitted to the data measured under initial reaction condition by means of a non-linear regression.

$$V = \frac{V_{max} \cdot [\mathbf{A_1}] \cdot [\mathbf{A_2}]}{(K_{M,\mathbf{A_1}} + [\mathbf{A_1}]) \cdot (K_{M,\mathbf{A_2}} + [\mathbf{A_2}])} \qquad \textbf{eq. 3-7}$$

The kinetic parameters calculated from Equation (eq. 3-7) are $K_{M,\mathbf{A_1}}$ = 77 mM (± 19 mM) for benzaldehyde and $K_{M,\mathbf{A_2}}$ = 310 mM (± 80 mM) for acetaldehyde, respectively. V_{max} was calculated to be 48 U mg^{-1} (± 10 U mg^{-1}). With an enzyme concentration of 0.087 µM, this corresponds to a turnover frequency[15] *tof* = 9 min^{-1}. The model represents the experimental data with a reasonable correlation of higher than 96% (Figure 3.34). However, in this case of using aqueous buffer for biotransformation V_{max} is only of theoretical value, because of the limited solubility of benzaldehyde under these conditions ($K_{M,\mathbf{A_1}}$ is greater than the maximal solubility of about 50 mM). No product inhibition by 2-HPP was observed.

[15] Turnover frequency *tof* is defined as the number of converted molecules per unit of time; *tof* = mole converted starting material / time / mole of catalyst.

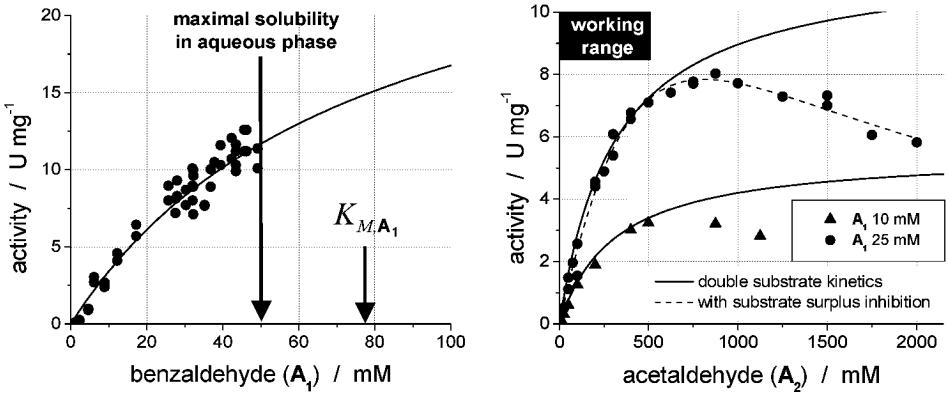

Figure 3.34: **Initial activity as a function of the concentrations of benzaldehyde (A_1, left) and acetaldehyde (A_2, right) (0.5 mM ThDP, 50 mM phosphate buffer, pH 7, 25°C, left: 500 mM A_2).**

By adding the mass balances (eq. 3-8) to the kinetic model (eq. 3-7), it is possible to simulate batch reactions (Figure 3.35). At the same time, this is proof of the applicability of the determined kinetic parameters.

$$\frac{d[\mathbf{A_1}]}{dt} = -v \cdot [cat]$$
$$\frac{d[\mathbf{A_2}]}{dt} = -v \cdot [cat] \qquad \text{eq. 3-8}$$
$$\frac{d[\mathbf{B}]}{dt} = v \cdot [cat]$$

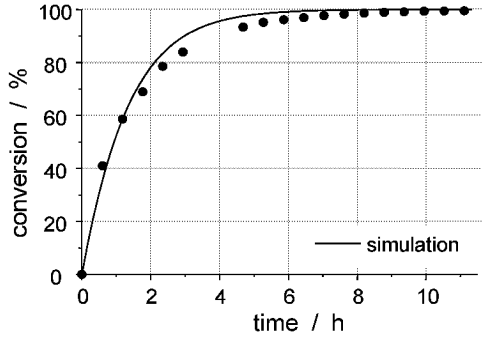

Figure 3.35: **Simulation of a typical batch reaction for the BFD-catalyzed carboligation to (*S*)-2-HPP (B) (12.5 mM benzaldehyde (A_1), 250 mM acetaldehyde (A_2), 0.5 mM ThDP, 50 mM phosphate buffer pH 7, 20°C, 0.6 U mL^{-1} BFD).**

The efficiency of the carboligation strongly depends on the temperature (Figure 3.36). The carboligation activity is enhanced by a factor of about 2 by raising the temperature from 25°C to 40-50°C. As activation energy for the carboligation of $\mathbf{A_1}$ and $\mathbf{A_2}$ to **B**, 45 ±2 kJ mol^{-1} has

been calculated, using the *Arrhenius* equation *[Arrhenius 1889]*. This is within the normal range of activation energies (20 – 60 kJ mol^{-1}) as reported for enzyme-catalyzed reactions in the literature *[Segel 1975; Wilcocks, Ward 1991]*.

The enantioselectivity of asymmetric C-C bond formations catalyzed by wild-type BFD can be influenced by three different parameters: temperature, benzaldehyde concentration, and electronic as well as steric properties of aromatic substituents on the donor aldehyde (**A_1**). As is evident from the literature, a number of methods have already previously been developed to improve the enantio- or regioselectivity of enzymes. The major ones comprise:

- Modification of the biocatalyst *[Reetz, et al. 2001]*.
- Selective change of the reaction conditions (temperature *[Pham, et al. 1989; Pham, Phillips 1990]*.
- Changing the solvent *[Carrea, Sergio Riva 2000; Klibanov 2001]*.
- Adjusting the pH *[Lam, et al. 1986]*).
- Modifying the substrate *[Lam, et al. 1986; Carrea, Sergio Riva 2000; Klibanov 2001; Reetz, et al. 2001]*.

It is well known that steric effects largely govern the enantioselectivity in asymmetric catalytic reactions; however, more recently, electronic effects originating from the substrate have also been found to influence the enantioselectivity *[Kunieda, et al. 1992; Zhang, et al. 1996; Moussou, et al. 1998; Watanabe, et al. 2001; Speare, et al. 2002]*.
Our kinetic investigations have shown for example that in the case of the C-C bond formation between benzaldehyde (**A_1**) and acetaldehyde (**A_2**)the enantioselectivity of the resulting (*S*)-2-HPP (**B**) depends on the temperature in an inverse manner, as demonstrated in Figure 3.36, right. It has to be mentioned that the lower optical purity obtained at higher reaction temperatures is a function of the enzyme selectivity rather than of the stability of (*S*)-2-HPP. Surprisingly, the enantiomeric excess of the resulting hydroxy ketone (**B**) is also increased, if the initial concentration of benzaldehyde (**A_1**) is lowered. The highest *ee* values (> 94%) were obtained using a low concentration of the donor substrate benzaldehyde (**A_1** < 1 mM) and performing the enzymatic coupling at low temperatures (4°C).

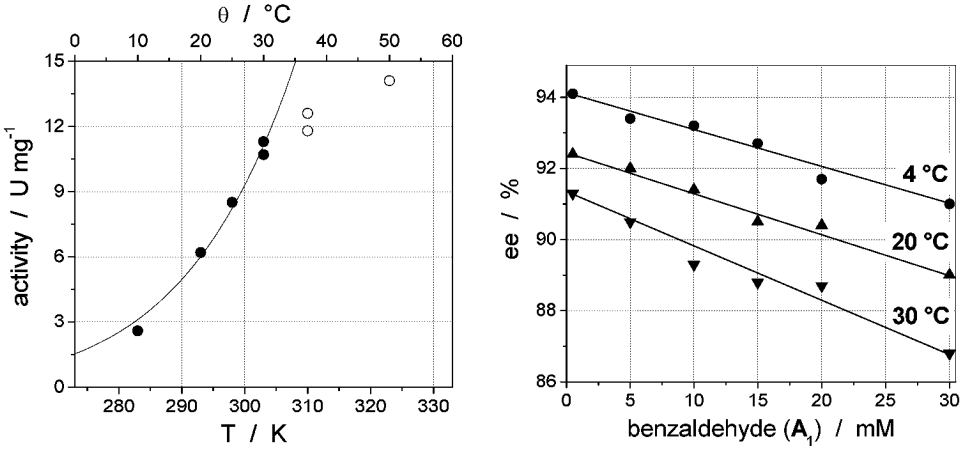

Figure 3.36: Influence of the temperature on the activity (left) and enantiomeric excess (right) of the carboligation of benzaldehyde and acetaldehyde to (*S*)-2-HPP (B) (500 mM acetaldehyde (A_2), 0.5 mM ThDP, 50 mM phosphate buffer pH 7, 6.4 U mL^{-1} BFD, left: 25 mM benzaldehyde (A_1)).

The transition states of the catalytic reaction were modeled[16] based on the X-ray crystallographic data published for wild-type BFD *[Hasson, et al. 1998]* with the benzaldehyde bound to the C-2 of the thiazole ring in thiamine diphosphate (Figure 3.33, **2**) *[Iding, et al. 2000]*. A model was developed for the two possible orientations of the enamine-carbanion intermediate (Figure 3.33, **2**) at the active site of BFD. These two possible orientations of **3** at the active site correspond to two conformations **X** and **Y** (Figure 3.37), which are considered to be in a kinetically controlled equilibrium with each other. In **X**, the phenyl ring of $\mathbf{A_1}$ is positioned between the two phenyl rings of Phe464 and Phe397, which are directed approximately perpendicular to each other, resulting in a stabilizing edge-to-face conformation frequently found in proteins *[Burley, A. 1985]*. By contrast in **Y**, the edge-to-face interactions are missing due to a different orientation of the phenyl ring of $\mathbf{A_1}$ attached to the C2-atom of the thiazole ring. Furthermore, the phenyl ring in **Y** gets into close proximity to His70, which results in higher steric strain; therefore, **X** is favored over **Y**. On the basis of these two conformations and assuming that catalytic processes occur only in the cavity restricted by Ala460, Phe464, His70, the protein backbone, and ThDP bound **3**, only four transition states during carboligation are conceivable theoretically, which result from *Re*- or *Si*-attack, respectively, on the acceptor $\mathbf{A_2}$ (Figure 3.37). The preferred orientation $\mathbf{X}_{Re}$ leads to (*S*)-2-HPP (**B**), whereas the unfavorable orientations $\mathbf{X}_{Si}$ and $\mathbf{Y}_{Si}$ are proposed to result in the formation of the minor enantiomer (*R*)-2-HPP. The two conformations **X** and **Y** are believed to be in a kinetically controlled equilibrium that can be shifted by temperature and the benzaldehyde concentration, resulting in different values of enantiomeric excess.

[16] Joachim Grötzinger, Institute of Biochemistry, RWTH Aachen, Germany, together with PD Dr. Martina Pohl, carried out the modeling.

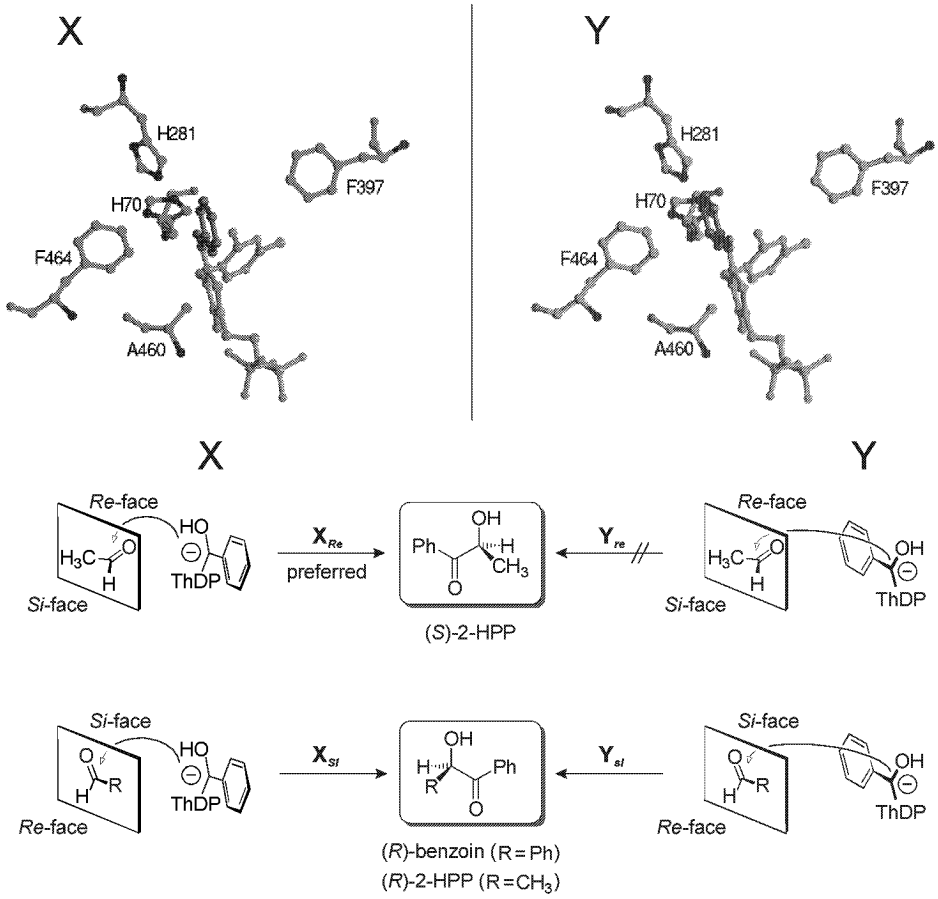

Figure 3.37: **The two possible orientations of the donor substrate-ThDP complex 3 in the active site of BFD: Computer-modeled complex based on crystallographic data (top) and schematic representation of the *Re*- and *Si*-attack of the carbanion-enamines X or Y *[Iding, et al. 2000]*.**

Aside from temperature and donor aldehyde concentration ($\mathbf{A_1}$) the enantioselectivity of the BFD-catalyzed carboligation is also influenced by the electronic as well as the steric properties of aromatic substituents on the donor aldehyde ($\mathbf{A_1}$). The range of compatible substrates for the BFD-mediated C-C-bond formation between $\mathbf{A_1}$ and $\mathbf{A_2}$ has been characterized *[Iding, et al. 2000]*. Different substituents in the *para*- and *meta*-position of the benzaldehyde demonstrate a broad range in the resulting enantiomeric excess of the carboligation products. We were able to demonstrate that in the case of *para*-substituents the enantiomeric excess rudimentary follows the *Hammett correlation* (Figure 3.38, left).

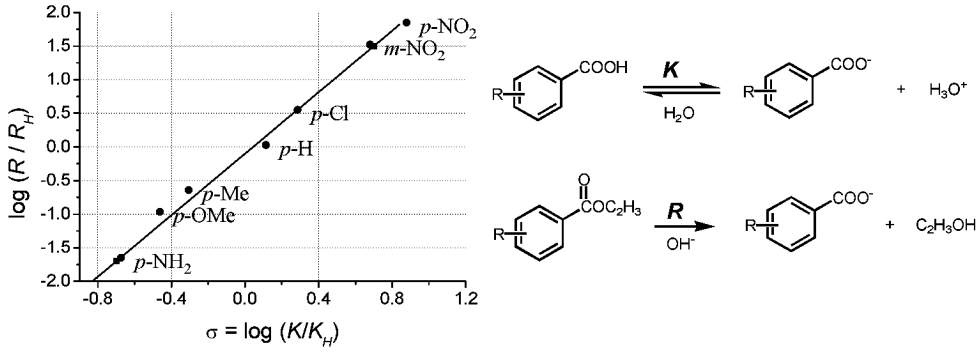

Figure 3.38: ***Hammett*** **correlation of the ratio of the dissociation constants of benzoic acids with rates of alkaline hydrolysis of benzoic esters** ***[Hammett 1937].***

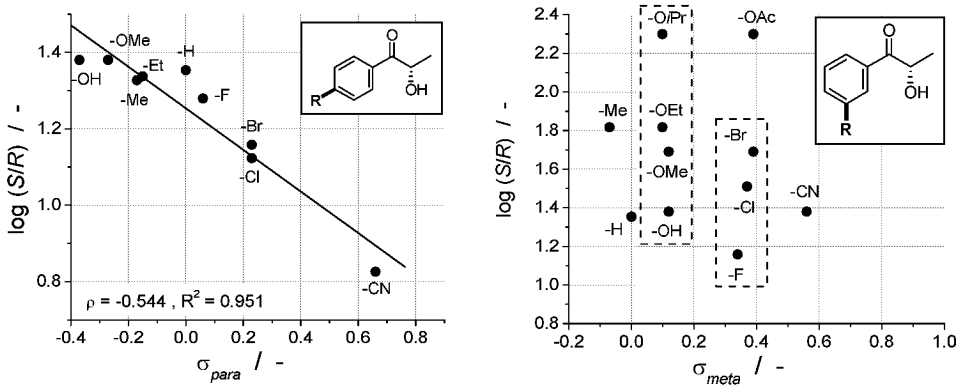

Figure 3.39: **Logarithm of the molar ratio of the enantiomers (*S*/*R*) of synthesized B as a function of the respective substituent constants σ_{para} (left) and σ_{meta} (right, dotted boxes indicate dominating steric parameters).** ***Hammett*** **parameters taken from** ***[Hansch, Leo 1979].***

The *Hammett* equation correlates the ratio of the dissociation constants of benzoic acids with the rates of alkaline hydrolysis of benzoic esters (Figure 3.38) *[Hammett 1935, 1937; Shorter 1985]*. In other words, it denotes the electronic properties of the different substituents when attached to aromatic moieties. In the case of the enantioselective carboligation catalyzed by wild-type BFD the logarithm of the molar ratio of *S*- to *R*-enantiomer can be correlated with the σ-constant of the *Hammett* equation (Figure 3.39) *[Hansch, Leo 1979]*. For the systems investigated here, this correlation is only satisfactory for *para*-substituted $\mathbf{A_1}$ in contrast to a seemingly random influence, if the substituents are in *meta*-position (Figure 3.39).

Log (*S*/*R*) is governed by the difference in the rates of formation of the *S* and *R* enantiomers, which in turn correlate with the electronic properties of the substituents according to the *Hammett* equation. We attribute the increase of *ee* observed for *para*-substituents (lower σ-values) to an increasing +I-effect resulting in an increase of the electron density in the

intermediate **3**. Increasing the electron density in the phenyl ring of $\mathbf{A_1}$ should lead to an increasing edge-to-face stabilization of **X**, which is a prerequisite for $\mathbf{X}_{Re}$-attack (or (*S*)-2-HPP formation). Moreover, a higher electron density would augment the nucleophilicity of the transitional **3**, facilitating nucleophilic attack of $\mathbf{X}_{Re}$, while at the same time increasing the repulsive forces for an $\mathbf{X}_{Si}$-attack.

The reason for the poor *Hammett*-correlation of the *meta*-substituents is most likely due to the close proximity of the substituents to the site of catalysis; i.e., the steric hindrance of the substituents prevails over possible electronic effects. It is conceivable that substituents in *meta*-position of $\mathbf{A_1}$ gradually limit the space in the catalytic cavity leaving $\mathbf{A_2}$ no other choice but to approach **3** as in $\mathbf{X}_{Re}$. More interestingly, the data for the *meta*-substituted case show how the *ee* increases with an increase of the size of a substituent for a given σ-value (Figure 3.39, right). Here, the *ee* is mainly determined by the steric constraints with almost no influence of electronic effects (see dotted boxes in Figure 3.39, right; substituents in increasing order of log (*S*/*R*) (or *ee*)):

$\sigma_{meta} \sim 0.37$: F < Cl < Br

$\sigma_{meta} \sim 0.10$: OH < OMe < OEt < O*i*Pr

Instead, the molar refractivity (*MR*) can be used to correlate the observed trend for the *meta*-substituents with parameters that account for the steric demand of the substituents. *MR* gives a reasonable linear correlation with log (*S*/*R*) (Figure 3.40).

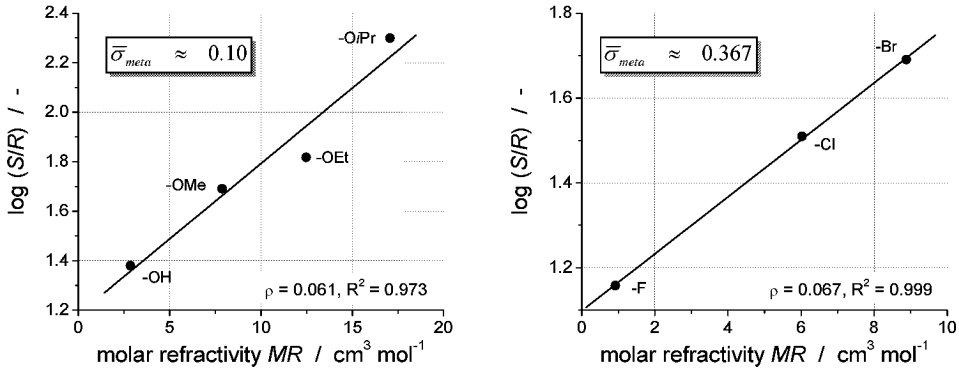

Figure 3.40: Plot of log (*S*/*R*) against the molar refractivity (*MR*) for substituents with similar electronic properties

In Equation eq. 3-9 describing the molar refractivity *MR*, the expression MW/δ stands for the molar volume (*MV*), which relates to the size of a substituent. The refractive index-related correction term $\frac{n^2-1}{n^2-2}$ in *MR* accounts for the polarizability of a substituent. Since the refractive index *n* varies only slightly for most organic compounds, the molar volume (*MV*) is often highly consistent with *MR [Kubinyi 1993]*.

$$MR = \frac{MW}{\delta} \cdot \frac{n^2 - 1}{n^2 - 2}$$ **eq. 3-9**

MR	$cm^3\ mol^{-1}$	molar refractivity
MW	$g\ mol^{-1}$	molecular weight
δ	$g\ cm^{-3}$	density
n	-	refractive index

The catalysis of benzoylformate decarboxylase is influenced by electronic as well as steric parameters. Even if the correlation in the *para*-case is not ideal, it shows at least a trend, and no significant strong influence of the steric parameters is observed. In the *meta*-case the opposite is true. Here a strong dependency on steric parameters is demonstrated, which can also be correlated via the molecular refraction. The *Hammett* correlation in the *para*-case should not be over interpreted, but the comparison of the *meta*- to the *para*-case provides predictive power and allows one to choose an appropriate substrate in order to achieve higher enantiomeric excess.

Continuous synthesis of (*S*)-2-hydroxy-1-phenylpropanone

Prior to establishing a production process for (*S*)-2-hydroxy-1-phenylpropanone (**B**), there are two points to be considered, which are an outcome of the investigations of the system as outlined above:

- High *ee* is reached at low temperature.
- High *ee* is reached at low benzaldehyde ($\mathbf{A_1}$) concentrations.

In view of reaching a high space-time yield, in general high concentrations are aimed at. Knowing the main characteristics of the three fundamental reactor types *[Bailey, Ollis 1986; Kragl, Liese 1999; Levenspiel 1999; Biselli, et al. 2002]*, the appropriate reactor can be chosen:

- Stirred tank reactor (str) or 'batch'.
- Plug flow reactor (pfr).
- Continuously operated stirred tank reactor (cstr).

As opposed to the stirred tank reactor, which is operated batchwise, the latter ones are operated continuously. The *stirred tank reactor* is operated in a non-stationary way (Figure 3.41, top). Stating ideal mixing, the concentration is the same in every volume element as a function of time. Starting up with a high starting material concentration, with advancing conversion $\mathbf{A_1}$ would be decreased and the product concentration **B** would be increased. A steady state is only reached at equilibrium conversion. In the *plug flow reactor* the starting material concentration $\mathbf{A_1}$ decreases slowly over the length of the reactor (Figure 3.41,

middle); therefore, the average reaction rate is faster than in the continuously operated stirred tank reactor. In each single volume element in the reactor the concentration is constant in the steady state. In other words, the dimension of time is exchanged with the dimension of place in comparison to the stirred tank reactor. Both reactors are not ideal for the above restrictions that apply here.

The *continuously operated stirred tank reactor* works under product outflow conditions, meaning that the concentrations in every volume element are the same as those at the outlet of the reactor (Figure 3.41, bottom). If the steady state is reached, the concentrations are independent on time and place. The conversion is controlled by the catalyst concentration and the residence time τ. This reactor is suited the best for the restrictions of this reaction system. In the steady state at high conversion only a low residual concentration of benzaldehyde $\mathbf{A_1}$ is yielded.

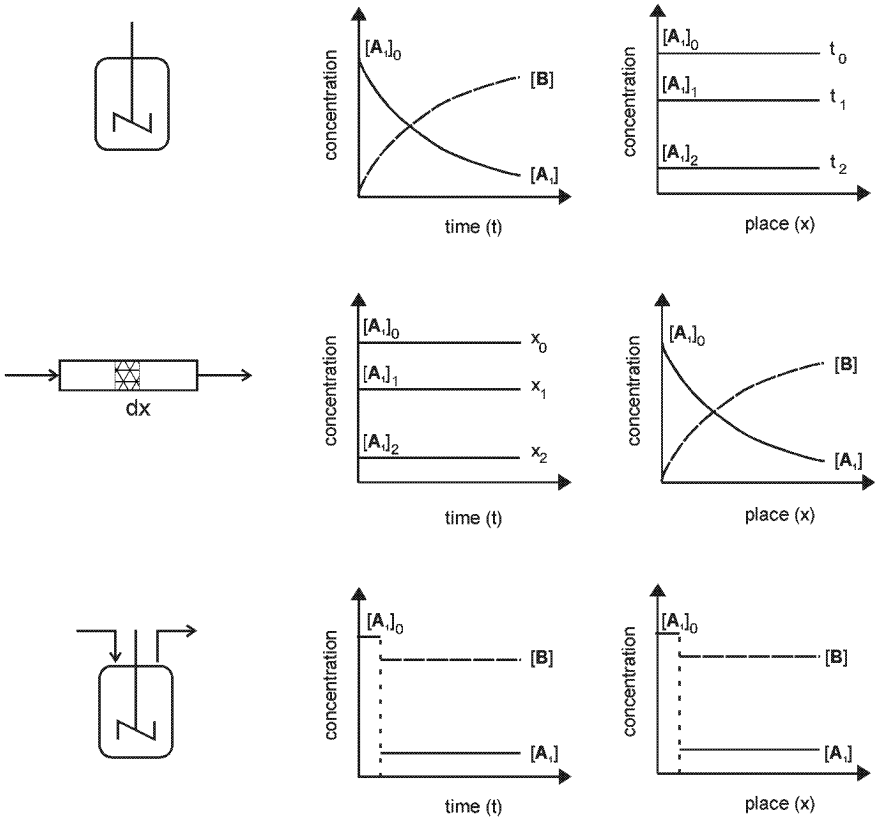

Figure 3.41: Fundamental types of reactors (from top to bottom: batch, pfr, cstr).

Therefore, a continuously operated stirred tank reactor (cstr) equipped with an ultrafiltration membrane (enzyme membrane reactor) was used. Since BFD was rapidly deactivated by stainless steel, polyether ether ketone is used as reactor material. The enzyme is also stable

versus polypropylene, but this material absorbs benzaldehyde. The ultrafiltration membrane retains BFD, whereas the substrates, products, and cofactors can pass the membrane. This permits the application of a high benzaldehyde concentration (**A_1**, 10 mM) at the inlet, which in case of 90% conversion results in an actual low concentration of 1 mM in the reactor. The conversion is controlled by the concentration of the enzyme and the residence time. The enzyme membrane reactor was operated continuously over a period of 180 h (Figure 3.42, left; data shown 0-90 h). (*S*)-2-HPP (**B**) was produced with an enantiomeric excess of 92.5% and a space-time yield of 34.2 g L^{-1} d^{-1}. By changing the reaction temperature of the cstr from 25°C to 17°C the influence of the temperature on the *ee* could be verified (Figure 3.42, right). In Figure 3.43 the space-time yield and enantiomeric excess are compared on the basis of the operation temperature of the cstr. As can be clearly seen, decreasing the temperature results in an increase of the *ee* and at the same time in a decrease of space-time yield because of a lowered enzyme activity with decreasing temperature. After recrystallization the *ee* was above 99 %.

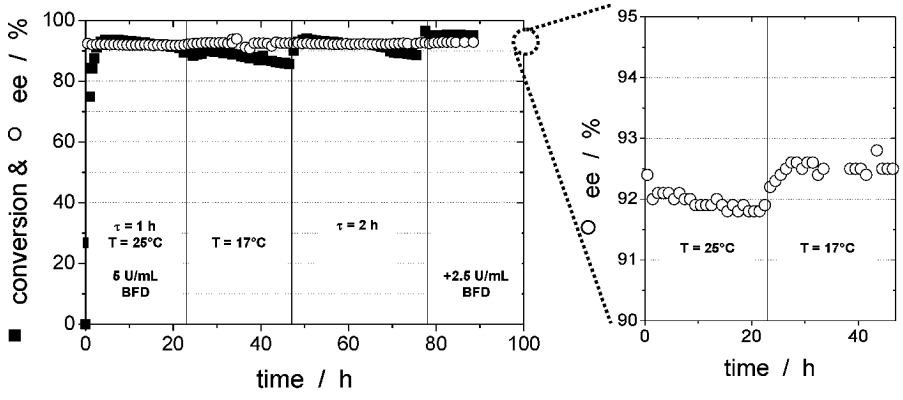

Figure 3.42: Conversion and *ee* as a function of time for a continuously operated membrane reactor operated at 25°C and 17°C (left). Right: Increase of *ee* upon lowering the temperature (10 mM benzaldehyde (A_1), 100 mM acetaldehyde (A_2), 4 mM ThDP, 0.5 mM $MgCl_2$, 50 mM phosphate buffer pH 7).

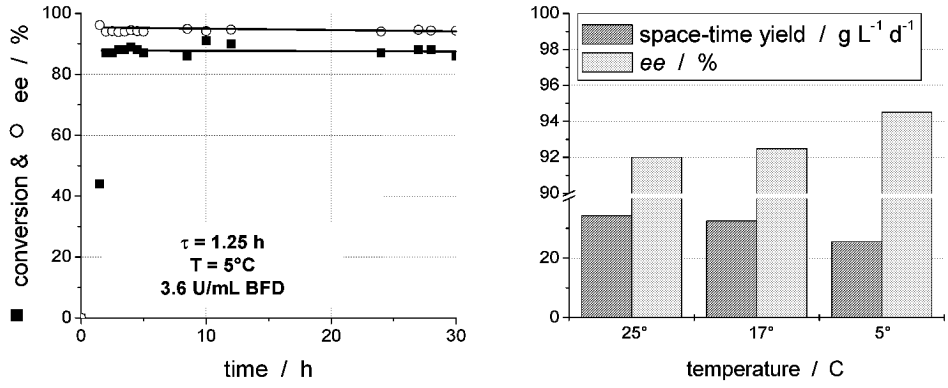

Figure 3.43: **Conversion and *ee* as a function of time for a continuously operated membrane reactor operated at 5°C (left). Comparison of space-time yield and *ee* for different temperatures (10 mM benzaldehyde (A_1), 100 mM acetaldehyde (A_2), 0.5 mM ThDP, 0.5 mM $MgCl_2$, 50 mM phosphate buffer pH 7).**

3.2.1.2 BAL catalyzed enantioselective carboligation to (*R*)-2-hydroxy-1-phenylpropanone

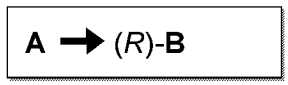

In contrast to the BFD-catalyzed carboligation, the reaction product of the BAL-catalyzed C-C bond formation is the enantiocomplementary compound (*R*)-2-hydroxy-1-phenylpropanone (2-HPP, (*R*)-**B**) that is formed with an *ee* > 99%. BAL catalyzes different reactions (Figure 3.44):

1. The carboligation of two benzaldehydes (**A_1**) to (*R*)-benzoin (𝔻).
2. The cleavage of (*R*)-benzoin (𝔻) to (*R*)-2-hydroxy-1-phenylpropanone ((R)-**B**).
3. The carboligation between benzaldehyde (**A_1**) and acetaldehyde (**A_2**) to (*R*)-2-hydroxy-1-phenylpropanone ((*R*)-**B**).

Additionally, also a racemic resolution can be catalyzed, if in reaction 2 racemic benzoin is chosen as starting material. (*S*)-Benzoin is not converted by BAL.

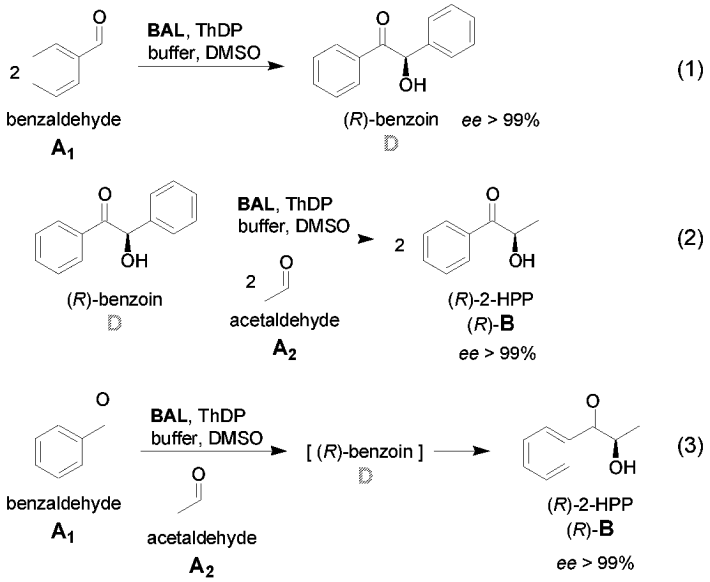

Figure 3.44: Different types of reactions catalyzed by BAL.

During the course of reaction 3 the formation of (*R*)-benzoin (**D**) is always observed (Figure 3.45, left). However, at the end of the reaction $\mathbf{A_1}$ is quantitatively converted to (*R*)-**B**. Nevertheless, it is not proven yet, if benzoin is formed as the first reaction step of the carboligation to (*R*)-2-HPP ((*R*)-**B**) or in a parallel reaction. The solubility of (*R*)-benzoin (**D**) is only 1.5 mM in the presence of 30 vol% DMSO. This is a crucial point to watch out for, since if this reaction were transferred to a continuously operated membrane reactor, precipitation of benzoin would cause blocking of the ultrafiltration membrane.

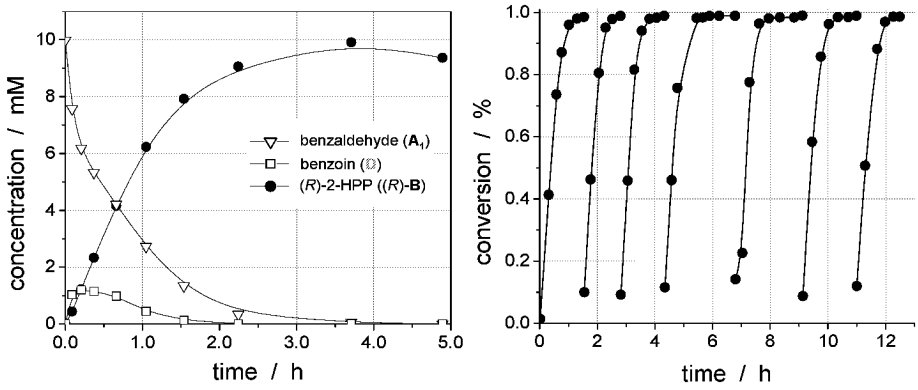

Figure 3.45: Batch conversion of benzaldehyde ($\mathbf{A_1}$) and acetaldehyde ($\mathbf{A_2}$) to (*R*)-2-HPP ((*R*)-B**) with benzoin (**D**) as transitional side product, left, and repetitive batch operation, right (10 mM benzaldehyde, 60 mM acetaldehyde, 30 vol% DMSO, 0.35 mM ThDP, 0.35 mM $MgSO_4$, 35 mM TEA buffer, pH 8.0, left: 3 U mL^{-1} BAL, right: 0.05 mg mL^{-1} BAL).**

As can be seen from the course of the repetitive batch experiment (Figure 3.45, right), BAL is a very stable catalyst. The initial reaction rate remains almost unchanged over 8 repetitive batches, and each time 100% conversion is reached. In analogy to the results with the BFD, here as well polyether ether ketone proves to be the best reactor material.

Because of the high stability and activity of BAL it is possible to run continuously operated reactors with a very small residence time of 6 or even 3 min. As a consequence very high fluxes are resulting in a 10 mL or 3 mL reactor. The standard design of an enzyme membrane reactor (EMR) incorporates a flat sheet membrane, in other words, a dead-end filtration is carried out *[Flaschel 1983; Cheryan 1986]*. To choose the right reactor size for very short residence times, the resulting membrane specific fluxes F need to be compared (Table 3.5).

Table 3.3: Volume-dependent reactor parameters:

Parameter	EMR 1		EMR 2	
volume / L	0.003	0.003	0.01	0.01
membrane area / m^2	0.00156	0.00156	0.00317	0.00317
residence time τ / h	0.05	0.1	0.05	0.1
membrane specific flux F / kg h^{-1} m^{-2}	38.5	19.2	63.1	31.5

At the same residence time, the EMR 1 (3 mL) has a lower membrane specific flux F, which means that a lower pressure drop is expected over the membrane. Therefore, EMR 1 was chosen. In the continuous experiment a conversion of 88% at a residence time of 6 min, respectively 75% conversion at 3 min, and an *ee* > 99.5% is reached. This correlates with a space-time yield (τ = 6 min) of 650 g L^{-1} d^{-1}, respectively a space-time yield (τ = 3 min) of 1,120 g L^{-1} d^{-1}. No benzoin precipitation was observed.

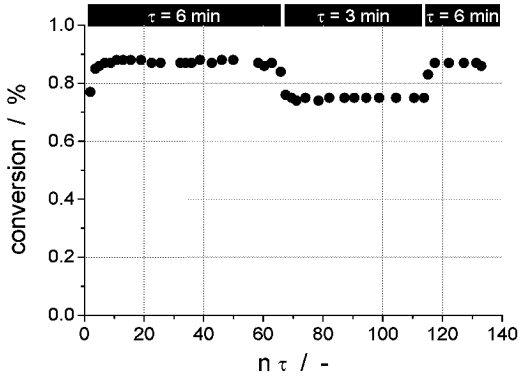

Figure 3.46: Continuous synthesis in the enzyme membrane reactor (20 mM benzaldehyde, 80 mM acetaldehyde, 30 vol% DMSO, 0.35 mM ThDP, 0.35 mM $MgSO_4$, 35 mM TEA buffer, pH 8).

One disadvantage of using DMSO as a cosolvent is the laborious 6-step downstream processing, resulting in a yellow oil or oily solid of ((*R*)-**B**). However, a cosolvent is needed to reach high conversion and to stabilize BAL *[Demir, et al. 2001]*. Up until now, it is only known that the enzyme tolerates up to 30 vol% DMSO or 15% polyethylene glycol (PEG 400). This was the motivation to carry out a screening of other organic solvents, which might be compatible with BAL. The storage stability of BAL in different two-phase systems was investigated at 5°C (Figure 3.47). Substituted ethers turned out to cause the lowest deactivation of BAL, especially methyl *tert*-butyl ether (MTBE) and diisopropyl ether performed rather well. Because of safety reasons MTBE was selected. In further investigations MTBE was used as cosolvent instead of DMSO. In a batch reaction, where the aqueous phase is saturated with MTBE, the same reaction rates and selectivities are reached, as it is the case in the system with 30 vol% DMSO.

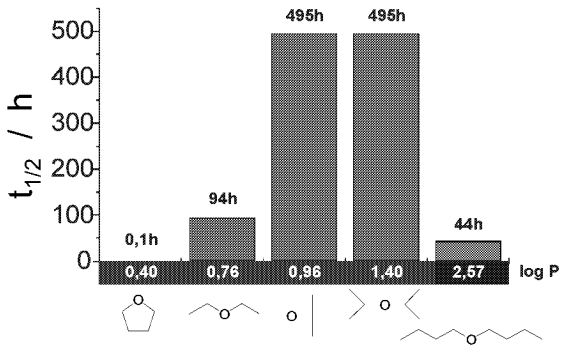

Figure 3.47: Storage stability of BAL in different aqueous-organic two-phase systems (5°C).

As can be seen from Figure 3.48 the two washing steps with water and brine can be omitted by using the MTBE saturated reaction solution. Additionally, a much cleaner product, a white solid instead of a yellowish oily solid is yielded. By this means 14.3 g (*R*)-2-hydroxy-1-phenylpropanone ((*R*)-**B**) with an *ee* > 99.5% could be isolated. Using this new protocol the downstream processing is much faster and more effective.

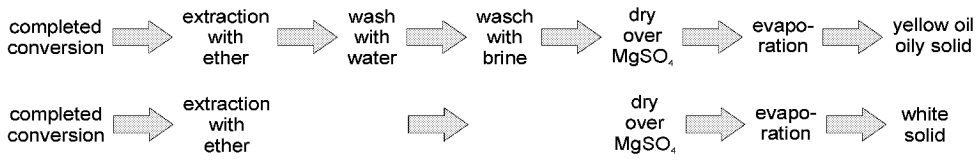

Figure 3.48: Comparison of downstream processing steps of a reaction solution with 30 vol% DMSO (top) and saturated with MTBE (bottom).

3.2.1.3 ADH-catalyzed enantioselective reduction to all stereoisomers of 1-phenylpropane-1,2-diol (C)

In this chapter the second step of the reaction sequence leading to vicinal diols is studied. For this purpose we screened secondary alcohol dehydrogenases that would accept both enantiomers of **B** (Figure 3.49) and reduce them diastereospecifically to the corresponding 1-phenylpropane-1,2-diols. We found the recombinant *Lactobacillus brevis* alcohol dehydrogenase (rec*Lb*-ADH, EC 1.1.1.2) *[Hummel 1997; Hummel 1999; Wolberg, et al. 2000]* to catalyze the reduction of the prochiral keto function of both (*S*)-**B** and (*R*)-**B**. Thereby an *S* configuration is being generated at the newly formed chiral center, leading to (1*S*,2*S*)-phenylpropane-1,2-diol [(1*S*,2*S*)-**C**], and (1*S*,2*R*)-1-phenylpropane-1,2-diol [(1*S*,2*R*)-**C**] respectively. An alcohol dehydrogenase from thermophilic *Thermoanaerobium species* (*Th. sp.*-ADH, EC 1.1.1.2) reduces the keto function of both (*S*)-**B** and (*R*)-**B** furnishing the *R* configuration at the newly formed chiral center of (1*R*,2*S*)-1-phenylpropane-1,2-diol [(1*R*,2S)-**C**] and (1*R*,2*R*)-1-phenylpropane-1,2-diol [(1*R*,2*R*)-**C**], respectively.

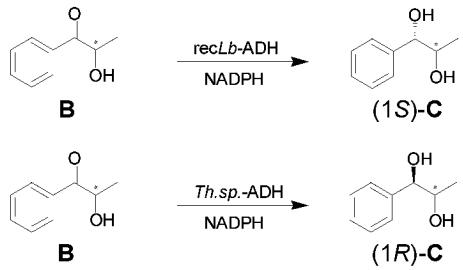

Figure 3.49: Enantioselective alcohol dehydrogenase (ADH)-catalyzed reduction of 2-HPP (B) to (1*S*)- or (1*R*)-1-phenylpropane-1,2-diol.

Both alcohol dehydrogenases used for the hydroxy ketone reduction are NADPH-dependent. In anticipation of a possible scale-up we decided to demonstrate the feasibility of an integrated cofactor regeneration system in an enzyme-coupled and a substrate-coupled approach (for a detailed explanation and discussion see ➲ chapter 4.4, page 161. When using *Thermoanaerobium sp.*-ADH for reduction at 40°C the regeneration of the cofactor was achieved with an excess (100-fold higher concentration) of 2-propanol in the substrate-coupled approach. The relatively high reaction temperatures of above 40°C required for sufficient activity when employing *Th.sp.*-ADH limits the alternatives for cofactor regeneration to the enzyme itself or other thermostable NADPH-dependent enzymes. A repetitive batch, employing a thermophilic hydrogenase from *Pyrococcus furiosus* for regeneration of the NADPH cofactor during the enantioselective reduction of (*S*)-**B** to (1*R*,2S)-**C**, is shown in ➲ Figure 4.32, page 133 *[Mertens, et al. 2002]*. The hydrogenase

utilizes molecular hydrogen as reduction equivalents. It must be pointed out, however, that at these relatively high temperatures the stability of the cofactor NADPH as well as of the enzyme is limited.

In the case of the reduction with rec*Lb*-ADH at 20°C it could be shown that both an enzyme- and substrate-coupled regeneration system are applicable. The advantage of the NADPH-dependent FDH (EC 1.2.1.2) *[Tishkov, et al. 1996; Tishkov, et al. 1999a]* system lies in the favorable equilibrium strongly shifted towards CO_2 and NADPH *[Shaked, Whitesides 1980]*. In addition, the CO_2 co-product can easily be removed and, compared to the 2-propanol-acetone system, does not inhibit the regeneration or reduction reaction, whereas acetone does. Table 3.4 summarizes the kinetic data for the reduction and preferred regeneration system.

Table 3.4: Kinetic parameters for the reduction and regeneration reactions.

Product	Kinetic parameters of the enzyme-substrate-pair under reaction conditions	System used for NADPH regeneration and selected kinetic parameters under reaction conditions
(1*S*,2*S*)-**C**	Reduction of (*S*)-**B** with rec*Lb*-ADH V_{max} = 1.50 ± 0.05 U mg^{-1} $K_{M,\,(S)\text{-}\mathbf{B}}$ = 2.36 ± 0.30 mM $K_{M,\,NADPH}$ = 0.41 ± 0.02 mM	FDH in the presence of 300 mM HCOONa V_{max} = 1.01 ± 0.08 U mg^{-1} $K_{M,\,HCOO^-}$ = 22.6 ± 3.1 mM $K_{M,\,NADP^+}$ = 0.23 ± 0.03 mM
(1*S*,2*R*)-**C**	Reduction of (*R*)-**B** with rec*Lb*-ADH V_{max} = 1.09 ± 0.05 U mg^{-1} $K_{M,\,(R)\text{-}\mathbf{B}}$ = 7.48 ± 1.10 mM	
(1*R*,2*S*)-**C**	Reduction of (*S*)-**B** with *Th.sp.*-ADH V_{max} = 1.35 ± 0.02 U mg^{-1} $K_{M,\,(S)\text{-}\mathbf{B}}$ = 0.1 ± 0.02 mM	*Th. sp.*-ADH in the presence of 100 mM 2-propanol V_{max} = 8.10 ± 0.18 U mg^{-1} $K_{M,\,2\text{-prop.}}$ = 3.4 ± 0.4 mM
(1*R*,2*R*)-**C**	Reduction of (*R*)-**B** with *Th.sp.*-ADH V_{max} = 0.90 ± 0.05 U mg^{-1} $K_{M,\,(R)\text{-}\mathbf{B}}$ = 0.21 ± 0.04 mM	

Fortunately, the specific activities of both ADHs towards the reduction of (2*S*)-**B** and (2*R*)-**B** are of the same order of magnitude. In consequence, we did not find a significant preferential reduction of one enantiomer of **B** by either ADH. Thus, all stereoisomers of the diol are equally well accessible. Moreover, a racemic resolution of **B** by selective reduction with the ADHs mentioned should not be possible.

3.2.1.4 Diastereoselective production of *vic*-diols with a reaction sequence

By combination of enantioselective lyases and enantioselective alcohol dehydrogenases it is possible to synthesize all four stereoisomers of 1-phenylpropane-1,2-diol (**C**) selectively

starting up from the bulk chemicals benzaldehyde (**A**$_1$) and acetaldehyde (**A**$_2$) (Figure 3.50). All four diastereomers of **C** have been synthesized with diastereoselectivities (*de*) > 98% and overall yields of > 80%. Utilizing wild-type BFD for carboligation, prior to the reduction step the enantiomeric excess needs to be increased by recrystallization from 94% to 99%.

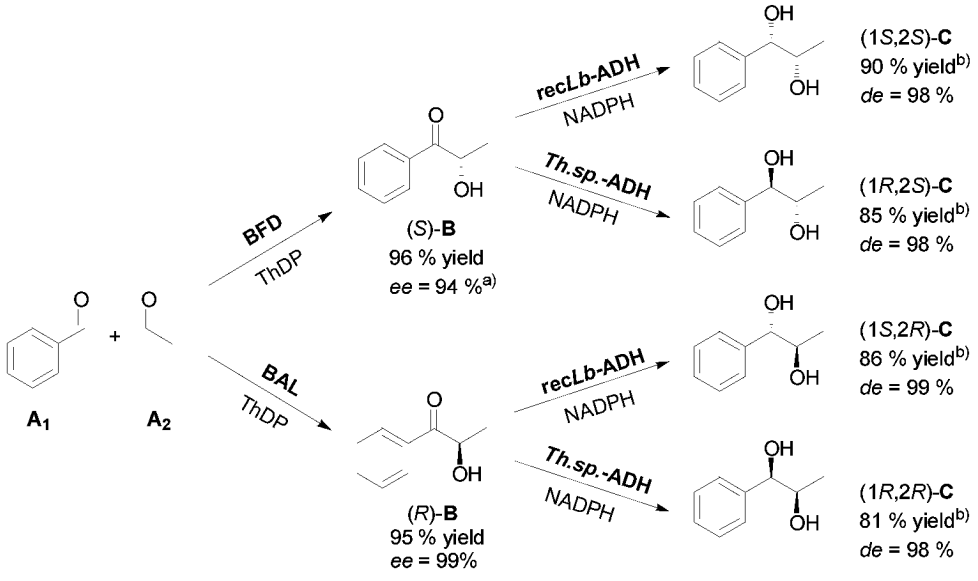

Figure 3.50: Enantio- and diastereoselective enzymatic synthesis of 1-phenylpropane-1,2-diol stereoisomers in a reaction sequence. [a] After crystallization ee > 99%; [b] yields of diols are given as overall yields for the 2 reaction steps.

A similar approach using pyruvate decarboxylase (PDC) as an alternative catalyst for the C-C bond formation is conceivable and has been shown to function for yeast cells containing PDC and alcohol dehydrogenases albeit with only the (1*R*,2*S*)-**C** as the major product being formed ((1*R*,2*S*)-**C** : (1*R*,2*R*)-**C** : (1*S*,2*S*)-**C** : (1*S*,2*R*)-**C** = 89 : 6 : 5 : 0) *[Mochizuki, et al. 1995]*. A problem that arises in a stepwise approach using purified PDC is the high susceptibility of the intermediate (1*R*)-hydroxy-1-phenylpropanone towards oxidation to the dione during work-up. Furthermore, to the best of our knowledge, the *S*-enantiomer is not yet accessible with high enantiomeric excess by this method *[Pohl, et al. 1998]*, making this approach unfavorable for diol syntheses.

To be able to apply the multicatalyst system efficiently, a continuous reactor set-up for the successive C-C bond formation and reduction reaction has been developed (Figure 3.51). In the first reaction vessel an ultrafiltration membrane retains BFD. Under the reaction conditions given in the legend to Figure 3.52 a converion of 85% regarding **A**$_1$ was reached in the first reaction vessel. The formed (2*S*)-**B** and an excess of acetaldehyde (**A**$_2$, 100 – 300 mM), which is needed because of the high K_M-value for acetaldehyde (310 mM) are found in the outlet of the first reaction vessel.

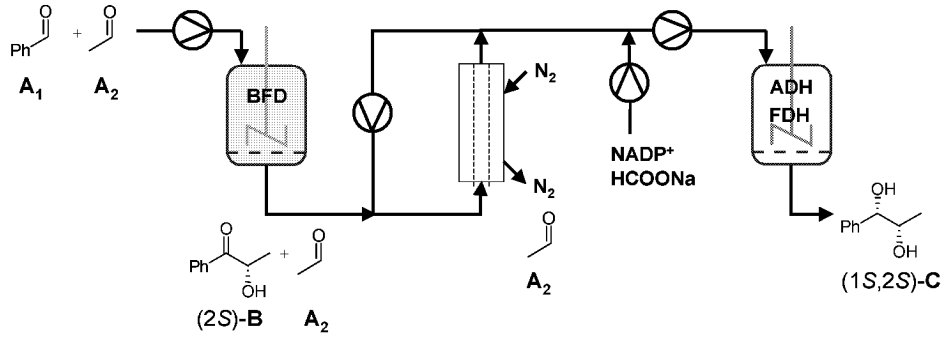

Figure 3.51: Flow scheme of the reactor for the sequential diol synthesis.

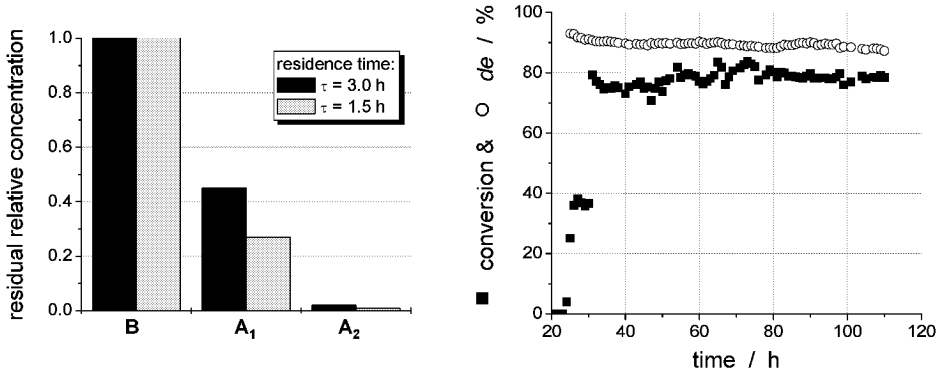

Figure 3.52: Extraction efficiency of the gas-liquid contactor, left, and course of conversion and *de* for the overall continuously operated process, right (left: Initial concentrations: 162 mM acetaldehyde, 2 mM benzaldehyde, 8 mM 2-HPP, 0.5 L min^{-1} N_2, 0.35 L min^{-1} circulation of reaction solution; right: 10 mM benzaldehyde, 200 mM acetaldehyde, 0.5 mM ThDP, 2.5 mM $MgSO_4$, 84 U mL^{-1} BFD, 10 mM NADP$^+$ and 3 M formate (feed rate 1 mL h^{-1}, resulting in 0.9 mM NADP$^+$ and 270 mM formate), 11.4 U mL^{-1} ADH, 4 U mL^{-1} FDH, 50 mM phosphate buffer, pH 7, 20°C).

Acetaldehyde (**A2**) is also a substrate for the ADH, which exhibits an increased specific activity (1,138 U mL^{-1}) by factor of 19 in comparison to that of (2*S*)-**B** (60 U mL^{-1}) at a comparable K_M-value. Therefore, acetaldehyde (**A2**) is separated inline by stripping with nitrogen in a membrane-based gas-liquid contactor. Benzaldehyde (**A1**, up to 45 % removal) and acetaldehyde (**A2**, up to 98 % removal) are selectively extracted in the presence of the intermediate hydroxy ketone (2*S*)-**B** (Figure 3.52, left). By this means the unspecific aldehyde reduction catalyzed by the ADH in the second reaction vessel is suppressed. To the depleted reaction solution NADP$^+$ and sodium formate is added prior to the second reaction vessel. By addition of NADP$^+$ at this late point, the residence time of the cofactor is reduced and its deactivation is lowered (Figure 3.52, right). In the second reaction vessel the enantioselective reduction of (2*S*)-**B** is catalyzed by rec*Lb*-ADH. The cofactor is regenerated by FDH. Because

of the application of the wild type BFD in this reactor system, the *ee* yielded for the intermediate (2*S*)-**B** is only 92% at 20°C. Therefore, the *de* was only 90% (ratio of (1*S*,2*S*)-**C** to (1*S*,2*S*)-**C** and (1*S*,2*R*)-**C** = 95:5). The enantioselectivity of the carboligation can be increased, if the new BFD mutant L476Q is applied, which yields an *ee* for (2*S*)-**B** of 96% under same conditions. Additionally, the K_M-value for acetaldehyde is reduced by a factor of approximately 3 in comparison to the wild type. At a residence time τ = 1 h in the first reactor and τ = 0.9 h in the second reactor, (1*S*,2*S*)-**C** is produced in the overall process with a space-time yield of 32 g L^{-1} d^{-1}.

3.2.1.5 Summary

- Transfer of the *1st biological principle*, namely *reaction sequences*, to technical asymmetric catalysis could be proven for the *in vitro* synthesis of *vic*-diols starting from bulk chemicals, i.e., benzaldehyde and acetaldehyde.
- All four stereoisomers of 1-phenylpropane-1,2-diol (**C**) have been synthesized with diastereoselectivities (*de*) > 98% and overall yields of > 80% in a reaction sequence, comprising an enantioselective carboligation and an enantioselective reduction.
- Applying physical organic principles like the *Hammett* postulate and using molar refractivity allows to predict the enantiomeric excess in benzoylformate dehydrogenase-catalyzed carboligations.
- (2*S*)-Hydroxypropiophenone was continuously produced by benzoylformate decarboxylase-catalyzed carboligation with an ee of 92.5% (25°C) and a space-time-yield of 34.2 g L^{-1} d^{-1}.
- (2*R*)-Hydroxypropiophenone was continuously produced by benzaldehyde lyase-catalyzed carboligation with an ee > 99% and a space-time-yield of 1,100 g L^{-1} d^{-1}.

3.2.2 Synthesis of polyols with *in vitro* multicatalyst systems[17]

Carbohydrates are polyols. They occur all over in nature and are produced by photosynthesis on the scale of approximately 200 billion tons per year *[Lindhorst 2000]*. This is one of the typical examples, how nature is applying reaction sequences in synthesizing complex structures. The main applications of polysaccharides in nature are scaffold materials, energy storage and water absorbent materials. Especially oligosaccharides promise to play an important role as drugs in future due to their role in biological recognition processes *[McAuliffe, Hindsgaul 1997; Alper 2001]*. The major fraction of the outer cell surface is covered by carbohydrates attached to lipids and proteins. They are thought of to play an important role in cell-cell interactions. Depending on the type of linkage to the lipids and proteins, these carbohydrate structures can be subdivided in N-glycans and O-glycans. O-glycans are in general attached to hydroxyl groups of certain amino acids, e.g. serine and threonine. They are further subdivided depending on the nature of the amino acid residue and the sugar group involved in the carbohydrate-protein linkage. In the following we are investigating the synthesis of different so-called core structures as subtypes of the mucin type O-glycans, where N-acetylgalactosamine (GalNAc) is linked to serine or threonine.

3.2.2.1 Optimizing the reaction selectivity

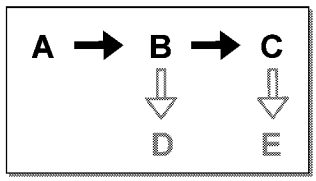

Core 2-based and core 3-based O-glycan structures play a key role in mucin-type O-glycosylation patterns *[Brockhausen 1995; Wilkins, et al. 1996; Varki, et al. 1999; Snapp, et al. 2001]*. These branched oligosaccharides attached to the respective protein backbone are involved in a variety of different biological processes *[Varki 1993]*. The core 2 trisaccharide is biosynthesized by the

[17] **Parts of this chapter are published in:**

1. G. Dudziak: *Reaktionstechnische Untersuchungen zur enzymatischen Glycosylierung von Peptiden, PhD-thesis*, University of Bonn, 1999
2. C. Hoh: *Optimierung der enzymatischen core2-Trisaccharid Synthese*, diploma thesis, University of Bonn, 1999
3. G. Dudziak, N. Bézay, T. Schwientek, H. Clausen, H. Kunz, A. Liese: *Cyclodextrin-assisted glycan chain extension on a protected glycosyl amino acid*; Tetrahedron 56 (32) (2000) 5865-5869
4. N. Bézay, G. Dudziak, A. Liese, H. Kunz: *Chemoenzymatisch-chemische Synthese eines (2-3)-Sialyl-T-Threonin-Bausteins und dessen Einsatz in der Synthese der N-terminalen Sequenz von Leukämie-assoziierten Leikosialin (CD34)*; Angew. Chemie 113 (12) (2001) 2350-2352; Angew. Chem. Int. Ed. 40, (2001) 2292-2295
5. C. Hoh, G. Dudziak, A. Liese: *Optimization of enzymatic synthesis of O-glycan core 2 structure by use of a genetic algorithm*; Bioorganic & Medicinal Chemistry Letters 12 (7) (2002) 1031-1034
6. N. Brinkmann, M. Malissard, M. Ramuz, U. Römer, T. Schumacher, E. G. Berger, L. Elling, C. Wandrey, A. Liese: *Chemo-enzymatic synthesis of the Galili epitope Galα(1→3)Galβ(1→4)GlcNAc on a homogeneously soluble PEG polymer by a multi-enzyme system*; Bioorganic & Medicinal Chemistry Letters 11 (2001) 2503-2506

enzyme family of the β1,6-GlcNAc transferases (GlcNAcTs) (Figure 3.53).

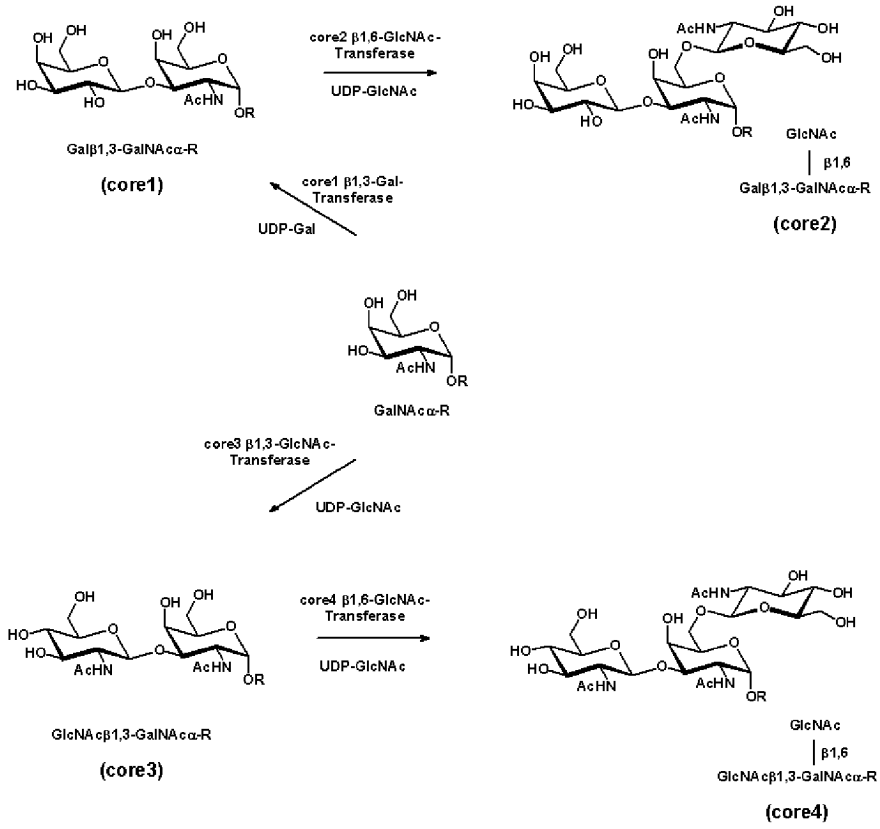

Figure 3.53: The core structures core 1 to core 4 (R = protein).

So far, three homologous GlcNAcTs have been cloned and characterized *[Bierhuizen, Fukuda 1992; Schwientek, et al. 2000]*. Since the acceptor substrate of all these enzymes for the synthesis of the core 2 trisaccharide is the core 1 [Gal-β1,3-GalNAc-α1-OR] disaccharide, several approaches have been undertaken for its synthesis *[Hedbys, et al. 1989; Fernández-Mayoralas 1997; Suzuki, et al. 1997]*. Despite the very recent cloning and expression of the cDNA of the appropriate β1,3-galactosyltransferase *[Canfield, et al. 2001]*, the use of a β–galactosidase from bovine testes proved to be a potent alternative method for generating this structure. Several approaches using this enzyme effectively have been made including the combined use of the β-galactosidase with a sialyltransferase in order to avoid product hydrolysis *[Kren, Thiem 1995; Gambert, Thiem 1999]* or the use of over-saturated solutions of the donor molecule *[Lio, Thiem 1999]*.

The intention of our work was to optimize the two-step reaction sequence leading to the core 2-Bn (**C**, Figure 3.54) in such a way that the secondary hydrolysis of the core 2-Bn (**C**)

by the β-galactosidase is discriminated and the formation of the undesired core 6-Bn (**E**) is avoided.

In the first step of this reaction sequence the core 1-Bn (**B**) is formed by transfer of the galactose residue from the lactose (donor) on the GalNAc-α1-OBn acceptor (**A**). This step is catalyzed by the β-galactosidase. In the consecutive reaction core 2-Bn (**C**) is then formed by transfer of the N-acetylglucosamine (GlcNAc) residue from UDP-GlcNAc to the core 1-Bn (**B**) by GlcNAcT. Eventual transglycosylation products other than core 1-Bn formed by β-galactosidase catalysis (e.g. 1,4-linked disaccharides) are not accepted by GlcNAcT.

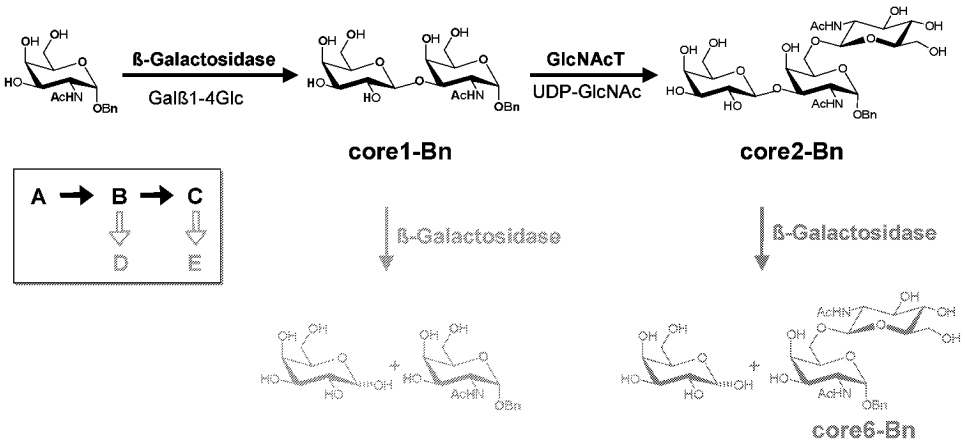

Figure 3.54: Synthesis of the core 2 trisaccharide in a reaction sequence catalyzed by β-galactosidase and recombinant β-1,6-GlcNAc transferase (GlcNAcT). Side reactions are introduced by the non-regioselective β-galactosidase from bovine testes leading to galactose, GalNAc-α1-OBn and core 6-Bn.

The undesired secondary hydrolyses of the core 1-Bn (**B**) and the core 2-Bn (**C**) are catalyzed by the β–galactosidase to form the core 6-Bn (**E**) and the GalNAc-α1-OBn (**D** = **A**), respectively. Calf intestine alkaline phosphatase (CIAP; EC 3.1.3.1) was added as a third enzyme in order to overcome inhibition of GlcNAcT by UDP, cleaved in the GlcNAcT reaction step.

Because of the high complexity of the reaction system due to many cross inhibitions and the poor regioselectivity of the β-1,3 linkage by the β-galactosidase *[Hedbys, et al. 1989; Fernández-Mayoralas 1997]* the optimization of this synthesis was carried out by means of a non-model based 'black-box' optimization method.

3.2.2.2 Genetic algorithm as tool for optimization of multi parameter systems

One of the most effective techniques for empirical optimization of multi parameter non-linear

systems (black-box systems) is the use of genetic algorithms (GAs) *[Goldberg 1989]*. This optimization strategy is based on the principles of evolution and was developed by Holland between 1962 and 1975 *[Holland 1975, 1992]*. GAs provide a robust tool for optimizing systems that are difficult to predict or whose parameters cannot be identified. This renders the GAs principle an attractive concept for optimizing complex systems. GAs-type algorithms have been used in many different approaches, such as optimization of fermentation media *[Weuster-Botz, et al. 1995; Weuster-Botz, Wandrey 1995]*, optimization of aqueous two-phase extractions *[Selber, et al. 2000]*, reaction engineering of enzymatic syntheses *[Uhlenbrock 1994]*, and on-line optimization of fermentation conditions *[Moriyama, Shimizu 1996]*. Furthermore, GAs permit the easy handling of complex data and the optimization of noisy systems. In contrast to gradient methods, their application is independent upon the choice of the starting point and can be used to cover the entire parameter space. They are thus able to determine global maxima independent of the starting conditions, thereby avoiding to get stuck on local maxima *[Ablay 1987; Goldberg 1989]*.

The basics for genetic algorithms were already laid in 1953 by the two biochemists *Watson* and *Crick*, when they published their results and assumptions regarding the structure and function of desoxyribonucleinic acid (DNA) *[Watson, Crick 1953]*. The complete information contained in the DNA is encoded via the 4 different bases adenine (A), thymine (T), cytosine (C) and guanine (G). The genetic structure of each individual is defined on the basis of this code (genotype), which then determines the appearance / look of each individual (phenotype) (Figure 3.55).

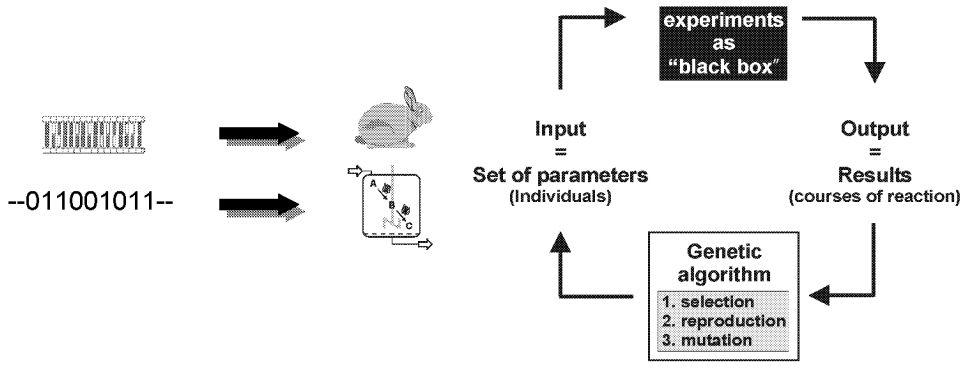

Figure 3.55: Left: Geno- and phenotype of individuals; right: principle of genetic algorithm.

Like nature, the genetic algorithm differentiates between a genotype and a phenotype. Thus, it is possible to encode selected parameters into binary bit strings and thereby simplify the data handling procedure. Very simple bit strings can represent difficult and highly complex structures. Once the data are encoded, it is very easy to perform all of the genetic operations that exist in nature (selection, crossover, and mutation). Important parameters for the program

are the number of individuals per generation, the crossing rate (which is the probability that two individuals exchange their genes, a much faster method for overall improvement compared to mutation), and the mutation rate (which represents the probability of a point mutation in one bit of a chromosome). Selection (survival of the fittest) determines which individuals survive and may thus reproduce to form the basis of the next generation. By this method, successful traits in individuals are passed along and are optimized over the course of generations. The flow chart shown in Figure 3.56 illustrates the steps carried out for the entire optimization procedure.

A general optimization procedure based on the genetic algorithm is exemplified by the following:

1. Initially, one set of **experiments** (individuals) is carried out (= 1 generation). The results of the experiments are compared and evaluated in respect to previously determined selection criteria.
2. To illustrate the **selection**, one can imagine a wheel of fortune, where the most successful experiment represents the largest area, and the worst one the smallest. Now the wheel of fortune is turned twice, and two new "parent" strings are selected.
3. Then these two parent strings are crossed over, and equal parts of the strings are exchanged in a process called **crossing over**.
4. To prevent that the evolution is restricted to local areas, punctual **mutations** are allowed, enabling new experimental conditions that were not investigated yet.
5. (= 1.) A new generation with new experimental conditions (individuals) as established in steps 1 – 4 is started.

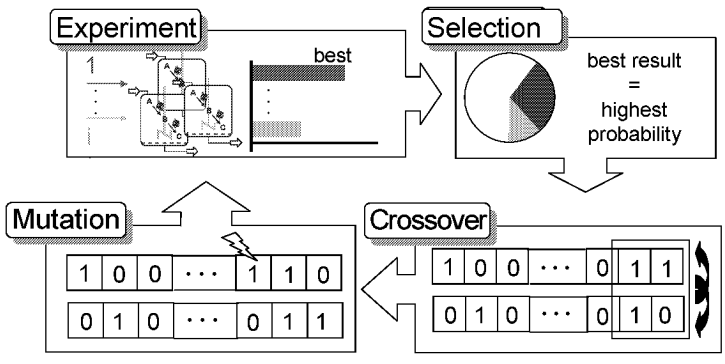

Figure 3.56: Principle of the genetic algorithm.

The probability of crossing over and mutation are fixed prior to the start of the algorithm. It is important not to limit the system at this stage, neither in the range of parameters nor in the step widths. If in doubt, it is advisable to use a large separation parameter space rather than to exclude a possible optimum, which could have been found. On the other hand, a wide parameter range in combination with small steps will dramatically increase the number of possible experiments. Another consideration for choosing the correct balance of freedom and constraint is the number of experiments possible. As a rule, the number of individuals per generation should be at least equal to the number of bits needed to encode the genes of those individuals.

3.2.2.3 Optimization of the core 2 trisaccharide synthesis

In Figure 3.57 a batch transformation of the above-described reaction sequence is outlined *[Dudziak, et al. 1998]*. The main product is core 6-Bn (E), which is the hydrolyzed side product of the core 2-Bn (**C**) structure. Therefore, the aim of this work was to find reaction conditions suitable for generating the desired product core 2-Bn (**C**) in high concentration and with high selectivity.

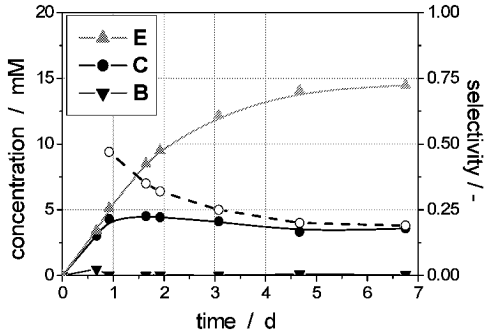

Figure 3.57: **Synthesis of core 2-Bn via a biocatalytical reaction sequence *[Dudziak 1999]*.** [0,5 M Lac; 20 mM GalNAc-Bn; 25 mM UDP-GlcNAc; 250 mU/mL galactosidase; 50 mU/mL GlcNAcT; 10 U/mL CIAP; 50 mM MES; pH 6; 37°C].

To optimize this reaction sequence the above-described genetic algorithm was applied. The GA calculations were carried out using the GALOP[18] software, version 2.20, which was developed at the Institute of Biotechnology 2 (Forschungszentrum Jülich GmbH, Jülich, Germany) *[Möllney, et al. 1993]*. The following two selection criteria were chosen with a weighting of 1:1:

[18] GALOP: *genetic algorithm for the optimization of processes*

1. Maximum core 2-Bn (**C**) concentration,
2. high selectivity of core 2-Bn formation at the point of the maximum product concentration, expressed as the ratio $\frac{C_{core\ 2-Bn}}{C_{core\ 6-Bn}}$.

After choosing the selection criteria, parameters were to be identified, which might have an influence on the reaction system. In total, 7 parameters were varied throughout 4 generations of optimization. The respective parameters and their range of variation are summarized in Table 3.5:

Table 3.5: Parameters and their range of variation[19]:

Parameter	Dimension	Range of Variation	Stepwidth (#)
GalNAc-Bn	mM	10-40[a]	10 (4)
lactose	mM	100-800	100 (8)
UDP-GlcNAc	mM	10-40	5 (7)
β-galactosidase	mU/mL[b]	250-1000[b]	125 (7)
C2GnT	mU/mL[b]	50-250	50 (5)
pH	-/-	5.0-7.5[c]	0.5 (6)
temperature	°C	10-50	10 (5)

[a] Maximal solubility of GalNAc-Bn is slightly over 40 mM.
[b] Enzyme activities of the experiment in Figure 3.57 were selected as the lowest value, because the reaction sequence should be accelerated.
[c] Maximal range of MES-buffer.

The concentration of the alkaline phosphatase was not varied, since it was used in excess relative to its activity to prevent any inhibition by UDP. Likewise, no parameter was assigned to the concentration of the applied MES-buffer (50 mM), since prior investigations had shown that the GlcNAcT exhibits its highest activity in this buffer *[Dudziak 1999]*. The values of the different parameters are encoded in the binary system (Figure 3.58). The resulting string is named a gene. For example: For GalNAc-Bn there are 4 possible parameter values allowed, resulting in a 2 bit string (4 = 2 • 2); in the case of lactose 8 different parameter values are allowed resulting in a 3 bit string (8 = 2 • 2 • 2). The whole string for all parameters consists of 20 bits. In total there are 235 200 different experiments possible[20], which are encoded.
The program GALOP allows for different methods, in which way the best individuals from one generation are transferred to the next one. The method applied here is called "*keep best,*

[19] All reactants of interest were quantified by HPLC analysis (conditions: Aminex HPX-87-H column, 6 mM H_2SO_4, 0.6 mL/min, T = 65 °C, UV-detection at λ = 195 nm, typical retention times: GalNAc-α1-OBn = 33.5 min, core 1-Bn = 19.1 min, core 2-Bn = 13.5 min, core 6-Bn = 20.4 min).
[20] 235 200 = 4 • 8 • 7 • 7 • 5 • 6 • 5

ball-bearing". This method ensures that the best individuals in regard to the selection criteria are transferred unchanged into the next generation. As a consequence, the best genes of one generation are not lost. This is of special relevance, if all successors and mutants of one generation are worse than their parents. Additionally, this method permits the proof of the (experimental) reproducibility. The crossing over rate was set to 0.95, which means that 95% of all individuals are crossing their genome. The mutation probability was set to 0.05, resulting in one mutation per string as a mean value. Each generation consisted of 14 experiments (individuals), with twice double the amount of parameters to be varied.

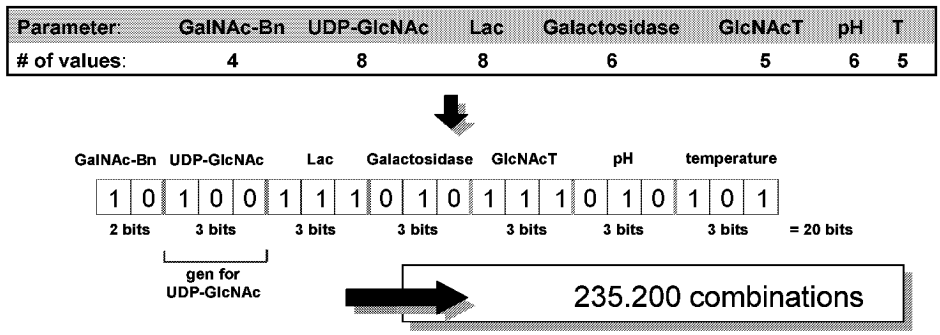

Figure 3.58: One string is encoding one possible phenotype, which equals one set of reaction parameters for the synthesis of core 2-Bn.

3.2.2.4 Results of the optimization

After four generations of optimization in a total of 56 from 235 200 possible experiments, the genetic algorithm found two local maxima regarding the selection criteria. The individuals of a fifth generation did not leave any hope to expect any more improvements and were therefore discarded.

To judge the success of an optimization two values are most interesting:

1. Development of any best individual per generation.
2. Development of the whole population of one generation, expressed as *total fitness*.

The developments for both selection criteria are shown in Figure 3.59. The results of the first generation are astonishingly good. The respective best individuals are not reached again until in the fourth generation. This observation needs to be explained. Because of the applied method *keep best, ball-bearing* is the best individual transferred unchanged to the following generation. But as can be seen from Figure 3.59, the same experiments have led to different results. This is because of an inadequate pH control during the first generation, a shortcoming, which that was solved from the second generation onwards.

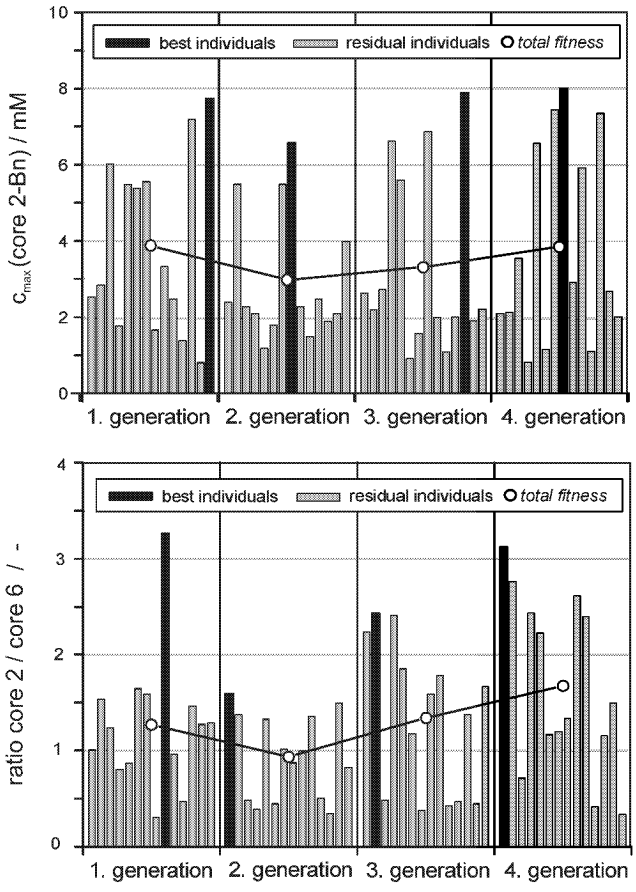

Figure 3.59: Development of all individuals as well as of the *total fitness*.

In regard to the two selection criteria the following maxima were found:

- The **maximum concentration of the core 2-Bn** trisaccharide reached was 8 mM. Although this product concentration corresponds to a yield of only 27%, the selectivity of the core 2-Bn formation (**C**) at this point was 55%. Compared to *Dudziak [Dudziak, et al. 1998]* the concentration of core 2-Bn could be doubled under these conditions (see Figure 3.60 left).

- The individual showing the **highest ratio core 2-Bn / core 6-Bn** for core 2-Bn formation (**C**) generated the desired trisaccharide in a maximum concentration of 2.1 mM, corresponding to 74% selectivity at the point of maximum product concentration and a yield of 21% (see Figure 3.60 right).

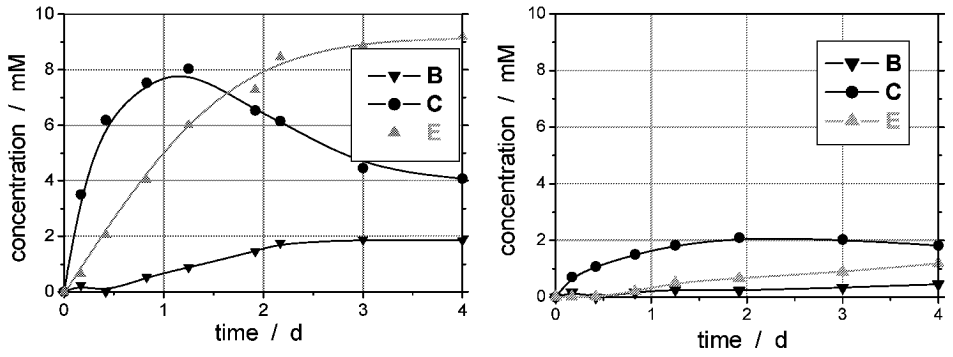

Figure 3.60: **Best individuals regarding maximal concentration of core 2-Bn (left) and ratio core 2-Bn / core 6-Bn (right).**
[max. core 2-Bn: 0.5 M Lactose, 30 mM GalNAc-Bn, 30 mM UDP-GlcNAc, 10 mM $MgCl_2$, 250 mU/mL β-galactosidase, 150 mU/mL C2GnT, 10 U/mL calf intestine alkaline phosphatase, 0.5 mg/mL BSA, MES buffer 50 mM, pH 6.5, 30°C
ratio core 2-Bn / core 6-Bn: 0.6 M Lactose, 10 mM GalNAc-Bn, 10 mM UDP-GlcNAc, 10 mM $MgCl_2$, 375 mU/mL β-galactosidase, 150 mU/mL C2GnT, 10 U/mL calf intestine alkaline phosphatase, 0.5 mg/mL BSA, MES buffer 50 mM, pH 6.5, 10°C].

Depending on the selection criteria, different values of the relevant parameters turned out to be ideal. Regarding the criteria of high product concentration, a reaction temperature of 30°C is optimal. In contrast, a high selectivity for the core 2-Bn concentration (**C**) could exclusively be found at 10°C, although low temperatures lowered the product concentration drastically.
For both criteria of selection, a pH value of 6.5 was found to be best choice. Compared to the system of *Dudziak [Dudziak, et al. 1998]* suitable for generating the core 6-Bn disaccharide (E), this value obviously marks the optimum conditions for core 2-Bn formation (**C**) considering both activity and stability of the β-galactosidase and GlcNAcT.
Not surprisingly, high lactose concentrations were found to be crucial for high product concentration and high product selectivity. The donor molecule of the β-galactosidase for generating the core 1-Bn disaccharide must be present in high excess, since hydrolysis of lactose is much faster than the respective transglycosylation reaction yielding the substrate for GlcNAcT.
To generate high product concentrations *and* high selectivities for core 2-Bn formation, the optimal GlcNAcT-concentration was found to be 150 mU/mL. This finding is rather unexpected since one might predict high amounts of GlcNAcT for fast and selective core 2-Bn synthesis. However, the highest enzyme level allowed for GA was set to 250 mU/mL, but this enzyme concentration proved to be inappropriate for effective core 2-Bn synthesis.
Since a system generating selectively the desired trisaccharide core 2-Bn (**C**) will have to discriminate the secondary hydrolysis of core 6-Bn (E) and core 1-Bn (**B**), respectively, the optimal β-galactosidase activity is expected to be rather low. In fact, the best two individuals regarding the selection criteria (Figure 3.60) both showed values for the β-galactosidase at the

very lower limit of this parameter namely 250 and 375 mU mL^{-1}, respectively.
In summary, we could show that optimization of a complex multi-enzyme system generating different O-glycan core structures can be achieved by using the method of a genetic algorithm. The selectivity for the core 2-Bn trisaccharide formation at the point of maximum product concentration has been doubled relative to the results of *Dudziak* et al., i.e., from 34% *[Dudziak, et al. 1998]* to 74% (Figure 3.60 left).
As an appropriate reactor type (➲ Figure 3.41, page 59) for this multicatalyst system qualifies a batch or as a continuous version the plug flow reactor. A cstr would not be appropriate, because in this reactor type the concentration of the final product (**C**) will always be the highest one. Instead, in a batch reactor the concentration of (**C**) is slowly increasing during the course of the reaction.

3.2.2.5 Comparison to synthesis with two separated reaction steps

The effectiveness of the reaction sequence for the synthesis of core 2-Bn becomes obvious, if this sequence is compared to an arrangement, where both reaction steps *[Dudziak 1999]* are carried out separately. As reaction conditions for both separate steps those were chosen, which individually yield the highest activity of the respective biocatalyst. It turns out that the yield of core 2-Bn (**C**) is higher in the reaction sequence catalyzed by the multicatalyst system than when carrying out both steps separately. The reason for this behavior is the otherwise only low yield of core 1-Bn (**B**), the product of the transglycosylation catalyzed by the β-galactosidase (Figure 3.61).

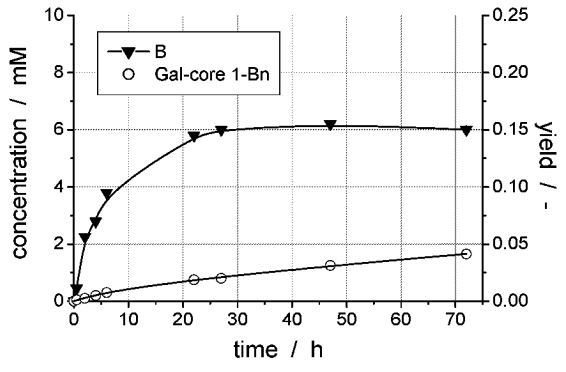

Figure 3.61 **Separate biotransformation of only first step.**
[40 mM GalNAc-Bn, 600 mM lactose, 100 mU/mL β-galactosidase, citrate-buffer, pH = 4.3, T = 37°C].

The maximal yield is 15%. Furthermore, a small amount of an additional side-product, Gal-core 1-Bn (○), is formed. This by-product is synthesized as well as core 1-Bn in a transglycosylation reaction, but by contrast to the latter one, here core 1-Bn itself acts as a glycosyl acceptor. As a consequence, even when assuming a quantitative conversion in the GlcNAcT-catalyzed step, a maximal overall yield of only 15% is reachable in the multicatalyst system. The first step is the yield limiting one, if the reaction system is carried out in two separate steps; therefore, application of this multicatalyst system as a reaction sequence is more effective than the separation of both reaction steps.

3.2.2.6 Overcoming problem of secondary hydrolysis by designing new reaction cascade[21]

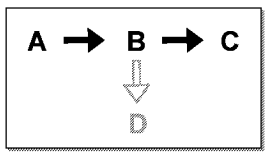

The problem of the secondary hydrolysis of product **C** can be overcome, if the structure of **C** is altered in such a way, that it is not any more a substrate for the first biocatalyst, the β-galactosidase. This is achieved by applying a sialyltransferase, which converts Neu5Ac into the intermediate **B**.

The reaction system as studied here starts from the protected *O*-glycosyl amino acid Fmoc-Thr(GalNAcα1)-*Ot*Bu **A** (Figure 3.62), which is accessible by chemical synthesis *[Liebe, Kunz 1997a, 1997b]*. In the first step of the reaction cascade the Fmoc-Thr-protected intermediate **B** (T antigen derivative Fmoc-Thr[Gal(β1-3)GalNAcα1]-OtBu) is obtained by transgalactosidation catalyzed by the β-galactosidase [E.C. 3.2.1.23] from bovine testes. In the subsequent reaction step **B** is sialylated yielding **C** (Fmoc-Thr[Neu5Ac(α2-3)Gal(β1-3)GalNAcα1]-OtBu; Sialyl-T-core 1-Thr), catalyzed by the core 1-specific human α2,3-sialyltransferase[22] [E.C. 2.4.99.4] *[Sadler, et al. 1979; Chang, et al. 1995]*. In contrast to **B**, the conjugate **C** is not anymore a substrate for the β-galactosidase.

[21] This study was carried out in collaboration with the working group of Professor Kunz at the University of Mainz, Germany.

[22] A soluble form of α2,3-SiaT was expressed in Sf9 cells grown in serum-free medium and partially purified by consecutive chromatography on Amberlite IRA-95, DEAE- and SP-Sepharose as described previously. In an alternative approach, purification by chromatography was avoided. The sialyltransferase-containing medium was diafiltrated against MES buffer using an ultrafiltration membrane. Thus, a crude enzyme preparation was obtained.

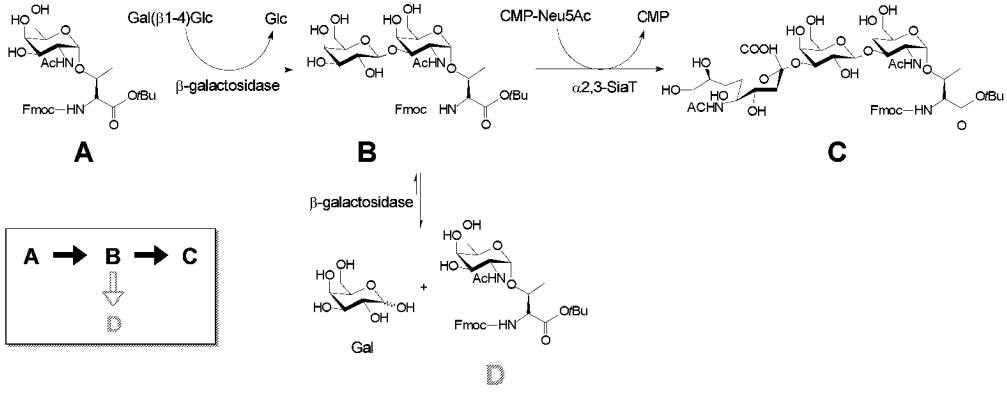

Figure 3.62: Simplified reaction scheme of the galactosidase/sialyltransferase catalyzed synthesis of Fmoc-Thr[Neu5Ac(α2-3)Gal(β1-3)GalNAcα1]-OtBu (Sialyl-T-core 1-Thr, C).

The glycoconjugate **C** is an important intermediate in the synthesis of the *N*-terminal glycopeptide sequence in Leucosialin (CD43) *[Fukuda 1991]*. The tumor-associated sialyl-T antigen [Neu5Ac(α2-3)Gal(β1-3)GalNAc(α1–*O*)Ser/Thr] is found on the leucocytes of patients with acute myeloic leukemia *[Fukuda, et al. 1986]*. Additionally, the (2-3)-sialyl-T structure was proven to be an antigen on breast cancer cells *[Brockhausen, et al. 1995]*. Therefore, glycopeptides with (2-3)-sialyl-T structure represent interesting targets for the development of anti-tumor vaccines.

The one-pot reaction as described above was elaborated using benzyl-α-N-acetylgalactosamine (GalNAc[α1-OBn]) as a model compound and optimized to 90% yield. First attempts to adapt this procedure to the protected amino acid glycan suffered from its low solubility in water. The solubility of the protected GalNAc-Thr acceptor is only 1 mM under reaction conditions. A non-protected threonin derivative of the sialyl-T containing building block **C** was synthesized by *Gambert* and *Thiem [Gambert, Thiem 1999]*. Organic co-solvents might be used for glycosylation of genuine building blocks, but in many cases they are not tolerated by the enzymes. Therefore, enzymatic glycosylations of protected amino acids gave yields of 15% or lower depending on the solubility of the substrate *[Cantacuzene, Attal 1991]*. By a galactosidase-catalyzed transglycosylation with DMF as a co-solvent, *Ajisaka* and coworkers achieved a yield of 23% with regard to the amino acid substrate *[Suzuki, et al. 1997]*. A further possibility is the application of two-phase systems *[Mori, et al. 1997]*. Nevertheless, there is no organic solvent known yet that is tolerated by the β-galactosidase from bovine testes and the α2,3-sialyltransferase at the same time. Alternatively, the addition of cyclodextrin derivatives as complexing agents were tested. Cyclodextrins are six-, seven- or eight-member glucose oligomers with cavity diameters ranging from 0.47 to 0.83 nm *[Li, Purdy 1992]*. Already in the case of in the aqueous phase poorly soluble aromatic ketones it could be demonstrated that addition of dimethylated cyclodextrins promote the solubility

[Zelinski, et al. 1999].

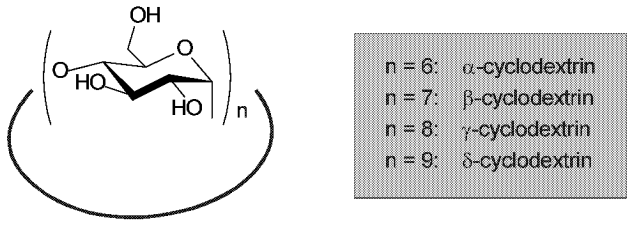

Figure 3.63: Cyclodextrins

β-Cyclodextrins are sufficiently large to enclose extended aromatic systems like the Fmoc-residue (Figure 3.63). Methylated cyclodextrins usually form more stable complexes than the unsubstituted cyclodextrins. Therefore, 2,6-di-O-methyl-β-cyclodextrin was used *[Casu, et al. 1979; Wenz 1994]*. In addition, hydroxypropyl-β-cyclodextrin and γ-cyclodextrin were investigated. Figure 3.64 shows the enhanced solubility of substrate **A** as a function of cyclodextrin concentrations. The best result was actually obtained with the dimethyl derivative. The cavity of the γ-cyclodextrin seems to be too large for efficient complexation, whereas hydroxypropyl-β-cyclodextrin shows poor inclusion properties and limited solubility.

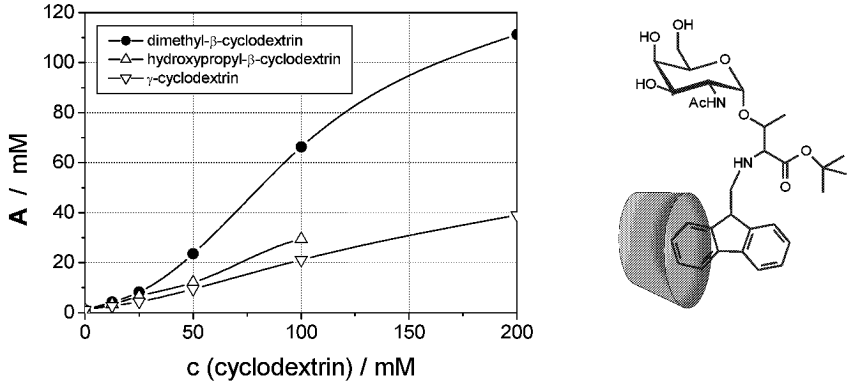

Figure 3.64: Enhancing the solubility of Fmoc-Thr(GalNAcα1)-O*t*Bu A by the addition of cyclodextrins (50 mM MES; pH 6,5). Left: Solubility of A as function of cyclodextrin concentration; right: schematic drawing of complexation of Fmoc residue of A.

Kinetic characterization of the galactosidase-catalyzed transgalactosylation from lactose to Fmoc-Thr(GalNAcα1)-OtBu **A** showed that the cyclodextrin complex is accessible for the enzyme. Although the K_M-value of 17 mM for the acceptor **A** is even lower than that for the model compound GalNAc(α1-OBn), the enzyme shows less activity towards **A**. In Table 3.6 the kinetic parameters are presented.

Table 3.6 **Kinetic data of the transgalactosylation reaction employing lactose as a donor.**

substrate	K_M / mM	relative v_{max} / -
GalNAc(α1-OBn)	50 ± 14	1
Fmoc-Thr(GalNAcα1)-O*t*Bu **A**	17 ± 5	0.25
lactose	78 ± 26	

In contrast to the synthesis with the model compound GalNAc(α1-OBn), another peak could be detected in the HPLC data during the course of the reaction. Most likely, it represents a regioisomer of the core 1 glycan **B**, though unfortunately, we could not isolate and characterize it. This assumed lack of regioselectivity of the galactosidase does not affect the synthesis of Fmoc-Thr[Neu5Ac(α2-3)Gal(β1-3)GalNAcα1]-OtBu **C**, because the regioisomer cannot be converted any further by the sialyltransferase.

On an analytical scale the reaction yielded 67% of sialyl-T-core 1-Thr **C**. In order to reduce enzyme consumption, preparative batches were carried out with lower enzyme activities yielding 50% of the trisaccharide **C**. The course of a representative preparative batch synthesis is shown in Figure 3.65. Although 20 mM of **A** were added, the starting concentration was lower due to precipitation of the acceptor substrate after dilution of the stock solution. After 16 h, the remaining substrate was dissolved completely. The α2,3-sialyltransferase does not convert the regioisomer of **B** (core 1-Thr). In total, 100 mg of the trisaccharide **C** were isolated.

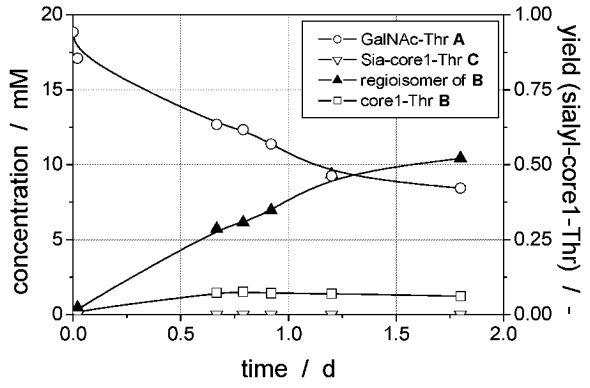

Figure 3.65: **Course of reaction of the one pot synthesis yielding sialyl-core 1-Thr C.**
[0.5 M lactose, 20 mM GalNAc-Thr **A**, 40 mM dimethyl-β-cyclodextrin, 25 mM CMP-Neu5Ac, 1 U/mL β-galactosidase, 200 mU/mL SiaT, 10 U/mL CIAP, 50 mM MES, pH 6.5].

3.2.2.7 Summary:

- The biological principle of reaction sequences was successfully demonstrated with the one-pot, two-step synthesis of the core 2-Bn trisaccharide.
- Optimization of complex multi-enzyme systems generating different O-glycan core structures can be achieved by using the method of a genetic algorithm.
- Principles of biological evolution have been transferred to technical evolution by using genetic algorithms for the optimization of reaction conditions of a one-pot biocatalytic reaction sequence.
- The selectivity for the core 2-Bn trisaccharide formation at the point of maximum product concentration has been doubled relative to the results of *Dudziak* et al., i.e., from 34% *[Dudziak, et al. 1998]* to 74%.
- The application of the multicatalyst system in a one-pot reaction sequence for core 2-Bn synthesis is more effective than the separation of both reaction steps.
- Syntheses of sialyl T threonine esters in a one-pot biocatalytic reaction sequence starting from N-Fmoc-(O-N-acetylgalactosaminyl)threonine *tert*-butyl ester was carried out.
- The solubility of a protected amino acid glycan could be enhanced up to 100-fold by the use of cyclodextrins.
- The one-pot reaction employing a β-galactosidase in combination with an α2,3-sialyltransferase opens up a new way to readily synthesize sialylated core 1 amino acid conjugates that are potentially interesting as building blocks for the syntheses of complex glycopeptides.

3.3 *In vitro* reaction sequences by combination of electrochemical with biocatalytical steps[23]

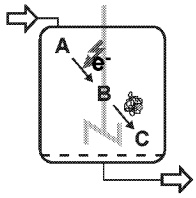

Often chemical asymmetric catalysis and enantioselective biocatalysis are complementary; sometimes they are even competitive as in the production of fine chemicals. In view of atom- and energy-efficiency the combination of both fields is becoming more and more important. Electroenzymatic synthesis utilizes electrons as cheap redox equivalents. The advantages of enzymes as enantioselective catalysts are combined here with the waste-free electrochemical *in situ* generation or regeneration of reagents. In contrast to whole cells in nature, where by necessity energy and mass transport are always coupled, - as for example in the respiratory chain or in photosynthesis, - *in vitro* it is possible to separate both processes. This is a very stimulating, positive difference, however, to the before formulated *6th biological principle: energy and mass transport are coupled* (➲ box page 3). In electroenzymatic synthesis, electrons can be directly transferred from an electrode to enzymes or mediators. The feasibility of supplying redox equivalents directly via an electrode was demonstrated before on some selected examples (for reviews see *[Steckhan 1994; Steckhan, et al. 2001; Schmid, et al. 2002a]*). This enables new possibilities in setting up reaction sequences according to the *1st biological principle: Complex chemicals are synthesized in reaction sequences* (➲ box page 3). Here electrochemical and biocatalytical steps are combined favorably in sequences or cycles and result in a method, which has been named "electroenzymatic synthesis".

Furthermore, utilization of the almost mass-free electrons as redox equivalents allows setting up redox reactions without side products. Both components of the electroenzymatic synthesis concept are intrinsically environmentally friendly *[Genders, Pletcher 1996]*. In addition, electrons are at the same time, - besides oxygen and hydrogen, - the cheapest redox equivalents available, especially on an industrial scale (Figure 3.66).

[23] **Parts of this chapter are published in:**

1. I. Schröder: *2,2'-Azinobis(3-ethylbenzothiazolin-6-sulfonsäure) (ABTS) als Mediator für die elektrochemische Oxidation von Nukleotidkofaktoren*; PhD-thesis, University of Bonn (2003)
2. I. Schröder, E. Steckhan, A. Liese: *In situ NAD(P)$^+$ regeneration using 2,2'-azinobis(3-ethylbenzothiazolin-6-sulfonate) as an electron transfer mediator*, J. Electroanal. Chem. 541 (2003) 109-115
3. S. Lütz: *Elektroenzymatische Reaktionen mit Chloroperoxidase aus Leptoxyphium fumago*; diploma thesis, University of Bonn (2000)
4. S. Lütz: *Prozeßentwicklung und Scale-Up Elektroenzymatischer Reaktionen*; PhD-thesis, University of Bonn (in progress)
5. A. Liese, S. Lütz: *Relevanz der Elektrochemie in oxidativen Biotransformationen*; GDCh Monographie der GDCh-Fachgruppe Angewandte Elektrochemie: Elektronentransfer in Chemie und Biochemie (J. Russow, H.J. Schäfer) 23 (2002) 305-308

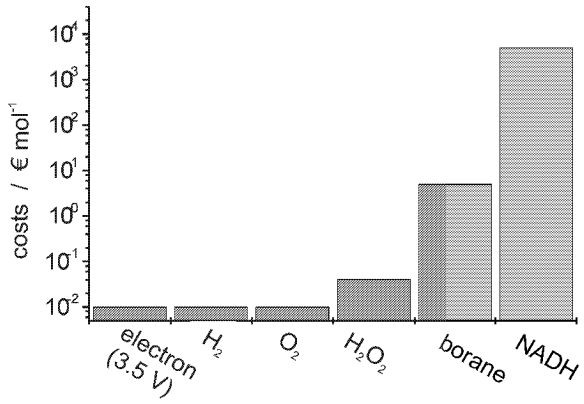

Figure 3.66: Costs of redox reagents compared on bases of 1 mole (logarithmic scale).

Three different methods for carrying out redox reactions can be differentiated, of which those for the oxidation of a substrate are outlined in Figure 3.67). The simplest method is to apply stoichiometric amounts of an oxidation reagent (Figure 3.67, top). The disadvantage of this method is that also stoichiometric amounts of waste are formed in form of the spent oxidation reagent, which is also unattractive from an economical point of view. Alternatively, two electrochemical methods can be applied: Electrochemical regeneration of catalytic amounts of the oxidation reagent (indirect electrolysis, Figure 3.67, bottom left) or the direct electrochemical oxidation of the substrate, omitting the oxidation reagent altogether (Figure 3.67, bottom right).

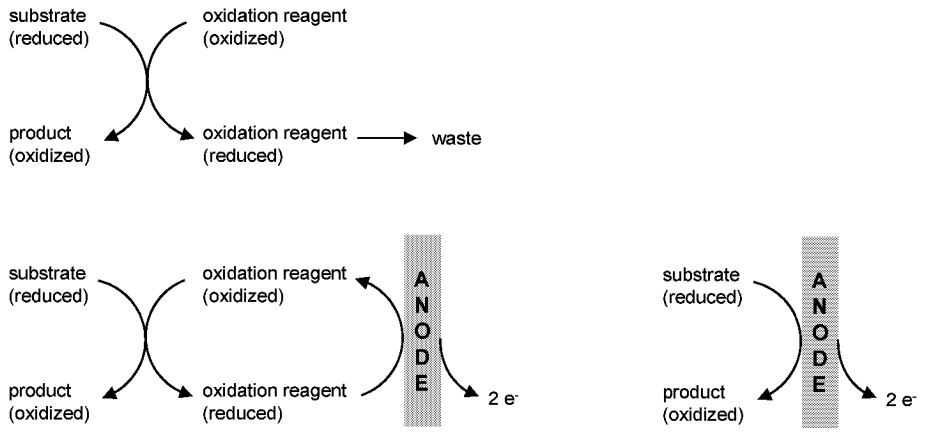

Figure 3.67: Comparison of oxidation reactions with the need of stoichiometric oxidant equivalents. Top: stoichiometric oxidant with waste production; bottom, left: electrochemical regeneration of catalytic amounts of oxidant; bottom, right: direct electrochemical regeneration *[Steckhan, et al. 2001]*.

Obviously, oxidoreductases are ideally suited for their combination with electrochemical steps. For all the reactions they catalyze, stoichiometric amounts of redox equivalents in relation to the starting material are needed. Since natural redox equivalents are often very expensive (see NADH in Figure 3.66) they need to be regenerated if applied in asymmetric catalysis on a technical or even industrial scale. At this point, electrochemistry comes into play. In contrast to enzymatic regeneration methods of e.g. nicotinamide cofactors, no side product, caused by the regeneration, are produced electrochemically *[Wong, Whitesides 1994]*. In electroenzymatic synthesis, - as is seen in Figure 3.68, the enzymatic regeneration of NAD^+ is replaced by either indirect cofactor regeneration via a mediator or by direct electrochemical regeneration (not shown), sparing out the mediator. The reversed procedure can also be applied for regeneration of the reduced nicotinamide cofactor.

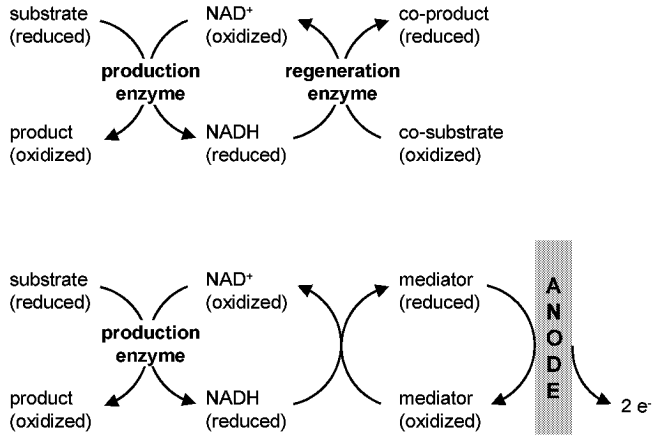

Figure 3.68: Substitution of a regeneration enzyme with its co-substrate and formed co-product by waste a free-electrochemical cofactor regeneration with catalytic amounts of mediator *[Steckhan, et al. 2001]*.

In the literature, several examples of electroenzymatic synthesis have been reported. So far, the major application thereof is the regeneration of cofactors, where mainly indirect electrolyses are applied. The FAD prosthetic group in ethylphenolmethylene hydroxylase is regenerated indirectly with the water-soluble 1,ω-bisferrocenyl-polyethyleneglycol *[Frede, Steckhan 1991; Brielbeck, et al. 1994]*. NAD(P)H is reported to be efficiently regenerated with the water-soluble polyethyleneglycol-bound Cp*Rh(bipyridyl)-complexes as mediators in continuously operated membrane reactors *[Ruppert, et al. 1987; Steckhan, et al. 1991; Westerhausen, et al. 1992; Steckhan 1994; Hollmann, et al. 2001; Schmid, et al. 2001b; Hollmann, et al. 2002]*. Likewise, methyl viologen and several other mediators are used for the regeneration of the reduced cofactors *[Delecouls-Servat, et al. 2002; Schmid, et al. 2002a]* (see also ➲ chapter 4.2.1, page 122). The aforementioned rhodium-complex acts as a totally selective redox catalyst, transferring a hydride only to the 4-position of NAD^+ and

$NADP^+$. For the regeneration of the oxidized cofactors, 1,10-phenanthrolin-5,6-dione or the respective N-methylated compound could be successfully applied *[Hilt, Steckhan 1993; Hilt, et al. 1997a; Hilt, et al. 1997b]*. Turnover frequencies *tof* = 35 h^{-1} were reached. An elegant electrochemical approach was published by *Biade* et al. for the de-racemization of racemic lactate *[Biade, et al. 1992]*, see Figure 3.69. The L-selective lactate dehydrogenase does only oxidize L-lactate to pyruvate that is subsequently electrochemically reduced to racemic lactate. By this means D-lactate is produced as left over. Besides the regeneration of cofactors, direct electron transfer to enzymes at electrodes has also been described. Prominent examples are hydrogenases *[Gros, et al. 1996; Butt, et al. 1997; Delecouls, et al. 1999; Smith, et al. 2001; Morozov, et al. 2002]*.

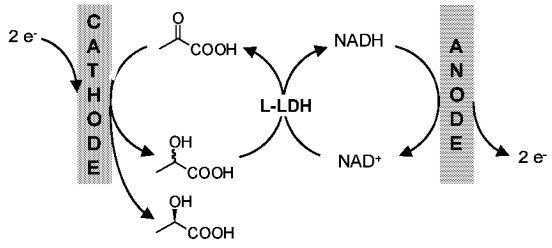

Figure 3.69: Direct anodic regeneration of NAD^+ coupled to the racemic cathodic reduction of pyruvate (LDH = lactate dehydrogenase).

Despite the success of the concept of electroenzymatic synthesis on a laboratory scale, so far no electroenzymatic synthesis was scaled up yet to an industrial process. The reason might be that optimization of such electroenzymatic syntheses in view of process engineering is still a rarely treated or attempted subject *[Bergel, DevauxBasseguy 1996; Delecouls, et al. 1998; Delecouls-Servat, et al. 2002]*.

Here the enantioselective oxidation of thioanisole to (*R*)-methylphenylsulfoxide, catalyzed by chloroperoxidase (CPO, EC 1.11.1.10), is investigated. The oxidation reagent H_2O_2 was *in situ* generated by cathodic reduction of oxygen. In both cases, highly enantioselective biotransformations yielding chiral fine chemicals were combined with an electrochemical supply of redox equivalents. Only upon applying reaction engineering a highly efficient production processes could be developed.

3.3.1 Electrochemical *in situ* generation of reactants

Besides the above discussed regeneration of cofactors and direct activation of enzymes, electrochemistry can also be used to generate reactants *in situ*. A promising target is the *in situ* generation of H_2O_2 as redox equivalent for peroxidases. Peroxidases catalyze a broad spectrum of reactions as depicted in Figure 3.70. Their application as biocatalysts for selective reactions as oxidations of non-activated carbons, epoxidations, hydroxylations, and sulfoxidations has been extensively reviewed *[van Deurzen, et al. 1997b; Adam 1999;*

Colonna, et al. 1999; van de Velde, et al. 2001; Schmid, et al. 2002a]. As oxidants, H_2O_2, alkyl hydroperoxides and *tert*-butyl hydroperoxide can be utilized. Especially hydrogen peroxide is attractive both, because of its economics and because water is being formed as the only co-product. Nevertheless, technical application of peroxidases is hampered by their instability towards high concentrations of the co-substrate hydrogen peroxide. For example, the heme peroxidase chloroperoxidase (CPO, EC 1.11.1.10), from the mold *Caldariomyces fumago*, is rapidly deactivated at 50 µM H_2O_2 (half-life $\tau_{1/2}$ = 38 min) *[Seelbach 1997; Seelbach, et al. 1997]*. To overcome this limitation different procedures have been established that are summarized later on. Recently, the heterologous expression of CPO as well as site-directed mutagenesis in the active site has also been carried out. But disappointingly, the resulting peroxidase yielded a much lower initial rate *[Rai, et al. 2000; Rai, et al. 2001; van de Velde, et al. 2001]*. The enantioselective sulfoxidation of thioanisole to (*R*)-methylphenyl-sulfoxide (*ee* = 99%, Figure 3.70 structures at bottom) catalyzed by chloroperoxidase *[Allain, et al. 1993; Dexter, et al. 1995; Lakner, Hager 1996]* was chosen as a reference system to explore its suitability for technical development. The asymmetric synthesis of sulfoxides is of industrial interest, because they can serve as chiral building blocks for the syntheses of e.g. β-hydroxy acids *[Mioskowski, Solladie 1980]* and pharmaceuticals like sulindac or omeprazole (Figure 3.70, right).

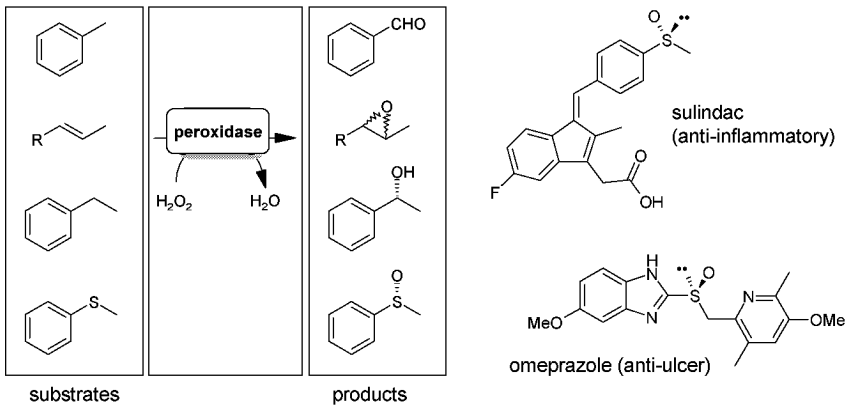

Figure 3.70: Selected examples of peroxidase-catalyzed reactions (left) and two industrial applications of thioanisoles (right).

Several approaches to controlling H_2O_2 at a constant low concentration have been reported that were recently reviewed *[van de Velde, et al. 2001; Schmid, et al. 2002a]*. They can be divided into two principles: feed-on-demand and *in situ* generation. The simplest method is the continuous slow addition of H_2O_2 *[Lakner, Hager 1996]*. Major drawback of this method is that the rate of the H_2O_2 addition needs to be adjusted to the rate of reaction. This can be further improved by sensor-controlled addition of hydrogen peroxide (feed-on-demand), adjusting the delivery rate according to the progress of the reaction *[Seelbach, et al. 1997;*

van Deurzen, et al. 1997a]. Using this method, a 20-fold increase in the *ttn*[24] for the CPO-catalyzed oxidation of indole to 2-oxindole has been achieved. Still one disadvantage of the feed-on-demand methods is that at the titration point locally a high concentration of H_2O_2 is resulting. The concentration of the titration solution of H_2O_2 needs to be high to prevent drastic increases of the reaction volume. This can be circumvented, if H_2O_2 is generated *in situ* by the reduction of oxygen. This can be carried out either by using a chemical reducing agent like ascorbic acid or with glucose oxidase that is oxidizing glucose at the same time to gluconic acid while hydrogen peroxide is formed as coproduct (Figure 3.71) *[Okrasa, et al. 2000; van de Velde, et al. 2000]*. The disadvantage of this method is obvious: A second starting material needs to be introduced stoichiometrically into the reaction system, and consequently a side-product is also synthesized and accumulates stoichiometrically.

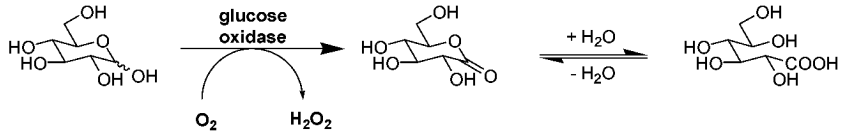

Figure 3.71: ***In situ*** **generation of hydrogen peroxide by glucose oxidase catalyzed oxidation of glucose.**

An alternative approach was published by *Laane* et al. *[Laane, et al. 1986]*. For the CPO-catalyzed chlorination of barbituric acid Laane produced the required H_2O_2 by cathodic reduction of oxygen. The advantage of this approach is that no side products are formed, whatsoever and that electrons are used as cheap redox equivalents. Within the scope of this study, this procedure has been transferred and scaled up to the technical utilization of chloroperoxidase to catalyze enantioselective sulfoxidations (Figure 3.72).

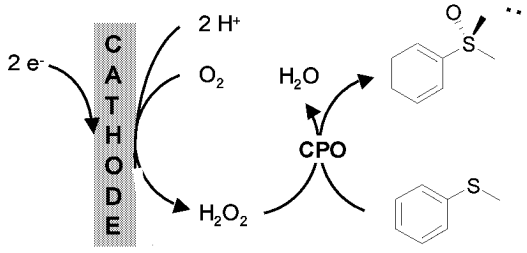

Figure 3.72: ***In situ*** **generation of hydrogen peroxide by cathodic reduction of oxygen coupled to the subsequent CPO-catalyzed sulfoxidation of thioanisole.**

[24] *ttn* = total turnover number (mole product formed / mole catalyst used)

3.3.1.1 System investigations

To determine reaction conditions that yield the highest efficiency in the two sequential reaction steps, namely both the electrochemical and the biocatalytical steps, compromises had to be made. The following milestones during our electroenzymatic process development are discussed in the following:

- Identification of uniform reaction conditions for both steps.
- Development of an electro-enzymatic reactor with a three-dimensional electrode.
- Characterization and optimization of electrochemical parameters.
- Scale up.

Identification of uniform reaction conditions for both steps

Theoretically, two electrons are needed to produce one hydrogen peroxide molecule, and each hydrogen peroxide molecule reacts to produce one (*R*)-methylphenylsulfoxide molecule. Therefore, the theoretical space-time yield (*sty*) of the sulfoxidation can be calculated (eq. 4-17):

$$sty = \frac{\text{current} \cdot \text{molecular mass of sulfoxide}}{2 \cdot \textit{Faraday}\,\text{constant} \cdot \text{volume}} = \text{current} \cdot 628\ \text{g L}^{-1}\ \text{d}^{-1}\ \text{A}^{-1} \qquad \textbf{eq. 3-10}$$

$9.64846\ 10^4$	C mol^{-1}	*Faraday* constant
sty	g L^{-1} d^{-1}	space-time yield
	A	current
	L	volume
	g mol^{-1}	molecular mass

The only factor influencing the *sty* of the process is the current that can be passed through the electrolyte. The reaction conditions reported in the literature[25] for CPO-catalyzed reactions*[Seelbach, et al. 1997; van Deurzen, et al. 1997a]* were found to be inferior from an electrochemical point of view. Since reaction conditions influence both the electrochemical and biocatalytic part, the impact on both had to be studied. For the integration of electrochemistry and biocatalysis the key parameters to be considered are listed in Table 4.5.

Table 3.7: Key parameters to be considered in electroenzymatic synthesis.

electrochemical parameters	biocatalytical parameters
current efficiency	enzyme activity
conductivity	enzyme stability
buffering capacity	

[25] Reported ‚standard' reaction conditions: 100 mM sodium phosphate buffer (pH 5), 30 vol% *tert*-BuOH, T = 20°C, substrate concentration 20 mM.

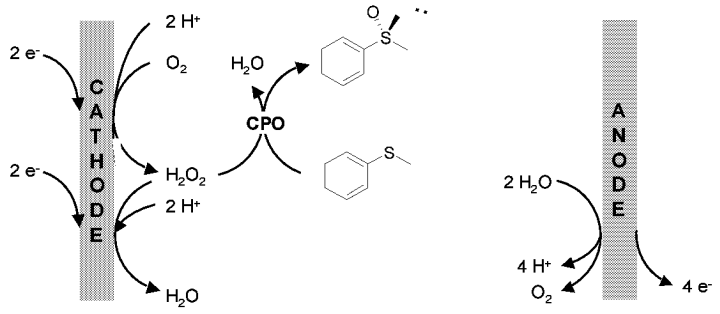

Figure 3.73: Complete electroenzymatic reaction system with both electrode reactions.

As derived from literature reports, the optimal pH for the biotransformation was found to be within the range of 4-6. Mostly, 100 mM sodium phosphate buffer was used, which has no buffering capacity in the desired pH range. Since the electrochemical reaction 'produces' protons at the anode and 'consumes' protons at the cathode (Figure 3.73), it was replaced by a 100 mM acetate / 50 mM sodium sulphate buffer that exhibits a higher buffer capacity. In this buffer system current efficiencies[26] of up to 95% have been reached.

In CPO-catalyzed biotransformations with poorly soluble substrates like thioanisole, *tert*-butanol is often used as a cosolvent. Therefore, the influence of the cosolvent on the conductivity as well as on the enzyme activity was determined. As shown in Figure 3.74, left, the conductivity of the buffer solution dropped significantly from ~ 13 mS cm^{-1} without *tert*-butanol to ~ 4 mS cm^{-1} in the presence of 30 vol% cosolvent. The decrease in activity as a function of the *tert*-butanol content up to 20 vol% is not that drastic. However, the *tert*-butanol content does have a high influence on the solubility of the starting material thioanisole (Figure 3.74, right).

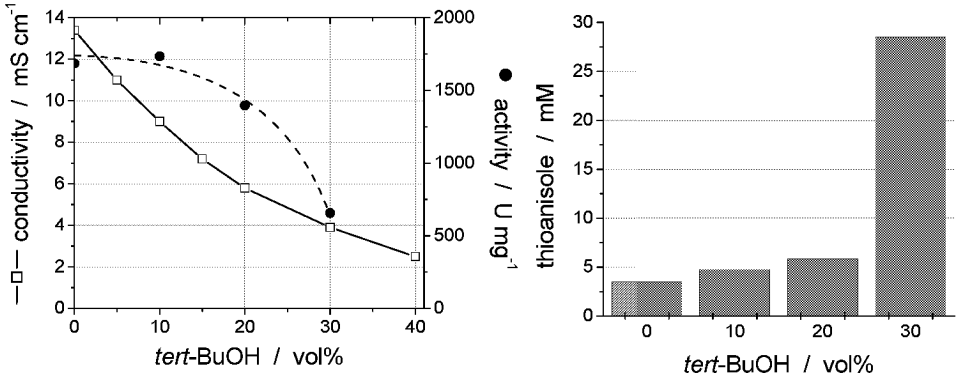

Figure 3.74: Left: Conductivity (left) and solubility of thioanisole (right) as function of the *tert*-BuOH content.

[26] Current efficiency is defined as the ratio of the current needed theoretically for the desired reaction to the current that is needed in practice.

As a consequence, if a lower butanol content is chosen because of the electrochemical parameters (i.e. conductivity), then a fed-batch technique must be applied to supply the same amount of starting material. Using the electroenzymatic method, however, no emulsions occur, since non-dissolved substrate is absorbed on the graphite electrode. We found that with 10 vol% of *tert*-butanol the system still worked satisfactory. The pH and the temperature were not altered, since we found no higher activities than those reported in the literature for sulfoxidations. As a compromise between electrochemical and biocatalytic demands the following standard reaction conditions were selected:

3.3.1.2 Development of an electroenzymatic reactor with a three-dimensional electrode

As a standard electrochemical cell for electroenzymatic synthesis a 300 mL thermostated glass beaker with a carbon felt cathode on steel insert was developed. With this setup a divided electrolysis cell has been realized, separating the anode compartment with a dialysis membrane (Sigma). In an undivided cell only moderate enantioselectivity was detected (~ 80% *ee*). However, by separating the enzyme from the anode via a membrane the *ee* could be increased up to 98%. Using the prior determined standard reaction conditions for the electroenzymatic sulfoxidation a space-time yield of 9 g $L^{-1}d^{-1}$ was reached.

To increase the ratio of cathode surface to reaction volume for the cathodic reduction of O_2 a 3-dimensional flow-by cell was designed, based on an earlier developed electrochemical method for the removal of dissolved oxygen from water *[Vuorilehto, et al. 1995]*. In this prior art, oxygen-rich water was passed through the three-dimensional cathode and the dissolved oxygen was reduced on the cathode surface to water *[Tamminen, et al. 1996]*. Based on the above cell as detailed in the literature, a three-compartment cell was designed, shown in Figure 3.75.

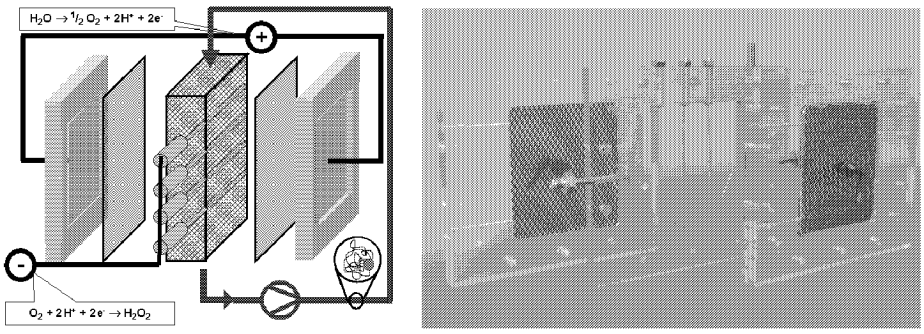

Figure 3.75: Left: Cell assembly. From the left: Anode, cation exchange membrane, packed bed cathode with current feeders, cation exchange membrane, anode. Right: Photo, from the left: Anode frame with anode net, cathode frame with current feeders, anode frame with anode net.

The cell consists of a packed bed cathode and two anodes, one on each side of it. Two anodes were needed to keep the ionic pathways as short as possible. The cathodic electrolyte (catholyte) flowed vertically downwards through the bed, and the current flowed horizontally. At both anodes, there was a separate anode chamber.

As the cathode a three-dimensional packed bed (80 mm x 90 mm x 10 mm) was used. Since the desired hydrogen peroxide-producing reaction takes place at the cathode, the choice of the right material was of high importance. At most cathode materials, oxygen is reduced to water (four electrons/mole). At carbon, gold, and mercury oxygen is preferentially reduced to hydrogen peroxide (two electrons/mole). The current efficiency of the hydrogen-peroxide producing reaction should be as high as possible, because the supply of oxygen (low solubility) and current (low conductivity) are limited in the system. Therefore, five different cathode materials were tested in regard to the current efficiency (Figure 3.76). Desulco graphite grains were chosen for additional experiments, since they yielded the highest current efficiency. Silver was chosen as current feeder material, because graphite itself is of low conductivity.

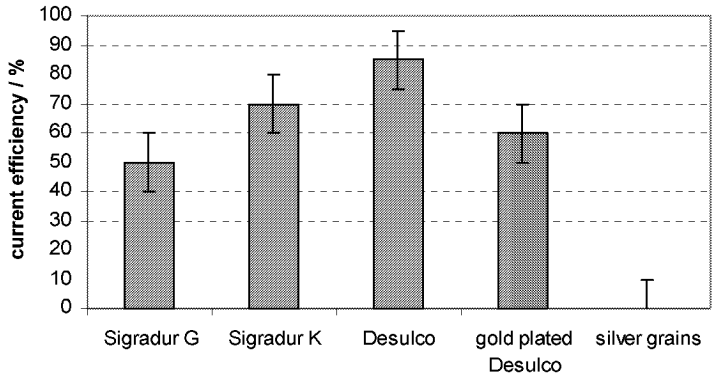

Figure 3.76: Evaluation of cathode materials (50 mM sodium sulphate, 3D flow cell, 100 mL min^{-1} flow rate, cell voltage 1.8 V for graphite, gold plated particles estimated from 2/3 bed length, no hydrogen peroxide detected with silver grains).

To avoid ohmic losses, the anodes were placed directly at the membranes. To avoid activation overpotential at the anodes, special oxygen evolution compatible anodes were used (Metakem, Germany), made out of titanium nets. Titanium is a suitable base material for this purpose, as it resists corrosion at anodic potentials. The nets were coated with iridium-based oxide as catalytic material. Since acrylic plastic as well as polycarbonate is unstable in the presence of thioanisole, stainless steel was used for the cathode frame. A cation exchange membrane (Nafion 424) was used to separate the cathode bed from the anode and to prevent *R*-sulfoxide and CPO from reacting on the anode. Positive cations can migrate through them, but not negative anions.

With this newly designed 3-D flow cell the electroenzymatic process could be improved further, since the packed bed of graphite particles allowed high ratios of electrode area (~ 900 - 1350 cm^2) to reaction volume (~ 90 mL) and, therefore, higher total currents than the simple setup in a beaker cell. The flow cell was integrated into a loop reactor, where oxygen was supplied via a separate aeration unit. The reaction system scheme is shown in Figure 3.77.

As pointed out in Equation eq. 3-10, the main factor influencing the space-time yield of the process is the current that can be passed through the electrolyte. By using the prior determined reaction conditions to yield a high conductivity of the reaction solution together with the optimised 3-D electrolysis cell, a space-time yield of 104 g $L^{-1}d^{-1}$ could be reached for (*R*)-methylphenylsulfoxide (*ee* > 99%) in the electroenzymatic sulfoxidation. A total turnover number (*ttn*) of 145.000 was reached for the CPO and a 75% current efficiency.

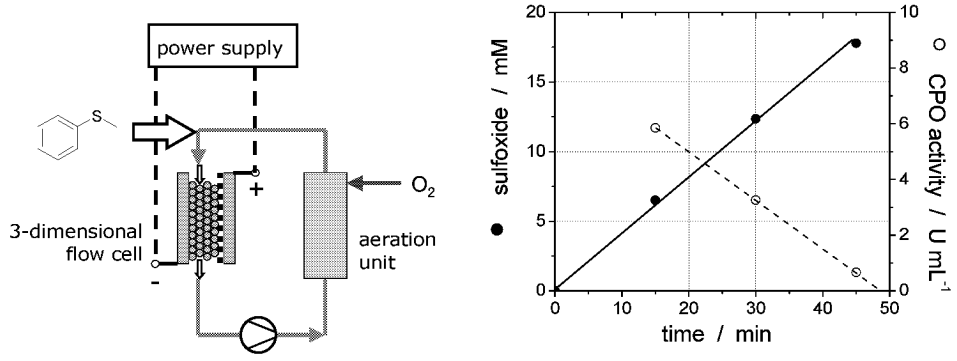

Figure 3.77: Left: Flow scheme of the circulation reactor. Right: Batch reaction in the circulation reactor with the 3-dimensional cathode (1.95 V, 220 mA, 0.6-1.0 mm graphite grains, 20 mM thioanisole, 1005 U CPO).

In practice, some current was lost due to side reactions (water and hydrogen production, respectively), and some hydrogen peroxide was dissociated. A total current efficiency of approximately 80% was measured in most experiments.

If the *ttn* reached in this electroenzymatic sulfoxidation is compared to that yielded by other methods, it is within the same range as with the feed-on-demand (*ttn* = 148,000) *[Seelbach, et al. 1997]*. With *in situ* generation of H_2O_2 utilizing the glucose oxidase, a *ttn* of even 250,000 has been achieved *[van de Velde, et al. 2000]*. Nevertheless, the electrochemical *in situ* generation of H_2O_2 brings about several advantages over the other two methods. In comparison to feed-on-demand no additional increase of volume is observed. In the feed-on-demand method only diluted H_2O_2 solutions can be added, thereby preventing enzyme deactivation at the titration point. This results in an increase of the reaction volume. There are two advantages in comparison to the *in situ* generation with glucose oxidase: On the one hand, no side-products as gluconic acid are formed, and on the other hand, the reaction rate can be easily controlled by the production rate of hydrogen peroxide, as all hydrogen peroxide

produced is immediately consumed by the enzyme. Since the enzymatic reaction is limited in hydrogen peroxide and the hydrogen peroxide production rate is controlled by the current, the total reaction can easily be controlled via the power source by choosing the desired voltage (Figure 3.78).

In a technical cost projection, assuming enzyme costs of 2500 €/kg protein[27], the production costs for 1 kg of (*R*)-methylphenylsulfoxide (*ee* > 99%) would be 17 €. If available through good expression systems, peroxidases for oxidation reactions have a huge potential as versatile biocatalysts in industrial biotransformations. Combined with the electrochemical *in situ* supply of hydrogen peroxide, a peroxidase-catalyzed biotransformation could be the first electroenzymatic process transferred to a technical scale.

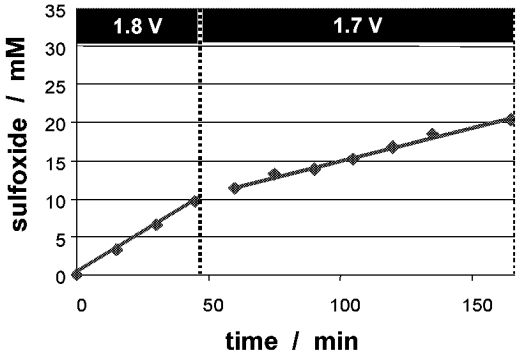

Figure 3.78: Regulation of reaction rate in a batch transformation (0-45 min: 1.8 V, 80 mA, *sty* = 43 g L^{-1} d^{-1}; 45-135 min: 1.7 V, 40 mA, *sty* = 20 g L^{-1} d^{-1}, 1.0 - 1.4 mm graphite grains, 12 U mL^{-1} CPO).

3.3.1.3 Summary

- The first biological principle, namely reaction sequences, can be transferred to unnatural conditions (e.i., electroenzymatic synthesis).
- A new electroenzymatic reactor, comprising an integrated 3-dimensional electrolysis cell, has been developed and successfully applied.
- In the newly developed reactor (*R*)-methylphenylsulfoxide could be produced in an electroenzymatic reaction sequence with an *ee* > 99% and a space-time yield of 104 g $L^{-1}d^{-1}$.
- Electroenzymatic sequential reactions are easily controllable from the outside, if the electrochemical reaction step is rate limiting.

[27] BASF, 2002

"At one level we can 'explain' enzyme catalysis -
what an enzyme does is bind,
and thus stabilise selectively the transition state
for a particular reaction.
But our current level of understanding
faces the more severe, practical test -
that of designing and making artificial enzyme systems
with catalytic efficiencies
which rival those of natural enzymes."

Angew. Chem., Intl. Ed. Engl. 1996, 35, 707-724

4 Second biological principle: Macromolecular catalysts[28]

The biological catalysts, the enzymes, inspire this area of research. Enzymes are ideal catalysts, optimized by nature over several generations. They are homogeneously soluble, highly selective biocatalysts of high molecular weight. This allows for their retention by e.g. ultrafiltration membranes due to their size *[Jandel, et al. 1980; Flaschel 1983]*. Thus, the recycling of such catalysts is possible, for example, by use of a continuously operated enzyme membrane reactor (EMR) *[Kula, Wandrey 1987]*. In this study, this so-called '*second biological principle*', namely, *biological catalysts are macromolecular and in general homogeneously soluble*, has been transferred to classical chemical catalysis. Metal ligands have been covalently bound via linkers to polymeric backbones of high molecular weight. Fur this purpose, the polymeric backbone and the linkers are chosen in such a way that the resulting *chemzyme* is - in contrast to the biocatalysts - homogeneously soluble in the solvent of choice, thus not restricted to water and can be retained using membranes. This is the application of the *3rd biological principle: Membranes retain macromolecular, homogeneously solubilized catalysts.* In this fashion, the major restriction to using biocatalysts has been overcome, namely that enzymes are typically limited to water as the solvent *[Buchholz, Kasche 1997]*.

Today, homogeneously soluble chemical catalysts can reach enantioselectivities and

[28] **Parts of this chapter are published in:**

1. S. Laue, L. Greiner, J. Wöltinger, A. Liese: *Continuous application of chemzymes in a membrane reactor: Asymmetric transfer hydrogenation of acetophenone*; Advanced Synthesis & Catalysis 343 (6-7) (2001) 711-720

chemoselectivities similar to those of enzymes *[Ojima 1993]*. But in contrast to most enzymes, these catalysts can also be employed in organic solvents. Nevertheless, a continuous operation with such catalysts is still difficult, although promising approaches - such as two-phase systems *[Herrmann, Kohlpaintner 1992; Malmström, Andersson 1999]* and heterogenization methods *[Cornils, Wiebus 1996; Sandee, et al. 2001]* - have been optimized *[Cornils, Herrmann 2000; Vos, et al. 2000]*.

In order to combine the advantages of the chemical and the enzymatic approach, chemical catalysts (oxazaborolidines *[Felder, et al. 1997; Giffels, et al. 1998; Wöltinger, et al. 2001a]* and amino alcohols for diethylzinc reduction *[Kragl, Dreisbach 1996]*) have been bound to homogeneously soluble polymers (polystyrenes, polymethacrylates). The resulting soluble polymer-bound catalysts (*chemzymes* = *chem*ical en*zymes*) can now be retained by ultrafiltration membranes like enzymes; therefore, they can now be applied in a *chemzyme membrane reactor* (CMR) *[Kragl, et al. 1996a; Rissom, et al. 1999; Kragl, Dwars 2001; Wöltinger, et al. 2001a; Bergbreiter 2002]*. Similar approaches have been developed for other classes of catalysts attached to polymers *[Bayer, Schurig 1975; Steckhan, et al. 1990; Leadbeater, Marco 2002]* or dendrimers *[Köllner, et al. 1998; Brinkmann, et al. 1999; Hovestad, et al. 1999]*. Even the direct retention of a DuPHOS ligand by a nanofiltration membrane has been described in the literature *[Smet, et al. 2001]*.

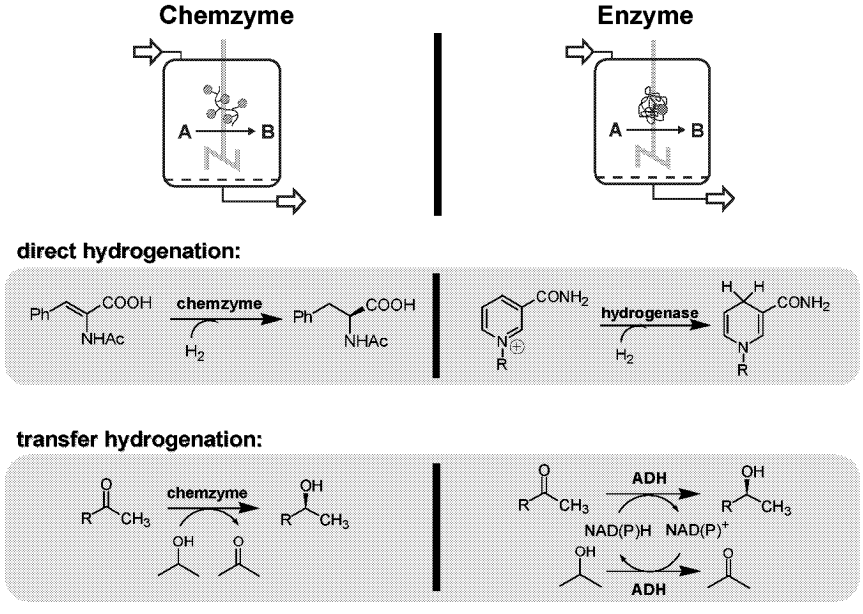

Figure 4.1: Comparison of chemzymes to enzymes in enantioselective hydrogenations (ADH = alcohol dehydrogenase).

In this chapter, the syntheses and application of new chemzymes is described. The main focus is the kinetic elucidation of the systems as well as the design of appropriate reactors that meet all the requirements of the chemzymes as well as of the enzymes. The results obtained upon optimizing the chemzyme approach will be compared to those of the respective enzyme-catalyzed systems (➲ chapter 4.5, page 169). An overview of the investigated catalytic systems is given in Figure 4.1. In the case of direct hydrogenation molecular hydrogen - that can be used in large excess - is used as reduction equivalent (Figure 4.1, top). In addition, H_2 can easily be removed, thus not interfering with downstream processing. As a typical example of a chemical catalyst the homogeneous hydrogenation catalyst PyrPhos was chosen (➲ chapter 4.1, page 103), whereas the hydrogenase I from the hyperthermophilic archeon *Pyrococcus furiosus (PF*H) represents the enzymatic approach (➲ chapter 4.2, page 119). Both catalysts activate molecular hydrogen, - the PyrPhos system for the enantioselective reduction of activated double bonds, whereas the *PF*H is capable of heterolytic cleavage of molecular hydrogen and regioselective 1,4-hydride addition to the oxidized form of the phosphorylated nicotinamide cofactor: $NADP^+$. In order to establish continuous operation with the chemzyme as well as with the enzyme, a special hydrogenation technology for the supply of the gaseous starting material hydrogen to the liquid phase had to be developed. For a detailed discussion of this topic see ➲ chapter 4.1.1, page 107.

In the case of transfer hydrogenation, 2-propanol is used as the reduction equivalent, which becomes oxidized to acetone (Figure 4.1, bottom). Transfer hydrogenation represents a promising method for the production of secondary alcohols *[Zassinovich, et al. 1992; Palmer, Wills 1999]*. Due to the low costs of 2-propanol, no hazardous hydrogen - in contrast to the very successful hydrogenation methods as described in the literature *[Noyori 1994; Burk, et al. 1995a]* - has used in this context. As follows from Figure 4.1, bottom, 2-propanol can also be used as a hydrogen source for enzyme-catalyzed reductions in aqueous solution, if it is applied at concentrations that do not destabilize the enzyme. One major difference of the enzyme-catalyzed approach is the need of a cofactor acting as a hydrogen mediator. This cofactor has to be regenerated during the course of reaction, because of its high price. Fortunately, effective methods could be developed for economically recycling the cofactor, as is outlined in the following.

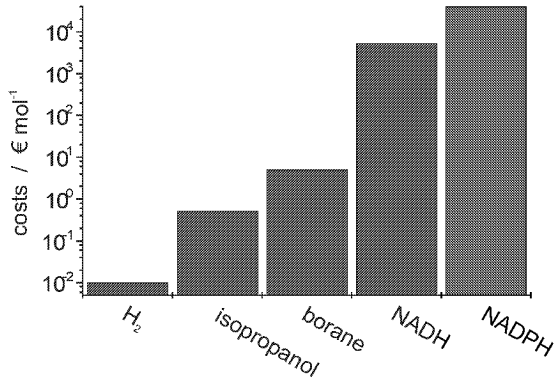

Figure 4.2: Costs of different reduction equivalents compared on the bases of 1 mole (logarithmic scale).

The costs of 1 mole each are compared for different reduction equivalents in Figure 4.2. As follows from this chart, molecular hydrogen is by far the cheapest one. Borane - that is used in oxazaborolidine-catalyzed reductions *[Corey, et al. 1987]* - is cost -wise more unattractive as 2-propanol. By far the most expensive reduction equivalents are the nicotinamide cofactors NADH and NADPH. Therefore, if these cofactors are to be used as hydrogen mediators, they need to be regenerated.

4.1 Direct hydrogenation with chemzymes[29]

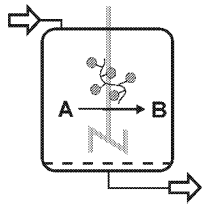

Historically, the starting point for applying homogeneously catalyzed reductions by soluble metal complexes represent the investigations of *Wilkinson [Osborn, et al. 1966]*. He showed that it is possible to reduce alkenes to alkanes under mild conditions with molecular hydrogen, utilizing rhodium triphenylphosphine as the catalyst (*Wilkinson's catalyst*). As is outlined in Figure 4.3, it is assumed that initially hydrogen is thereby oxidatively added to the central Rh followed by coordination of the alkene. Further investigations showed that the formation of the rhodium dihydride forms the first step of the catalytical cycle *("dihydride route") [Halpern, Wong 1973]*. Proceeding from these results *Knowles* and *Sabacky* developed the first industrial asymmetric hydrogenation process starting from cinnamic acid derivatives to synthesize L-Dopa (3,4-dihydroxyphenylalanine), which is used in the treatment of Parkinson's disease, Figure 4.4 *[Knowles, Sabacky 1968]*. Their homogeneously soluble catalyst is a cationic rhodium bisphosphine complex, in which the enantioselectivity is induced by the chiral bisphosphine ligand. Total turnover numbers of their "Rh-DIPAMP" catalyst is > 10,000, and an *ee* = 0.96 is reached. The optically pure L-dopa is separated from the catalyst by crystallization. In contrast to the *Wilkinson* catalyst *Halpern [Halpern 1982]* and *Brown [Brown, Chaloner 1980a, 1980b]* could show that in case of the cinnamic acid derivative as the substrate, the first step of the catalytic cycle involves complexation of the alkene to the central Rh atom, which is followed by the oxidative addition of hydrogen to the resulting complex *("unsaturated route")*. Later on *Kagan* and coworkers showed that the chirality of the phosphor-containing ligand could be shifted to the backbone. This was demonstrated for the first time through the synthesis of the ligand DIOP[30] *[Kagan, Dang 1972; Dumont, et al. 1973; Kagan 1982]*, which represents a fundamental structure acting as a basis for a vast variety of related bisphosphane ligands. Based on *Kagan's* findings new ligands and catalyst systems were subsequently developed. For an overview the following reviews are recommended *[Knowles 1983; Jacobsen, et al. 1999; Brunner 2000]*. The most prominent

[29] **Parts of this chapter are published in:**

1. L. Greiner: *Prozessentwicklung für die katalytische Reduktion mit molekularem Wasserstoff*, PhD-thesis, University of Bonn (2002)
2. L. Greiner, D. Müller, E. van den Ban, J. Wöltinger, C. Wandrey, A. Liese: *Membrane aerated hydrogenation: Enzymatic and chemical homogeneous catalysis*, Advanced Synthesis & Catalysis 345 (2003) 679-683
3. S. Laue, L. Greiner, J. Wöltinger, A. Liese: *Continuous application of chemzymes in a membrane reactor: Asymmetric transfer hydrogenation of acetophenone*; Advanced Synthesis & Catalysis 343 (6-7) (2001) 711-720
4. A. Bommarius, H.-P. Krimmer, D. Reichert, J. Almena, A. Karau, J. Wöltinger, K. Drauz, A. Liese, L. Greiner, C. Wandrey: *Volumenbegasung*, German patent application *DE 101 63 168.5 (21.12.2001)*

[30] DIOP = 2-dimethyl-4,5-bis-(diphenylphosphanyl)-pyrrolidine

ligands are derived from components of the "chiral pool", i.e., BPPM[31] derived from proline *[Achiwa 1976]*, or PyrPhos[32] derived from tartaric acid by the group of *Nagel [Nagel 1984; Nagel, Kinzel 1986; Nagel, et al. 1986]*. Another important family of ligands represents DuPhos[33] and derivatives thereof, developed by *Burk* at DuPont (➲ Figure 3.3 and Figure 3.4, page 22) *[Burk 1991a, 1991b]*.

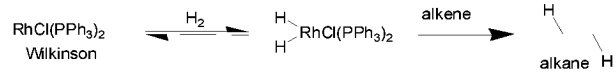

Figure 4.3: Hydrogenation of alkenes catalyzed by the *Wilkinson* catalyst.

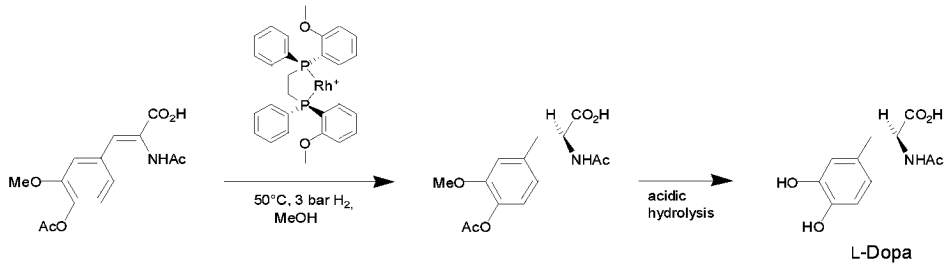

Figure 4.4: Synthesis of L-dopa using the Rh-DIPAMP catalyst (*ttn* > 10,000, *ee* = 0.96).

More recently, *Noyori* introduced the BINAP[34] ligand for the asymmetric reduction of carboxylic acids lacking the acetamido functionality *[Miyashita, et al. 1980]*. Complexes of Ru(II) with BINAP are extremely powerful catalysts for enantioselective hydrogenations of prochiral α,β- and β,γ-unsaturated carboxylic acids, enamides, allylic and homoallylic alcohols, imines, etc. *[Noyori 1994; Koten, Leeuwen 1999]*. BINAP ligands are applied on an industrial scale for several asymmetric reactions as for example the hydrogenation to (*S*)-naproxen by Syntex (Figure 4.5) or the synthesis of (-)-menthol from myrcene by Takasago *[Koten, Leeuwen 1999]*.

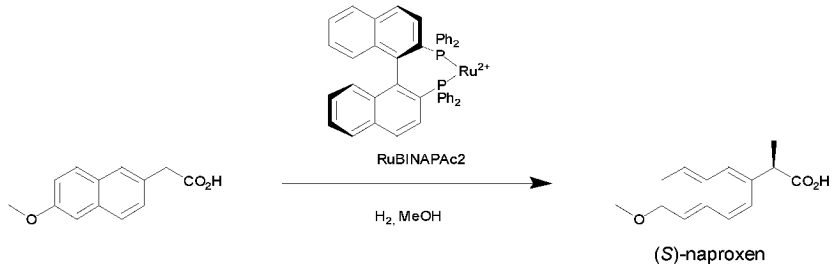

Figure 4.5: Synthesis of (*S*)-naproxen using Ru-BINAP (*ttn* = 200, *ee* = 97%).

[31] BPPM = ethyl 4-diphenylphosphanyl-2-[(diphenylphosphanyl)-methyl]-pyrrolidine-1-carboxylate
[32] PyrPhos = 1-phenyl-3,4-bis-(diphenylphosphanyl)-pyrrolidine
[33] DuPhos = 1,2-bis(2,5-dimethylphospholanyl)-benzene
[34] BINAP = 2,2'-bis-phosphanyl-[1,1']binaphthalenyl

As newer additions to the growing family of asymmetric ligands, JosiPhos and PhanePhos represent another class of hydrogenation catalyst that contain more than one centers of chirality. They exhibit axial as well as central chirality *[Burk 1991a; Pye, et al. 1997; Muniz, Bolm 2000]*. Finally, a very special ligand, XyliPhos, needs to be mentioned that is used for the production of (*S*)-metolachlor on a scale of 10,000 t a^{-1} by Syngenta (Figure 4.6). This ligand reaches a very high *ttn* of 100,000 and a *tof* of up to 20,000 h^{-1} *[Pugin, et al. 2002]*.

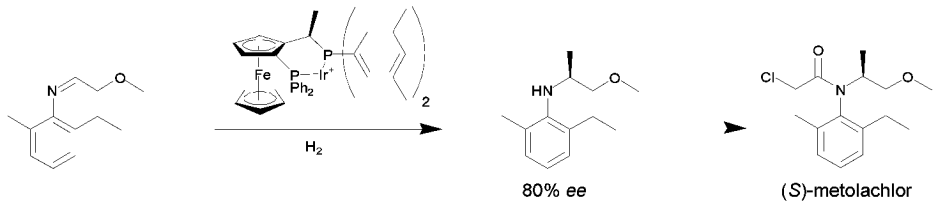

Figure 4.6: Synthesis of (*S*)-metolachlor using the ferrocene-based Ir-XyliPhos ligand (*ttn* = 100,000, *tof* ≥ $2 \cdot 10^5$ h^{-1}).

To establish a model system for reaction engineering of the asymmetric, catalytic hydrogenation, PyrPhos has been selected in this study as an attractive ligand *[Nagel 1984; Nagel, Kinzel 1986]*, because of its easy access via a short synthesis[35] starting from tartaric acid *[Nagel, et al. 1986; Beck, Nagel 1988]*.

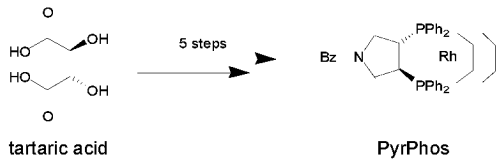

Figure 4.7: Synthesis of PyrPhos (also called DeguPhos) strating from tartaric acid.

The ligand complexes Rh as the precious metal. The enantioselective hydrogenation of 2-*N*-acetyl-acetoamido cinnamic acid has been selected as the model reaction used for this catalyst system in this investigation (Figure 4.8, *ee* = 94%, quantitative conversion). The criteria applied in selecting this catalyst are outlined in the following:

1. The catalyst PyrPhos is available via a short synthesis starting from tartaric acid. Since tartaric acid is a natural product, it is available in both enantiomeric forms at a very low price, which means that both enantiomers of the catalyst can readily be prepared.

2. The nitrogen atom of the pyrrolidine ring of the PyrPhos ligand incorporates a C_2-symmetry axis. Coupling the ligand via the nitrogen to a polymer does not destroy the symmetry thereof, which should minimize negative influences on the selectivity of the

[35] PyrPhos was kindly supplied by Dr. Jens Wöltinger (degussa, Hanau, Germany).

catalyst.

3. The electronic properties of the central metal, here Rh, can easily be modified *[Inoguchi, Achiwa 1990]*. This enlarges the substrate spectrum, if ketones are to be reduced.

4. The catalyst has already been produced on a large scale, and the synthesis as well as the catalysis therewith have already been optimized empirically and have been found to be very reproducible *[Beck, Nagel 1988]*.

5. From pre-investigations it was already known that the enantioselectivity achieved is independent of the hydrogen pressure and the temperature *[Nagel, Kinzel 1986]*.

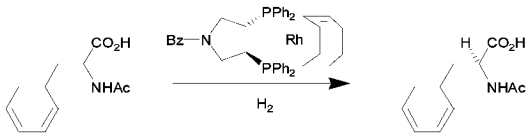

Figure 4.8: Enantioselective hydrogenation of 2-acetoamido cinnamic acid catalyzed by PyrPhos (*ee* = 94%, quantitative conversion).

Prior to its use in catalysis, the ligand needs to be activated by liberation of the 1,5-cyclooctadiene (COD) (Figure 4.8) *[Burk, et al. 1998]*. The exact mechanism of this activation in the case of PyrPhos is not known yet. In the case of other catalysts like DIOP, however, the activation process has been investigated, and two alternative reaction pathways have been proposed in the literature *[Nindakova, Shainyan 2001]*:

1. Hydrogenation of COD, thereby liberating the activated complex.
2. Displacement of COD by the solvent, followed by inheriting the freed coordination places at the Rh to the substrate.

The synthesis[36] of the chemzyme used in this study was carried out via a convergent synthesis in analogy to published protocols *[Bergbreiter, et al. 1998; Bergbreiter 2002]*. The PyrPhos ligand was covalently bound to a poly(*N-iso*-propyl-methacrylamide) (Figure 4.9). Furthermore, other polymer-enlarged PyrPhos systems have also been described in literature *[Malmström, Andersson 1999; Malmström, Andersson 2000]*. The advantage of this particular chemzyme is the additional spacer unit that prevents interactions or interference with the polymeric backbone thanks to the increased distance. In contrast to other polymer-coupled PyrPhos systems, the selectivity of this polymer-bound system is not changed with the preparation of this chemzyme relative to its low-molecular relative.

[36] The synthesis was carried out by Dr. Jens Wöltinger (degussa, Hanau, Germany) and kindly supplied within the scope of a collaboration.

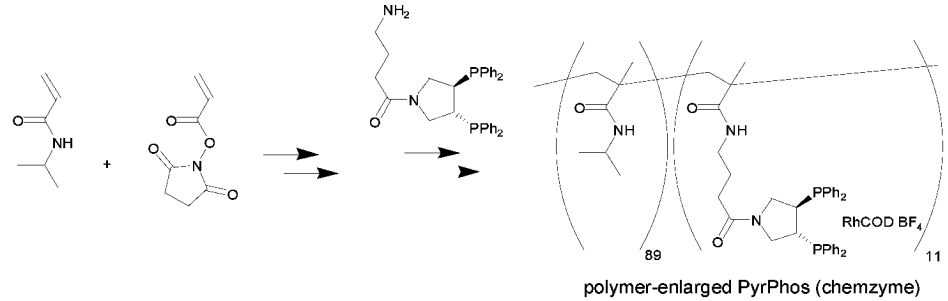

Figure 4.9: Synthesis of the homogeneously soluble polymer-enlarged PyrPhos ligand (chemzyme).

The fundamental properties of the native PyrPhos and the chemzyme are compared in Table 4.4.

Table 4.1 Comparison of non-immobilized PyrPhos and the respective chemzyme.

	PyrPhos (monomer)	PyrPhos (chemzyme)
molecular weight / g mol^{-1}	827.5	$30 \cdot 10^3$
active sites	1	11
ee / %	94	94

4.1.1 Supply of hydrogen

Because of the low solubility of hydrogen in the liquid phase, hydrogenations show the characteristics of a 'fed-batch' reaction regarding hydrogen. H_2 is fed into the reacting solution from the gaseous reservoir according to the coupled equilibrium between the gas and the liquid phase. *Henry's* law describes this equilibrium (eq. 4-17). The solubility of hydrogen at equilibrium in the liquid phase $[H_2]_{eq}$ is proportional to the partial pressure of H_2 in the gas phase, p_{H_2}, and is correlated by the specific *Henry* coefficient H_{H_2}, which is uniquely different for each individual system.

$$p_{H_2} = H_{H_2} \cdot [H_2]_{eq}$$

eq. 4-1

with:			
	p_{H_2}	bar	hydrogen pressure in gas phase
	H_{H_2}	bar mM^{-1}	specific *Henry* coefficient for H_2
	$[H_2]_{eq}$	mM	equilibrium solubility

For the reaction to occur, hydrogen has to move from the gas into the liquid phase; therefore, its diffusion determines the maximum rate of the over-all reaction. The mass transport from the gas phase into the organic phase can be described by the two-film theory *[Whitman 1923]*. Alternatively, other theories can be used, but they essentially yield the same results, but

require more sophisticated mathematics *[Levenspiel 1993, 1999]*.

The area of the interface A and the mass transport coefficient k_l determine the rate of hydrogen solvation. In general A and k_l are not directly accessible by experimental methods. In different literature references it is documented that the rate of solvation is limiting the overall reaction rate *[Sun 1996; Sun, et al. 1997]*. Different methods have been established to overcome this limitation. The two standard solutions to this problem are: Application of an increased hydrogen pressure within an autoclave to increase the gradient of the hydrogen concentration as driving force or to incorporate appropriate stirrers to increase the limiting interface. Several authors describe a dependency of the reaction rate on the speed of agitation; commonly the reaction is started by stirring *[Sun 1996; Sun, et al. 1997]*. Only increasing the area of the interface and reduction of the diameter of the liquid film leads to an increased overall reaction rate.

Here, a new methodology for hydrogenations has been developed *[Bommarius, et al. 2001]* that will be applied in the following throughout in hydrogenations using chemzymes or enzymes: If a dense membrane replaces the gas/liquid interface, the two parameters A and k_l become decoupled (Figure 4.10). Additionally, the overall pressure p is now separated into the two partial pressures, p_g and p_l, for the gas- and the liquid phase, respectively. By this means it is possible to establish a pressure difference between the gas and the liquid phase. This method has already been successfully established and applied previously for the supply of oxygen to the liquid phase via dense silicon membranes (silicon tubings) in fermentations of mammalian cells *[Noll, et al. 1996]* as well as in biotransformations *[Bongs, et al. 1997; Rissom, et al. 1997]*.

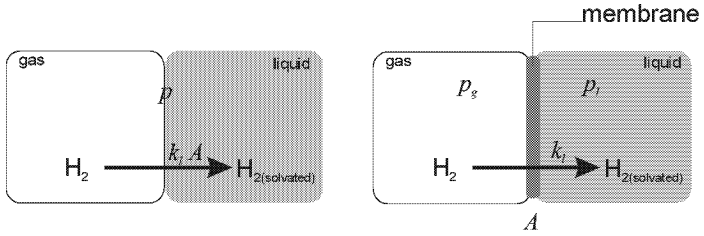

Figure 4.10: Decoupling of A and k_l by replacing the interface by a dense membrane (left: classical gas/liquid interface, right: membrane-separated gas and liquid phase).

When applying continuously operated membrane reactors, as with chemzymes and enzymes, additional advantages arise: On the retentate side of the membrane reactor, which correponds to the actual reaction volume, no gas phase is involved. By this means the control of the residence time in the reactor is simplified. In comparison to classical autoclaves, where the gas volume accounts for one third to one half of the reactor volume, the effective gas volume in the reactor is reduced drastically in the approach as chosen here. Besides practical aspects, this does also minimize the risks introduced by using gaseous hydrogen.

As appropriate tubing materials, different polymers were characterized in view of their mass transport characteristics for hydrogen. The mass transport over a dense polymer membrane is comparable to heat transfer *[Fitch, et al. 1993; Gieck, Gieck 1995; Compan, et al. 1999]*, and the same laws can be applied. The mass transport $\dot{n}$ is proportional to the differential pressure Δp and anti proportional to the thickness of the membrane d_o - d_i (eq. 4-2 and Figure 4.11, left). The material-specific constant κ depends on the type of gas and the membrane material used (for a detailed deviation of eq. 4-2 see *[Greiner 2002]*).

$$\dot{n} = \frac{\kappa_{H_2} \pi l \Delta p}{\ln d_o - \ln d_i}$$

with:				
	$\dot{n}$	mol s^{-1}	mass transport	
	κ_{H_2}	mol s^{-1} m^{-1} bar^{-1}	material-specific transport coefficient	**eq. 4-2**
	l	m	tubing length	
	Δp	bar	differential pressure	
	d_o	m	outer diameter	
	d_i	m	inner diameter	

The higher the differential pressure, the thinner the membrane, and the larger the area A, the higher is the mass transport. However, the thicker the membrane, the higher is the pressure, which the membrane has to retain. But at the same time, higher pressures need to be applied to achieve the same level of mass transport.

In Figure 4.11, right, different tubing materials (membranes) are compared in regard to their material-specific constants κ_{H_2}. PTFE (polytetrafluoroethylene) exhibits the highest mass transport coefficient κ_{H_2} for molecular hydrogen. Furthermore, it is commercially available in different shapes and diameters.

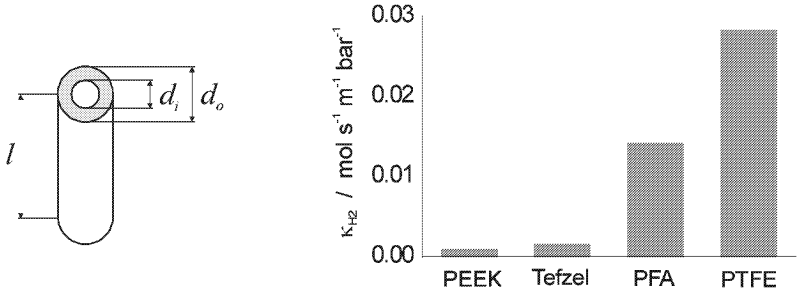

Figure 4.11: Left: dimensions of a tubing; right: mass transport coefficient κ_{H_2} compared for different polymer materials (PEEK = poly(ether-ether ketone), Tefzel = ethylene tetrafluoro-ethylene, PFA = perfluoroalkoxy, PTFE = polytetrafluoroethylene).

4.1.2 Volume aerated membrane reactor

The proposed membrane aeration was realized via a newly developed module. A membrane tubing consisting out of Teflon was placed concentrically into the center of stainless steal tubing as outlined in Figure 4.12, unit 4. This set up is similar to that of a concentric double-pipe heat exchanger, with the only difference that instead of heat the gaseous compound hydrogen is transported from one chamber into the other. Additionally, it is easily scalable via a tube bundle. The gaseous hydrogen is defusing out of the gaseous volume through the membrane into the liquid medium on the opposite side of the membrane. There, hydrogen is solubilized in the liquid medium. The transmembrane pressure drop is the driving force for the permeation of the H_2, and the rate thereof can conveniently be controlled by selecting and maintaining the inner pressure of the tubular aeration membrane independently from the pressure within the liquid phase using a back pressurizing valve. As a result an effective decoupling of the gas and liquid pressure can be achieved within the limits of the burst pressure of the aeration membrane employed. For continuous membrane filtration a closed liquid volume is favorable, because the residence time of the reactants can thus be controlled by flow control of the liquid alone, making mass balancing for the gas phase unnecessary. The flow scheme of the newly developed continuously operated reactor for hydrogenations with molecular hydrogen catalyzed by chemzymes as well as by enzymes (➲ chapter 4.2.4, page 129) is shown in Figure 4.12 (photo Figure 4.13). The filtration module also serves as a heat exchanger thermostating the whole liquid volume of the reactor.

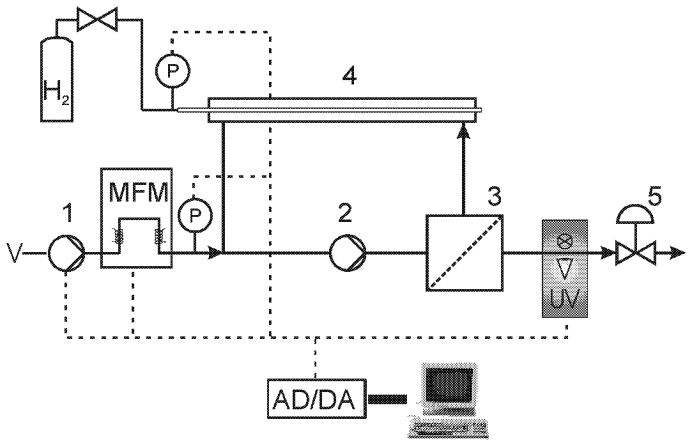

Figure 4.12: Flow scheme of the volume aerated membrane reactor (1: starting material feeding pump, 2: circulation pump, 3: ultrafiltration membrane unit, 4: volume aeration, 5: membrane valve, AD/DA: analog-digital/digital-analog converter, MFM: mass flow meter, p: pressure detection, UV: UV detection)

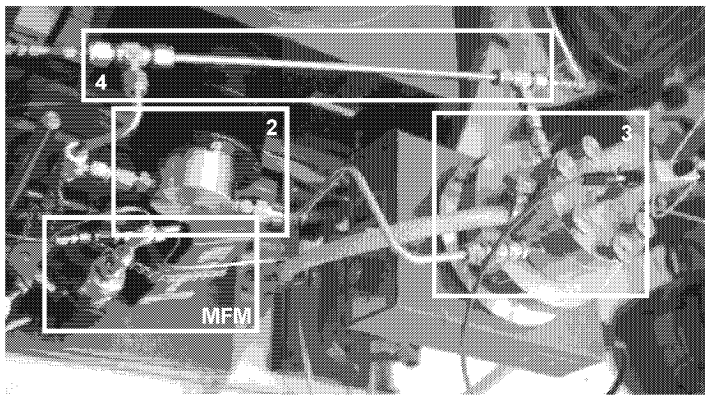

Figure 4.13: Photo of the volume aerated membrane reactor.

The starting material is supplied using an alternating piston pump. It is advantageous to apply a gear pump as a circulation pump to establish turbulent flow conditions in the aeration module, thus avoiding concentration gradients over the cross section of the aeration module. The surface to volume ratio in the aeration module is 3.8 $cm^2\ mL^{-1}$. The fraction of the gas volume on the total reactor volume is 10^{-3}.

Concentration gradients in the double-pipe heat exchanger are circumvented by establishing turbulent flow *[Levenspiel 1999]*. The respective minimal flow rates can be calculated for different solvents via the definition of the dimensionless *Reynolds* number *Re* (eq. 4-3) *[Gieck, Gieck 1995]*.

$$Re = \frac{\upsilon\, d_h\, \rho}{\eta}$$

eq. 4-3

with:			
	Re	-	*Reynolds* number
	υ	$m\ s^{-1}$	liquid velocity
	d_h	m	hydraulic diameter
	ρ	$kg\ L^{-1}$	density
	η	$Pa\ s = kg\ m^{-1}\ s^{-1}$	dynamic viscosity

The geometry of the aeration module is taken into consideration in the definition of the hydraulic diameter d_h (eq. 4-4).

$$d_h = 4\frac{A_Q}{\pi\left(d_i' + d_o\right)}$$

eq. 4-4

with:			
	A_Q	m^2	cross section of flow area
	d_i'	m	inner diameter of outer tubing

The flow rate F is accessible via the definition of the velocity of the liquid υ (eq. 4-5).

$$\upsilon = \frac{F}{A_Q} \qquad \text{eq. 4-5}$$

with: F $m^3\ s^{-1}$ flow rate

Turbulent flow is established, if $Re > 2320$ *[Gieck, Gieck 1995]*. The minimal required flow rate F_{min} to reach turbulent flow is correlated to the sum of the characteristic diameter $d_i' + d_o$ and dependent on the material-specific constant. Therefore, a minimal diameter of both tubings needs to be chosen. F_{min} can be calculated by using eq. 4-3 (substituted with equations eq. 4-4 and eq. 4-5, $Re = 2320$). In Table 4.2 the resulting minimal flow rates F_{min} in the volume aeration module are listed for different solvents. All experiments were carried out by establishing the minimal required flow rate.

Table 4.2: **Minimal flow rates F_{min} that are needed to reach turbulent flow ($Re > 2320$) in the membrane aeration module for different solvents ($d_i' = 4.0$ mm, $d_o = 1.6$ mm, $T = 40$°C).**

solvent	dynamic viscosity η / 10^{-4} Pa s	Density ρ / kg L^{-1}	minimal flow rate F_{min} / L min^{-1}
water	6	0.98	0.38
THF	2	0.89	0.14
methanol	8	0.81	0.61
ethanol	9	0.76	0.74
2-propanol	10	0.65	0.96

4.1.3 System characterization

To kinetically characterize the PyrPhos catalysts as well as the PyrPhos chemzyme, standard reaction conditions needed to be established. This does also include a constant hydrogen pressure throughout the kinetic experiment, because otherwise the effective hydrogen concentration in the liquid phase would change. In a classical autoclave the hydrogen pressure is decreasing during the course of the reaction, since hydrogen is consumed as reduction equivalent. The result is an alteration of the driving force for the phase transition of hydrogen. Therefore, a constant pressure autoclave was set up as shown in the flow scheme Figure 4.14. A constant hydrogen flow is measured using with a mass flow meter (MFM). The hydrogen flow is regulated with the control valve 2.

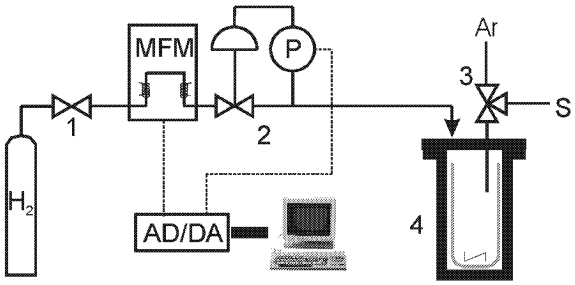

Figure 4.14: **Flow scheme of the constant pressure autoclave (1: valve, 2 control valve, 3 three way valve, 4: autoclave, AD/DA: analog-digital/digital-analog converter, MFM: mass flow meter, p: pressure detection, S: starting material).**

The whole setup is controlled and regulated via a computer. The recorded real-time data can then be used for kinetic investigations. The results of a typical experiment are shown in Figure 4.15. At first an activation of the catalyst is observed, which results in an oscillation of the hydrogen flow caused by the closed loop control unit. After activation of the PyrPhos an even hydrogen flow results that can be used to determine the reaction rate in the range of the zeroth order reaction. In this range of the reaction the activation is finalized as can be seen from Figure 4.15.

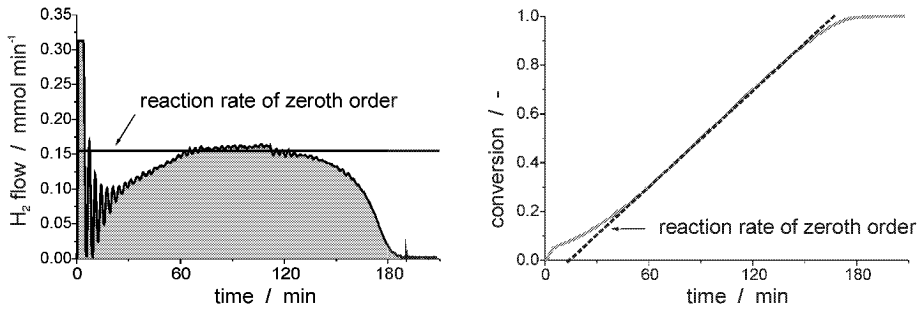

Figure 4.15: **Typical reaction course of a hydrogenation and resulting zeroth order reaction rate (p_{H2} = 10.0 bar constant, 0.5 mM PyrPhos, 0.5 M 2-acetoamido cinnamic acid, T = 25°C, methanol).**

The activation of the catalyst proceeds via liberation of the 1,5-cyclooctadiene *[Burk, et al. 1998]*. During the course of the activation the kinetic parameters cannot be determined.

As simple kinetics the following rate equation is assumed to describe the PyrPhos catalyst appropriately (eq. 4-6). Here, one important assumption is that the mass transport of molecular hydrogen is not rate limiting. This is true for a slow catalytic reaction and results from the linear fraction of the rate as function of the catalyst concentration [*cat*].

$$\upsilon = [cat]\frac{tof \cdot [AA]}{K_M + [AA]}$$

with:				eq. 4-6
	υ	mmol L^{-1} min^{-1}	reaction rate	
	tof	min^{-1}	turnover frequency	
	$[AA]$	mM	2-acetoamido cinnamic acid	
	$[cat]$	mM	catalyst	
	K_M	mM	*Michaelis-Menten* constant	

In case of high substrate concentrations $[AA] >> K_M$ the following approximation is valid (eq. 4-7):

$$\upsilon = [cat]tof \qquad \text{eq. 4-7}$$

In other words: Within the range of catalyst saturation (zeroth order), the reaction rate is linear in respect to the catalyst concentration. This is shown in Figure 4.16 for the non-immobilized PyrPhos catalysts and the PyrPhos chemzyme. The non-immobilized catalyst reaches a $tof = 20$ min^{-1} up to a catalyst concentration of 0.2 mM, - which is valid irrespective of the solvent applied. The non-linearity at higher catalyst concentrations is introduced by a limitation in the hydrogen supply. The difference between the characteristics of the two solvents is caused most likely by their different viscosities (Table 4.2, page 112). The PyrPhos chemzyme is approximately eight times slower than its non-immobilized variant ($tof = 2.7$ min^{-1}) in relation to the active sites (Rh).

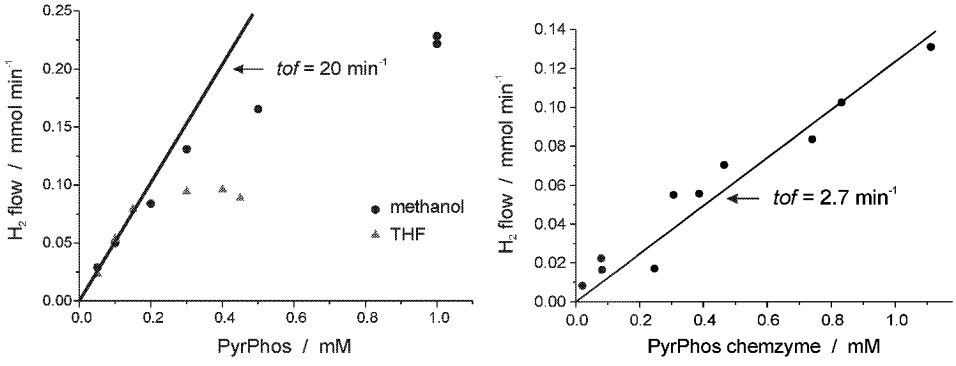

Figure 4.16: Hydrogen flow as function of the catalyst concentration: left: non-immobilized PyrPhos, right: PyrPhos chemzyme (p_{H2} = 10.0 bar constant, 0.5 M 2-acetoamido cinnamic acid, T = 25°C).

The hydrogen pressure determines the solubility of hydrogen in the liquid phase as defined by *Henry's* law (eq. 4-1). By increasing the hydrogen pressure the hydrogen concentration is increased as well. The turnover frequency is a linear function of the hydrogen pressure in the investigated range (eq. 4-8), respectively the hydrogen concentration in the liquid phase, as

can be seen from Figure 4.17.

$$tof_{p_{H2}} = K_{tof_{pH2}} \cdot p_{H_2} \qquad \text{eq. 4-8}$$

with:			
	$tof_{p_{H2}}$	min^{-1}	p_{H2} dependent turnover frequency
	$K_{tof_{pH2}}$	$min^{-1}\ bar^{-1}$	p_{H2} dependent correlation constant

The non-immobilized catalyst reaches $K_{tof_{pH2}} = 2.3 \pm 0.1\ min^{-1}\ bar^{-1}$. With the *Henry* constant for methanol of $H_{H2} = 0.27\ bar\ mM^{-1}$ equation eq. 4-8 can be reformulated as a function of the hydrogen concentration. The respective constant is then $K_{tof_{[H2]}} = 0.62 \pm 0.1\ min^{-1}\ mM^{-1}$. This dependence of the adsorption kinetics of the catalyst is astonishing, since normally a hyperbolic function would be expected *[Sun, et al. 1997]*. The linear correlation between the hydrogen pressure, respectively the hydrogen concentration, and the turnover frequency demonstrates that the affinity between the catalyst and hydrogen is low. An extrapolation to the saturation limit is not valid. Investigations by other authors have shown that the linear range goes up to twice the pressure of $p_{H2} = 50$ bar *[Nagel, et al. 1986]*. In the case of the chemzyme a $K_{tof_{pH2}} = 0.27 \pm 0.5\ min^{-1}\ bar^{-1}$ is reached.

The linear dependency on the hydrogen concentration has two consequences for practical applications of the catalyst:

- The saturation limit of the catalyst in regard to H_2 is not reached within the range of the applied pressure.
- To reach reasonably high activities, a corresponding pressure p_l needs to be applied onto the liquid phase (Figure 4.10 and eq. 4-2, page 108).

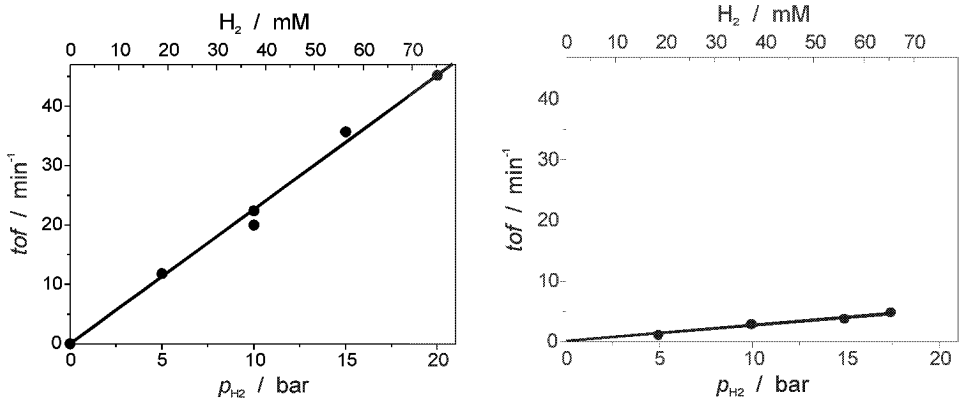

Figure 4.17: Turnover frequency as function of the hydrogen pressure, respectively the hydrogen concentration. Left: non-immobilized PyrPhos, right: PyrPhos chemzyme (p_{H2} = 10.0 bar constant, 0.5 M 2-acetoamido cinnamic acid, 0.5 mM PyrPhos, 1 g L^{-1} chemzyme = 0.5 mM (Rh), T = 25°C).

The reaction product (*R*)-*N*-acetyl-phenylalanine can be recrystallized from water. After fractional crystallization an *ee* > 99.5% is reached. In total, over 100 g of (*R*)-*N*-acetyl-phenylalanine were produced during all these kinetic experiments.

4.1.4 Synthesis in the volume aerated membrane reactor

To prove the applicability and suitability of the volume aeration unit, at first a batch reaction was carried out. For this reason, we used a simplified setup, leaving out the ultrafiltration unit (Figure 4.12 without 1, 3 and MFM). The aeration unit was replaced by a larger one, providing a larger membrane area (400 cm^2). Using this setup a batch reaction, - or in respect to hydrogen a fed-batch reaction, - was performed. The hydrogen flow was measured, which is necessary to keep the pressure constant on the gaseous side of the membrane. During the reaction the differential pressure was raised from 3 to 4 bar. The conversion calculated from the hydrogen flow matches the conversion as estimated by independent analysis from samples withdrawn during the reaction (Figure 4.18). The enantiomeric excess was not altered compared to previous findings *[Nagel, et al. 1986]*.

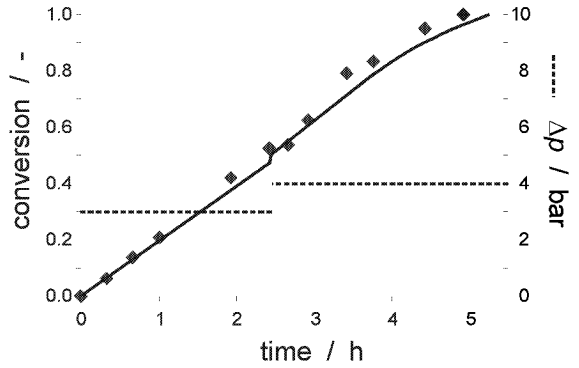

Figure 4.18: Batch conversion in the volume aerated membrane reactor; the squares represent the conversion calculated on GC measurements, and the line represents the conversion calculated based upon the hydrogen flow (p_l = 8.0 bar, 0 – 2.4 h: p_{H2} = 11.0 bar constant, 2.4 – 5 h: p_{H2} = 12.0 bar constant, 0.25 M 2-acetoamido cinnamic acid, 1 mM PyrPhos, T = 30°C).

The continuous process was carried out in the volume aerated membrane reactor as outlined in Figure 4.12, page 110. In comparison to the above-described batch reaction, a smaller membrane area of the PTFE tubing was used (14 cm^2). Nevertheless, the surface to volume ratio in the aeration module itself even increased from 3.6 to 3.8 cm^2 mL^{-1}.

In Figure 4.19 the conversion is plotted as a function of the number of residence times for one continuous experiment. At a residence time of τ = 2.0 h the hydrogen supply via the PTFE membrane seems to be limiting, and only a low conversion is reached. By increasing the residence time to τ = 5.7 h, the conversion is approximately doubled. A further addition of

catalyst after 97 h (17 residence times of 5.7 h) leads to a maximal conversion of 0.6, which is instable. Furthermore, a fast decrease of the conversion is observed. Non-linear regression of the conversion decrease delivers an apparent retention of r = 0.78 for the chemzyme. The dotted line denotes the case, where no retention of the chemzyme would be given. The value of the apparent retention differs drastically from the independently determined retention of r = 0.99 *[Wöltinger 2001]*. Possibly the chemzyme or the precious metal Rh exhibits either a worse retention as compared to before the activation or the chemzyme is deactivating faster under real reaction conditions. After the experiment, a black precipitation was observed on the surface of the ultrafiltration membrane. This precipitate might have been rhodium, which could not be verified, however.

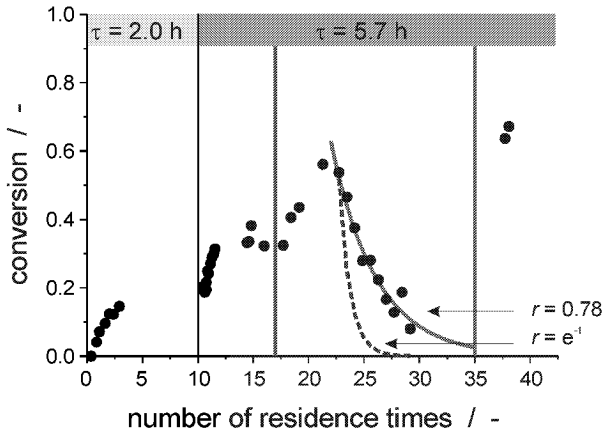

Figure 4.19: Hydrogenation in the continuously operated volume aerated membrane reactor with the PyrPhos chemzyme (p_t = 9.0 bar, p_{H2} = 24.0 bar constant, 0.1 M 2-acetoamido cinnamic acid, T = 40°C).

4.1.5 Summary

- The bisphosphine catalyst PyrPhos was immobilized on a homogeneously soluble polymer *N-iso*-propyl-polymethacrylamide yielding a chemzyme corresponding to 11 catalytic active sites.
- The non-immobilized PyrPhos catalyst as well as the chemzyme has been investigated and characterized kinetically. In case of the chemzyme, the selectivity stays unchanged, but the turnover frequency is reduced by factor 8.
- The PyrPhos chemzyme demonstrates in continuous experiments a very low stability, preventing efficient usage thereof.
- A constant-pressure autoclave was developed incorporating flow measurement and

control of the hydrogen.

- A new membrane aeration technique for supplying defined quantities of gaseous hydrogen was developed that can be applied for chemo- as well as for biocatalysis (chapter 4.1.1, page 107). Polytetrafluoroethylene (PTFE) proved to be the best membrane material in view of its hydrogen permeability and chemical stability. The advantages are:
  - A defined interfacial area,
  - the liquid and the gas pressure can be controlled separately, thereby allowing for a precise control of the mass transition.

- For continuous operation a circulating reactor with a double-pipe aeration module was setup (surface to volume ratio in the aeration module of 3.8 cm^2 mL^{-1}).

- The applicability of the newly developed hydrogen aeration technology has been demonstrated using both a batch and a continuous hydrogenation as typical examples.

- In total, over 100 g (*R*)-*N*-acetyl-phenylalanine were produced with an *ee* > 99.5% after fractional crystallization.

4.2 Direct hydrogenation with enzymes[37]

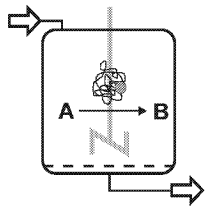

In this chapter, hydrogenations with molecular hydrogen as reduction equivalents catalyzed by biological catalysts, the hydrogenases, are discussed. The same physical and chemical laws apply here as with the already discussed chemical catalyst (➲ chapter 4.1, page 103). Also the suitability of the volume aeration method developed for chemical hydrogenations (➲ chapter 4.1.2, page 110) will be demonstrated for biocatalyzed hydrogenations. After a short introduction devoted to hydrogenases the generation and regeneration of NADPH with molecular hydrogen will be discussed.

Classical hydrogenases are bi-directional enzymes that catalyze the production *[Selvaggi, et al. 1999; Woodward, et al. 2000a; Woodward, et al. 2000b]* and oxidation *[Ma, et al. 2000]* of molecular hydrogen. The enzymatic reaction is represented by the equation:

$$H_2 \rightleftharpoons 2\,H^+ + 2\,e^-$$

Actually, the enzymatic cleavage of H_2 is herein heterolytic: $H_2 \Rightarrow H^+ + H^-$ *[Krasna 1978]*. The enzymes may differ in many properties, e.g., in their specificities for electron carriers, which are either reduced with H_2 or from which hydrogen can be evolved *[Schlegel, Schneider 1978]*. Generally, the hydrogenases are divided into two major groups on the basis of the metal content of their respective dinuclear catalytic centers: the "iron-only" [FeFe]-hydrogenases and the [NiFe]-hydrogenases *[Nicolet, et al. 2000; Frey, et al. 2001; Lemon, Peters 2001; Frey 2002]*. [FeFe]-hydrogenases contain only [FeS]-clusters, of which one

[37] **Parts of this chapter are published in:**
This project was carried out in close collaboration with the working groups of Dr. H. Haaker, University of Wageningen, The Netherlands and of Prof. F. Hagen, University of Delft, The Netherlands.

1. L. Greiner: *Prozessentwicklung für die katalytische Reduktion mit molekularem Wasserstoff*, PhD-thesis, University of Bonn (2002)
2. R. Mertens: *Reaktionstechnische Charakterisierung der Darstellung von NADPH mit Pyrococcus furiosus Hydrogenase I*, diploma thesis, University of Bonn (2001)
3. R. Mertens: *Prozessentwicklung für biokatalytische Hydrierungen mit molekularem Wasserstoff*, PhD-thesis, University of Bonn (in progress)
4. L. Greiner, D. Müller, E. van den Ban, J. Wöltinger, C. Wandrey, A. Liese: *Membrane aerated hydrogenation: Enzymatic and chemical homogeneous catalysis*, Advanced Synthesis & Catalysis 345 (2003) 679-683
5. R. Mertens, L. Greiner, E. C. D. van den Ban, H. Haaker, A. Liese: *Practical applications of hydrogenase I from Pyrococcus furiosus for NADPH generation and regeneration*, Journal Molecular Catalysis B, Enzymatic 24-25 (2003) 39-52
6. A. Buchholz, L. Greiner, C. Hoh, A. Liese: *Genetic algorithms as tool for capillary electrophoresis method development*, Journal of Capillary Electrophoresis and Microchip Technology 7(3&4) (2002) 51-60
7. E. van den Ban, H. Haaker, L. Greiner, R. Mertens, A. Liese: *Verfahren zur enzymatischen Reduktion von Substraten mit molekularem Wasserstoff*, German patent application DE 101 39 958.8 (21.08.2001)
8. A. Bommarius, H.-P. Krimmer, D. Reichert, J. Almena, A. Karau, J. Wöltinger, K. Drauz, A. Liese, L. Greiner, C. Wandrey: *Volumenbegasung*, German patent application DE 101 63 168.5 (21.12.2001)

functions as the "H-cluster", binding the hydrogen. The latter usually tends to be more reactive towards the hydrogen production, whereas the former [NiFe]-hydrogenases are less reactive and more involved in the hydrogen oxidation in the electron flow chain *[Adams 1990]*. The hydrogen activation takes place at the dinuclear catalytic center (Figure 4.20) *[Albracht 1994]* It is proven that oxidation of hydrogen, respectively the reduction of protons, takes place separated from other processes at the α-subunit. The protons are solvated and the electrons are transferred internally to the β-subunit. Although the exact catalytic mechanism remains to be elucidated. The hydrogenase applied here is derived from *Pyrococcus furiosus* and belongs to the class of the [NiFe]-hydrogenases. The reduction of $NADP^+$ takes place at the FAD-binding site (Figure 4.20):

$$NADP^+ + H^+ + 2e^- \rightleftharpoons NADPH$$

There might be different reasons for the separation of the oxidation and the reduction. For one, the enzyme can function as a switch in metabolism, since the electrons can be transferred to different acceptors. Additionally, the separation prevents deactivation of the acid-labile NADPH by the generated proton. By this means local pH-minima are prevented on the site of reduction, which would lead to a fast deactivation of the NADH and NADPH.

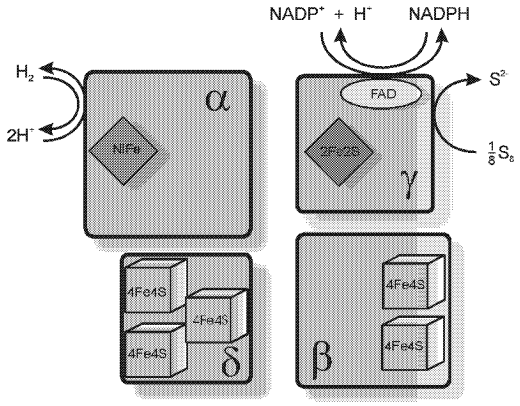

Figure 4.20: Hetero-tetrameric structure of the hydrogenase from *Pyrococcus furiosus* and the redox-active metal centers as well as the FAD binding site *[Silva, et al. 1999]*.

The organism hosting the hydrogenase used in this study, *Pyrococcus furiosus* (DSM 3638), was originally isolated from geothermally heated marine sediments near Vulcano, Italy (1986) and is a strictly anaerobic hyperthermophilic archaeon. It harbors two soluble [NiFe]-hydrogenases, namely Hydrogenase I and Hydrogenase II *[Bryant, Adams 1989a; Ma, et al. 2000]*. *P. furiosus* is a heterotroph that grows optimally at temperatures above 90°C *[Fiala, Stetter 1986]*. Due to its unusual ability to grow without elemental sulfur, large-scale cultures of *P. furiosus* can be grown in conventional fermenters *[Adams 1991; Krahe, et al. 1996;*

Biller, et al. 2002]. In the absence of S^0, the role of *PF*H I was proposed to be H_2 production using NADPH as the electron donor *[Ma, et al. 1994]*. In contrast, kinetic studies could show, that the reduction of $NADP^+$ with hydrogen *in vitro* proceeds almost 10 times faster than the oxidation of NADPH *[Silva, et al. 2000; van den Ban 2001]*. Therefore, detailed insight into the *in vivo* function of this enzyme will require additional analyses and studies, which are currently in progress in several research groups.

The soluble *PF*H I, formerly known as *PF* sulfhydrogenase, was purified to homogeneity *[Bryant, Adams 1989b]* and the genome sequence is known *[Payen, et al. 1983]*. However, up until now no expression system is known allowing overproduction in another organism. It is capable of generating the cofactor NADPH directly from the oxidized β-nicotinamide adenine dinucleotide phosphate cofactor ($NADP^+$) with hydrogen as reducing agent without producing any by-products other than protons (Figure 4.21). The reduction of $NADP^+$ is 1,4-regioselective. Because of the conjugation of the double bonds, the 1,6-dihydropyridine is the energetically favored one that is not produced by the *PF*H I. NADPH was found to be the physiological substrate *[Ma, et al. 1994]*. Therefore, the high biotechnological potential of *PF*H I for the synthesis of NADPH, as well as for the enzyme-coupled *in situ* NADPH-regeneration is evident (Figure 4.22).

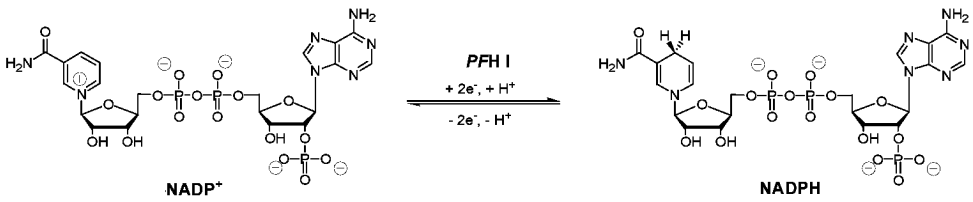

Figure 4.21: Regioselective 1,4-reduction of the pyridine in $NADP^+$ catalyzed by the hydrogenase I (*PF*H I) from *Pyrococcus furiosus*.

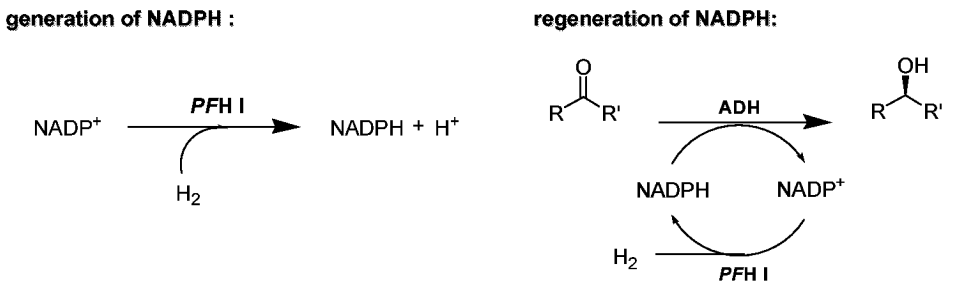

Figure 4.22: Left: Generation of NADPH; right: regeneration of NADPH in an enzyme-coupled system.

4.2.1 Generation of NADPH

The synthesis of NADPH can be carried out by means of chemical, electrochemical or enzymatic methods. However, not many processes for the direct generation of reduced β-nicotinamide adenine dinucleotide phosphate have been published. The enzyme–free chemical (Figure 4.23) and direct electrochemical methods suffer from low selectivity and undesirable side reactions *[Day, et al. 1972; Chenault, Whitesides 1987a; Peters 1998a]*.

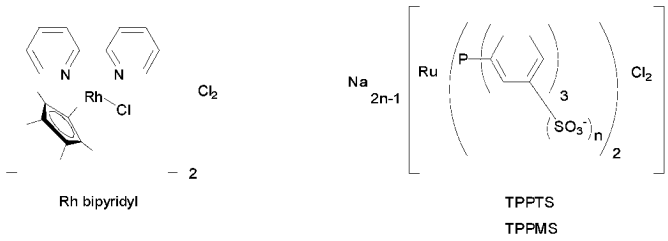

Figure 4.23: Homogeneous catalysts for the regioselective 1,4-hydride addition to NAD^+ and $NADP^+$ ***[Ruppert, et al. 1988b; Steckhan, et al. 1990; Hembre, et al. 2000].***

Indirect electrochemical processes circumvent these problems by using mediators, but these agents often interfere with downstream processing *[Ruppert, et al. 1988a]*. In 1983 Eguchi *et al. [Eguchi, et al. 1983]* reported the utilization of resting methanogenic bacteria cells as biocatalysts in the reduction of $NADP^+$ with formate or hydrogen. With a maximum conversion of 60 %, they could achieve an analytical yield of approximately 6 g/L NADPH. However, the limiting factor was the cultivation of the strictly anaerobic cells. An enzymatic generation of NADPH from $NADP^+$ and L-malic acid was achieved with the soluble L-malic:$NAD(P)^+$ oxidoreductase from *Achromobacter parvulus* IFO-13182 (EC 1.1.1.39-40) *[Suye, Yokoyama 1985]*. Under optimized conditions, quantitative conversion yielded about 8.9 g/L NADPH after 4 h. Another common enzymatic method is the D-glucose-6-phosphate dehydrogenase (G6P-DH; EC 1.1.1.49)-catalyzed reduction of β-$NADP^+$ with glucose-6-phosphate *[Wong, Whitesides 1981]*. Since the thermodynamics of this reversible reaction is in favor of the substrate, this process has to be carried out with a surplus of expensive glucose-6-phosphate. More favorable thermodynamics and less interference of by-products are encountered according to a method using a recombinant $NADP^+$-specific formate dehydrogenase (EC 1.2.1.2). This approach has gained much attention, since it reduces $NADP^+$ utilizing formate as a cheap substrate, generating only gaseous CO_2 and NADPH *[Tishkov, et al. 1999b]*. Isolated hydrogenases are so far, - up to our knowledge, - only applied for the regeneration of the nicotinamide cofactors and not for their production. For this purpose, not many systems are known, which involve a hydrogenase as regenerating enzyme *[Klibanov, Puglisi 1980; Wong, et al. 1981; Klibanov 1983; Okura, et al. 1987a, 1987b; Otsuka, et al. 1989; Hasumi, et al. 1995]*. This restriction stems from the availability of $NADP^+$-specific hydrogenases. To

date, there are only the *Alcaligenes eutrophus* H16 hydrogenase, the *Desulfovibrio fructosovorans* hydrogenase, a hydrogenase from *Anacystis nidulans,* and a membrane-bound hydrogenase from *Klebsiella pneumoniae,* which utilize NAD(H) - besides the *PF*H I and *PF*H II known to be capable to utilize NADP(H) as a redox equivalent *[Schneider, Schlegel 1976; Peschek 1979; Keefe, et al. 1995; De Luca, et al. 1998; Steuber, et al. 1999]*. These enzymes are mainly applied for the regeneration of NADPH (➲ chapter 4.2.5, page 130).

4.2.2 Analytics

For a characterization of the hydrogenase a quantitative analytical procedure for the determination of $NADP^+$ and NADPH must be established. Often a photometrical method is applied to determine NADPH ($\lambda_{max,\ NADPH}$ = 340 nm) *in situ*. $NADP^+$ is in general determined by an enzymatic transformation to NADPH. For an exact quantification of the hydrogenation this is not sufficient. To establish a mass balance, all reactants need to be quantified at the same conversion point. Additionally, the reaction product NADPH is not very stable, as will be shown later on (➲ chapter 4.2.3, page 124). These constraints required the development of a new analytical procedure. Capillary electrophoresis (CE) proved to be the appropriate method. CE allows for the electrophoretic separation of individual substances and their detection by various means, e.g., by direct or indirect UV-VIS absorbance, as well as by fluorescence or mass spectrometric detection. To optimize the separation quality a genetic algorithm was used *[Buchholz, et al. 2002]*. Genetic algorithms were already successfully applied for the optimization of selectivity and yield in a biotransformation (➲ chapter 3.2.2.2, page 72). In the following approach, six parameters were considered for optimization, namely: injection time, voltage, buffer pH, buffer concentration, temperature, and overlaid pressure. After four generations, the mean separation quality was increased and the analysis time was reduced. At the same time all β-nicotinamide adenine dinucleotide cofactors can be analyzed (Figure 4.24, left) and additionally the decomposition product of NADPH can be analyzed (Figure 4.24, right, $\lambda_{max,\ NADP^+}$ = 254 nm, $\lambda_{max,\ decomposed\ NADPH}$ = 266 nm).

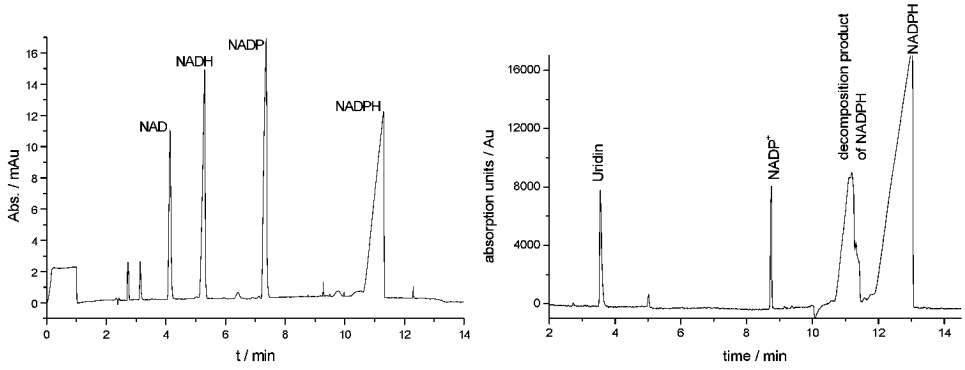

Figure 4.24: Electropherogram of the β-nicotinamide adenine dinucleotide cofactors (left: phosphorylated and non-phosphorylated, right: phosphorylated including decomposition product of NADPH; buffer: 40 mM phosphate & 10 mM borate, pH 8.5, 40°C, 30 kV, 1 mM uridine as internal standard, UV-detection: λ = 254 nm).

System investigations

The reduction of $NADP^+$ to NADPH by molecular hydrogen is a redox reaction. The respective equilibrium constant is defined via the law of mass-action (eq. 4-9). The equilibrium is far on the side of the products with an equilibrium constant of $K_{eq,\,PFHI} = 1.1\ 10^3$ *[Greiner 2002]*. The protons formed are removed from the equilibrium by titration or by buffering of the pH. Additionally, the initial concentration of molecular hydrogen is kept constant by the equilibrium of gas and liquid phase, which also shifts the reaction equilibrium onto the side of the products. The equilibrium constant is in the same order of magnitude as the one for the reduction of NAD^+ to NADH catalyzed by formate dehydrogenase (FDH) utilizing formate ($K_{eq,\,FDH} = 0.42\ 10^3$) *[Goldberg, et al. 1993]*.

$$1\ NADP^+ + 1\ H_2 \rightleftharpoons 1\ NADPH + 1\ H^+$$

$$K_{eq,PFHI} = \frac{[H^+]_{eq}[NADPH]_{eq}}{[H_2]_{eq}[NADP^+]_{eq}} = 1.1 \cdot 10^3 \quad (298\,K) \qquad \text{eq. 4-9}$$

So far, it has not been possible to carry out a detailed kinetic study, because the activation mechanism is not yet understood. This will become especially evident during the discussion of the repetitive batch experiments (➲ Figure 4.27, page 127).

One major point to still consider is the limited stability of the reaction product NADPH. There are some general tendencies regarding the stability of β-nicotinamide adenine dinucleotide cofactors *[Chenault, Whitesides 1987b]*:

- The reduced cofactors are less stable than their oxidized forms.
- The oxidized forms are more stable than the reduced ones in an acidic milieu.
- The reduced forms are more stable than the oxidized ones in an alkaline milieu.
- The phosporylated ones deactivate faster.

The pH range from 6.5 to 9, shown in Figure 4.25, is most relevant for oxidoreductases. Most industrial reductive biotransformations are carried out in this pH range *[Liese, et al. 2000; Liese, et al. 2002]*. Total turnover numbers up to 600,000 for NADH have been reached *[Hummel, et al. 1987]*.

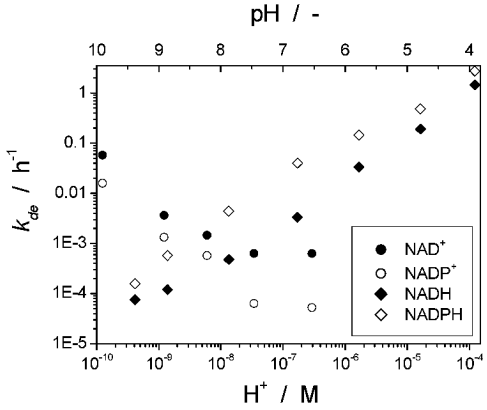

Figure 4.25: Deactivation constant k_{de} for β-nicotinamide adenine dinucleotide cofactors as function of pH after *[Chenault, Whitesides 1987b]* (0.1 mM cofactor, 50 mM buffer: pH 3-6 acetate, pH 6-8 TEA, pH >9 carbonate, T = 25°C)

The reduction of $NADP^+$ (**A**) is an almost quantitative reaction followed by an irreversible decomposition of NADPH (**B**) to ℂ. From a kinetic point of view this is the classical situation of a multi-step reaction sequence, as already discussed in (➲ chapter 3, page 19). The only difference to the systems discussed before is, that ℂ is the side product and **B** is the reaction product. The assumption of an irreversible reaction of first order is a simplification; also the observation of intra- and intermolecular reactions has been reported *[Wu, et al. 1986b]*.

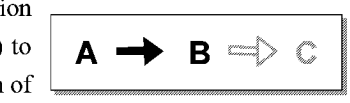

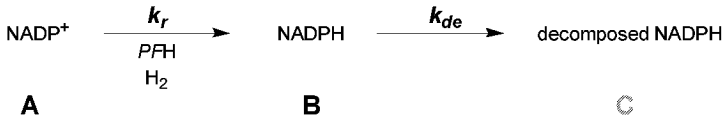

The typical course of a reaction as later shown in Figure 4.26 is caused by the simultaneous interplay of the NADPH formation (k_r) and decomposition (k_{de}) (eq. 4-10 and eq. 4-11).

$$\frac{d[\mathrm{NADP^+}]}{dt} = -k_r\,[\mathrm{NADP^+}] = -k\,[PF\mathrm{H}][\mathrm{NADP^+}] \qquad \textbf{eq. 4-10}$$

$$\frac{d[\mathrm{NADPH}]}{dt} = -k_{de}\,[\mathrm{NADPH}] + k_r\,[\mathrm{NADP^+}] \qquad \textbf{eq. 4-11}$$

Two typical conversion plots at 40°C in two different buffer systems are shown in Figure

4.26, left. Total turnover numbers (*ttn*) of 4,600 (EPPS buffer) and 7,060 (Tris-HCl buffer), respectively, could be reached in terms of NADPH with turnover frequencies (*tof*) of 28.7 h^{-1} and 44.0 h^{-1}. Although the activity of the hyperthermophilic enzyme increases exponentially with temperature and has its maximum above 80°C *[Ma, et al. 1994; van den Ban 2001]*, the reactions were performed at lower temperature (40°C) to compromise enzyme activity and thermal stability of NADPH *[Wong, et al. 1981; Wu, et al. 1986a]*. Nevertheless, the limiting factor still seems to be the low stability of NADPH at elevated temperatures. The course of the yield-conversion plot shows the typical characteristics for a reaction sequence **A** ⟶ **B** ⟶ ℂ, with **B** as reaction product decomposing ℂ (Figure 4.26, right). This decrease is initiated by the chemical decomposition of the cofactor under these reaction conditions, which are necessary in order to achieve a sufficient enzyme activity. The amount of the decomposition product formed in the EPPS-buffered process is higher than in the Tris-buffered reaction. The exact mechanism thereof and the decomposition product still have to be elucidated. Preliminary analytical measurements using capillary electrophoresis and IC-MS/MS techniques showed that the unknown substance has the same molecular mass as NADPH, but with an absorption maximum at 266 nm instead of 340 nm. No decay products of $NADP^+$ could be detected. Whether the decomposition product inhibits the enzyme has not yet been investigated.

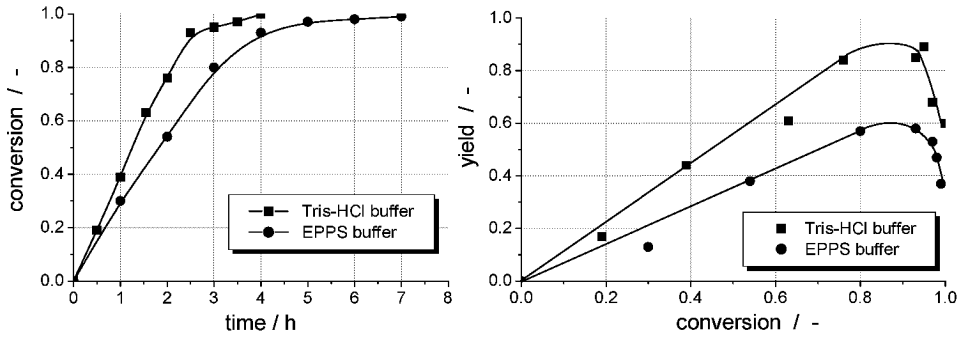

Figure 4.26: Batch hydrogenations in two different buffer systems; left: conversion as function of time, right: yield of NADPH as function of conversion. Lines are only drawn as visual aids (12 mM $NADP^+$, 200 mM EPPS-buffer (•) or 100 mM Tris-HCl buffer (■), pH 8.0, 0.26 mg/mL *PF*H I, p_{H2}1.1 bar, 40 °C).

To investigate the stability of the *PF*H I under reaction conditions a repetitive batch series was carried out. A reactor equipped with an ultrafiltration membrane was used for the repetitive batch process. Two separate experiments of 8 runs each were performed. The progression curves are shown in Figure 4.27. After reaching > 95% conversion, the reactor content was concentrated to approx. 7% residual volume and refilled with freshly prepared substrate solution. Within the first repetitive batch-series (Figure 4.27, left) a hydrogen pressure of 5.0 bar was applied for the first 6 runs. Since the initial reaction rate began to decrease, a higher hydrogen pressure of 7.5 bar was applied to find out, whether there were

any mass transfer limitations. This seemed not to be the case. During the whole course of the eight repetitive batch cycles no further dosage of *PF*H I was necessary. Over 8 runs, total turnover numbers (*ttn*) of 9,800 and 10,000, respectively, were achieved with the maximum analytical NADPH yield taken as a basis and the partially purified *PF*H I preparation treated as if it was pure hydrogenase.

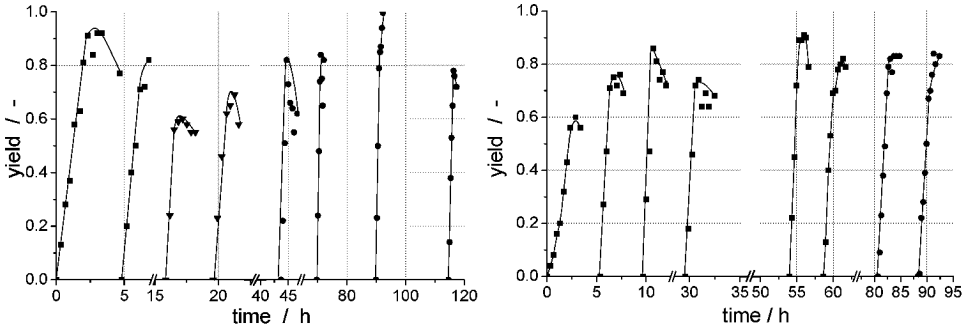

Figure 4.27: **NADPH production in two series of repetitive batch experiments, consisting of 8 runs each at different hydrogen pressures as indicated: (▼) p_{H2} = 2.5 bar, (■) p_{H2} = 5.0 bar, (•) p_{H2} = 7.5 bar. (12 mM $NADP^+$, 200 mM EPPS buffer, pH 8.0, 1.0 mg/mL *PF*H I, T = 40°C, YM10 membrane).**

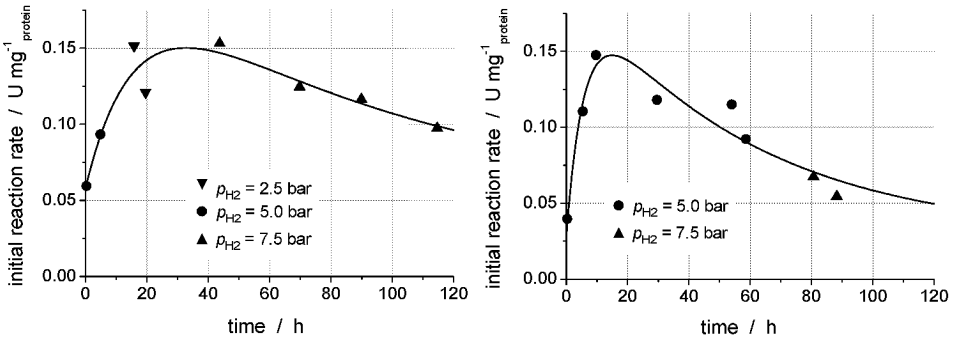

Figure 4.28: **Initial reaction rate of each individual batch as function of time for two independent repetitive batch series. Black line denotes the simulated course of initial activity based on eq. 4-12 (for reaction conditions see Figure 4.27).**

Astonishingly, a "reproducible" activation of the *PF*H is observed during the first three runs in two independent repetitive batch series (Figure 4.28), before a decrease, probably caused by deactivation of the *PF*H I, has been encountered. It is known, that [NiFe]-hydrogenases in general and the *PF*H I in particular need to be reductively activated prior to their use. Therefore, the crude *PF*H I preparation was pre-incubated at 80°C for 5 min under hydrogen atmosphere, following a standard protocol *[Silva, et al. 1999; Frey, et al. 2001]*, before transferring it avoiding oxygen into the reaction mixture.

This phenomenon can be kinetically described, if it is assumed that an "unready" *PF*H* is

irreversibly activated (k_{act}) to *PF*H, followed by an irreversible inactivation (k_{de}) leading to *PF*H†.

$$PFH^* \xrightarrow{k_{act}} PFH \xrightarrow{k_{de}} PFH^-$$

Even though the redox processes leading to different activation states of the enzyme, have been investigated and differentiated by electron spin resonance studies (EPR), as described in the literature, and found to be reversible *[Silva, et al. 1999]*, it is still unclear how they can account for the resulting activity *[Bryant, Adams 1989b; Silva, et al. 1999]*. An irreversible activation is the simplest assumption leading to a quite appropriate description of the observed phenomenon. The resulting activity / concentration of the *PF*H in the subsequent reaction can be described by the term as outlined in eq. 4-12 *[Greiner 2002]*.

$$[PFH] = [PFH]_0 + [PFH^*]_0 \cdot k_{act} \left(\frac{e^{-k_{act} t}}{k_{de} - k_{act}} + \frac{e^{-k_{de} t}}{k_{act} - k_{de}} \right) \qquad \textbf{eq. 4-12}$$

with:			
	$[PFH]$	U mg^{-1}	activated *PF*H
	$[PFH]_0$	U mg^{-1}	initially activated *PF*H at startup
	$[PFH^*]_0$	U mg^{-1}	non-activated *PF*H at startup
	k_{act}	h^{-1}	activation constant
	k_{de}	h^{-1}	deactivation constant

Upon fitting the parameters to the course of the initial activity for the two repetitive batch series with non-linear regression the data collected in Table 4.3 are received. The simulated course of the initial activity is shown in Figure 4.28 by the black line.

Table 4.3: Parameter of the time-dependent activation of *PF*H for the two repetitive batch series in Figure 4.28.

parameter	1. series	2. series	unit
k_{act}	17.1 ± 7.8	6.0 ± 4.3	10^{-2} h^{-1}
k_{de}	1.7 ± 0.7	1.3 ± 0.1	10^{-2} h^{-1}
$[PFH^*]_0$	15.5 ± 3.0	14.0 ± 5.6	10^{-2} U mg^{-1}
$[PFH]_0$	2.8 ± 1.6	5.8 ± 1.4	10^{-2} U mg^{-1}
$\Sigma\ [PFH]$	18.3 ± 4.6	19.8 ± 7.0	10^{-2} U mg^{-1}

A comparable total concentration of *PF*H $\Sigma\ [PFH] = [PFH^*]_0 + [PFH]_0$ within the margin of error is calculated. The sum is the possible total activity of the *PF*H. This means, that in spite of the fact that the rate of activation (k_{act}) differs significantly for both repetitive batch series, a comparable total amount of enzyme concentration is resulting. The deactivation constant is also comparable for both repetitive batch series. The conclusion is that there must be at least one parameter that was not controlled, which seems to have a very high impact on the activation. To identify the identy of this parameter is in the focus of presently ongoing

investigations.
It is unclear why the activation effect occurs. Presumably, the applied [NiFe]-hydrogenase was not fully converted to the catalytically active state by temperature-induced activation. However, these findings are interesting, since the *PF*H I preparation was purified under anaerobic and reducing conditions. There still remain many questions to be answered concerning the mechanism of the enzyme. Although a consensus is slowly being reached, the exact roles of the different active site components have not yet been fully established *[Fontecilla-Camps, Ragsdale 1999]*. In other words: there is still a great potential to even increase the effectiveness of the hydrogenase I from *Pyrococcus furiosus* by understanding the activation mechanism in more detail and establishing a more effective protocol for the activation.

4.2.4 Continuous production of NADPH in the volume aerated membrane reactor

To carry out the continuous production of NADPH the newly developed volume aerated membrane reactor was applied, as already described in ➲ chapter 4.1.2, page 110 (flow scheme: Figure 4.12, page 110). Figure 4.29 shows the concentration ratio of NADPH to the sum of $NADP^+$ and NADPH as a function of the number of residence times. A steady-state with almost quantitative conversion was reached at a residence time of 2.0 h. After adjusting the flow rate to the shorter residence time of 1.5 h, the supply with hydrogen proved to be the limiting factor. Raising the differential pressure from 0.9 to 1.5 bar compensated for this decrease. The slow decline of the concentration ratio to about 0.85 over the period of 120 h can be accounted for by a deactivation of the enzyme. In order to make the degradation effects and the capabilities of the enzyme visible, no stabilizer, - as for example the antioxidant sodium dithionite, - was added. The reactor outflow was directly cooled down to 4°C to prevent further decomposition of the reaction product NADPH. In the continuous experiment a space-time yield (*sty*) of 130 g L^{-1} d^{-1} was reached. The total turnover number (*ttn*) of the enzyme was calculated to be 66,000. This value certainly is a too low estimate, since it was neglected that only approximately one fifth of the protein in the enzyme preparation is active hydrogenase.

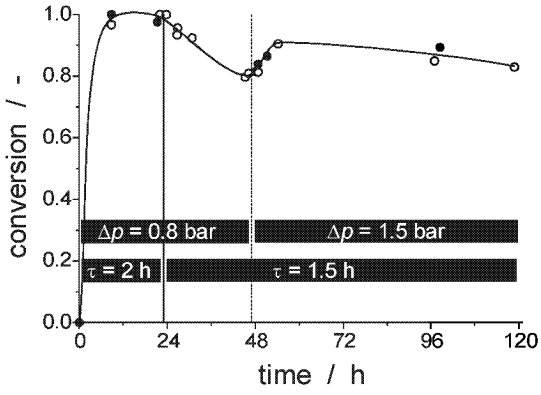

Figure 4.29: Course of the continuous NADPH synthesis in the volume aerated membrane reactor (12 mM $NADP^+$, 1.9 mg mL^{-1} *PF*H, 100 mM KPi buffer, pH 8.0, T = 40°C, YM10 membrane, p_l = 5.0 bar, p_{H2} = 5.8 bar from 47 h onwards p_{H2} = 6.5 bar, conversion[38] based on • quantified and ○ qualitative data).

4.2.5 Regeneration of NADPH

Among several *in situ* regeneration techniques, enzymatic processes are presently applied with success *[Hummel 1999; Liese, et al. 2000; Leonida 2001; Vrtis, et al. 2002]*. Two different approaches are known, namely the substrate-coupled and the enzyme-coupled system. In the substrate-coupled system the enzymatic conversion of a cheap co-substrate, e.g. 2-propanol to acetone, regenerates the reduced cofactor (Figure 4.30, left). In the case of the enzyme-coupled *in situ* regeneration instead, a second enzyme, which regenerates the cofactor directly, is added to the reaction system (Figure 4.30, right). A well-known example for the enzyme-coupled cofactor regeneration is the formate dehydrogenase (FDH), which catalyzes NADPH-regeneration through conversion of formate to carbon dioxide *[Seelbach, et al. 1996; Tishkov, et al. 1999a]*. Another approach is to use a hydrogenase, which produces the reduced cofactor at the expense of the cheapest reducing agent, namely of hydrogen *[Klibanov, Puglisi 1980; Wong, et al. 1981; Hilhorst, et al. 1983; Okura, et al. 1987a, 1987b; Otsuka, et al. 1989; Hasumi, et al. 1995]*. To date, no study has been published to our knowledge, which describes the direct regeneration of NADPH with a hydrogenase.

[38] Because of problems with the internal standard in the samples withdrawn, several samples could not be quantified (open circles).

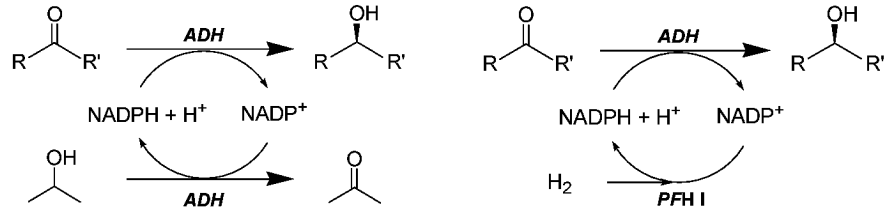

Figure 4.30: Comparison of substrate-coupled (left) and enzyme-coupled (right) cofactor regeneration.

In case of the cofactor regeneration with hydrogen, the position of the reaction equilibrium is determined by the respective reduction potentials of the substrates, since the corresponding oxidation potential is per definition zero. In the case of the hydrogenation of double bonds, the two hydrogen atoms of molecular hydrogen are transferred as opposed to the hydrogenation of $NADP^+$, where a hydride is transferred and a proton is a byproduct. Therefore, the equilibrium of carbonyl reduction is not influenced by the pH during cofactor regeneration in contrast to the $NADP^+$ reduction (➲ eq. 4-9, page 124). The substrate-coupled cofactor regeneration will be discussed in detail in ➲ chapter 4.4, page 161.

To study the difference between substrate- and hydrogenase-coupled cofactor regeneration, respectively, the *in situ* NADPH regeneration using the thermophilic NADPH-dependent alcohol dehydrogenase from *Thermaoanaerobium spec.* (ADH) was studied. It was found that the ADH catalyzed the enantioselective reduction of acetophenone to (1*S*)-phenyl ethanol at 40°C at the same time. This system was compared to the enzyme-coupled *in situ* NADPH regenerating system with *PF*H I under comparable conditions. Figure 4.31, left, shows the progression curves obtained of the 2-propanol-coupled NADPH regeneration using two different initial cofactor concentrations. Regardless of the initial $NADP^+$ concentration applied, equilibrium conversions X_{eq} = 93% were reached after 2 h and 2.5 h, respectively. The difference in reaction rates between the batches with 0.5 mM and 0.1 mM is due to the kinetics (for ADH: $k_{M,\ NADPH} \approx 0.5$ mM). In contrast, quantitative conversions > 99% were reached after 3 h with the *PF*H I - catalyzed NADPH regenerating system (Figure 4.31, right). These results proof that the substrate-coupled NADPH regeneration reaction is thermodynamically limited, whereas the enzyme-coupled system overcomes this limitation by enabling the usage a strong reducing agent.

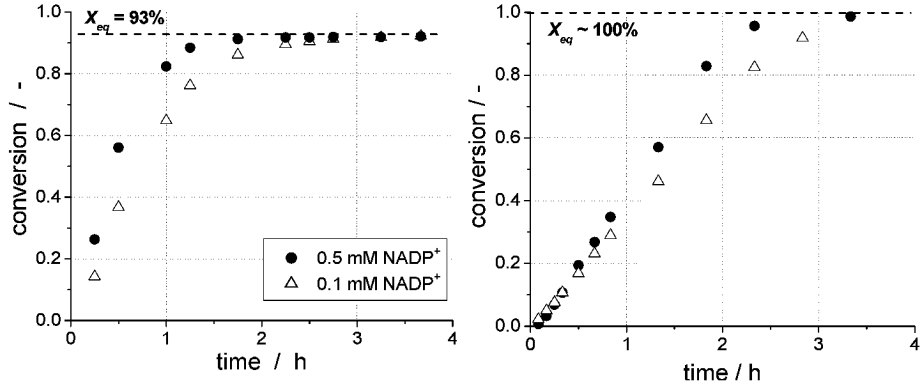

Figure 4.31: Comparison of the substrate-coupled (left) and the enzyme-coupled (right) cofactor regeneration in case of the enantioselective reduction of acetophenone to (*R*)-phenylethanol. The substrate coupled cofactor regeneration (left) is carried out with 2-propanol by the same ADH also catalyzing the enantioselective reduction. Enzyme-coupled cofactor regeneration with *PF*H (right) (10 mM acetophenone, 0.5 and 0.1 mM $NADP^+$, 50 mM phosphate buffer, pH = 8.0, 0.3 mg mL^{-1} ADH, 40°C, left: 300 mM 2-propanol, right: 1 mg mL^{-1} *PF*H, p_{H2} = 1.1 bar).

The total turnover number (*ttn*) of the redox mediator NADP+ amounts to 93 (0.1 mM $NADP^+$) and 19 (0.5 mM $NADP^+$). The product alcohol could be produced with an enantioselectivity of over 99.5% in all of the experiments throughout. By these means, it has been proved that the stereoselectivity of the alcohol dehydrogenase catalyzed reduction of acetophenone to (1*R*)-phenyl ethanol is not influenced by the type of regenerating system used.

To increase the turnover number of the cofactor, it is a common practice to decrease the initial concentration of the critical cofactor in the system. Another approach follows the linear dependence of the *ttn* on the initial substrate concentration. An increase in substrate concentration should also lead to higher total turnover numbers and thus to a higher efficiency. Since we have already shown (Figure 4.31) that lowering the $NADP^+$ concentration results in inefficient use of the enzymes, we selected the latter technique, but utilizing a substrate of higher solubility than acetophenone[39]. Consequently, the *PF*H I was applied in an enzyme-coupled cofactor regeneration system with the ADH catalyzing the enantioselective reduction of (2*S*)-hydroxy-1-phenyl-propanone[40], which is the product of the enantioselective C-C bond formation (➲ chapter 3.2.1, page 45), to the corresponding (1*R*,2*S*)-diol with a *de* > 98% (Figure 4.32). The reaction was carried out in a repetitive batch mode regarding the enzymes. Because of the limited stability of the ADH under the reaction conditions applied, 0.3 mg mL^{-1} ADH needed to be fed for starting up each batch.

[39] The maximum solubility of acetophenone in 50 mM KP_i buffer, pH 8.0, T = 40°C, totals to 20 mM (L. Greiner, D. Müller, personal communication, 2001).

[40] The maximum solubility of (2*S*)-hydroxy-1-phenyl-propanone (HPP) in 50 mM KP_i buffer pH 7.0, T = 20°C, totals to 120 mM (D. Kihumbu, personal communication, 2002).

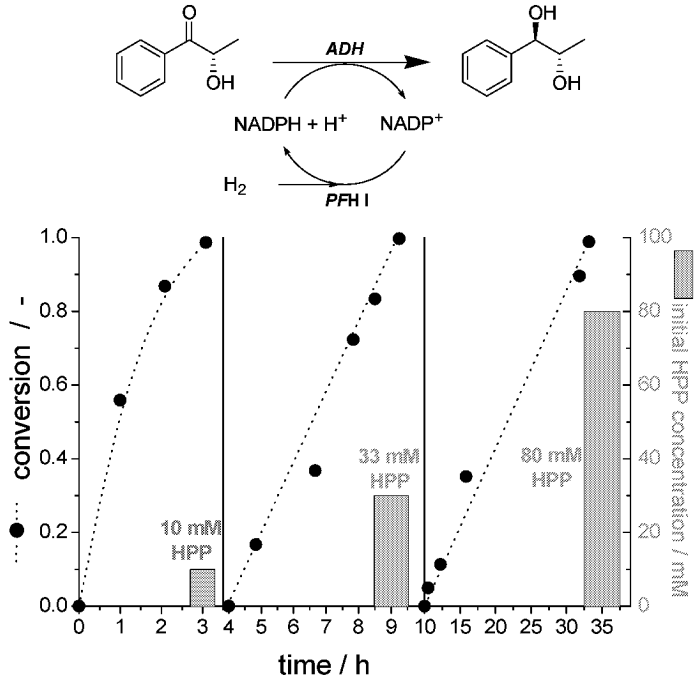

Figure 4.32: **Enantioselective reduction of (2*S*)-hydroxy-1-phenyl-propanone (HPP) to (1*R*,2*S*)-phenyl-propane-1,2-diol with *PF*H I catalyzed NADPH regeneration in a repetitive batch mode consisting of 3 cycles with different initial substrate concentrations (1.: 10 mM HPP, 2.: 30 mM HPP, 3.: 80 mM HPP, 0.5 mM $NADP^+$, 50 mM KP_i buffer, pH 8.0, 0.3 mg mL^{-1} ADH, 1.0 mg mL^{-1} *PF*H I, p_{H2} = 1.1 bar, 40°C, YM10 membrane).**

Each of the three runs yielded quantitative conversion. The initial concentration of the (2*S*)-hydroxy-1-phenyl-propanone (HPP) was subsequently increased from 10 mM to 80 mM, and a maximum *ttn* of 160 for NADPH could be reached.

In these experiments,e the advantage of the hydrogenase-coupled cofactor regeneration over the substrate-coupled one can be impressively demonstrated. With the substrate-coupled cofactor regeneration using 2-propanol as second substrate only an equilibrium conversions X_{eq} = 51% is reached (Figure 4.33).

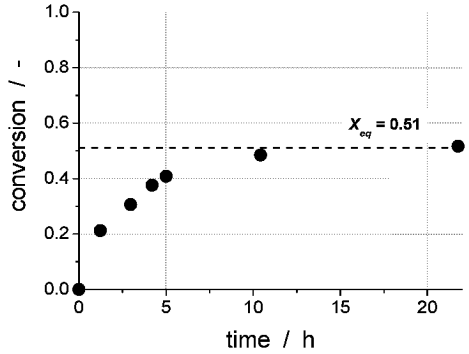

Figure 4.33: Enantioselective reduction of (2*S*)-hydroxy-1-phenyl-propanone (HPP) to (1*R*,2*S*)-phenyl-propane-1,2-diol with substrate-coupled NADPH regeneration (85 mM HPP, 150 mM 2-propanol, 0.5 mM $NADP^+$, 50 mM KP_i buffer, pH 8.0, 1 mg mL^{-1} ADH, 40°C, YM10 membrane).

4.2.6 Summary

- NADPH was produced by utilizing molecular hydrogen in combination with the hydrogenase from *Pyrococcus furiosus* without the production of any side products.
- An increase in the activity of the hydrogenase was observed in repetitive batch experiments, pointing to a not yet fully understood activation process of the hydrogenase. This offers a great potential to yield even higher activities upon understanding the activation mechanism.
- The newly developed volume aeration membrane reactor for chemical hydrogenation has also been efficiently applied for the continuous production of NADPH catalyzed by hydrogenase with a:
  - space-time yield of 130 g L^{-1} d^{-1} for NADPH,
  - total turnover number of 66,000 for the *PF*H.
- The hydrogenase can be efficiently used for regenerating NADPH in enzyme-coupled systems.
- In contrast to the substrate-coupled cofactor regeneration, which is thermodynamically limited, quantitative conversions are reached by applying the hydrogenase for cofactor regeneration.

4.3 Transfer hydrogenation with chemzymes[41]

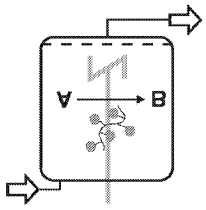

In the thirties it was discovered that special alumina alkoxides are able to reduce carbonyl compounds *[Graauw, et al. 1994]*. This type of reaction is called *Meerwein-Pondorf-Verley reduction*. From 1967 onwards transition metal complexes were also used for the transfer hydrogenation, which in the midst of the eighties were combined with chiral ligands *[Gladiali, Mestroni 1998]*. For a long time, the transfer hydrogenation approach was not accepted as a real alternative to the "classical" hydrogenation, due to its low reaction rate. This changed significantly in 1991, when Bäckvall published the addition of catalytical amounts of base as a promoter (e.g. sodium hydroxide). By this means, the activity of the transition metal complexes could be increased drastically for the first time *[Chowdhury, Bäckvall 1991]*.

In our study, the transfer-hydrogenation catalyst as published by Gao-Noyori in 1996 *[Gao, et al. 1996b]* was chosen as a starting point for the synthesis and investigation of a transfer-hydrogenation chemzyme. The enantioselective reduction of acetophenone was chosen as model reaction. The Gao-Noyori catalyst utilizes 2-propanol as the hydrogen donor. (2*S*)-Phenylethanol is formed with an ee up to 97% and a *tof* of 30 h^{-1} is achieved at 45°C and 100 mM phenylacetone.

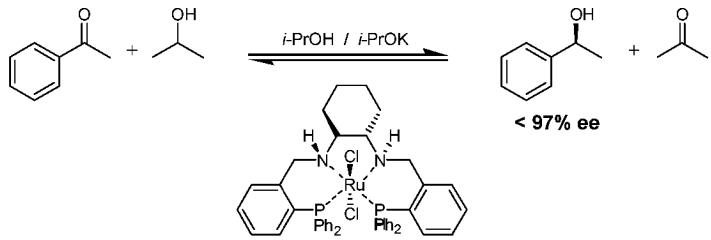

Figure 4.34: Transfer hydrogenation catalyzed by the Gao-Noyori catalyst *[Gao, et al. 1996b]*.

[41] **Parts of this chapter have been published in:**

1. S. Laue: *Asymmetrische Transferhydrierung im chemischen Membranreaktor*; PhD-thesis, University of Bonn (2002)
2. S. Laue, L. Greiner, J. Wöltinger, A. Liese: *Continuous application of chemzymes in a membrane reactor: Asymmetric transfer hydrogenation of acetophenone*; Advanced Synthesis & Catalysis 343 (6-7) (2001) 711-720
3. J. Wöltinger, O. Burkhardt, A. Bommarius, A. Karau, J.-L. Philippe, K. Drauz, J. Allgaier, A. Liese, C. Wandrey: *Polymervergößerte Katalysatoren*; German patent application DE 199 10 691.6-41 (11.03.1999); *Polymer enlarged catalysts*; world patent application WO 053305 A1 (14.09.2000)
4. A. Bommarius, K. Drauz, J. Wöltinger, S. Laue, A. Liese, C. Wandrey: *Verwendung von molekulargewichtsvergrößerten Katalysatoren in einem Verfahren zur asymmetrischen kontinuierlichen Hydrierung, neue molekulargewichtsvergrößerte Liganden und Katalysatoren*; German patent application DE 100 02 975.2 (24.01.2000)

The main reason to select this ligand for the synthesis of a transfer-hydrogenation chemzyme was the expected high complex stability of the corresponding transition metal complex. In the Gao-Noyori catalyst the ruthenium is complexed by two amino and two phosphino groups, forming a stable chelate complex. This extraordinary complexing property could also be demonstrated through the examples of copper and silver complexes *[Wong, et al. 1996]*. The motivation for the synthesis of the chemzyme has been its intended application in a continuously operated membrane reactor. Hereby it is important to guarantee that the polymer-enlarged ligand (chemzyme) is retained together with the transition metal.

4.3.1 Synthesis of the chemzyme

The synthesis of the chemzyme was carried out via a 12 step convergent synthesis, whereby a ruthenium-based transfer hydrogenation catalyst could be linked via hydrosilylation to a polysiloxane (**13**). For that purpose, we developed two routes leading to the key compounds **4** and **10** (Figure 4.35 and Figure 4.36).

According to the first route, a palladium-catalyzed phosphination of 2-bromobenzaldehyde allowed the effective introduction of the diphenylphosphine into the ligand (85%). In this fashion, the reaction was possible without prior protecting the aldehyde as previously described in literature *[Hoots, et al. 1982]*. Next, the selective mono functionalization of (1*R*,2*R*)-diaminocyclohexane (**3**) was achieved by slow addition of **2** to **3**. The course of the reaction was monitored by NMR, because the imine proton of the mono- and difunctionalized product can be clearly distinguished.[42] However, the attempt to isolate the monofunctionalized imine by aqueous work-up yielded up to 10% of difunctionalized imine as a byproduct. This was most likely caused by hydrolytic regeneration of **2**, which reacted to the difunctionalized imine during the removal of the solvent. Therefore, subsequent to generating the monofunctionalized imine, this intermediate was directly converted to the corresponding amine **4** by reduction with sodium borohydride. The purification of the product was carried out by precipitation as hydrochloride (51%).

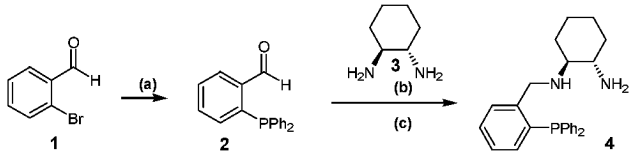

Figure 4.35: Synthesis of the monofunctionalized diamine half unit 4. Reagents and conditions: (a) 1.3 equiv. $HPPh_2$, 0.6% $Pd(PPh_3)_4$, Et_3N, toluene, reflux; (b) 4-fold excess of 3, slow addition of 2, EtOH, 0°C; (c) EtOH, $NaBH_4$, rt

[42] ^{1}H-NMR ($CDCl_3$), imine signal monofunctionalized: 8.74 (1H, d, CH), - difunctionalized 8.62 (2H, d, CH).

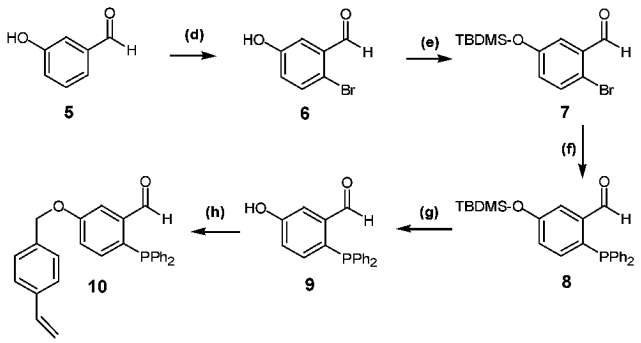

Figure 4.36: Synthesis of the linker half unit 10. Reagents and conditions: (d) Br $_2$, $CHCl_3$; (e) TBDMSCl, imidazole, DMF; (f) 1.3 equiv. $HPPh_2$, 0.6% $Pd(PPh_3)_4$, Et_3N, toluene, reflux; (g) KF, aqueous HBr (48 %), DMF; (h) NaH, vinylbenzylchloride, DMF

The effective phosphination reaction as described in Figure 4.35 was also used for the preparation of the second key compound **10**. For this purpose, 2-hydroxy-benzaldehyde (**5**) was brominated according to literature procedures *[Hodgson, Greensmith Beard 1925]* yielding **6** with a moderate yield of 65%. The hydroxyl group was protected with *tert*-butyltrimethylsilylchloride (TBDMSCl), yielding compound **7** (97%). The phosphination was performed under analogous conditions as detailed above, with 80% yield of **8**. The cleavage of the TBDMS-ether of **8** afforded **9** (81%). The resulting alcohol **9** was subjected to an ether synthesis with 4-vinylbenzylchloride, giving **10** with a moderate yield of 56%. The vinyl function of **10** served as linking moiety for the successive polymer linkage (Figure 4.37).

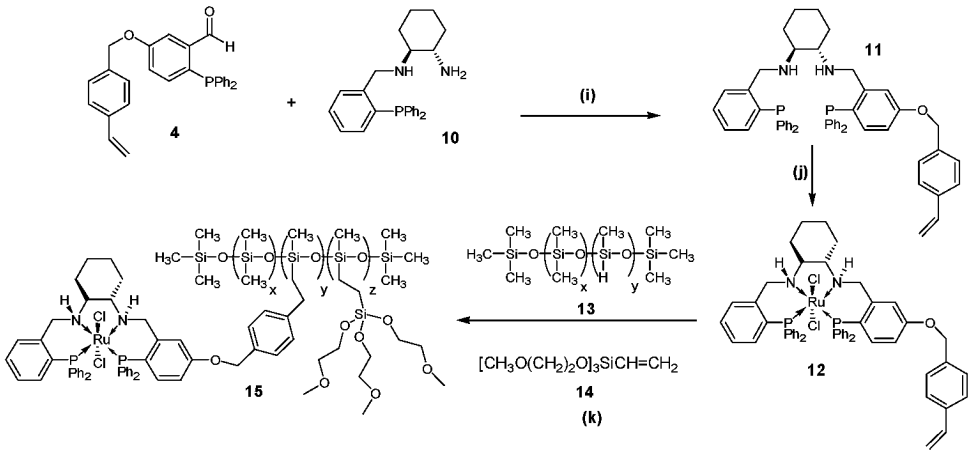

Figure 4.37: Synthesis of chemzyme 15. Reagents and conditions: (i) EtOH, reflux; $NaBH_4$, EtOH, rt; (j) $Ru(DMSO)_4Cl_2$, toluene, reflux (k) platinum-divinyltetramethyl-disiloxane, toluene, 50°C

Both convergent routes were combined by reacting **4** and **10** as shown in Figure 4.37 followed by immediate reduction of the resulting imine leading to **11** (79%). The ruthenium was introduced by ligand exchange of dichlorotetrakis(dimethyl sulphoxide)ruthenium *[Evans 1973]* with **11**. The resulting linkable catalyst **12** was purified by column chromatography (56%). Finally, **12** was attached to the hydro-siloxane moieties of the methylhydrosiloxane - dimethylsiloxane copolymer[43] **13** via an effective hydrosilylation reaction (> 99%) *[Ojima 1989]*. Due to the quantitative linking reaction, various exact grades of polymer functionalization were achieved,namely 2, 2.9, 5, and 10% with catalyst. A polysiloxane-polymer was chosen as the backbone, because coupling of ligands via linkers to siloxane-based matrixes is an established method *[Ojima 1989]*. For an industrial application a more hydrolysis-stable polymer has to be chosen. The remaining Si-H groups of **13** were end-capped by attaching polar tris-(2-methoxyethoxy)vinylsilane **14** to the polymer backbone via the same quantitative catalytic linking reaction (Figure 4.38). In this fashion, the solubility of the polymer-bound catalyst (chemzyme) **15** in polar solvents is increased. Thus the described technique provides for the possibility to adjust functionalization and solubility of the chemzyme **15** as shown in Table 4.4. The resulting chemzyme consists of the following three subunits as shown in Figure 4.38 that are denominated with "X" (dimethylsiloxane unit of polymeric backbone), "Y" (unit with attached ligand), and "Z" (unit with tris-(2-methoxyethoxy)vinylsilane as solubilizer). For further functionalization 2.9% was chosen, because of its highest activity and good solubility. The average molecular weight (M_n) thereof was calculated to be 20658 g/mol. By means of GPC-measurements[44] a molecular weight of 21130 g/mol and a dispersity of 2.1 was determined. The resulting polymer was purified by ultrafiltration, and 8.2 g of the chemzyme was yielded.

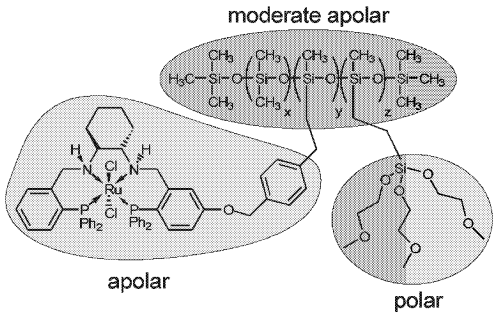

Figure 4.38: Subunits X, Y, Z of the chemzyme and relative polarity.

[43] The methylhydrosiloxane-dimethylsiloxane copolymer (CAS: [68037-59-2]) was kindly provided by Dr. Winkhofer, Wacker-Chemie GmbH, Germany. The polymer has an average molecular (M_n) weight of 11735 g/mol with a dispersity of 1.7 (GPC in THF versus polystyrene standards). The Si- H functionalization is 19% according to ^{29}Si-NMR analysis.

[44] GPC = gel permeation chromatography (versus polystyrene standards in THF).

Table 4.4 Influence of functionalization on initial reaction rate and solubility.

functionalization [%]	X	Y	Z	M_n[a] [g/mol]	tof_0[b] [min^{-1}]	solubility[c]
2	135	3.3	22.7	19710	0.94	good
2.9	135	4.7	21.3	20658	1.1	good
5	135	8.1	17.8	23039	1.01	good
10	135	9.7	9.7	28630	0.43	moderate

[a] Calculated from gel permeation chromatography results and functionalization of original polymer.

[b] Initial turnover frequency (250 mM acetophenone, 1 mM isopropoxide, 45°C).

[c] in 80 vol% 2-propanol and 20 vol% methylene chloride

4.3.2 System investigations

The newly synthesized chemzyme as outlined above has been applied to a batch reaction to investigate its applicability (Figure 4.39). The course of this reaction was found to be comparable to a batch reaction catalyzed by the non-polymerbound catalyst *[Laue 2002]*. In respect to the enantiomeric excess, there are two major points that can be recognized from this batch reaction:

1. The enantiomeric excess is increasing during the first hour from 85% to 94%. This effect cannot be explained yet. Blackmond observed a similar activation phenomenon for a cinchona-modified heterogeneous Pt-catalyst *[Sun, et al. 1997]*. These authors could not explain their observations either. Here it could be proven, however, that the substrate concentration had no significant influence. Furthermore, at lower isopropoxide concentration in the batch reaction (0.25 – 0.5 mM), enantiomeric excesses of up to 96% have been reached. However, a very long pre-incubation time (12 h) with isopropoxide leads to a lowered enantiomeric excess of only 80%. This gives a hint to a possible rearrangement of the catalyst, since it was already demonstrated in the literature that different conformational isomers of the pre-catalyst exist *[Stoop, et al. 2000]*. The maximal enantiomeric excess achieved is comparable to that obtained using the non-polymer enlarged catalyst *[Laue 2002]*.

2. After reaching the maximum enantiomeric excess, the *ee* decreases with increasing conversion. The explanation thereof is the reversibility of the transfer hydrogenation. Because of a reverse reaction, the enantiomeric excess is decreasing again, as will be discussed in detail later on (➲ Figure 4.48, page 152).

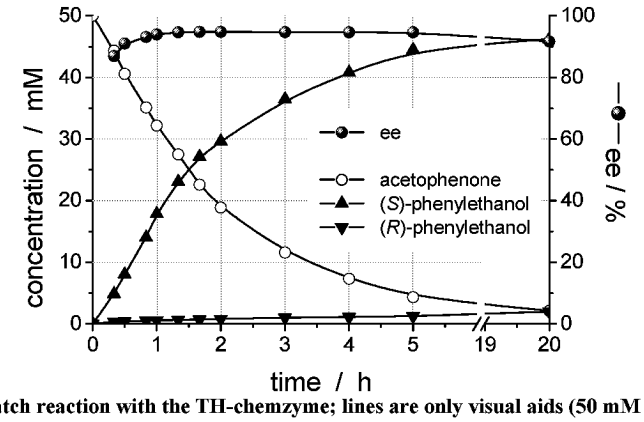

Figure 4.39: **Batch reaction with the TH-chemzyme; lines are only visual aids (50 mM acetophenone, 0.5 mM TH-chemzyme, 1 mM potassium isopropoxide, 80 vol% 2-propanol, 20 vol% methylene chloride, 45°C).**

Influence of moisture

Transfer hydrogenations described in the literature are generally carried out in absolute organic solvents. A possible reason might be the influence of water on the catalyst activity *[Bellefon de, Tanchoux 1998]*. If 2-propanol is used as the solvent, however, the water content is no less than 0.005 weight%, even after drying it over calcium hydride. The water content of methylene chloride dried over molecular sieve ranges in the same order of magnitude. A water concentration of 0.01 weight% correlates to approximately a 5 mM H_2O concentration, resulting in a 10-times higher concentration than that of the catalyst (0.5 mM) itself. Therefore, the affinity of water molecules to the catalyst must be low. We have found, however, that the catalyst, once deactivated by water can successfully be regenerated by addition of isopropoxide, as can be seen in Figure 4.40. Isopropoxide is assumed to displace the coordinated water molecules from the catalyst, a process, which is comparable to the initial activation or formation of the catalyst. This assumption would be in accordance with Noyori´s observations during his work on ruthenium diamine-based catalysts *[Haack, et al. 1997]*, which showed that the addition of base in batch reactions is required only for the formation of the active catalyst, but not for maintaining the catalytic reaction.

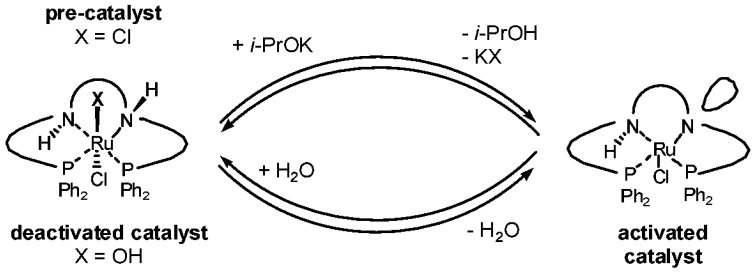

Figure 4.40: **Activation of the pre-catalyst (X = Cl) and regeneration of the catalyst with 2-propanol (X = OH) because of its deactivation by water.**

Furthermore we found that the addition of 20 vol% methylene chloride, which was needed to increase the solubility of the chemzyme, did not have any significant influence on the equilibrium conversion. Nevertheless, the activity of the catalyst decreased by approximately 30%.

Influence of isopropoxide

As was already stated above, the addition of isopropoxide is needed because of two reasons (Figure 4.40):

1. Activation of the pre-catalyst
2. Regeneration of the catalyst deactivated by water

Equilibrium is assumed between the pre-catalyst and the activated catalyst. Since neither the concentration of the pre-catalyst nor that of the activated catalyst can be determined experimentally, no value for this equilibrium constant can be given. However, addition of isopropoxide does affect the initial turnover frequency (tof_0) as well as the enantiomeric excess (*ee*) at the same time after activation of the chemzyme as can be seen from Figure 4.41. This influence can be quantified by separately determining the kinetic parameters of isopropoxide for the *S*- as well as for the *R*-selective reaction utilizing the kinetic equations **eq. 3-1** – eq. 4-14. K_{base} describes the base concentration that is needed to reach half the maximal catalyst activity ($tof_{max}/2$). The enantiomeric excess is calculated based on the enantiospecific initial turnover frequencies (Equation eq. 4-15).

$$tof_{(S)0} = tof_{(S)\max}\frac{[base]}{K_{base(S)}+[base]} \qquad \textbf{eq. 4-13}$$

$$tof_{(R)0} = tof_{(R)\max}\frac{[base]}{K_{base(R)}+[base]} \qquad \textbf{eq. 4-14}$$

$$ee_0 = \frac{tof_{(S)0}-tof_{(R)0}}{tof_{(S)0}+tof_{(R)0}} \qquad \textbf{eq. 4-15}$$

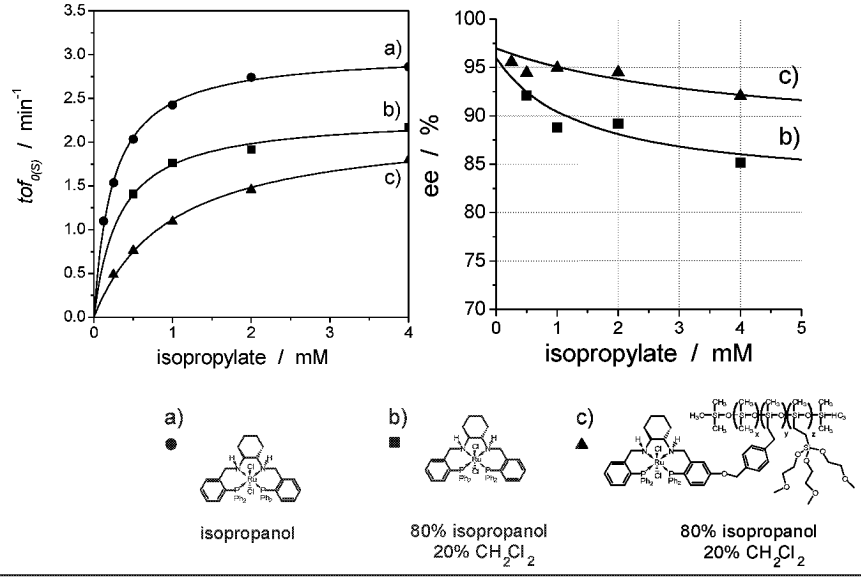

(*S*)-selective reaction			
$K_{base\ (S)}$ [mM]	0.23 ± 0.01	0.32 ± 0.04	0.97 ± 0.07
$tof_{S\ (max)}$ [min^{-1}]	3.02 ± 0.03	2.30 ± 0.07	2.20 ± 0.06
(*R*)-selective reaction (data plot not shown)			
$K_{base\ (R)}$ [mM]	1.4 ± 0.3	1.5 ± 0.8	4.3 ± 2.2
$tof_{R\ (max)}$ [min^{-1}]	0.46 ± 0.04	0.22± 0.05	0.15 ± 0.04

Figure 4.41: Influence of the isopropoxide concentration on the initial turnover frequency of the (*S*)-selective reaction (left) and *ee* (right). (250 mM acetophenone, 0.5 mM chemzyme, 80 vol% 2-propanol, 20 vol% methylene chloride, 45°C, pre-incubation of the catalyst with base for 45 min).

The influence of the polymer linkage and the solubilizer were investigated separately (free catalyst with and without solubilizer: curves **a** and **b** in Figure 4.41; polymer-bound catalyst with solubilizer: curve **c** in Figure 4.41). Since the main activity of the catalyst is determined by the (*S*)-selective reaction, the main trends are discussed using this enantiomer as an example:

- On the addition of 20 vol% methylene chloride, the $tof_{(S)max}$ is reduced by 24% (3.02 min^{-1} to 2.30 min^{-1}) in the case of the free catalyst (curves **a** and **b** in Figure 4.41, left).
- The value of $tof_{(S)max}$ is comparable (5% difference) between the free and the polymer-bound catalyst (curves **b** and **c** in Figure 4.41, left).
- A drastic difference between the free and the polymer-bound catalyst can be observed in regard to K_{base}. The $K_{base(S)}$ is increased by 300% for the polymer-bound catalyst

(from 0.32 mM to 0.97 mM). The reason is a side reaction of isopropoxide with the polysiloxane backbone, as discussed later on (➲ chapter 4.3.3, page 153). In contrast to the initial reaction rate, the enantiomeric excess (*ee*) is decreasing with increasing isopropoxide concentration (Figure 4.41, right). The *ee* achieved with the polymer-bound catalyst might be somewhat increased, because of a side reaction with the polysiloxane backbone (➲ chapter 4.3.3, page 153) that leads to a lower residual isopropoxide concentration.

This leads to the conclusion that a compromise between activity and enantioselectivity has to be made. For an investigation of the kinetics, the isopropoxide concentration was chosen at a magnitude comparable to that of the $K_{base(S)}$ value. At this point, the half maximal reaction rate is reached, and the negative influence on the enantioselectivity is still low.

Thermodynamics

The transfer hydrogenation is an equilibrium reaction; therefore, the maximal conversion that can be reached is determined by the thermodynamic equilibrium constant. To carry out any simulations of the reaction system, the thermodynamics has to be accounted for besides the kinetics. The equilibrium constant can be determined via the free standard heat of formation of the reactants. Since these values were not available for the systems as investigated here, a procedure was applied utilizing the corresponding redox potentials. These were determined electrochemically *[Adkins, et al. 1949]*: acetophenone 118 mV, acetone 129 mV. The *Nernst* equation can be simplified to eq. 4-16, if it is assumed that all reactants are at their equilibrium concentrations. At that stage, the redox potential of the cell is 0.

$$E^0 = (RT/\nu F) \; ln\, K_{eq}$$

E^0	V	standard redox potential	
R	8.31441 J K^{-1} mol^{-1}	ideal gas constant	**eq. 4-16**
F	9.64846 10^4 C mol^{-1}	*Faraday* constant	
T	K	temperature	
ν	-	number of redox electrons	

E^0 consists of the redox potentials of the half-cells and has been determined to be –11 mV (Equation eq. 4-17). With this information, $\nu = 2$ and $T = 318.15$ K (45°C) the equilibrium constant can be derived to be 0.4482 after conversion of eq. 4-16.

$$E^0 = E^0_{ox} - E^0_{red} \quad \Rightarrow \quad E^0 = 118 - 129 = -11\,\text{mV} \qquad \textbf{eq. 4-17}$$

$$1\,AP + 1\,IP \rightleftharpoons 1\,PE + 1\,AC$$

$$K_{eq} = \frac{[PE]_{eq}[AC]_{eq}}{[AP]_{eq}[IP]_{eq}} = 0.4482 \quad (318.15\,K) \qquad \text{eq. 4-18}$$

The calculation[45] of the equilibrium conversions X_{eq} of acetophenone is based on the law of mass action (Equation eq. 4-18), upon substituting the respective equilibrium concentrations with terms based on the initial concentrations $[AP]_0$ and $[IP]_0$ as well as X_{eq}.

$$K_{eq} = \frac{[AP]_0^2 \cdot X_{PE}^2}{[AP]_0 \cdot (1 - X_{PE}) \cdot ([IP]_0 - [AP]_0 \cdot X_{PE})} \qquad \text{eq. 4-19}$$

The resulting quadratic equation (eq. 4-19) is then solved for X_{eq}. The solution corresponding to negative concentration is discarded because of obvious reasons. Using the positive solution, the equilibrium conversion X_{eq} can be calculated for different starting concentrations $[AP]_0$ and $[IP]_0$. The resulting dependencies are outlined in Figure 4.42[46].

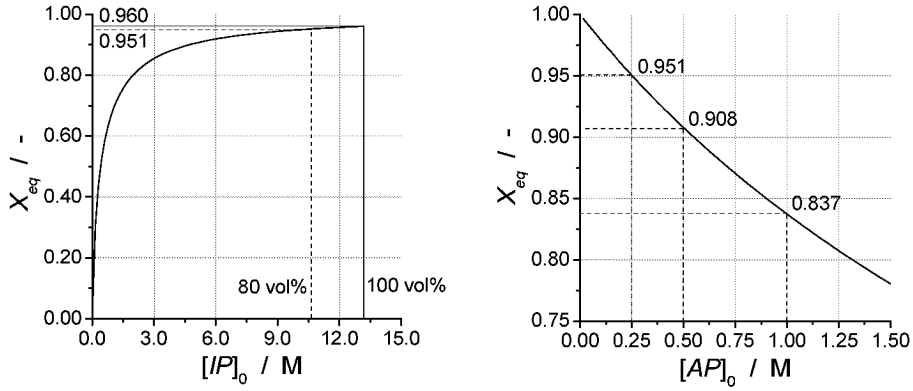

Figure 4.42: Equilibrium conversion X_{eq} of acetophenone as a function of $[IP]_0$ with $[AP]_0 = 250$ mM (left) and of $[AP]_0$ in 80 vol% of 2-propanol (right).

The maximal conversion that can be reached is 96.0%, if 100 vol% 2-propanol are used (Figure 4.42, left). By applying 80 vol% 2-propanol the maximal obtainable conversion (X_{eq}) is reduced marginally to 95.1%. Equimolar amounts of 2-propanol only lead to a conversion of 40.1%. As can be seen from Figure 4.42, right, doubling the acetophenone concentration from 250 mM to 500 mM results in a decrease of conversion from 95.1% to 90.8%.

[45] For a detailed derivation see **Laue S (2002)** Asymmetrische Transferhydrierung im chemischen Membranreaktor [Ph.D. thesis]. Bonn: University of Bonn.

[46] The concentration of 2-propanol is plotted up to a concentration of 13.061 M corresponding to 100 vol%.

Kinetics

An investigation of the kinetics is a key point to understand the reaction system and to allow simulations of continuously operated processes at different points of operation. The reduction of the acetophenone catalyzed by the chemzyme consists of two reversible reactions leading to the (*S*)- and the (*R*)-enantiomer of phenylethanol. In the literature three different reaction mechanisms are discussed for the transfer hydrogenation *[Alonso, et al. 1999]*. *Noyori* performed detailed mechanistic studies *[Yamakawa, et al. 2000]*. Based on the investigations of these authors as well as of our own using electronspray-ionization measurements *[Laue 2002]*, a *ping-pong-bi-bi mechanism [Cornish-Bowden 1995]* can be concluded, as is illustrated in Figure 4.43.

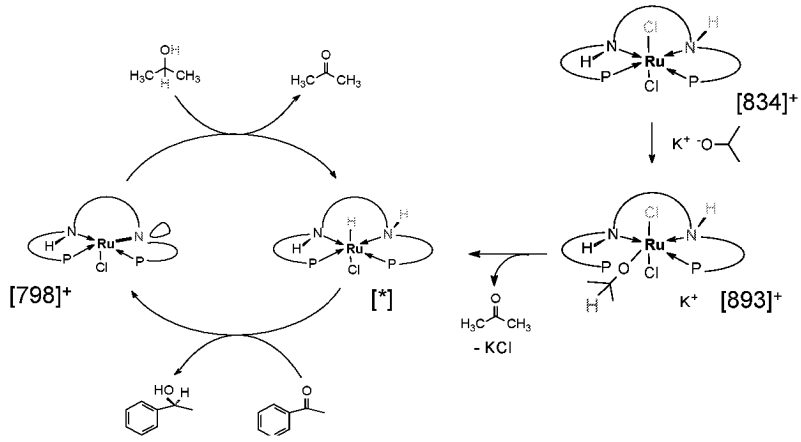

Figure 4.43: Proposed mechanism for the transfer hydrogenation with the Gao-Noyori catalyst. [798]+ [893]+ [834]+ proven by ESI-MS *[Laue 2002]* and [*] = proven by NMR *[Gao, et al. 1996a]*.

A kinetic modeling of this mechanism requires the detailed knowledge of all rate and equilibrium constants, an ambition that would be too extensive. Therefore, a simplified model was chosen from a practical point of view. Instead of considering a successive reaction of all partners with the catalyst, a simultaneous interaction of all reaction partners with catalyst via a ternary transition state was chosen (Figure 4.44). Thereby it has been assumed that the adsorption of the two substrates acetophenone and 2-propanol takes place in a random order. The reaction products leave the catalyst in a random sequence as well. Because of the 'principle of microscopic reversibility', all reaction steps are assumed to be reversible *[Biselli 1991]*. This type of reaction mechanism has been previously baptized the *random-bi-bi mechanism [Cornish-Bowden 1995]*.

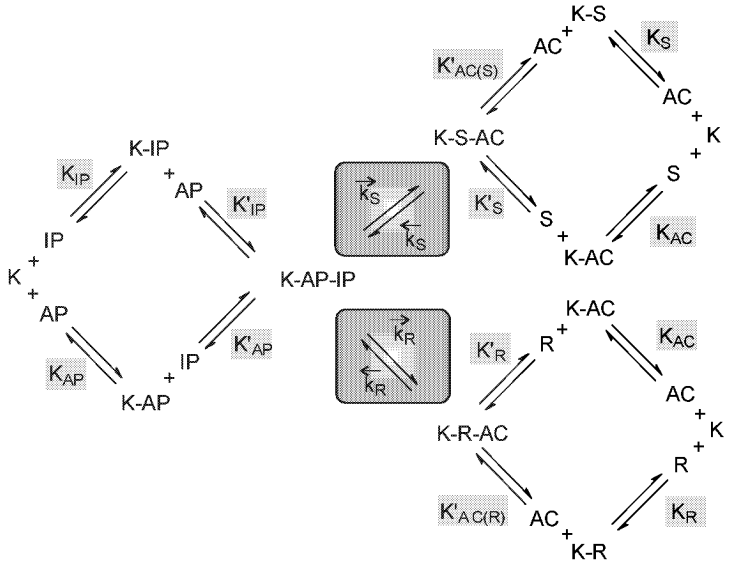

Figure 4.44: Reaction scheme of a *random-bi-bi mechanism* leading over a ternary transition state to the enantioselective transfer hydrogenation (K = catalyst, AP = acetophenone, S = (1*S*)-phenylethanol, R = (1*R*)-phenylethanol, IP = 2-propanol, AC = acetone).

For the description of this reaction system 12 parameters are required:

- The four rate constants $\vec{k}_S$, $\overleftarrow{k}_S$, $\vec{k}_R$, $\overleftarrow{k}_R$,
- five dissociation constants K_{AP}, K_{IP}, K_S, K_R, and K_{AC},
- in each case, one of the following dissociation constants K'_{AP} / K'_{IP}, K'_S / $K'_{AC(S)}$, respectively K'_R / $K'_{AC(R)}$. The respective other constant is calculated via the law of mass action, e.g. $K_S \cdot K'_{AC(S)} = K'_S \cdot K_{AC}$.

The rate limiting steps correspond to the gray shaded reactions in Figure 4.44. The rate constants $\vec{k}_S$ and $\overleftarrow{k}_S$ with the dimension [time^{-1}] describe the maximal activity in the case that only the ternary complexes [K-AP-IP] and [K-S-AC] are present. However, binding of other reactants during the course of the catalysis does reduce the reaction rate. The resulting reaction rates for (*S*)- as well as for the (*R*)-enantiomer are given in the following equations (eq. 4-20).

$$tof_S = \frac{\frac{\vec{k}_S}{K_{AP}\cdot K_{IP}}\cdot[AP]\cdot[IP] - \frac{\overleftarrow{k}_S}{K_S\cdot K_{AC}}\cdot[S]\cdot[AC]}{1+\frac{[AP]}{K_{AP}}+\frac{[IP]}{K_{IP}}+\frac{[S]}{K_S}+\frac{[R]}{K_R}+\frac{[AC]}{K_{AC}}+\frac{[S]\cdot[AC]}{K_S\cdot K_{AC}}+\frac{[R]\cdot[AC]}{K_R\cdot K_{AC}}}$$

$$tof_R = \frac{\frac{\vec{k}_R}{K_{AP}\cdot K_{IP}}\cdot[AP]\cdot[IP] - \frac{\overleftarrow{k}_R}{K_R\cdot K_{AC}}\cdot[R]\cdot[AC]}{1+\frac{[AP]}{K_{AP}}+\frac{[IP]}{K_{IP}}+\frac{[S]}{K_S}+\frac{[R]}{K_R}+\frac{[AC]}{K_{AC}}+\frac{[S]\cdot[AC]}{K_S\cdot K_{AC}}+\frac{[R]\cdot[AC]}{K_R\cdot K_{AC}}}$$

eq. 4-20

A more detailed derivation of the kinetic model (eq. 4-20) can be found in *Laue [Laue 2002; Laue, et al. in preparation]*. Here only some short remarks are given:

- The quotient of the reaction rate v_S and the catalyst concentration $[cat]_0$ delivers the activity normalized to the catalyst concentration tof_S (turnover frequency). The overall reaction rate of one enantiomer is expressed as the difference between the forward and backward reaction rate.
- A simplification is introduced, since the reactant 2-propanol also functions as the solvent at the same time. 2-Propanol occurs in excess in comparison to all other reactants[47]; therefore, the concentration of 2-propanol remains almost constant during the course of the reaction, and its influence on the kinetics is negligible. As a consequence, an experimental determination of K_{IP} is not possible, since the 2-propanol concentration cannot be varied; therefore the value of K_{IP} is set per definition equal to the 2-propanol concentration at the start of the reaction $[IP]_0$.
- During the course of fitting the kinetic parameters to the measured data, it turned out that K_{AP} and K'_{AP} are of the same value. This leads to the conclusion that the adsorption and desorption processes of acetophenone are independent of the binding of 2-propanol to the catalyst. Therefore, replacing K'_{AP} with K_{AP} reduces the number of kinetic parameters, which thereby simplifies the system.
- The reverse reaction is not measurable via initial reaction rate experiments, since at high concentrations of acetone an aldol condensation is observed in the presence of the base isopropoxide that is needed for the activation of the catalyst (Figure 4.45).

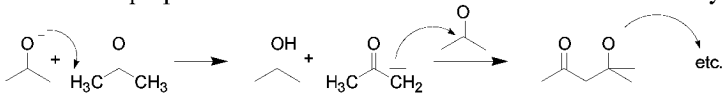

Figure 4.45: Aldol condensation of acetone catalyzed by isopropoxide.

Alternatively, the kinetic parameters of the reverse reaction may be determined by another method. Considering the already mentioned 'principle of microscopic

[47] The high concentration of 2-propanol in the range of 10-13 M in comparison to the concentration of the reactants in the area of 0.25 M is the real driving force of the reaction.

reversibility' *[Biselli 1991]*, measurements of the inhibition of the forward reaction can also be used to determine the kinetic parameters of the reverse reaction. As a simplification it is assumed that the inhibition constant of an inhibitor represents the dissociation constant at the same time. Using this assumption, K_S, K_R, and K_{AC} were determined. Nevertheless, by this means the kinetic parameters $K'_{AC(S)}$ and $K'_{AC(R)}$ cannot be determined. Therefore, the same simplification as in the case of K'_{AP} is introduced. $K'_{AC(S)}$ and $K'_{AC(R)}$ are treated as equivalent to the dissociation constant of K_{AC}, which has been determined by inhibition measurements.

- The rate constants $\overleftarrow{k_S}$ and $\overleftarrow{k_R}$ for the reverse reaction are determined via their correlation with the thermodynamic equilibrium constant K_{eq} (eq. 4-18). When stating a thermodynamic equilibrium, the rate constants of the forward and the reverse reactions are the same; therefore, tof_S and tof_R are both zero. This means that at thermodynamic equilibrium a racemate is formed. Setting equation eq. 4-20 to zero, multiplying it with the adsorption term[48], and rearranging the resulting term according to the law of mass action leads to eq. 4-21.

$$\overleftarrow{k_S} = 2 \cdot \frac{\overrightarrow{k_S} \cdot K_S \cdot K_{AC}}{K_{eq} \cdot K_{AP} \cdot K_{IP}} \qquad \text{eq. 4-21}$$

$$\overleftarrow{k_R} = 2 \cdot \frac{\overrightarrow{k_R} \cdot K_R \cdot K_{AC}}{K_{eq} \cdot K_{AP} \cdot K_{IP}}$$

Table 4.5: Kinetic parameters of the chemzyme-catalyzed transfer hydrogenation.

kinetic parameter	value	standard deviation	unit
$\overrightarrow{k_S}$	1.81	± 0.007	min^{-1}
$\overleftarrow{k_S}$	0.27	± 0.015	min^{-1}
$\overrightarrow{k_R}$	0.048	± 0.015	min^{-1}
$\overleftarrow{k_R}$	0.016	± 0.008	min^{-1}
K_{AP}	81	± 10	mM
K_{IP}	10641	-	mM
K_S	116	± 21	mM
K_R	262	± 82	mM
K_{AC}	245	± 41	mM

[48] adsorption term = denominator

The kinetic parameters, which are accessible via initial rate measurements, were determined by means of non-linear regression. In Figure 4.46 the parameter fit for the (*S*)-selective reaction is shown exemplarily. In Table 4.5 all determined kinetic parameters are summarized.

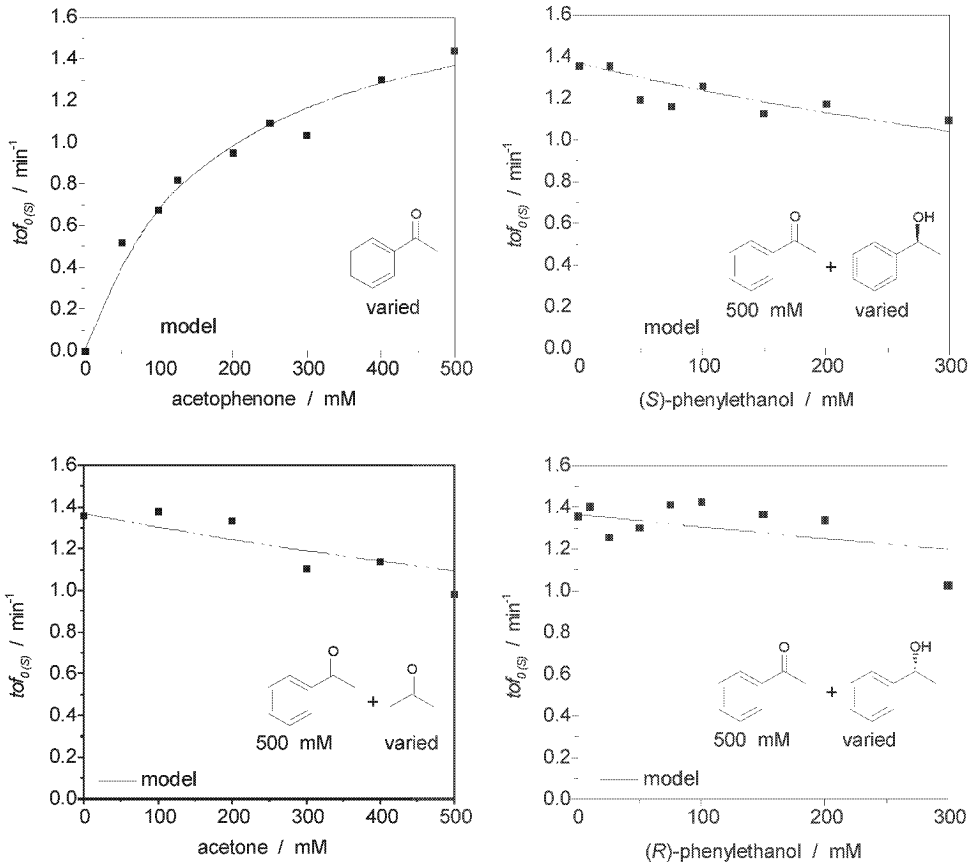

Figure 4.46: Kinetics of the (*S*)-selective reaction, lines are generated with kinetic model (0.5 mM chemzyme, 1 mM isopropoxide, 80 vol% 2-propanol, 20 vol% methylene chloride, 45°C).

Under initial reaction rate conditions, this means with no products formed yet and no reverse reaction, the enantiomeric excess is only determined by the ratio of $\vec{tof}_{S(0)}$ to $\vec{tof}_{R(0)}$. The enantiomeric excess can then be expressed as in eq. 4-22. This is at the same time the maximal achievable *ee* = 94.7%, since the reverse reaction introduces a decrease of the *ee*.

$$ee = \frac{\vec{k}_S - \vec{k}_R}{\vec{k}_S + \vec{k}_R} = 0.947 \qquad \text{eq. 4-22}$$

Simulations of batch experiments

Prior to applying the kinetics for the simulation and optimizing the operating points of continuously operated reactors, batch simulations have been carried out to proof the applicability of the model. For the simulation of a batch reactor the respective mass balances are needed, for which purpose the following equations (eq. 4-23) are solved numerically.

$$\begin{aligned}
\frac{d[AP]}{dt} &= -(tof_S + tof_R)\cdot[cat] \\
\frac{d[IP]}{dt} &= -(tof_S + tof_R)\cdot[cat] \\
\frac{d[S]}{dt} &= tof_S \cdot [cat] \\
\frac{d[R]}{dt} &= tof_R \cdot [cat] \\
\frac{d[AC]}{dt} &= (tof_S + tof_R)\cdot[cat]
\end{aligned} \qquad \textbf{eq. 4-23}$$

Figure 4.47 shows the result of such a simulation. The kinetic model predicts the course of the reaction quite well. During the start of the batch experiment a difference between the measured and simulated concentrations is observed. The reason is the initial activation of the catalyst that is not accounted for yet in the present kinetic model. The enantiomeric excess is also described well after the activation phase. During the course of the reaction the enantiomeric excess is decreasing from 94% to 92%. The simulations did also show that two terms in the adsorption term of eq. 4-20 could be omitted. The simulations shown in Figure 4.47 are carried out with this simplified kinetic model (Equation eq. 4-24).

$$tof_S = \frac{\frac{\vec{k}_S}{K_{AP}\cdot K_{IP}}\cdot[AP]\cdot[IP] - \frac{\overleftarrow{k}_S}{K_S\cdot K_{AC}}\cdot[S]\cdot[AC]}{1+\frac{[AP]}{K_{AP}}+\frac{[IP]}{K_{IP}}+\frac{[S]}{K_S}+\frac{[R]}{K_R}+\frac{[AC]}{K_{AC}}} \qquad \textbf{eq. 4-24}$$

$$tof_R = \frac{\frac{\vec{k}_R}{K_{AP}\cdot K_{IP}}\cdot[AP]\cdot[IP] - \frac{\overleftarrow{k}_R}{K_R\cdot K_{AC}}\cdot[R]\cdot[AC]}{1+\frac{[AP]}{K_{AP}}+\frac{[IP]}{K_{IP}}+\frac{[S]}{K_S}+\frac{[R]}{K_R}+\frac{[AC]}{K_{AC}}}$$

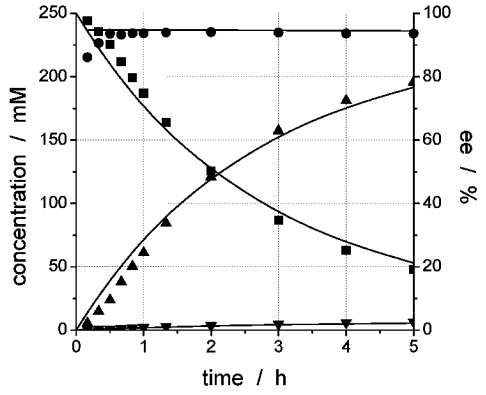

Figure 4.47: Simulation of a batch reaction; ■ acetopheone, ▲ (*S*)-phenylethanol, ▼(*R*)-phenylethanol, ● ee (250 mM acetophenone, 2 mM isopropoxide, 1 mM chemzyme, 80 vol% 2-propanol, 20 vol% methylene chloride, 45°C).

Based on the above-developed model and the determined reaction parameters, the behavior of the reactor can be simulated for arbitrary time ranges. By this means it is possible to reach the thermodynamic equilibrium conversion. This means that the system is investigated under *thermodynamic conditions*. Additionally, this concept can be used to investigate the decrease of the enantioselectivity at high conversion as has already been observed during the batch experiments under *kinetic conditions*. Figure 4.48, left, shows the results of a simulation up to the equilibrium conversion with a starting concentration of 500 mM acetophenone. It is observed that from a conversion of 84% on the reaction rate drops drastically to reach the equilibrium conversion of 90.8% after 4000 h. Furthermore, it is observed that the initially reached *ee* of 94.7% is continuously decreasing to a value of zero. The reason for this can be seen in Figure 4.48, right. The (*S*)-selective reverse reaction has a much higher impact on the (*S*)-product formation than is the case for the (*R*)-product. The (*S*)-forward reaction namely is producing relevant amounts of the (*S*)-product at a much higher rate, which serves as the starting material for the reverse reaction. The consequence is a faster decline of tof_S compared to tof_R. The value of tof_S is negative after 27 h, since $\overleftarrow{tof}_S$ gets much bigger than $\overrightarrow{tof}_S$. In contrast to the turnover frequency tof_R that stays always positive.

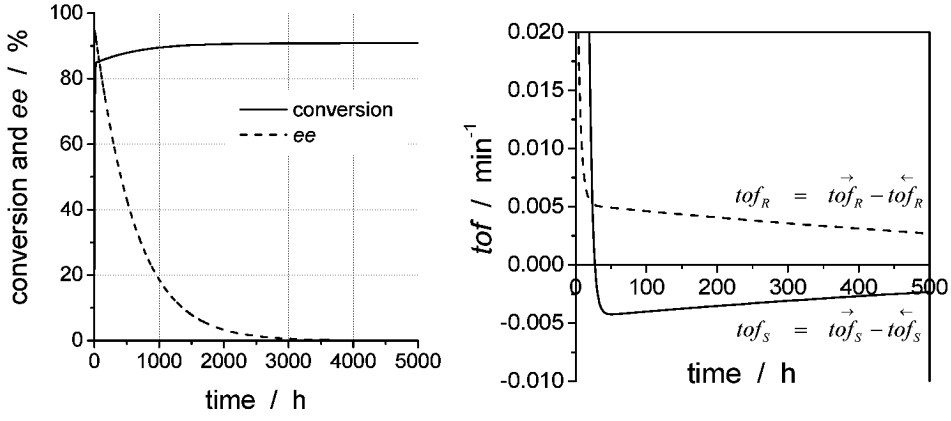

Figure 4.48: **Simulation of a batch reaction under thermodynamic conditions, left: conversion and ee as function of time, right: *tof* as function of time (500 mM acetophenone, 1 mM chemzyme, 80 vol% 2-propanol).**

Simplified summary of the kinetic and thermodynamic analysis of the transfer hydrogenation system

From a thermodynamic point of view, the final product must be a racemate, since at thermodynamic equilibrium the entropy is maximized. The simulation model correctly describes this situation, since the enantiomeric excess formed under kinetic conditions is totally reduced to a racemic situation under thermodynamic conditions.

A physical model consisting of 3 volumes that are connected via tubings can also explain this situation (Figure 4.49): The amount of the starting material acetophenone and the product enantiomers (*R*) and (*S*) corresponds to the reservoir of the experimental set up as shown in Figure 4.49.

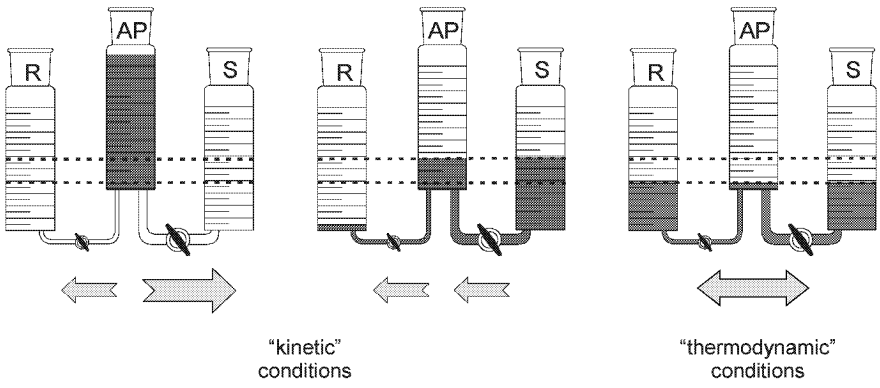

Figure 4.49: **Principle of communicating tubes for visualization the changing product concentrations.**

Hereby it is of major importance that the tubing leading from the reservoir containing the starting material acetophenone to the product reservoir of the (*S*) enantiomer has a considerably larger diameter than that leading to the (*R*) reservoir. According to the kinetic model, this demonstrates the much higher reaction rate leading to the (*S*) than to the (*R*) enantiomer. During the course of a "reaction" the following phases can be differentiated:

1. After starting the reaction (opening of both valves), the two product reservoirs of the (*R*)- and (*S*)-enantiomers are filled up at different rates. This situation describes the *kinetic conditions* of the batch reactor simulation.
2. After a special time period, the same filling height is reached in the reservoir of the starting material acetophenone and in the reservoir of the product (*S*)-enantiomer. At the same time, there is only a low volume contained in the (*R*)-reservoir, since the tubing leading to this reservoir is much smaller. In this situation, a high excess of the (*S*)-product occurs, since equilibrium conditions are not reached yet, which is expressed by the dotted line. This relates to high enantiomeric excess. The (*R*)-reservoir as well as the (*S*)-reservoir are not at equilibrium (different filling heights); therefore, the direction of the flow is changed from the (*S*)-reservoir to the (*R*)-reservoir.
3. Only after reaching equal filling heights in all reservoirs, *thermodynamic conditions* are established. At this point, the same amounts of the (*S*)- and (*R*)-enantiomer (racemate) are being formed.

4.3.3 Operation and simulation of continuously operated reactors

The set up of the reactor system is shown schematically in Figure 4.50 and as a photo in Figure 4.51. The continuous synthesis was carried out in membrane reactors with reactor volumes of 3 or 10 mL, respectively, that were thermostated to 45°C. A nanofiltration membrane MPF-50 (Koch-Membrane Systems, Germany) was used to retain the chemzyme. Stainless steel or polyether ether ketone (PEEK) served as the reactor materials. Chemical-resistant sealings were custom made out of Teflon or polyfluorinated polymers, and stainless steel capillaries were used as tubings. All other reactor materials were made out of Teflon. The flow rate established by alternating piston pumps was measured with mass flow meters and regulated by a PID-controller.

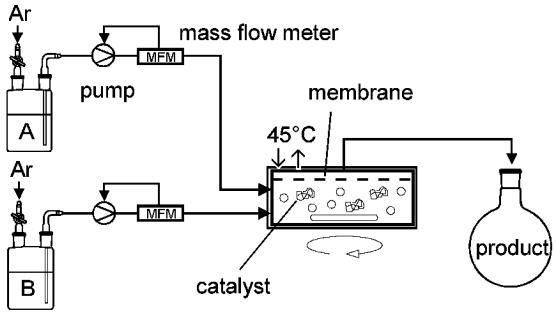

Figure 4.50: Flow scheme of the continuously operated chemical membrane reactor (CMR).

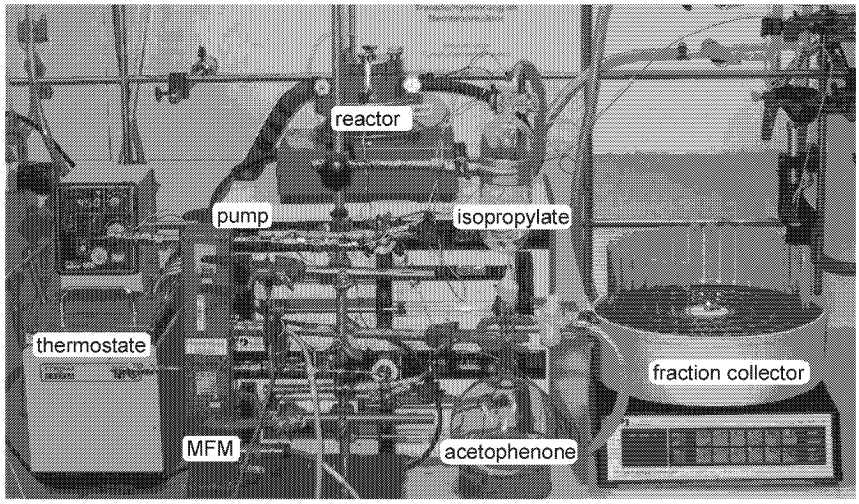

Figure 4.51: Photo of the continuously operated chemical membrane reactor.

Oxygen had to be strictly excluded from the reaction system, because otherwise the catalyst became deactivated irreversibly.Furthermore, as recognized with several other transfer hydrogenation catalysts, the catalyst is sensitive to water *[Bellefon de, Tanchoux 1998]*. This could be shown in batch reactions, in which a strong dependency of the activity on the water content was observed (data not shown). Presumably, as demonstrated with similar complexes *[Stoop, et al. 2000]*, water molecules are able to coordinate to the activated catalyst (➲ Figure 4.40, page 140). Because of this sensitivity, the water content in the feed stream had to be minimized. By use of the Karl-Fischer-Method, titration showed that the water content could be reduced to 0.005% by drying the feed stream over molecular sieves. Nevertheless, in a continuous application, depending on different concentrations of water in the feed stream, a significant deactivation took place (Figure 4.52, 0-32 number of residence times). The reason for this was a cumulative catalyst deactivation caused even by the small amounts of water, which still passed through the reactor over time. This deactivation is reversible, however, as

can be seen by the response to a second pulse with isopropoxide (Figure 4.52, residence times 32-51) and compensation by a continuous low isopropoxide dosage (1.2 mM) (Figure 4.52, residence times 52-180).

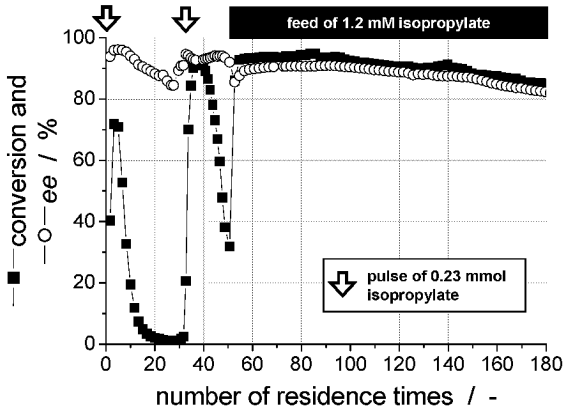

Figure 4.52: Time plot of the results of a continuous experiment in the chemzyme membrane reactor (13 mM acetophenone, 2-propanol as shown, 23 mM catalyst, 80 vol% 2-propanol, 20 vol% methylene chloride, 45°C, τ = 30 min).

As a consequence of the continuous dosage of added base, two side effects were observed: High concentrations of isopropoxide resulted in a decreased enantioselectivity of the catalyst, possibly due to an abstraction of the second chloride, which might cause a change in the catalyst geometry. Furthermore, a side reaction of the isopropoxide with the polysiloxane-polymer resulted in fragmentation of the polymer (Figure 4.53).

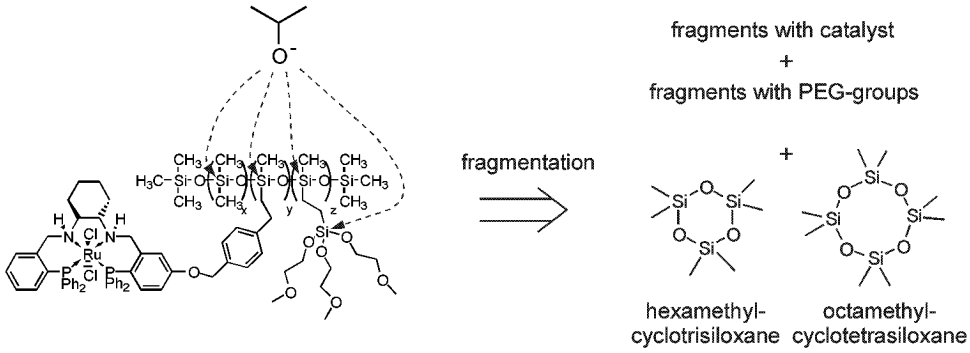

Figure 4.53: Possible side products as the result of isopropoxide reacting with the chemzyme.

This effect became noticeable by the increased amount of small cyclosiloxane fragments as a product of fragmentation *[Noll 1968]* (especially octamethylcyclotetrasiloxane $[\text{-Si}(CH_3)_2\text{O-}]_4$), which could be monitored in the reactor outlet by GC. As seen in Figure 4.54, minimal fragmentation and high enantioselectivities were achieved upon careful

adjustment of the isopropoxide concentration. Nevertheless, it could be shown, that even without any fragmentation (i.e., without adding base) the retention of the chemzyme is only 99.8%. This retention value was calculated from the amount of chemzyme that was isolated after 50 residence times. As a consequence of the fragmentation reaction at a continuous base dosage of 1 mM, this value is further decreased to 99.5%. Therefore, a continuous loss of catalyst took place. These losses (referred to as "wash out" of the catalyst) were compensated by continuously supplementing 0.5% chemzyme per residence time to the reactor. In addition to the fragmentation reaction, hydrolysis of the tris-(2-methoxyethoxy)-silane side group might result in a change of the solubility of the catalyst. However, an increase of the filtration backpressure was not observed, which would be expected to accompany a precipitation and associated blocking of the membrane due to insolubility of the catalyst. Furthermore, leaching of the transition metal was monitored. The observed ruthenium concentration, which was equal or even smaller than 0.5% of initial ruthenium concentration, could be attributed to the continuous losses of the catalyst as a result of the wash out. Therefore, we can conclude that leaching of uncomplexed transition metal may not be critical for the continuous reaction.

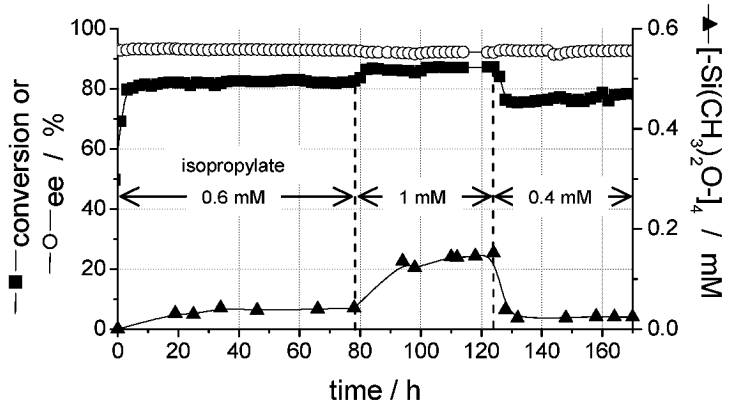

Figure 4.54: **Results of a continuous experiment in the chemzyme membrane reactor, showing conversion and *ee* as function of time (15 mM initial catalyst concentration, 0.075 mM continuous catalyst addition, initial isopropoxide concentration 15 mM, 100 mM acetophenone, 80 vol% 2-propanol, 20 vol% methylene chloride, 45 °C, τ = 60 min).**

Applying the reaction conditions as given in Figure 4.54, a continuous transfer hydrogenation was carried out with steady conversions of about 87%, enantiomeric excesses of 94%, and space-time yields of up to 255 g L^{-1} d^{-1}. The achievable total turnover number (*ttn*) can be calculated as the quotient of the catalyst activity under reaction conditions ($tof_{reaction}$ = 5.80 h^{-1}) and the catalyst consumption, given as the deactivation constant (k_{de} = 0.005 h^{-1}). This is equivalent to the continuous chemzyme replacement of 0.5% per residence time. Thus the *ttn* was determined to 1160.

To simulate continuously operated stirred tank reactors, the mass balances given for the batch reactor (eq. 4-23) need to be extended by a convection term (eq. 4-25). This term describes the outflow of reactants by reaction per residence time *[Levenspiel 1999]*.

$$\begin{aligned}
\frac{d[AP]}{dt} &= -(tof_S + tof_R)\cdot[cat] + \frac{[AP]_0 - [AP]}{\tau} \\
\frac{d[IP]}{dt} &= -(tof_S + tof_R)\cdot[cat] + \frac{[IP]_0 - [IP]}{\tau} \\
\frac{d[S]}{dt} &= tof_S \cdot [cat] - \frac{[S]}{\tau} \\
\frac{d[R]}{dt} &= tof_R \cdot [cat] - \frac{[R]}{\tau} \\
\frac{d[AC]}{dt} &= (tof_S + tof_R)\cdot[cat] - \frac{[AC]}{\tau}
\end{aligned} \qquad \textbf{eq. 4-25}$$

Based on the kinetic model and the mass balances, the influence of the process conditions (acetophenone concentration $[AP]_0$, catalyst concentration, and residence time τ) on the performance of the continuously operated membrane reactor (*ttn*, *sty*, *ee* and conversion) has been investigated and optimized. One important point to be stressed is that *ttn* is influenced by two factors: the retention and the stability of the chemzyme (eq. 4-26). The *ttn* is proportional to the $tof_{reaction}$ in the case that no deactivation (k_{de}) takes place; therefore the $tof_{reaction}$ values as determined by the simulation can directly be correlated to the *ttn*. Because of the chemzyme retention in the continuous process it is possible to apply high catalyst concentrations leading to high space-time yields. An increase of the space-time yields lead at constant catalyst concentration and constant conversion to an increase of the $tof_{reaction}$, repectively the *ttn*.

$$ttn \sim tof_{reaction} \quad \Rightarrow \quad ttn = \frac{tof_{reaction}}{k_{de}} \qquad \textbf{eq. 4-26}$$

Prior to starting the optimization, an additional correction term was integrated, accounting for the different activation of the catalyst in the continuous process as compared to the batch process, for which the kinetics has been determined *[Laue 2002]*. Here as well the continuous regeneration of deactivated catalyst by isopropoxide has been considered.

A simultaneous optimization of all four parameters (*ee*, space-time yield *sty*, conversion, $tof_{reaction}$) was not possible, since the conversion and the *ee* as well as the conversion and the *sty* showed opposite tendencies. The reason is that at high conversions the reaction rate of the chemzyme ($tof_{reaction}$) drops drastically, resulting in a decreased space-time yield (*sty*). Likewise the *ee* is decreasing with increasing conversion, as has already been shown in Figure 4.39 and Figure 4.48; therefore a minimum conversion of 80% was defined as a sensible limitation of the process parameters. In Figure 4.55 are outlined the development of *sty* and *ee*

as a function of the acetophenone concentration for two different conversions (80% and 85%, respectively). As can be seen, the space-time yield (*sty*) passes through a maximum with increasing acetophenone concentrations. The reason is a growing influence of the reverse reaction. The consequence is an increase of the residence time (τ) at constant catalyst concentration that leads to a decrease of the enantiomeric excess (*ee*). The high impact of the reverse reaction under continuous operation becomes especially visible, if these results of the simulation at 80% conversion are compared to those at 85% conversion (Figure 4.55, left). The 5% increase in conversion lowers the maximum achievable *sty* by approximately 40%. The reason is the decrease of the reaction rate ($tof_{reaction}$) at high conversions close to the thermodynamic equilibrium. As a consequence the residence time that is needed to reach very high conversion increases, resulting in low enantiomeric excess (*ee*), because of the reverse reaction.

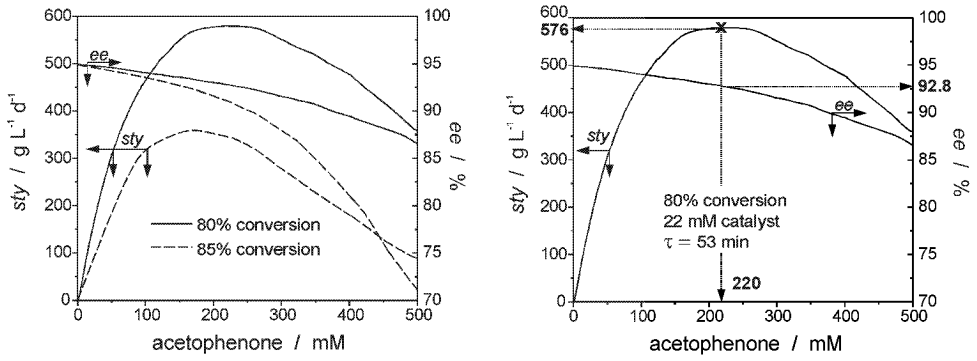

Figure 4.55: Simulation of the space-time yield (*sty*) and the enantiomeric excess (*ee*) as a function of the acetophenone concentration for two different conversion levels (left) and determination of the optimum at a conversion of 80% (steady state concentration of 1 mM isopropoxide).

In Figure 4.55, right, the determination of the optimal operating point is shown. At 80% conversion, a maximum space-time yield of 576 g L^{-1} d^{-1} is reached at 220 mM acetophenone with a respective residence time of 53 min. The enantiomeric excess of 92.8% is only 1.9% lower than the maximum achievable value of 94.7% (eq. 4-22, page 149). Based on the $tof_{reaction}$ = 13.3 h^{-1} a total turnover number of 2656 is calculated (eq. 4-26 with k_{de} = 0.005 h^{-1}).

To verify these optimum conditions, the continuous process shown in Figure 4.54 was continued with a changed set of operating parameters (Figure 4.56). As can be seen from Figure 4.55, left, the slightly increased acetophenone concentration did not have a high impact, neither on *sty* nor on *ee*. At a residence time of 60 min and an acetophenone concentration of 250 mM a conversion of 79% and a space-time yield of 578 g L^{-1} d^{-1} at 91% *ee* was achieved. Hereby the $tof_{reaction}$ was 13.16 h^{-1} and the *ttn* 2633. Lowering the steady-state isopropoxide concentration from 1 mM to 0.4 mM resulted, - as expected, - in a decrease

of the conversion and an increase of the *ee*.

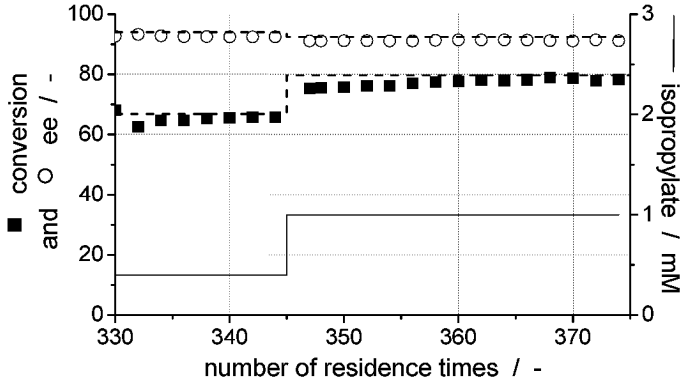

Figure 4.56: Continuation of the continuous experiment in Figure 4.54, showing the conversion and *ee* as function of time. The dotted lines are the results of simulations based on the kinetic model (15 mM initial catalyst concentration, 0.045 mM continuous catalyst addition, initial isopropoxide concentration 15 mM, 250 mM acetophenone, 80 vol% 2-propanol, 20 vol% methylene chloride, 45 °C, τ = 60 min).

The impact of the reverse reaction can easily be demonstrated, if a simulation is carried out omitting the reverse reaction. This can be established practically in such a way that the reaction product acetone is removed *in situ*. Methods that allow for the *in situ* removal of acetone are already established, i.e., online distillation or pervaporation. In the case of a substrate-coupled cofactor regeneration, the shifting effect of the reverse reaction on the equilibrium was already demonstrated *[Stillger, et al. 2002]*. The result of the corresponding simulation is shown in Figure 4.57. Without the reverse reaction, a constant enantiomeric excess of 94.7% is reached, as determined by the selectivity of the chemzyme (eq. 4-22, page 149). The space-time yield does not pass through a maximum in the absence of a reverse reaction, since when increasing the acetophenone concentration in this case, only a slight increase of the residence time is needed to yield the same conversion.

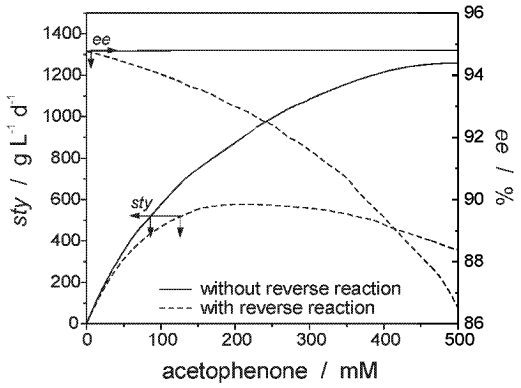

Figure 4.57: **Simulation of the space-time yield (*sty*) and the enantiomeric excess (*ee*) as a function of the acetophenone concentration with and without the reverse reaction (simulation conditions are the same as in Figure 4.55).**

4.4 Transfer hydrogenation with enzymes[49]

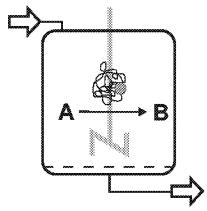

In this chapter transfer hydrogenations catalyzed by enzymes are discussed. In contrast to the transfer hydrogenations catalyzed by e.g. the *Gao-Noyori* catalyst (➲ chapter 4.3, page 135), enzymes do not catalyze a direct transfer hydrogentation. Most often nicotinamide cofactors, NAD(P)H, are needed as mediators for the reduction equivalents supplied by 2-propanol. Prior to the utilization of transition metal complexes *[Gladiali, Mestroni 1998]*, special alumina alkoxides were already applied in the thirties to reduce carbonyl compounds *[Graauw, et al. 1994]*. This type of reaction is called *Meerwein-Ponndorf-Verley* reduction (Figure 4.58) *[Meerwein 1925; Verley 1925; Ponndorf 1926]*.

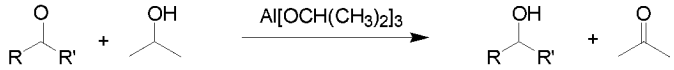

Figure 4.58: ***Meerwein-Ponndorf-Verley*** **reduction of ketones catalyzed by alumino alkoxides.**

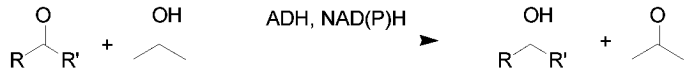

Figure 4.59: Mediated transfer hydrogenations catalyzed by alcohol dehydrogenases (ADH).

Alcohol dehydrogenases utilize nicotinamide cofactors as mediators for the asymmetric hydride transfer (➲ Figure 4.30, page 131). This topic has already been discussed in different chapters of this work. Mediated transfer hydrogenations catalyzed by alcohol dehydrogenases are essentially identical to the substrate-coupled cofactor regeneration (Figure 4.59). To regenerate the nicotinamide cofactor a sacrificial alcohol is needed as a co-substrate

[49] **Parts of this chapter are published in:**

1. T. Stillger: *Pervaporation in einem Hybridverfahren zur substratgekoppelten Cofaktorregenerierung*, diploma thesis, University of Bonn (2000)
2. L. Greiner: *Prozessentwicklung für die katalytische Reduktion mit molekularem Wasserstoff*, PhD-thesis, University of Bonn (2002)
3. M. de Oliveira Villela Filho: *Enantioselektive enzymatische Reduktion von Ketonen in Zwei-Phasen Reaktoren*, PhD thesis, University of Bonn (2003)
4. T. Zelinski, A. Liese, C. Wandrey, M.-R. Kula: *Asymmetric reduction in aqueous media: Enzymatic synthesis in cyclodextrin containing buffers*, Tetrahedron Asymmetry 10 (9) (1999) 1681-1687
5. T. Stillger, M. Bönitz, M. Villela Filho, A. Liese: *Überwindung von thermodynamischen Limitierungen in substratgekoppelten Cofaktorregenerierungsverfahren*, Chemie Ingenieur Technik 74(7) (2002) 1035-1039
6. T. Stillger, M. Villela, A. Liese, C. Wandrey: *Verfahren und Vorrichtung zur enzymatischen Co-Faktor-Regenerierung*, German patent application DE 100 60 602.4 (05.12.2000)
7. M. de Oliviera Villela Filho, W. Hummel, C. Wandrey, A. Liese: *Verfahren zur Herstellung von Alkoholen aus Substraten mittels Oxidoreduktasen, Zweiphasensystem umfassend eine wässrige Phase und eine organische Phase sowie Vorrichtung zur Durchführung des Verfahrens*, German Patent Application *DE 102 08 007.0 (26.02.2002)*

[Stampfer, et al. 2002]. This co-substrate has to meet different requirements:

- The co-substrate must be applicable in high concentrations without deactivating the alcohol dehydrogenase, to overcome thermodynamic limitations,
- the co-substrate must be a 'better' substrate than the substrate to be reduced in terms of k_M and V_{max},
- the co-substrate should be cheap in order to not increase the overall process costs,
- the oxidation product of the co-substrate should not inhibit the enzyme or react with any other reactant,
- the co-substrate and its oxidation product should be easy to separate and to remove.

Quite often in reductions, frequently also in bio-reductions, 2-propanol is applied as a sacrificial secondary alcohol that is oxidized to acetone. As already pointed out in different chapters throughout this work, thermodynamic limitations apply in the case of transfer hydrogenations (➲ chapter 4.3.2, page 139), respectively substrate-coupled cofactor regenerations. The equilibrium constant K_{eq} can be calculated via the redox potentials of the reactants utilizing the *Nernst* equation for a given set of reaction conditions, as outlined in equations eq. 4-16 – eq. 4-18. The equilibrium conversion X_{eq} for a given set of reaction conditions depends on the equilibrium constant K_{eq} and the excess ratio r_0 of the sacrificial co-substrate S_{red} to the starting material *Ox* (eq. 4-5).

$$Ox + S_{red} \rightleftharpoons Red + S_{ox} \qquad \textbf{eq. 4-27}$$

$$r_0 = \frac{[S_{red}]_0}{[Ox]_0}$$

Since the starting material *Ox* and the sacrificial co-substrate S_{red} both need to be accepted substrates of the enzyme, they are consequently closely related. Therefore, the difference of the standard redox potentials is often relatively small, if even not negative[50]. In the case of acetophenone (*Ox*) and 2-propanol (S_{red}) the difference of the standard redox potentials ΔE is – 11 mV, and K_{eq} is 0.462. As a consequence a high ratio r_0 has to be chosen due to thermodynamic reasons to yield a high conversion (see also ➲ Figure 4.42, page 144). Using eq. 4-18 and eq. 4-19[51] the equilibrium conversion X_{eq} can be calculated (eq. 4-28) after resolving the resulting quadratic equation[52].

[50] If the difference of the standard redox potentials is negative, the resulting equilibrium constant is smaller than one.

[51] *AP* equals *Ox* and *IP* equals S_{red}.

[52] For a detailed derivation see **Greiner L (2002)** Prozessentwicklung für die katalytische Reduktion mit molekularem Wasserstoff [PhD thesis]: Universtiy of Bonn..

$$X_{eq} = K_{eq} \frac{(r_0 + 1) - \sqrt{(1 - r_0)^2 + 4 K_{eq}^{-1} r_0}}{2 (K_{eq} - 1)} \qquad \text{eq. 4-28}$$

In the case of the transfer hydrogenation of acetophenone with 2-propanol catalyzed by an alcohol dehydrogenase the reachable equilibrium conversion under the conditions applied is X_{eq} = 93% with r_0 = 30 (Figure 4.60). It can be clearly seen from Figure 4.60, left, that the amount of mediator (= cofactor $NADP^+$) added does not influence the thermodynamics in view of the equilibrium conversion X_{eq}. But the cofactor concentration does have a high impact on the reaction rate, determined by the kinetics of the alcohol dehydrogenase (Figure 4.60, right). It is visible from the right graph that an increase in the cofactor concentration does result in an increased reaction rate v. In other words: The cofactor concentration does not influence the maximum reachable conversion but the time that is needed to reach it. The increase of the reaction rate up to a conversion of 0.4 is due to the fact that the oxidized cofactor needs to be reduced first when starting the batch batch, and should not be over-emphasized

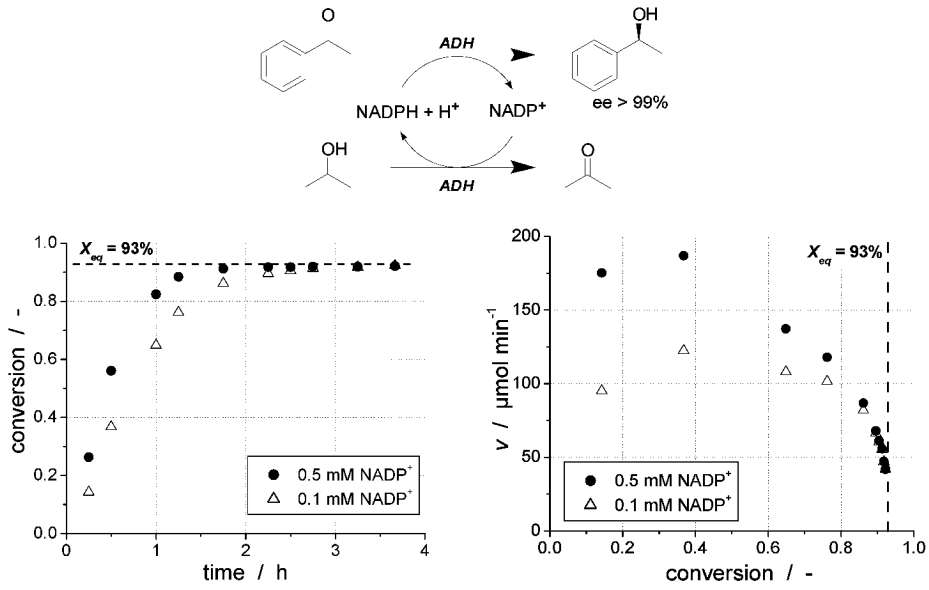

Figure 4.60: The enzyme-catalyzed mediated transfer hydrogenation exemplified by the enantioselective reduction of acetophenone. Conversion as function of time (left) and reaction rate as function of conversion (right) for two different cofactor concentrations. (10 mM acetophenone, 300 mM 2-propanol, 0.5 and 0.1 mM $NADP^+$, 50 mM phosphate buffer, pH = 8.0, 0.3 mg mL^{-1} ADH, 40°C).

As can be seen in Figure 4.61, the mediated transfer hydrogenation can also be efficiently applied for the enantioselective production of chiral alcohols, e.g. (1*S*)-2-naphthyl-ethanol, in

continuous operation. As enzyme a carbonyl reductase from *Candida parapsilosis* is utilized. Since the starting material 2-acetylnaphthalene, as well as the product is of low solubility, 50 mM hepta-(2,6-di-O-methyl)-β-cyclodextrin (DIMEB) was added. By this means the substrate solubility could be increased about 150-fold to 20 mM. The advantage of this method is, that no influence of the additive on the catalyst is observed. Besides using DIMEB to increase the starting material concentration, other approaches have been developed, such as adsorbing the substrate to anion exchange resins *[Anderson, et al. 1995]* or continuous extraction of the product *[Kragl, et al. 1996b; Kruse, et al. 1996; Rissom, et al. 1999]*. An excess ratio of the sacrificial co-substrate 2-propanol to the starting material 2-acetylnaphthalene of $r_0 = 13$ was chosen. At a residence time of $\tau = 2$ h, a conversion of 82% is reached. Reducing τ to 0.5 h, 71% conversion was obtained, corresponding to a space-time yield of 118 g L^{-1} d^{-1}.

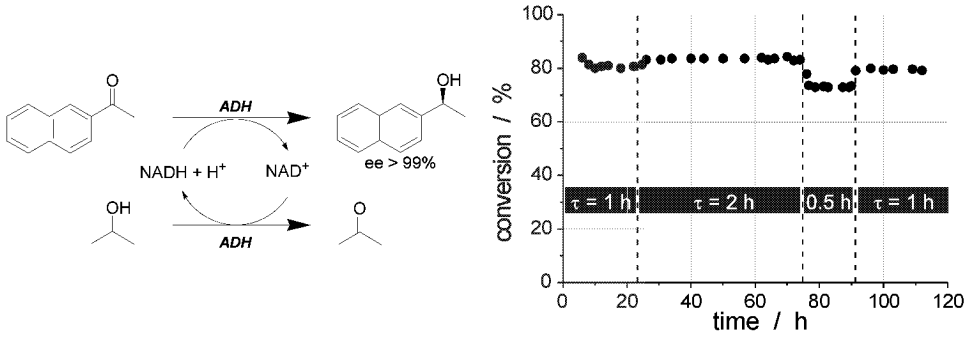

Figure 4.61: Continuous reduction of 2-acetylnaphthalene with alcohol dehydrogenase catalyzed mediated transfer hydrogenation (20 mM 2-acetylnaphthalene, 260 mM 2-propanol 0.5 mM NAD^+, 100 mM TEA buffer, pH 7.0, 2 mM DTT, 50 mM DIMEB, 4.6 U/mL *CP*CR (= *Candida parapsilosis* carbonyl reductase)) *[Zelinski, et al. 1999]*.

4.4.1 Overcoming thermodynamic limitations in transfer hydrogenation

As already explained above, the maximum reachable conversion is determined by the equilibrium constant. Therefore, substrate-coupled cofactor regenerations are very often thermodynamically limited. In general, there are two possibilities to overcome this situation:

1. Selection of a high excess ratio r_0 (eq. 4-27),
2. efficient *in situ* separation of the reaction product acetone.

In the following two different methods are presented for an efficient *in situ* removal of the reaction product acetone. For one, acetone can be separated with the membrane process of pervaporation. Secondly, acetone can be stripped from the reaction solution with air.

As a model system the enantioselective transfer hydrogenation of ethyl 5-oxohexanoate to ethyl (5*S*)-hydroxyhexanoate (*ee* > 99.5%) catalyzed by the carbonylreductase from *Candida*

parapsilosis (*CP*CR) has been investigated. Therein, the cofactor NADH is regenerated in a substrate-coupled manner with 2-propanol that is oxidized to acetone (Figure 4.62, left). A typical course of the reaction is shown in Figure 4.62, right. A maximum conversion of 75% is reached under the reaction conditions applied. In parallel to the synthesis of the chiral alcohol, acetone is stoichiometrically formed. To increase the conversion in this thermodynamically limited reaction pervaporation and stripping was tested for the *in situ* acetone removal.

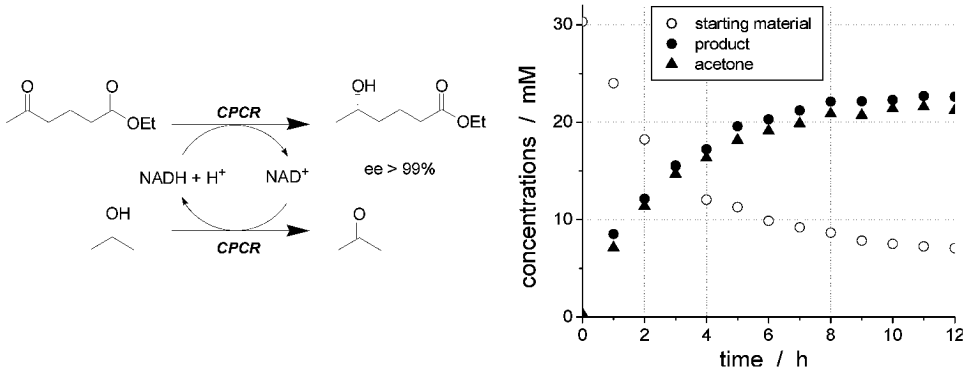

Figure 4.62: Enantioselective reduction of ethyl 5-oxohexanoate under thermodynamic limiting conditions catalyzed by *Candida parapsilosis* carbonylreductase without acetone separation. (30 mM ethyl 5-oxohexanoate, 130 mM 2-propanol, 0.2 mM NADH, 1 mM DTT, 0.15 U/mL *CP*CR, 100 mM TEA buffer pH 7.8, 35°C).

Pervaporation is the transport of compounds through a pore-free, polymer membrane with a phase transition from the liquid to the gaseous phase *[Lipnizki, et al. 2001]*. The separation principle is based on the preferred solubility and diffusion of the compounds to permeate into the polymeric membrane material *[Hänel, et al. 1994; Steinhauser, Brüschke 1994]*. The driving force for the transmembrane mass transport is the gradient of the chemical potential, resulting from the different in activities of the permeating compounds on the opposite sides of the membrane. The gradient is maintained by establishing a low pressure on the permeate side of the membrane. The flow scheme of the reactor setup is shown in Figure 4.63, left. As pervaporation membrane a composite membrane (PDMS, GKSS-Forschungszentrum Geesthacht[53], Germany) is used that consists of a selective separating layer made out of polydimethylsiloxan (PDMS, 1 µm thick), a supporting layer made out of polyetherimide (PEI), and a spun bound layer made out of polyethylene. The special characteristic of this pervaporation membrane is its high transmembrane flux. In Figure 4.63, right, the acetone and the 2-propanol flux are plotted as a function of the respective feed concentration. Acetone is the preferentially permeating compound, besides 2-propanol and water, the latter one with a

[53] The PDMS pervaporation membrane was supplied by Dr. Blümke, GKSS-Forschungszentrum Geesthacht, Germany.

constant flux of 0.9 kg h^{-1} m^{-1}.

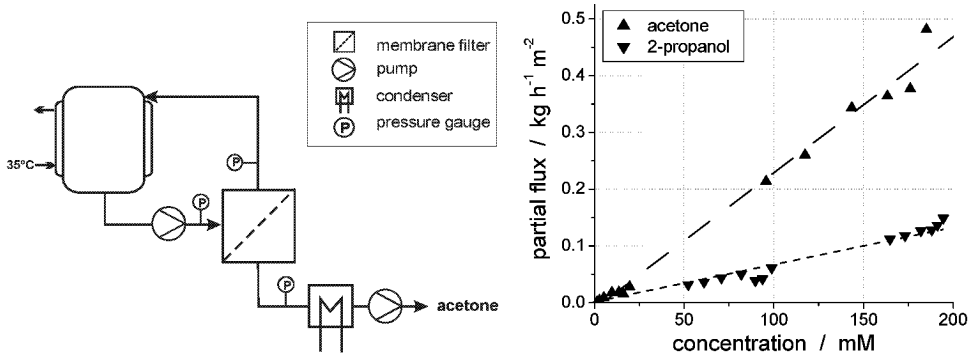

Figure 4.63: Left: Flow scheme of the pervaporation reactor; right: Partial flux of acetone and 2-propanol as function of concentration.

A second alternative for *in situ* acetone removal is stripping of the volatile compounds from the liquid phase, as already mentioned above. An inert gas stream (helium or nitrogen) is passed through the liquid, or the compound mixture to be separated is emerged to the stripping gas in a spray unit *[Sattler 1995]*. For the separation of the formed acetone during the biotransformation, compressed air is used as the most economical gas that is passed through the reaction solution. To prevent any loss of water, the compressed air is saturated with water prior to its use. Also here, as in the case of pervaporation, acetone is the predominately separated compound. The loss of 2-propanol could be compensated by a recharging of 2-propanol during the course of the experiment.

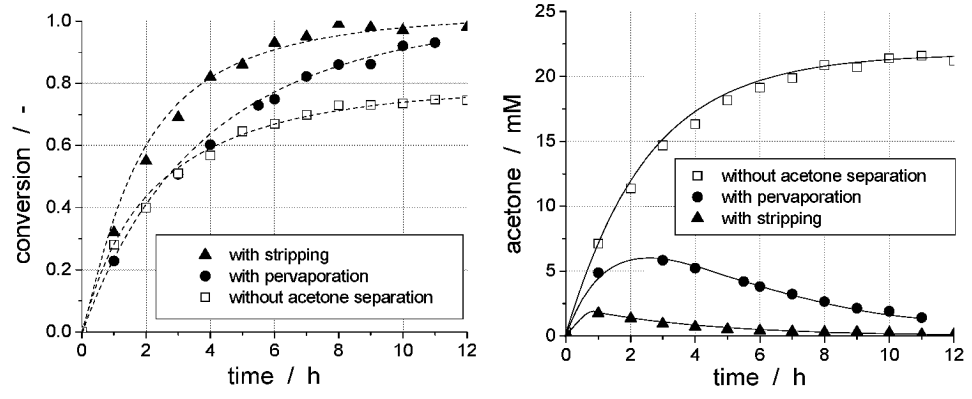

Figure 4.64: Comparison of the course of conversion and the respective acetone concentration for comparable experiments □ without acetone separation, ▲ with stripping and • with pervaporation (30 mM ethyl 5-oxohexanoate, 100 mM 2-propanol, 0.2 mM NADH, 1 mM DTT, 0.15 U mL^{-1} *CP*CR, 100 mM TEA buffer pH 7.8, 35°C; pervaporation: PDMS-pervaporation membrane, constant addition of 0.025 mL min^{-1} of 6.5 vol% aqueous 2-propanol; stripping: 0.5 L min^{-1} air, addition of 1.25 mmol 2-propanol every 20 min).

As can be seen from Figure 4.64, left, the thermodynamic limitation can be overcome by incorporating an *in situ* acetone separation. By this means, the thermodynamic driving force is maintained, enabling effective cofactor regeneration.

By applying pervaporation the acetone concentration could be maintained at a low concentration level, namely below 8 mM (Figure 4.64, right). The increase of the acetone concentration during start up of the batch is due to the high initial reaction rate. The acetone formation at high reaction rates cannot be compensated by the transmembrane flux of acetone. If the rate of acetone separation is higher than the rate of its formation, than the concentration is declining again. The reason for this phenomenon is the limited membrane area in the pervaporation unit as applied here. By using bigger pervaporation units with a higher membrane area this limitation can be circumvented, and even more selective membranes for acetone may be applied. Likewise, the *in situ* acetone separation via stripping with pre-wetted air does also work efficiently as can be seen from Figure 4.64. The acetone concentration did not pass 5 mM, and a final conversion > 97% was reached.

In both processes no total retention of 2-propanol was reached. Nevertheless, the industrial application of these hybrid processes is still attractive. The net gain in value of the product by significantly increasing the conversion by more than 20% can overcompensate a further addition step of 2-propanol and the capital investment associated with the installation of the *in situ* separation process. At a lab scale, the technical expenditure of the stripping process is lower. Stripping of protein-containing aqueous solutions often results in protein foam formation however, which can be prevented by the addition of additives. Unfortunately, the latter are often polymeric compounds that may complicate downstream processing. When scaling up the stripping process, a further recycling step of the separated compound needs to be established to meet the limits set by the government for gaseous emissions *[*Erste allgemeine Verwaltungsvorschrift zum Bundes-Immisionsschutzgesetz *cabinet decision, December 12th, 2001 2001 #1245]*. Therefore, namely because of both ecological and economical reasons, the recycling of the separated compound is required. Consequently, the additional step that needs to be integrated in large-scale operations results in a technical and energetic effort, which is comparable with those required for the pervaporation process. By contrast to the stripping process, it is possible in the pervaporation mode to influence and control the selectivity of the separation of the compound to be removed. With the stripping method, it is always the compound of highest volatility, which is the predominately removed compound.

Summary

- The substrate-coupled cofactor regeneration can be compared to the *Meerwein-Ponndorf-Verley* reduction and may be addressed as a mediated transfer hydrogenation. In this view the nicotinamide cofactor acts as a mediator for the reduction equivalents.
- The maximum reachable conversion depends on the equilibrium constant and the excess ratio of the sacrificial substrate.
- The thermodynamic limit of conversion is determined by thermodynamics, but the rate of approaching the equilibrium conversion is determined by the concentration of the mediator.
- In the continuous production of (1*S*)-2-naphthyl-ethanol (*ee* > 99%) a space-time yield of 118 g L^{-1} d^{-1} at a conversion of 71% and a residence time of 0.5 h has been reached.
- The thermodynamic limitation in transfer hydrogenation can be overcome by integration of an efficient *in situ* separation of the reaction product.
- It could be demonstrated that pervaporation as well as stripping can be used successfully for the separation of acetone to shift the reaction equilibrium.

What is a nine-letter word for "biotechnology"?
Chemistry!

Paul Swanson,
Dow Chemicals,
ACS Meeting Advances in Biocatalysis,
San Francisco, 3/26/00

4.5 Comparison of chemzymes to enzymes[54]

In the preceding chapters 4.1 – 4.4 the application of the second biological principle, macromolecular catalysts, has been discussed in detail. In the following a comparison between the man-made chemical catalysts and biocatalysts is carried out using reduction with molecular hydrogen and the transfer hydrogenation as characteristic examples.

The synthesis of chemzymes, the "man-made" or chemical equivalents of enzymes, qualifying in all the following aspects is difficult and not always successful:

- high molecular weight (> 15,000 g mol^{-1})
- low molecular weight per active site
- homogeneously soluble
- high chemical stability (high *ttn*)
- high turnover frequency (*tof*)
- retainable with > 99.99% retention

Two chemzymes were synthesized, the PyrPhos chemzyme for hydrogenations with molecular hydrogen, and the *Gao-Noyori* catalyst-based chemzyme for transfer hydrogenations. In the first case of the PyrPhos chemzyme, only the preparation of a specimen with a very low stability was achieved, thus preventing its efficient application. In the latter case of the transfer hydrogenation chemzyme, an active and moderately stable

[54] **Parts of this chapter are published in:**

1. S. Laue: *Asymmetrische Transferhydrierung im chemischen Membranreaktor*; PhD-thesis, University of Bonn (2002)
2. S. Laue, L. Greiner, J. Wöltinger, A. Liese: *Continuous application of chemzymes in a membrane reactor: Asymmetric transfer hydrogenation of acetophenone*; Advanced Synthesis & Catalysis 343 (6-7) (2001) 711-7201. L. Greiner: *Prozessentwicklung für die katalytische Reduktion mit molekularem Wasserstoff*, PhD-thesis, University of Bonn (2002)
3. R. Mertens: *Reaktionstechnische Charakterisierung der Darstellung von NADPH mit Pyrococcus furiosus Hydrogenase I*, diploma thesis, University of Bonn (2001)
4. R. Mertens: *Prozessentwicklung für biokatalytische Hydrierungen mit molekularem Wasserstoff*, PhD-thesis, University of Bonn (in progress)
5. L. Greiner, D. Müller, C. Wandrey, A. Liese: *Membrane aerated hydrogenation: Enzymatic and chemical homogeneous catalysis*, submitted (2003)

catalyst has been obtained. Both non-polymer enlarged catalysts catalyze enantioselective reductions. Their respective enantioselectivity was not changed in both cases upon polymer enlargement.

For both examples of hydrogenation methods it could be demonstrated that the same process development could be applied, independent of the origin of the catalyst, man-made or nature. In the case of the chemzymes as well as of the enzymes ultra- or nanofiltration membranes are applied to retain the respective catalyst. Since chemzymes can be applied in organic solvents, making use of the high solubility of hydrophobic reactants, solvent-stable membranes have to be applied. This is sometimes a considerable restriction, since up to now only a limited number of such membranes are available. In the last years, however, this situation is improving due to the broader availability of highly specialized ceramic ultrafiltration membranes, which qualify well already for small-scale applications.

For hydrogenations with molecular hydrogen as reducing equivalent the new technology of volume aeration via a fluoro polymer tubing has been developed in this study (➲ chapter 4.1.1, page 107). This technology can successfully be applied for chemical catalysts (➲ chapter 4.1, page 103) as well as for enzymes (➲ chapter 4.2, page 119) without any modifications. Especially for continuously operated processes this technology proves to be very convenient, since the volume of the hydrogen gas phase is reduced to a minimum. Additionally, the control of the residence times is simplified, since no gas phase is involved in the reactor volume itself.

In the following the results with the transfer hydrogenation chemzyme will be compared in detail to those of the enzyme-catalyzed mediated transfer hydrogenation on the example of the enantioselective reduction of the hydrophobic substrate, 2-acetylnaphthalene (➲ chapter 4.3, page 135 and ➲ chapter 4.4, page 161). Comparable to the chemical case, in which the concentration of the catalyst could be increased by adding the co-solvent methylene chloride, now in the enzymatic approach the substrate solubility can be increased about 150-fold, to 20 mM by addition of 50 mM hepta-(2,6-di-O-methyl)-β-cyclodextrin (DIMEB). Nevertheless, the chosen example demonstrates that the low solubility of the hydrophobic organic substrates remains one of the key problems in the enzyme approach. In both cases a comparable reactor setup using an ultrafiltration membrane reactor can be used. In the enzymatic case an aqueous buffer containing the substrate (20 mM) with the DIMEB and the sacrificial substrate 2-propanol (260 mM) was pumped through the reactor. High conversions of up to 82% yielding (1*S*)-2-naphthyl-ethanol with *ee* values of 99% have been achieved. The best results of both approaches are compared in Table 4.6.

Table 4.6: Comparison of chemical and enzymatic approach for the reduction of ketones to chiral alcohols via transfer hydrogenation.

parameter	unit	chemical reduction	enzymatic reduction	Comparison
molecular weight of catalyst	g mol^{-1}	21,000	78,000	
active centers per catalyst	-	5	1	
mass per active centers	g mol^{-1}	4,200	78,000	
[ketone]	mM	250	20	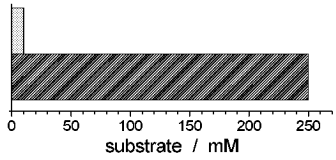
[catalyst]	mM	15	$0.04 \cdot 10^{-3}$	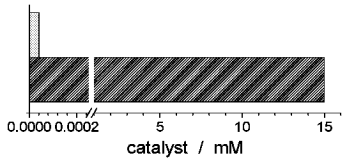
total turnover number (*ttn*)	-	2,630	$2.4 \cdot 10^{8}$	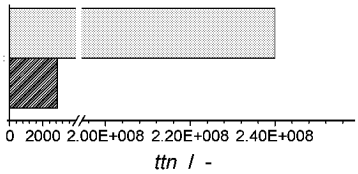
turnover frequency (*tof*)	min^{-1}	0.22	$2.3 \cdot 10^{4}$	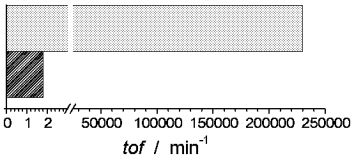
space-time yield (*sty*)	g L^{-1} d^{-1}	578	118	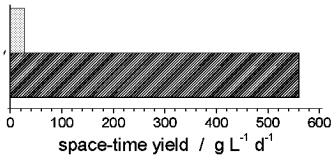
ee	%	91	> 99	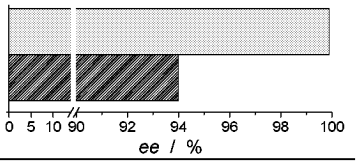

Despite the very high activity of the enzyme, but due to the low solubility of the substrate in water, only low space-time yields of 118 g L^{-1} d^{-1} can be achieved. With the unlimited substrate solubility as is the case in the organic solvent, the limiting aspect in the chemical

approach is the maximum catalyst concentration possible. To increase the solubility of the chemzyme 20 vol% methylene chloride had to be added. By retaining the catalyst, an economical use of the desirable high catalyst concentrations is obtained by decoupling the residence times of the reactants and the catalyst in this case as well. . Therefore, even with high catalyst concentrations, high *ttn* can be achieved. Furthermore, as result of the high catalyst concentration, even with low activities (up to 0.22 min^{-1} for the chemzyme compared to $2.3 \cdot 10^{-4}$ min^{-1} for the enzyme) high space-time yields of up to 578 g L^{-1} d^{-1} are possible. The application of high catalyst concentration can be achieved and tolerated, because it is possible to bind a number of catalysts to one polymer molecule. Thus, the molecular mass per active site is much lower for the chemzyme than for the enzyme. This enables a high catalyst concentration without critical increase of viscosity. The parameters in Table 4.6 clearly show that both approaches have their advantages and disadvantages. Nevertheless, in terms of stability, *ttn,* and enantioselectivity the high effectiveness of the enzyme approach is still not reached. One main reason for the high *ttn* is the effective retention of the biocatalyst. There is still some potential for improvement in case of the chemzyme, since the increase of retention by applying larger and inert polymer molecules would have a strong impact on the achievable *ttn* as shown in Figure 4.65. Increasing the retention from 99.5% to 99.9% would increase the *ttn* from 2633 to approximately 13,000. In comparison to a batch operation the *ttn* was already increased by a factor of 48, namely from 54 to 2633 (Figure 4.66).

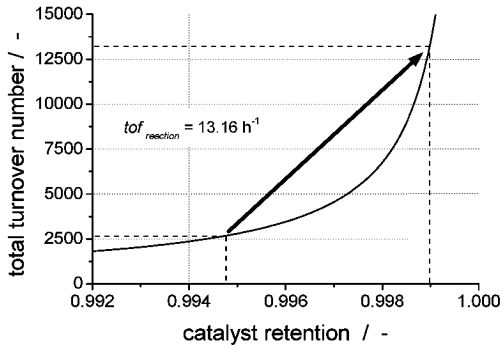

Figure 4.65: Influence of the chemzyme retention on the maximum *ttn* for a given *tof*. Retention value and *tof* are achieved with the experimental details as given in ➲ Figure 4.56, page 159.

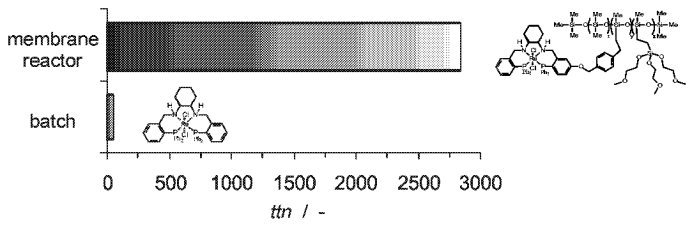

Figure 4.66: Maximum *ttn* in a batch and continuously operated membrane reactor for the chemzyme-catalyzed transfer hydrogenation.

One problem encountered in the chemzyme catalyzed transfer hydrogenation is the thermodynamic limitation. The same problem was observed before with the mediated transfer hydrogenation in the case of the enzyme-catalyzed substrate-coupled cofactor regeneration. As solution to this problem the *in situ* separation of reaction product acetone by pervaporationhas successfully been demonstrated. Likewise, this same technology can also be transferred from the bio- to the chemocatalysis, using online acetone separation. Utilizing the simulation model already established for the transfer hydrogenation chemzyme it can be predicted that space-time yields up to 1,600 g L^{-1} d^{-1} should be possible.

These investigations demonstrate that comparable reaction engineering is needed for the continuous application of chemzymes and enzymes. Both fields can learn from each other and an already established technology in one field, e.g. the volume aeration with molecular hydrogen or the *in situ* product removal by pervaporation can be efficiently transferred/applied in the corresponding field. These opens up a prospective that more engineers are needed that integrate the knowledge from both fields, enabling a faster process development.

In forecasting the future of scientific research
there is one quite general law to be noted.
The unexpected always happens.
So one can be quite sure
that the future will make any detailed predictions look rather silly.

J.B.S. Haldane (1892 – 1964),
in "The Future of Biology"

5 Discussion and outlook[55]

The results of the individual chapters have already already been extensively discussed in their places. At this place a compact discussion of the essential points and perspectives for the future will be provided.

The production of enantiopure compounds is of increasing importance to the chemical and biotechnological industries. Bioorganic transformations are predestined to meet this demand due to their inherent regio- and stereoselective nature. Indeed, a growing amount of enantiopure chemicals for pharmaceutical purposes are being produced biocatalytically today, in contrast to the production of racemic bulk commodities in the past. In this sense, biosynthesis needs to be understood as "chemistry by nature". The biological principles optimized over thousands of years experience a new renaissance when applied to technical asymmetric catalysis. Nevertheless, one key tool or prerequisite for their application is the appropriate technology, namely reaction engineering. As has been pointed out in this report, without technology no economically attractive transfer takes place. The *1st biological principle*, namely *complex chemicals are synthesized in reaction sequences* (➲ box, page 3), is presently becoming more and more attractive in view of a 'sustainable development', as has also been pointed out in the recent 'OECD Report on Biotechnology' *[OECD 2001]*. The OECD demands to increase sustainability by setting up cascades of reactions and integrating the syntheses of the precursors. This is nothing more or less than something equivalent to the above named *1st biological principle*. Thanks to the high regio- and stereoselectivity of biocatalysts, protection steps, which are required following classical routes of organic

[55] **Parts of this chapter are published in:**

1. C. Wandrey, A. Liese, D. Kihumbu: *Industrial biocatalysis: Past, present and future*; Organic Process Research & Development 4 (2000) 286-290
2. A. Liese, K. Seelbach und C. Wandrey: *Industrial Biotransformations*; VCH-Wiley, Weinheim, 2000
3. A. Liese: *Industrial applications and processes using biocatalysis*; in: Enzyme Catalysis in Organic Synthesis, 2nd edition, (K. Drauz, H. Waldmann, S.M. Roberts, eds.), VCH-Wiley, Weinheim (2002) 1419-1460

synthesis, become superfluous. Omitting them waste is drastically reduced and the starting materials are utilized much more economically. In addition, stages for the purification of intermediates can often be neglected in biocatalytic reaction sequences.

All of this can be achieved with isolated enzymes (➲ chapter 3.2.2, page 70, *demonstrated on the example of the one-pot synthesis of oligosaccharides using multicatalyst systems*), as well as with wild-type whole cells (➲ chapter 3.1.1, page 21, *demonstrated via the biocatalyzed diastereoselective reduction of 2,5-hexanedione*), and with genetically modified organisms. Starting up reaction sequences not beginning with already advanced intermediates, but instead with bulk chemicals (➲ chapter 3.2.1, page 45, *demonstrated by means of the example of the enzyme-catalyzed enantioselective carboligation starting from benzaldehyde and acetaldehyde*) enables an economically attractive production process. The classification of the aforementioned and referenced examples in this report is outlined in Figure 5.1. The possibility to discriminate undesired parallel and consecutive reactions in reaction sequences by means of reaction engineering or by means of genetic engineering for whole cell biotransformations may well bring about a renaissance to the field of technical asymmetric catalysis. Probably, there will also be a renaissance of whole cell biotransformations, whereby undesired side activities and further metabolizing steps (excluding the desired reaction) are suppressed by means of gene-disruption. Right now, work is going on to install non-natural cofactor regenerating systems in whole cells ("designer strains"). Especially the methods of non-natural evolution of enzymes - and in particular the possibility to combine such enzymes in one strain, - can be of great importance for biocatalysis in future.

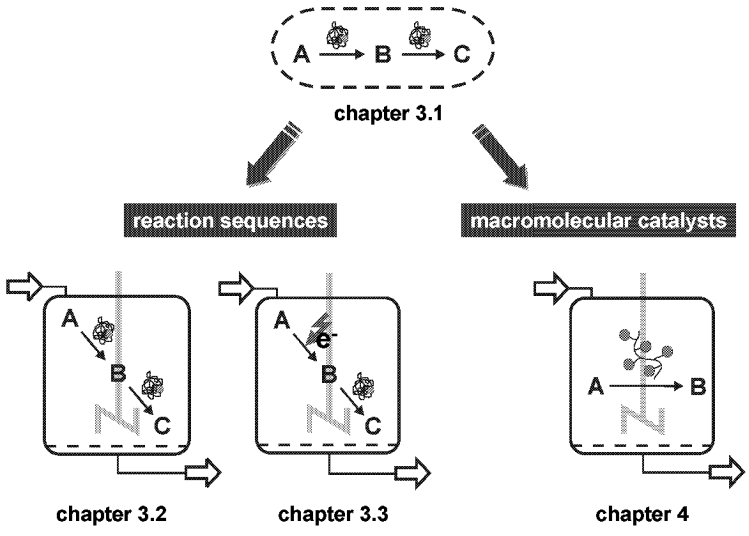

Figure 5.1: Biological principles applied to technical asymmetric catalysis.

In contrast to the latter described *in vivo* technologies, the realization of *in vitro* reaction sequences opens up ways to establish new reaction sequences that are not common in nature. Driving biotransformations with energy in form of electrons supplied by an external electrical power supply (➲ chapter 3.3.1, page 90, *demonstrated on the example of electrochemical in situ supply of H_2O_2 for enzyme-catalyzed sulfoxidations*) or by light using photosensitive electron-transfer mediators might become one of the new key technologies to accomplish redox biotransformations. Since this is a rather new field, however, it has only been exploited scarcely by a few pioneers, notably by the late *E. Steckhan* of the University of Bonn. It can be hoped, however, - and even be expected with confidence in the opinion of this author - that this concept will catch on and in due time. It will not only prove to be very attractive scientifically, but also technically, and quite likely even economically.

In the hopefully not too distant future a more detailed understanding of the physical organic basis of enzyme catalysis will be accessible. This prerequisite is required namely to optimize the reaction systems as well as the substrate (➲ chapter 3.2.1.1, page 49, *demonstrated on the example of the Hammett correlation and molecular refractivity*) and to carry out 'solvent engineering' (➲ chapter 3.2.1.2, page 61, *demonstrated on the example of organic (co)solvent addition*). Additionally, by means of elaborate reactor engineering (i.e., via multi-phase bioreactors) or by the development of solvent-resistant organisms/enzymes, the use of organic solvents for enzymatic reactions will probably become increasingly possible.

The *2nd biological principle*, namely *biological catalysts are macromolecular and in general homogeneously soluble*, points the way to the development of artificial *chemzymes* (*chem*ical en*zymes*) (➲ chapter 4.1, page 103, *demonstrated on the example of hydrogenations using molecular hydrogen* and ➲ chapter 4.3, page 135, *demonstrated on the example of transfer hydrogenation*). Nowadays, still most industrial applications of homogeneous catalysis are carried out in batch reactors with catalysts immobilized on a heterogeneous support. Here new technologies based on the *2nd biological principle* might initiate a change of the established production processes in the future, especially for the syntheses of chiral compounds.. Membranes can retain macromolecular catalysts, like enzymes, that are homogeneously soluble. By this means mass transfer limitations that are very often observed in conventional catalysis can be overcome, thereby increasing the productivity and decreasing the catalyst consumption.

In this report, hydrogenations with molecular hydrogen as well as transfer hydrogenations have been investigated using chemzymes. Furthermore, for the hydrogenation with molecular hydrogen a new aeration method for supplying H_2 has been developed, copying the biological principle and function of lungs. This concept could be proved to be applicable for catalysis using a homogeneous catalyst containing a transition metal (➲ chapter 4.1.2, page 110, *demonstrated on the example of hydrogenations catalyzed by PyrPhos*) or alternatively an enzyme (➲ chapter 4.2.4, page 129, *demonstrated on the example of hydrogenation catalyzed*

by a hydrogenase from Pyrococcus furiosus). Pervaporation could be proved as a suitable and selective method for the removal of acetone in mediated transfer hydrogenations using enzymes (➲ chapter 4.4, page 161, *demonstrated on the example of substrate-coupled cofactor regeneration*). The same thermodynamic limitation as in the case of the substrate-coupled cofactor regeneration governs the transfer hydrogenation via organic transition metal catalysts. It can already be expected that the thermodynamic limitations can also be overcome in the latter case by removal of acetone by means of pervaporation. This would then represent another example of a successful transfer of technologies between the worlds of biology and chemistry.

But there is still another, not yet discussed point, with considerable potential, which may also impact technical asymmetric catalysis eventually. However, even though biocatalysts are efficient, active, and selective, there remains still one big disadvantage: At the present time, there is not yet an appropriate enzyme known or available for every given chemical reaction. It is estimated that there exist about 25,000 enzymes in nature, and 90% of these have still to be discovered *[Appel, et al. 1994; Bairoch 1994]*. Furthermore, approximately only 10% of all known/investigated enzymes are already available on an industrial scale. This represents a challenge and opens up a new 'playground' for chemists. For several fundamental, very important chemical reactions, no suitable enzymes have yet been described. Some examples for such voids are listed in Table 5.1.

Table 5.1: Organic chemical reactions where until now no isolated enzyme is known for.

Type of reaction	Formula
Heck reaction, *Stille*- and *Suzuki*-coupling	
hydroformylation of alkenes	
metathesis of alkenes	
hydrogenation of aromates	

Until recently, the very prominent Diels-Alder reaction would also have belonged to this table. But within the last two years reports have been published describing a biocatalytic Diels-Alder reaction *[Pohnert 2001]*. Nevertheless, the way to a routine application of "Diels-Alderases" might still be long. The challenge of the future will be to design chemzymes that can catalyze even those reactions, which are not yet feasible with enzymes. And an even further projection might be the successful combination of chemzymes with enzymes in

continuously operated reactors to synthesize complex products diastereoselectively starting from bulk chemicals.

In summary, understanding biological principles and processes both in organic chemical and physical terms is a prerequisite and represents the first step towards the development of novel engineered systems utilizing these biological principles. To implement these concepts requires engineers that integrate the knowledge of these diverse fields, namely of biocatalysis, physical organic chemistry, and biochemical engineering.

"If we wish to catch up with nature,
we shall need to use the same methods that she does."

Emil Fischer 1902, Nobel Lecture

6 Summary

Two major biological principles, namely *reaction sequences* and *homogeneously soluble, macromolecular catalyst*, were identified and have been transferred to technical asymmetric catalysis.

First biological principle: Reaction sequences

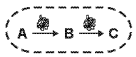

- The biological principle of reaction sequences simplifies the downstream processing.
- Utilizing *Lactobacillus kefir* **(2*R*,5*R*)-hexanediol** was produced in a newly designed, continuously operated process with an ***ee* and *de* > 99%** at a space-time yield of **64 g L^{-1} d^{-1}**. This process has been transferred to an industrial company.

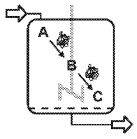

- Utilizing *in vitro* reaction sequences, **all four possible diastereomers of 1-phenylpropane-1,2-diol** were selectively synthesized with ***de* > 98%** by sequential use of a lyase and an oxidoreductase, starting from the bulk chemicals benzaldehyde and acetaldehyde.
- **(2*R*)-Hydroxypropiophenone** was continuously produced by benzaldehyde lyase-catalyzed carboligation with an ee > 99% and a space-time-yield of **1,100 g L^{-1} d^{-1}**.
- Applying **physical organic principles** like the *Hammett* postulate and using molar refractivity allows to **predict the enantiomeric excess** in benzoylformate dehydrogenase-catalyzed carboligations.
- **Principles of biological evolution** have been transferred to technical evolution by using **genetic algorithms** for the optimization of reaction conditions of the **core 2-Bn** synthesis in a **one-pot biocatalytic reaction sequence**
- Syntheses of **sialyl T threonine esters** in a **one-pot biocatalytic reaction sequence** starting from N-Fmoc-(O-N-acetylgalactosaminyl)threonine *tert*-butyl ester.

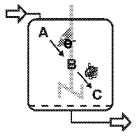

- In electroenzymatic reactions energy and mass transport can be separated, in contrast to reactions occurring in whole cells as practiced by nature.
- A newly designed three-dimensional electrode has successfully been applied for the cathodic reduction of O_2, the first step of the electroenzymatic reaction sequence.
- (*R*)-Methylphenylsulfoxide was produced with an ***ee* = 99%** and a space-time yield of **104 g L^{-1} d^{-1}** in a newly developed electroenzmyatic reactor, utilizing chloroperoxidase.

Second biological principle: Macromolecular catalysts

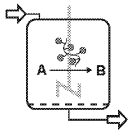

- Biological principles are even applicable and attractive under non-natural conditions.
- A **new aeration technology for supplying H_2** to catalytic reaction cycles has been developed, copying the biological function of lungs. This enables the easy operation of continuously operated hydrogenations with enzymes and chemzymes.
- Applying this technology, **NADPH** was produced via hydrogenation catalyzed by a **hydrogenase**, at a space-time yield of **130 g L^{-1} d^{-1}**.
- A new transfer hydrogenation **chemzyme** was developed, characterized kinetically, and applied successfully to the continuous production of **(1*S*)-phenylethanol (ee = 91%)** at a space-time yield of **578 g L^{-1} d^{-1}** and a ***ttn* = 2633** for the chemzyme.
- Thermodynamic limitations in oxidoreductase-mediated transfer hydrogenations have been overcome by integration of a selective acetone removal step, i.e., by means of pervaporation.

7 Literature

Ablay P (1987) Optimieren mit Evolutionsstrategien. Spektrum der Wissenschaft: 104-115.

Achiwa K (1976) Asymmetric hydrogenation with new chiral functionalized bisphosphine-rhodium complexes. JACS 98: 8265-8266.

Adam W, Fell RT, Mock-Knoblauch C, Saha-Möller CR (1996) Synthesis of optically active α-hydroxycarbonyl compounds by (salen)Mn(III)-catalyzed oxidation of silyl enol ethers and silyl ketene acetals. Tetrahedron Lett. 37: 6531-6534.

Adam W, Fell RT, Saha-Möller CR, Zhao C-G (1998a) Synthesis of optically active α-hydroxy ketones by enantioselective oxidation of silyl enol ethers with a fructose-derived dioxirane. Tetrahedron Asymm. 9: 397-401.

Adam W, Fell RT, Stegmann VR, Saha-Möller CR (1998b) Synthesis of optically active α-hydroxy carbonyl compounds by the catalytic, enantioselective oxidation of silyl enol ethers and ketene acetals with (salen)manganese(III) complexes. J. Am. Chem. Soc. 120: 708-714.

Adam W (1999) Biotransformations with peroxidases. Adv. Bio. Eng/Bio 63: 73-108.

Adams MWW (1990) The structure and mechanism of iron-hydrogenases. Biochim. Biophys. Acta 1020: 115-145.

Adams MWW (Ed) (1991): Baltimore: University of Maryland Press, College Park, MD.

Adkins H, Elofsin RM, Rossow RM, Robinson CC (1949) The oxidation potentials of aldehydes and ketones. J. Am. Chem. Soc. 71: 3622.

Ager DJ (1999) Handbook of Chiral Chemicals. New York: Marcel Dekker.

Albracht SPJ (1994) Nickel hydrogenases: in search of the active site. Biochim. Biophys. Acta 1188: 167-204.

Allain EJ, Hager LP, Deng L, Jacobsen EN (1993) Highly enantioselective epoxidation of disubstituted alkenes with hydrogen peroxide catalyzed by chloroperoxidase. J. Am. Chem. Soc. 115: 4415-4416.

Alonso DA, Brandt P, Nordin SJM, Andersson PG (1999) Ru(Arene)(amino alcohol)-catalyzed transfer hydrogenation of ketones - mechanism and origin of enantioselectivity. J. Am. Chem. Soc. 121: 9580-9588.

Alper J (2001) Searching for medicine's sweet spot. Science 291: 2338-2343.

Altenbach-Rehm J, Weuster-Botz D (1996) Einsatz von Fedbatch-Schüttelkolben zur Bioprozessentwicklung. Bio World 5: 22-23.

Altenbach-Rehm J, Weuster-Botz D, Drescher T, Wandrey C (1996) Fedbatch-Schüttelkolbentechnik - Werkzeug für die biotechnologische Prozeßentwicklung. Chem.-Ing.-Tech. 68: 1432-1436.

Anderson BA, Hansen MM, Harkness AR, Henry CL, Vinzenzi JT, Zmijewski MJ (1995) Application of a practical biocatalytic reduction to an enantioselective synthesis of the 5*H*-2,3-benzodiazepine LY200164. J. Am. Chem. Soc. 117: 12358-12359.

Appel RD, Bairoch A, Hochstrasser DF (1994) A new-generation of information-retrieval tools for biologists - the example of the expasy www server. Trends in Biochemical Sciences 19: 258-260.

Arrhenius S (1889) Über die Reaktionsgeschwindigkeit bei der Inversion von Rohrzucker durch Säuren. Z. phys. Chem. 4: 226-248.

Bailey JE, Ollis DF (1986) Biochemical engineering fundamentals. New York: McGraw Hill Publishing Company.

Bairoch A (1994) The enzyme data-bank. Nucleic Acids Res. 22: 3626-3627.

Bayer E, Schurig V (1975) Lösliche Metallkomplexe von Polymeren zur Katalyse. Angew. Chem. 87: 484.

Beck W, Nagel U (1988) Optisch aktive 3,4-Bis(diphenylphosphino)-pyrrolidone, diese als chirale Liganden enthaltende Rhodiumkomplexe und deren Verwendung. US Patent, EP 0151282.

Bellefon de C, Tanchoux N (1998) Effect of non-linear kinetics on the enantioselecctivity in the H-transfer asymmetric homogeneous reduction of arylketone with a rhodium diamine catalyst. Tetrahedron Asymm. 9: 3677.

Bergbreiter DE, Case BL, Liu U-S, Caraway JW (1998) Poly(*N*-isopropylacrylamide) soluble

polymer supports in catalysis and synthesis. Macromolecules 31: 6053-6062.

Bergbreiter DE (2002) Using soluble polymers to recover catalysts and ligands. Chem. Rev. 102: 3345-3384.

Bergel A, DevauxBasseguy R (1996) First attempts in bioelectrochemical engineering. J. Chim. Phys.-Chim. Biol. 93: 753-762.

Bewley CN, Faulkner DJ (1998) Steinschwämme: Stars unter den Naturstoffproduzenten oder Wirte des Stars? Angew. Chem.: 2281-2297.

Biade A-E, Bourdillon C, Laval J-M, Mairesse G, Moiroux J (1992) Complete conversion of L-lactate into D-lactate. A generic approach involving enzymatic catalysis, electrochemical oxidation of NADH, and electrochemical reduction of pyruvate. J. Am. Chem. Soc. 114: 893-897.

Bierhuizen MFA, Fukuda M (1992) Expression cloning of a cdna-encoding upd-glcnac-gal-beta-1-3-galnac-r (glcnac to galnac) beta-1-6glacnac transferase by gene-transfer into cho cells expressing polyoma large tumor-antigen. Proc. Nat. Acad. Sci. U.S.A. 89: 9326-9330.

Biller KF, Kato I, Märkl H (2002) Effect of glucose, maltose, soluble starch, and CO_2 on the growth of the hyperthermophilic archaeon *Pyrococcus furiosus*. Extremophiles 6: 161-166.

Biselli M (1991) Enzymkatalysierte Racematspaltung von Aminosäuren mit integrierter Rückführung - dargestellt am Beispiel der Umsetzung von D,L-Alanin zu L-Alanin [Dissertation]. Bonn: Universität Bonn.

Biselli M, Kragl U, Wandrey C (2002) Reaction engineering for enzyme-catalyzed biotransformations. In: Enzyme catalysis in organic synthesis. Edited by Drauz K, Waldmann H: Wiley-VCH; 185-258. vol 1.

Blaser H-U (1991) Enantioselective synthesis using chiral heterogeneous catalysts. Tetrahedron Asymm. 2: 843-866.

Bommarius A, Krimmer H-P, Reichert D, Almena J, Karau A, Wöltinger J, Drauz K, Liese A, Greiner L, Wandrey C (2001) Volumenbegasung. US Patent, German Patent Application DE 101 63 168.5.

Bongs J, Hahn D, Schörken U, Sprenger GA, Kragl U, Wandrey C (1997) Continuous production of erythrulose using transketolase in a membrane reactor. Biotechnol. Lett. 19: 213-215.

Bornscheuer U (2000) Industrial Biotransformations. In: Biotechnology-Serie. Edited by Rehm H, Reed G, Pühler A, Stadler P: Wiley-VCH; 277-294. vol 8b.

Bortolini O, Fantin G, Fogagnolo M, Giovannini PP, Guerrini A, Medici A (1997) An easy approach to the synthesis of optically active *vic*-diols: A new single-enzyme system. J. Org. Chem. 62: 1854-1856.

Bortolini O, Casanova E, Fantin G, Medici A, Poli S, Hanau S (1998) Kinetic resolution of *vic*-diols by *Bacillus stearothermophilus* diacetyl reductase. Tetrahedron Asymm. 9: 647-651.

Bradshaw CW, Hummel W, Wong C-H (1992) Lactobacillus kefir alcohol dehydrogenase: A useful catalyst for synthesis. J. Org. Chem. 57: 1532-1536.

Bredig G, Fiske PS (1912) Biochem. Z. 46: 7.

Brielbeck B, Frede M, Steckhan E (1994) Continuous electroenzymatic synthesis employing the electrochemical enzyme membrane reactor. Biocat. 10: 49-64.

Brinkmann N, Giebel D, Lohmer G, Reetz MT, Kragl U (1999) Allylic substitution with dendritic palladium catalysts in a continously operated membrane reactor. J. Cat. 183: 163.

Brockhausen I (1995) Biosynthesis of O-glycans of the N-acetylgalactosamine-alpha-Ser/Thr linkage type. In: Glycoproteins. Edited by Montreuil J, Schachter H, Vliegenthart JFG: Elsevier Science B. V.; 201-258.

Brockhausen I, Yang J-M, Burchell J, Whitehouse C, Taylor-Papadimitriu J (1995) Mechanisms underlying aberrant glycosylation of muc1 mucin in breast-cancer cells. Eur. J. Bioch. 233: 607.

Brown JM, Chaloner PA (1980a) Structural characterization of a transient intermediate in rhodium-catalyzed asymmetric homogeneous hydrogenation. J. Chem. Soc.-Chem. Commun.: 344-346.

Brown JM, Chaloner PA (1980b) The mechanism of asymmetric homogeneous hydrogenation - rhodium(I) complexes of dehydroamino acids containing asymmetric ligands related to bis(1,2-diphenylphosphino)ethane. J. Am. Chem. Soc. 102: 3040-3048.

Bruhn H, Pohl M, Mesch K, Kula MR (1995) Verfahren zur Herstellung von Acyloinen, dafür geeignete Pyruvatdecarboxylase sowie deren Herstellung und DNA-Sequenz des für diese kodierenden PDC-Gens. US Patent, 195 23 269. 0-41.

Brunner H, Amberger K, Wischert T, Wiehl J (1991) Asymmetrische Katalysen, 69[1], Enantioselektive Hydrierung von Dicarbonylverbindungen mit NaBr/L-(+)-Weinsäure modifizierten Nickelkatalysatoren. Bulletin des societes chimiques belges 100: 585-595.

Brunner H (2000) Hydrogenation. In: Applied Homogeneous Catalysis with Organometallic Compounds. Edited by Cornils B, Herrmann WA: VCH; 201.

Bryant FO, Adams MWW (1989a) Characterization of hydrogenase from hyperthermophilic archaebacterium, *Pyrococcus furiosus*. J. Biol. Chem. 264: 5070-5079.

Bryant FO, Adams MWW (1989b) Characterization of hydrogenase from hyperthermophilic archaebacterium, *Pyrococcus furiosus*. The Journal of Biological Chemistry 264: 5070-5079.

Buchholz A, Greiner L, Hoh C, Liese A (2002) Genetic algorithms as tool for capillary electrophoresis method development. Journal of Capillary Electrophoresis and Microchip Technology 7: 51-60.

Buchholz K, Kasche V (1997) Biokatalysatoren und Enzymtechnologie. Weinheim: VCH Verlagsgesellschaft mbH.

Bunce RA (1995) Recent advances in the use of tandem reactions for organic synthesis. Tetrahedron 51: 13103-13159.

Burk M, Harper G, Kalberg C (1995a) Highly enantioselective hydrogenation of beta-keto-esters under mild conditions. J. Am. Chem. Soc. 117: 4423-4424.

Burk MJ, Feaster JE, Harlow RL (1990) New electron-rich chiral phosphines for asymmetric catalysis. Organomet. 9: 2653-2655.

Burk MJ (1991a) C2-symmetric bis(phospholanes) and their use in highly enantioselective hydrogenation reactions. J. Am. Chem. Soc. 113: 8518-8519.

Burk MJ (1991b) Optically pure 1,4-diols. US Patent, US 5,021,131.

Burk MJ, Feaster JE, Harlow RL (1991) New chiral phospholanes; synthesis, characterization, and use in asymmetric hydrogenation reactions. Tetrahedron Asymm. 2: 569-592.

Burk MJ (1992) Chiral phospholanes via chiral 1,4-diol cyclic sulfates. US Patent, US 5,171,892.

Burk MJ, Gross MF, Martinez JP (1995b) Asymmetric catalytic synthesis of β-branched amino acids via highly enantioselective hydrogenation reactions. J. Am. Chem. Soc. 117: 9375-9376.

Burk MJ, Casy G, Johnson NB (1998) A three-step procedure for asymmetric catalytic reductive amidation of ketones. J. Org. Chem. 63: 6084-6085.

Burley SK, A. PG (1985) Aromatic-aromatic interaction - a mechanism of protein-structure stabilization. Science 229: 23-28.

Butt JN, Filipiak M, Hagen WR (1997) Direct electrochemistry of *Megaspaera elsdenii* iron hydrogenase. Eur. J. Bioch. 245: 116-122.

Cane DE (1990) Enzymatic formation of sesquiterpens. Chem. Rev. 90: 1089-1103.

Canfield WM, Cummings RD, Ju TUS (2001) US Patent, U.S. Patent WO 01/44478 A2.

Cantacuzene D, Attal S (1991) Enzymatic-synthesis of galactopyranpsyl-L-serine derivatives using galactosidases. Carb. Res. 211: 327-331.

Caron G, Kazlauskas RJ (1994) Isolation of racemic 2,4-pentanediol and 2,5-hexanediol from commercial mixtures of racemic and meso isomers by way of cyclic sulfites. Tetrahedron Asymm. 5: 657-664.

Carrea G, Sergio Riva S (2000) Enzyme in organischen Lösungsmitteln: Eigenschaften und Einsatz in der Synthese. Angew. Chem. 112: 2312-2341.

Casu B, Reggiani M, Sanderson GR (1979) Methylated cycloamyloses (cyclodextrins) and their inclusion properties. Carb. Res. 76: 59-66.

Chang ML, Eddy RL, Shows TB, Lau JTY (1995) Three genes that encode human beta-galactoside alpha 2,3- sialyltransferases. Structural analysis and chromosomal mapping studies. Glycobiology 5: 319-325.

Chen L-Y, Ghosez L (1991) Intramolecular cycloadditions of keteniminium salts. A practical asymmetric synthesis of prostaglandins. Tetrahedron Asymm. 2: 1181-1184.

Chenault HK, Whitesides GM (1987a) Regeneration of nicotinamide cofactors for use in organic synthesis. Appl. Biochem. Biotechnol. 14: 147-197.

Chenault HK, Whitesides GM (1987b) Regeneration of nicotinamide cofactors for use in organic synthesis. Appl. Biochem. Biotechnol. 14: 147-197.

Cheryan M (1986) Process design. In: Ultrafiltration handbook. Edited by: Technomic Publ. AG.

Chong JM, Clarke IS, Koch I, Olbach PC, Taylor NJ (1995) Asymmetric synthesis of *trans*-2,5-diphenylpyrrolidine: A C2-symmetric chiral amine. Tetrahedron Asymm. 6: 409-418.

Choudary MB, Chowdari NS, Madhi S, Kantam ML (2001) A trifunctional catalyst for the synthesis of chiral diols. Angew. Chem. 113: 4755-4759.

Chowdhury RL, Bäckvall J-E (1991) Efficient ruthenium-catalysed transfer hydrogenation of ketones by propan-2-ol. J. Chem. Soc., Chem. Commun.: 1063-1064.

Collins AN, Sheldrake GN, Crosby J (1992) Chirality in industry. New York: John Wiley & Sons, Inc.

Colonna S, Gaggero N, Richelmi C, Pasta P (1999) Recent biotechnological developments in the use of peroxidases. Tibtech 17: 163-168.

Compan V, López ML, Andrio A, López-Alemany A, Refojo MF (1999) Determination of the oxygen transmissibility and permeability of hydrogel contact lenses. J. Appl. Polym. Sci. 72: 321-327.

Corey EJ, Bakshi RK, Shibata S (1987) Highly enantioselective borane reduction of ketones catalyzed by chiral oxazaborolidines. Mechanism and synthetic implications. J. Am. Chem. Soc. 109: 5551-5553.

Corey EJ, Helal CJ (1998) Reduktion von Carbonylverbindungen mit chiralen Oxazaborolidin-Katalysatoren: eine neue enantioselektive Katalyse und leistungsfähige Synthesemethode. Angew. Chem. 110: 2092-2118.

Cornils B, Wiebus E (1996) Virtually no environmentally impact: the biphasic oxo process. Rec. Trav. Chim. Pays-Bas 115: 211-215.

Cornils B, Herrmann WA, Schlögl R, Wong C-H (1999) Catalysis from A to Z - A Concise Encyclopedia. Weinheim: Wiley-VCH.

Cornils B, Herrmann WA (2000) Homogeneous catalysts and their heterogenization and immobilization. In: Applied Homogeneous Catalysis with Organometallic compounds. Edited by Cornils B, Herrmann WA: Wiley-VCH; 575.

Cornish-Bowden A (1995) Fundamentals of Enzyme Kinetics. London: Portland Press Ltd.

Corrie JET (1998) Preparation and properties of unsymmetrical benzoins and related compounds. Tetrahedron 54: 5407-5416.

Cumbo CC (1981) Process for Preparing Alkanediols by Electrochemical Coupling of Halohydrins, Alkanediols, when Produced by such Process, and an Electrolytic Cell Suitable for Carrying out the Process. US Patent, EP 0 024 178 A2.

Cumbo CC (1982) Process for preparing alkanediols by electrochemical coupling of halohydrins. US Patent, US 4,324,625.

Curci R, D'Accolti L, Dinoi A, Fusco C, Rosa A (1996) Selective oxidation of O-isopropylidene derivatives of diols to 2-hydroxy ketones employing dioxiranes. Tetrahedron Lett. 37: 115-118.

Davis FA, Chen B-CC (1992) Asymmetric hydroxylation of enolates with N-sulfonyloxaziridines. Chem. Rev. 92: 919-934.

Day RJ, Kinsey SJ, Seo ET, Weliky N, Silverman HP (1972) Electrochemically driven biochemical reactions: I. Reduction of pyridine nucleotides in aqueous solution. Trans. N. Y. Acad. Sci. 34: 588-594.

De Luca G, De Philip P, Rousset M, Bélaïch J-P, Dermoun Z (1998) The NADP-reducing hydrogenase of *Desulfovibrio fructosovorans*: Evidence for a native complex with hydrogen dependent methyl viologen reducing activity. Biochem. Biophys. Research Commun. 248: 591-596.

De Vos WE, Vankelecom IJF, Jacobs P (2000) Chiral catalyst immobilization and recycling. Weinheim: Wiley-VCH.

Delecouls K, Basseguy R, Bergel A (1998) Some aspects of bioelectrochemistry - Prospects for using electrochemical processes at an industrial scale. Actual Chim.: 91-94.

Delecouls K, Saint-Aguet P, Zaborosch C, Bergel A (1999) Mechanism of the catalysis by *Alcaligenes eutrophus* H16 hydrogenase of direct electrochemical reduction of NAD(+). J. Electroanal. Chem. 468: 139-149.

Delecouls-Servat K, Basseguy R, Bergel A (2002) Designing membrane electrochemical reactors for oxidoreductase- catalysed synthesis. Bioelectrochemistry 55: 93-95.

DeMan JC, Rogosa M, Sharpe ME (1960) A medium for the cultivation of *Lactobacilli*. Journal of

Applied Bacteriology 21: 130-135.
Demir A, Dünnwald T, Iding H, Pohl M, Müller M (1999) Asymmetric benzoin reaction catalyzed by benzoylformate decarboxylase. Tetrahedron Asymm.: 4769-4774.
Demir AS, Pohl M, Janzen E, Müller M (2001) J. Chem. Soc., Perkin Trans. 1: 633.
Demir AS, Sesenoglu Ö, Eren E, Hosrik B, Pohl M, Janzen E, Kolter D, Feldmann R, Dünkelmann P, Müller M (2002) Enantioselective synthesis of alpha-hydroxy ketones via benzaldehyde lyase-catalyzed C-C bond formation reaction. Adv. Synth. Cat. 344: 96.
Dexter AF, Lakner FJ, Campbell RA, Hager LP (1995) Highly enantioselective epoxidation of 1,1-disubstituted alkenes catalyzed by chloroperoxidase. J. Am. Chem. Soc. 117: 6412-6413.
Dictionary AH (1992) edn 3rd: Houghton Mifflin Company.
Drauz K, Waldmann H (2002) Enzyme Catalysis in Organic Synthesis, vol I-III. Weinheim: Wiley-VCH.
Dudziak G, Zeng S, Berger EG, Gellego RG, Kamerling JP, Kragl U, Wandrey C (1998) *In situ* generated O-glycan core 1 structure as substrate for Gal(β1-3)GalNAc(β1-6)GlcNAc transferase. Bioorg. Med. Chem. 8: 2595-2598.
Dudziak G (1999) Reaktionstechnische Untersuchungen zur enzymatischen Glycosylierung von Peptiden [PhD thesis]. Bonn: Universtiy of Bonn.
Dumont W, Poulin J-C, Dang T-P, Kagan HB (1973) Asymmetric catalytic reduction with transition metal complexes. II. asymmetric catalysis by a supported chiral rhodium complex. JACS: 8295-8299.
Dünnwald T, Demir A, Siegert P, Pohl M, Müller M (2000) Enantioselective synthesis of (*S*)-2-hydroxy propanone derivatives by benzoylformate decarboxylase catalyzed C-C bond formation. Eur. J. Org. Chem.: 2161-2170.
Dünnwald T, Müller M (2000) Stereoselective formation of bis(α-hydroxyketones) via enzymatic carboligation. J. Org. Chem.: 8608-8612.
Eguchi S, Nishio N, Nagai S (1983) NADPH production from $NADP^+$ by a formate-utilizing methanogenic bacterium. Agric. Biol. Chem. 47: 2941-2943.
Enders D, Hoffmann R (1985) Asymmetrische Synthese. ChiuZ 19: 177-187.
Enders D, Kallfass U (2002) Ein effizienter nucleophiler Carben-Katalysator für die asymmetrische Bezoinkondensation. Angew. Chem. 114: 1822.
Endo T, Koizumi S (2000) Large-scale production of oligosaccharides using engineered bacteria. Curr. Opin. Struct. Biol. 10: 521-526.
Endo T, Koizumi S, Tabata K, Ozaki A (2000) A large-scale production of sialylated oligosaccharides. Glycobiology 10: 90.
Endo T, Koizumi S (2001) Microbial conversion with cofactor regeneration using genetically engineered bacteria. Adv. Synth. Cat. 343: 521-526.
Endo T, Koizumi S, Tabata K, Kakita S, Ozaki A (2001) Large-scale production of the carbohydrate portion of the sialyl-Tn epitope, alpha-Neup5Ac-(2 -> 6)-D-GalpNAc, through bacterial coupling. Carb. Res. 330: 439-443.
Engels S, Stolz R, Göbel W, Nawrocki F, Nowak A (1989) ABC Geschichte der Chemie. Leipzig: VEB Deutscher Verlag für Grundstoffindustrie.
Erste allgemeine Verwaltungsvorschrift zum Bundes-Immisionsschutzgesetz. **(cabinet decision, December 12th, 2001)**.
Evans IP (1973) Dichlorotetrakis(dimethyl sulphoxide) ruthenium (II) and its use as a source material for some new ruthenium (II) complexes. Journal of the Chemical Society, Dalton Transaction: 204.
Faber K (1995) Biotransformations in organic chemistry - a textbook. Berlin, Heidelberg, New York: Springer-Verlag.
Faber K (2000) Biotransformations in organic synthesis. Berlin: Springer.
Felder M, Giffels G, Wandrey C (1997) A polymer-enlarged homogeneously soluble oxazaborolidine catalyst for the asymmetric reduction of ketones by borane. Tetrahedron Asymm. 8: 1975-1977.
Fernández-Mayoralas A (1997) Top. Curr. Chem. 186: 1-21.
Fiala G, Stetter KO (1986) *Pyrococcus furiosus* sp. nov. represents a novel genus of marine heterotrophic archaebacteria growing optimally at 100°C. Arch. Microbiol. 145: 56-61.
Fitch MW, Koros WJ, Nolen RL, Carnes JR (1993) Permeation of several gases through elastomers

with emphasis on the deuterium/hydrogen pair. J. Appl. Polym. Sci. 47: 1033-1046.
Flaschel E (1983) Ultrafiltration for the separation of biocatalysts. Advances in Biochemical Engineering/Biotechnology 26: 73-142.
Fodor K (1999) Heterogeneous enantioselective catalysis: state of the art. Enantiomer 4: 497-511.
Folienserie (1985) Biotechnologie/Gentechnik. Folienserie des Fonds der Chemischen Industrie, 20.
Fontecilla-Camps JC, Ragsdale SW (1999) Nickel-iron-sulfur active sites: hydrogenase and CO dehydrogenase. Advances in Inorganic Chemistry 47: 283-333.
Frede M, Steckhan E (1991) Continuous electrochemical activation of flavoenzymes using polyethyleneglycol-bound ferrocenes as mediators - a model for the application of oxidoreductases as oxidation catalysts in organic-synthesis. Tetrahedron Lett. 32: 5063-5066.
Frey M, Fontecilla-Camps JC, Volbeda A (2001) Nickel-iron hydrogenases. In: Handbook of metalloproteins. Edited by Messerschmidt A, Huber R, Poulos T, Wieghardt K: John Wiley & Sons, Ltd.; 880-896. vol 2.
Frey M (2002) Hydrogenases: Hydrogen-activating enzymes. CHEMBIOCHEM 3: 153-160.
Fukuda M, Calsson SR, Klock JC, Dell A (1986) Structures of o-linked oligosaccharides isolated from normal granulocytes, chronic myelogenous leukemia cells and acute myelogenous leukemia cells. J. Biol. Chem. 261: 2796-2806.
Fukuda M (1991) Leukosialin, a major O-glycan-containing sialoglycoprotein defining leukocyte differentiation and malignancy. Glycobiology 1: 347.
Gala D, DiBenedetto D, Clark JE, Murphy BL, Schumacher DP, Steinmann M (1995) Preparation of antifungal Sch 42427/SM 9164: Preparative chromatographic resolution, and total asymmetric synthesis via enzymatic preparation of chiral α-hydroxy arylketones. Tetrahedron Lett. 37: 611-614.
Gambert U, Thiem J (1999) Multienzyme system for synthesis of the sialylated Thomsen-Friedenreich antigen determinant. Eur. J. Org. Chem. 1: 107-110.
Gao JX, Ikariya T, Noyori R (1996a) A ruthenium(II) complex with a C-2-symmetric diphosphine/diamine tetradentate ligand for asymmetric transfer hydrogenation of aromatic ketones. Organomet. 15: 1087-1089.
Gao JX, Wan HL, Wong WK, Tse MC, Wong WT (1996b) Synthesis and characterization of iron(2+) and ruthenium(2+) diimino-diphosphine, diamino-diphosphine and diamido-diphosphine complexes - X-ray crystal-structure of *trans*-$RuCl_2(P_2N_2C_2H_4)CHCl_3$. Polyhedron 15: 1241-1251.
Genders JD, Pletcher D (1996) Electrosynthesis - A tool for the pharmaceutical industry today? Chemistry & Industry: 682-686.
Gieck K, Gieck R (1995) Technische Formelsammlung edn 30. Germering: Gieck Verlag.
Giffels G, Beliczey J, Felder M, Kragl U (1998) Polymer enlarged oxazaborolidines in a membrane reactor: Enhancing effectivity by retention of the homogeneous catalyst. Tetrahedron Asymm. 9: 691-696.
Gladiali S, Mestroni G (1998) Transferhydrogenations. In: Transition metals for organic synthesis, edn 1. Edited by Beller M, Bolm C: Wiley-VCH; 97-119. vol 1.
Goldberg DE (1989) Genetic Algorithms in Search, Optimization and Machine Learning. Reading, MA: Addison Wesley Publishing.
Goldberg RN, Tewari YB, Bell D, Fazio K, Anderson E (1993) Thermodynamics of enzyme-catalyzed reactions: Part 1. Oxidoreductases. Journal of Physical and Chemical Reference Data 22: 515-582.
Gonzáles B, R. Vicuña JB, 2401 (1989) J. Bacteriol.: 2401.
Graauw Cd, Peters JA, Bekkum Hv, Huskens J (1994) Meerwein-Pondorf-Verley reductions and Oppenhauer oxidations: An integrated approach. Synthesis: 1007.
Greiner L (2002) Prozessentwicklung für die katalytische Reduktion mit molekularem Wasserstoff [PhD thesis]: Universtiy of Bonn.
Griengl H (2000) Biocatalysis. Berlin: Springer.
Gros P, Zaborosch C, Schlegel HG, Bergel A (1996) Direct electrochemistry of *Rhodococcus opacus* hydrogenase for the catalysis of NAD^+ reduction. J. Electroanal. Chem. 405: 189-195.
Gunsalus IC, Gunsalus CF, Stanier RY (1953) The enzymatic conversion of mandelic acid to benzoic acid. J. Bacteriol. 66: 538-542.
Haack K-J, Hashigushi S, Fujii A, Ikariya T, Noyori R (1997) The catalyst precursor, catalyst, and

intermediate in the ru(II)-promoted asymmetric hydrogen transfer between alcohols and ketones. Angewandte Chemie, International Edition English 36: 285.

Haberland J, Kriegesmann A, Wolfram E, Hummel W, Liese A (2002) Diastereoselective synthesis of optically active (2*R*,5*R*)-hexanediol. Appl. Microbiol. Biotechnol 58: 595-599.

Haberland J (2003) Verfahrensentwicklung zur Darstellung von (2*R*,5*R*)-Hexandiol mit *Lactobcillus kefir* DSM20587. Bonn: University of Bonn.

Halpern J, Wong CS (1973) Hydrogenation of tris(triphenylphosphine)chlororhodium(I). J. Chem. Soc.-Chem. Commun.: 629-630.

Halpern J (1982) Mechanism and stereoselectivity of asymmetric hydrogenation. Science 217: 401-407.

Hammett LP (1935) Some relations between reaction rates and equilibrium constants. Chem. Rev. 17: 125-136.

Hammett LP (1937) The effect of structure upon the reaction of organic compounds. Benzene derivatives. J. Am. Chem. Soc.: 96-103.

Hänel P, Heinzelmann W, Helmrich H, Hoffmann P (1994) Pervaporation and related processes: new fields of application by novel module concepts. In Synthetic Membranes in Science and Industry; Tübingen: Dechema e.V.: 507.

Hansch C, Leo A (1979) Substituent constants for correlation analysis in chemistry and biology. New York: Wiley.

Hasson MS, Muscate A, Henehan GTM, Guidinger PF, Petsko GA, Ringe D, Kenyon GL (1995) Purification and crystallization of benzoylformate decarboxylase. Prot. Sci. 4: 955-959.

Hasson MS, Muscate A, McLeish MJ, L.S. P, Gerlt JA, Kenyon GL, Petsko GA, Ringe D (1998) The crystal structure of benzoylformate decarboxylase at 1,6 A resolution: diversity of catalytic residues in thiamin pyrophosphate-dependent enzymes. Biochemistry 37: 9918-9930.

Hasumi F, Miyamoto Y, Okura I (1995) Synthesis of glutamate by reductive amination of 2-oxoglutarate with the combination of hydrogenase and glutamate dehydrogenase. Appl. Biochem. Biotechnol. 55: 1-4.

Hedbys L, Johansson E, Mosbach K, Larsson PO (1989) Synthesis of 2-acetatamido-2-deoxy-3-o-beta-d-galactopyrano-syl-d-galactosil by the sequential use of beta-d-galacto-sidases from bovine testes and *Escherichia coli*. Carb. Res. 186: 217-223.

Hegeman GD (1966) Synthesis of the enzymes of the mandelate pathway by Pseudomonas putida. J. Bacteriol. 91: 1155.

Hembre RT, Wagenknecht PS, Penney JM (2000) Enzymatic reductions with dihydrogen via metal catalyzed cofactor regeneration. US Patent, WO 00/53731.

Herrmann G, Ichikawa Y, Wandrey C, Gaeta F, Paulson JC, Wong C-H (1993) A new multi-enzyme system for a one-pot synthesis of sialyl oligosaccharides: combined use of β-galactosidase and α(2-6)-sialyltransferase coupled with regeneration in situ of CMP-sialic acid. Tetrahedron Lett. 4: 1193-1202.

Herrmann WA, Kohlpaintner CW (1992) Water-soluble ligands, metal complexes, and catalysts: synergism of homogeneous and heterogeneous catalysis. Angew. Chem. Int. Ed. Engl. 32: 1524.

Hildebrandt G, Klavehn W (1932) Deutsches Reichspatent Nr. 584 459.

Hilhorst R, Laane C, Veeger C (1983) Enzymatic conversion of apolar compounds in organic media using an NADH-regenerating system and dihydrogen as reductant. FEBS Letters 159: 225-228.

Hilt G, Steckhan E (1993) Transition-metal complexes of 1,10-phenanthroline-5,6-dione as efficient mediators for the regeneration of NAD^+ in enzymatic- synthesis. J. Chem. Soc.-Chem. Commun.: 1706-1707.

Hilt G, Jarbawi T, Heineman WR, Steckhan E (1997a) An analytical study of the redox behavior of 1,10- phenanthroline-5,6-dione, its transition-metal complexes, and its N-monomethylated derivative with regard to their efficiency as mediators of NAD(P)(+) regeneration. Chem.-Eur. J. 3: 79-88.

Hilt G, Lewall B, Montero G, Utley JHP, Steckhan E (1997b) Efficient *in-situ* redox catalytic NAD(P)(+) regeneration in enzymatic synthesis using transition-metal complexes of 1,10-phenanthroline-5,6-dione and its N-monomethylated derivative as catalysts. Liebigs Ann.-Recl.: 2289-2296.

Hinrichsen P, Gómez I, Vicuña R, Gene 1994, 137 (1994) Gene 144: 137.

Hodgson HH, Greensmith Beard H (1925) Bromoderivatives of *m*-hydroxybenzaldehyde. J. Chem. Soc.: 875.

Hoffmann N (1996) Bäckerhefe - ein lebendes Reagens für die organisch-chemische Synthese. ChiuZ 30: 201-213.

Holland JH (1975) Adaptaion in natural and artificial systems.

Holland JH (1992) Genetische Algorithmen. Spektrum der Wissenschaft: 44-51.

Hollmann F, Schmid A, Steckhan E (2001) The first synthetic application of a monooxygenase employing indirect electrochemical NADH regeneration. Angew. Chem.-Int. Edit. 40: 169-171.

Hollmann F, Witholt B, Schmid A (2002) [Cp*Rh(bpy)(H2O)](2+): a versatile tool for efficient and non- enzymatic regeneration of nicotinamide and flavin coenzymes. J. Mol. Catal. B-Enzym. 19: 167-176.

Hoots JE, Rauchfuss TB, Wrobleski DA (1982) Substituted TriarylPhosphines. 4 21: 175-179.

Horner L, Siegel H, Büthe H (1968) Asymmetrische katalytische Hydrierung mit einem homogen gelösten optisch aktiven Phosphin-Rhodium-Komplex. Angew. Chem. 80: 1034-1035.

Hovestad NJ, Eggeling EB, Heidbüchel HJ, Jastrzebski JTBH, Kragl U, Keim W, Vogt D, van Koten G (1999) Selektive Hydrovinylierung von Styrol im Membranreaktor: Anwendung mit hemilabilen P,O-Liganden. Angew. Chem. 111: 1763.

Hummel W, Schuette H, Schmidt E, Wandrey C, Kula MR (1987) Isolation of scl-phenylalanine dehydrogenase from Rhodococcus sp. M4 and its application for the production of scl-phenylalanine. Appl. Microbiol. Biotechnol 26: 409-416.

Hummel W (1990) Reduction of acetophenone to R(+)-phenylethanol by a new alcohol dehydrogenase from Lactobacillus kefir. Appl. Microbiol. Biotechnol 34: 15-19.

Hummel W (1997) New alcohol dehydrogenases for the synthesis of chiral compounds. Adv. Bio. Eng/Bio 58: 145-184.

Hummel W (1999) Large-scale applications of NAD(P)-dependent oxidoreductases: recent developments. Tibtech 17: 487-492.

Iding H, Dünnwald T, Greiner L, Liese A, Müller M, Siegert P, Grötzinger J, Demir AS, Pohl M (2000) Benzoylformate decarboxylase from *Pseudomonas putida* as stable catalyst for the synthesis of chiral 2-hydroxy ketones. Chem. Eur. J. 6: 1483-1495.

Ikeda H, Sako E, Sugai T, Ohta H (1996) Yeast-mediated synthesis of optically active diols with C2-symmetry and (R)-4-pentanolide. Tetrahedron 52: 8113-8122.

Imai T, Tamura T, Yamamuro A (1986) Organoboron compounds in organic synthesis. 2. asymmetric reduction of dialkyl ketones with (R,R)- or (S,S)-2,5-dimethylborolane. J. Am. Chem. Soc. 108: 7402-7404.

Inoguchi K, Achiwa K (1990) Efficient asymmetric hydrogenation of (*Z*)-2-acetamidocinnamic acid catalyzed by the rhodium complex of modified *N*-benzyl-(2*R*,4*R*)-3,4-bis(diphenylphosphino)pyrrolidine (DeguPhos). Chem. Pharm. Bull. 38: 818-820.

Itsuno S, Nakano M, Ito K, Hirao A, Owa M, Kanda N, Nakahama S (1985) Asymmetric synthesis using chirally modified borohydrides. Part 4. Enantioselective reduction of ketones and oximethers with a reagent prepared from borane and polymer-supported (S)-(-)-2-Amino-3-(p-hydroxyphenyl)-1,1-diphenylpropane-1-ol. J. Chem. Soc., Perkin Trans. 1 I: 2615-2619.

Izumi Y (1971) Methoden der asymmetrischen Synthese - enantioselektive katalytische Hydrierung. Angew. Chem. 83: 956-966.

Jacobsen EN, Marko I, Mungal WS, Schröder G, Sharpless KB (1988) Asymmetric dihydroxylation via ligand-accelerated catalysis. J. Am. Chem. Soc. 110: 1968-1970.

Jacobsen EN, Zhang W, Muci AR, Ecker JR, Deng L (1991) Highly enantioselective epoxidation catalyst derived from 1,2-diaminocyclohexane. J. Am. Chem. Soc. 113: 7063-7064.

Jacobsen EN, Pfaltz A, Yamamoto H (1999) Comprehensive asymmetric catalysis. Berlin, Heidelberg, New York: Springer Verlag.

Jandel L, Schulte B, Bückmann AF, Wandrey C (1980) Quantitative description of the rejection of polymeric catalysis by ultrafiltration membranes. J. Membr. Sci. 7: 185.

Jones JB, Sneddon DW, Higgins W, Lewis AJ (1972) Preparative-scale reductions of cyclic ketone and aldehyde substrates of horse liver alcohol dehydrogenase with *in situ* sodium dithionite recycling of catalytic amounts of NAD. J. Chem. Soc., Chem. Commun.: 856-857.

Kagan HB, Dang T-P (1972) Asymmetric catalytic reduction with transition metal complexes. I. A

catalytic system of rhodium(I) with (-)-2,3-O-isopropylidene-2,3-dihydroxy-1,4-bis(diphenylphosphino)butane, a new chiral diphosphine. JACS 94: 6429-6433.

Kagan HB (1982) Asymmetric synthesis using organometallic catalysts. In: Comprehensive Organometallic Chemistry. Edited by Wilkinson G, Stone FGA, Abel EW: Pergamon; 463-498. vol 8.

Kandler O, Kunath P (1983) *Lactobacillus kefir* sp. nov., a component of the microflora of kefir. System. Appl. Microbiol. 4: 286-294.

Kataoka M, Rohani LPS, Yamamoto K, Wada M, Kawabata H, Kita K, Yanase H, Shimizu S (1997) Enzymatic production of ethyl (*R*)-4-chloro-3-hydroxybutanoate: asymmetric reduction of ethyl 4-chloro-3-oxobutanoate by an *Escherichia coli* transformant expressing the aldehyde reductase gene from yeast. Appl. Microbiol. Biotechnol 48: 699-703.

Kataoka M, Rohani LPS, Wada M, Kita K, Yanase H, Urabe I, Shimizu S (1998) *Escherichia coli* transformant expressing the glucose dehydrogenase gene from *Bacillus megaterium* as a cofactor regenerator in a chiral alcohol production system. Biosci. Biotechnol. Biochem. 62: 167-169.

Kataoka M, Yamamoto K, Kawabata H, Wada M, Kita K, Yanase H, Shimizu S (1999) Stereoselective reduction of ethyl 4-chloro-3-oxobutanoate by *Escherichia coli* transformant cells coexpressing the aldehyde reductase and glucose dehydrogenase genes. Appl. Microbiol. Biotechnol 51: 486-490.

Katsuki T, Sharpless KB (1980) The first practical method for asymmetric epoxidation. J. Am. Chem. Soc. 102: 5974-5976.

Keefe RG, Axley MJ, Harabin AL (1995) Kinetic mechanism studies of the soluble hydrogenase from *Alcaligenes eutrophus* H16. Arch. Biochem. Biophys. 317: 449-456.

Kieboom AP, Moulijn J, Leeuwen PWNM, Santen RAv (1999) History of catalysis. In: Catalysis: An integrated approach, edn 2nd. Edited by Santen RAv, Moulijn J, Leeuwen PWNM, Averill BA: Elsevier; 3-28.

Kim M-J, Lee IS (1993) Combined chemical and enzymatic synthesis of (S,S)-2,5-dimethylpyrrolidine. Synlett: 767-768.

Kizaki N, Yasohara Y, Hasegawa J, Wada M, Kataoka M, Shimizu S (2001) Synthesis of optically pure ethyl (*S*)-4-chloro-3- hydroxybutanoate by *Escherichia coli* transformant cells coexpressing the carbonyl reductase and glucose dehydrogenase genes. Appl. Microbiol. Biotechnol 55: 590-595.

Klibanov A (2001) Improving enzymes by using them in organic solvents. Nature 409: 241-246.

Klibanov AM, Puglisi AV (1980) The regeneration of coenzymes using immobilized hydrogenase. Biotechnol. Lett. 2: 445-450.

Klibanov AM (1983) Biotechnological potential of the enzyme hydrogenase. Process Biochem. 18: 13-16.

Knowles WS, Sabacky MJ (1968) Catalytic asymmetric hydrogenation employing a soluble, optically active, rhodium complex. Chem. Comm.: 1445-1446.

Knowles WS (1983) Asymmetric hydrogenation. AccChemRes 16: 106-112.

Koike T, Murata K, Ikariya T (2000) Stereoselective synthesis of optically active alpha-hydroxy ketones and anti-1,2-diols via asymmetric transfer hydrogenation of unsymmetrically substituted 1,2-diketones. Org. Lett.: 3833-3836.

Koizumi S, Endo T, Tabata K, Nagano H, Ohnishi J, Ozaki A (2000) Large-scale production of GDP-fucose and Lewis X by bacterial coupling. J. Ind. Microbiol. Biotechnol. 25: 213-217.

Kolb HC, VanNieuwenhze MS, Sharpless KB (1994) Catalytic asymmetric dihydroxylation. Chem. Rev. 94: 2483-2547.

Köllner C, Pugin B, Togni A (1998) Dendrimers containing chiral ferrocenyl diphosphine ligands for asymmetric catalysis. J. Am. Chem. Soc. 120: 10274.

Koten Gv, Leeuwen PWv (1999) Homogeneous catalysis with transition metal complexes. In: Catalysis: An integrated approach. Edited by Santen RAv, Leeuwen PW, Moulijn JA, Averil BA: Elsevier; 289-342. [Delmon B, Yates JT (Series Editor): Studies in surface science and catalysis, vol 123.

Kragl U, Dreisbach C (1996) Kontinuierliche asymmetrische Synthese in einem Membranreaktor. Angew. Chem. 108: 684-685.

Kragl U, Dreisbach C, Wandrey C (1996a) Membrane reactors in homogeneous catalysis. In:

Applied homogeneous catalysis with organometallic compounds. Edited by Cornils B, Herrmann WA: VCH; 832-843. vol 2.

Kragl U, Kruse W, Hummel W, Wandrey C (1996b) Enzyme engineering aspects of biocatalysis: Cofactor regeneration as example. Biotech. Bioeng. 52: 309-319.

Kragl U, Liese A (1999) Biotransformations, engineering aspects. In: The Encyclopedia of Bioprocess Technology: Fermentation, Biocatalysis & Bioseparation. Edited by Flickinger MC, Drew SW: John Wiley & Sons; 454-464.

Kragl U, Dwars T (2001) The development of new methods for the recycling of chiral catalysts. Tibtech 19: 442-449.

Krahe M, Antranikian G, Märkl H (1996) Fermentation of extremophilic microorganisms. FEMS Microbiol. Rev. 18: 271-285.

Krasna AI (1978) Oxygen-stable hydrogenase and assay. Methods Enzymol. 53: 296-314.

Kren V, Thiem J (1995) A multienzyme system for one-pot syntheis of Sialyl T-antigen. Angew. Chem. Int. Ed. Engl. 34: 893-895.

Kruse W, Hummel W, Kragl U (1996) Alcohol-dehydrogenase-catalyzed production of chiral hydrophobic alcohols. A new approach leading to a nearly waste-free process. Rec. Trav. Chim. Pays-Bas 115: 239-243.

Kubinyi H (1993) QSAR: Hansch analysis and related approaches in methods and principles in medical chemisty. Weinheim: VCH.

Kula M-R, Wandrey C (1987) Continuous enzymatic transformation in an enzyme-membrane-reactor with simultaneous NADH regeneration. In: Method Enzymol. Edited by K. Mosbach e; 9-21. vol 136.

Kunieda N, Nokami J, Kinoshita M (1992) Substituent effect on the enantioface-differentiating reaction of (R)-[lithiomethyl para-tolyl sulfoxide]with eta-substituted or para-substituted acetophenones. Bull. Chem. Soc. Jpn. 65: 526-529.

Laane C, Weyland A, Franssen M (1986) Bioelectrosynthesis of halogenated compounds using chloroperoxidase. Enzyme Microb. Technol. 8: 345-348.

Lakner FJ, Hager LP (1996) Chloroperoxidase as enantioselective epoxidation catalyst: An efficient synthesis of (R)-(-)-mevalonolactone. J. Org. Chem. 61: 3923-3925.

Lam KP, Hui AHF, Jones JB (1986) Enzymes in organic-synthesis. 35. stereoselective pig-liver esterase catalyzed hydrolyzes of 3-substituted glutarate diesters-optimization on enantiomeric excess via reaction conditions control. J. Org. Chem. 51: 2047-2050.

Laue S (2002) Asymmetrische Transferhydrierung im chemischen Membranreaktor [Ph.D. thesis]. Bonn: University of Bonn.

Laue S, Greiner L, Wandrey C, Liese A (in preparation) Kinetics and reactor simultations of transfer hydrodrogenations catalyzed with a chemzyme.

Leadbeater NE, Marco M (2002) Preparation of polymer-supported ligands and metal complexes for use in catalysis. Chem. Rev. 102: 3217-3274.

Lemon BJ, Peters JW (2001) Iron-only hydrogenases. In: Handbook of Metalloproteins. Edited by Messerschmidt A, Huber R, Poulos T, Wieghardt K: John Wiley & Sons, Ltd.; 738-751. vol 2.

Leonida MD (2001) Redox enzymes used in chiral syntheses coupled to coenzyme regeneration. Current Medicinal Chemistry 8: 345-369.

Levenspiel O (1993) The chemical reactor omnibook. Corvallis: OSU Book Stores, Inc.

Levenspiel O (1999) Chemical reaction engineering edn third edition. New York: John Wiley&Sons, Inc.

Li S, Purdy WC (1992) Cyclodextrins and their applications in analytical chemistry. Chem. Rev. 92: 1457-1470.

Liebe B, Kunz H (1997a) Solid-phase synthesis of a tumor-associated sialyl-t-n antigen glycopeptide with a partial sequence of the "tandem repeat" of the muc-1 mucin. Angew. Chem. Int. Ed. Engl. 36: 618-621.

Liebe B, Kunz H (1997b) Solid-phase synthesis of a sialyl-tn-glycoundecapeptide of the muc1 repeating unit. Helv. Chim. Acta 80: 1473-1482.

Liese A, Villela Filho M (1999) Production of fine chemicals using biocatalysis. Curr. Opin. Biotech. 10: 595-603.

Liese A, Seelbach K, Wandrey C (2000) Industrial Biotransformations. Weinheim: VCH-Wiley.

Liese A, Kragl U, Kierkels H, Schulze B (2002) Membrane reactor development for the kinetic resolution of ethyl 2-hydroxy-4-phenylbutyrate. Enzyme Microb. Technol. 30: 673 - 681.

Lindhorst TK (2000) Struktur und Funktion von Kohlenhydraten. ChiuZ 34: 38-52.

Lio RG, Thiem J (1999) Chemoenzymatic synthesis of spacer-linked oligosaccharides for the preparation of neoglycoproteins. Carb. Res. 317: 180-190.

Lipkin D, Stewart TD (1939) J. Am. Chem. Soc. 61: 3295.

Lipnizki F, Hausmanns S, Laufenberg G, Field R, Kunz B (2001) Use of pervaporation-bioreactor hybrid processes in biotechnology. Chem. Eng. Technol. 23: 569-577.

Lohmann W, Schuster G (1937) Biochem. Z.: 188-193.

Ma K, Zhou ZH, Adams MWW (1994) Hydrogen production from pyruvate by enzymes purified from the hyperthermophilic archaeon, *Pyrococcus furiosus*: A key role for NADPH. FEMS Microbiol. Lett. 122: 245-250.

Ma K, Weiss R, Adams MWW (2000) Characterization of hydrogenase II from the hyperthermophilic archaeon *Pyrococcus furiosus* and assessment of its role in sulfur reduction. J. Bacteriol. 182: 1864-1871.

Maier ME, Reuter S (1997) Double asymmetric dihydroxylation of 1,5-hexadiene. Liebigs Annalen/Recueil: 2043-2046.

Malmström T, Andersson C (1999) Enantioselective hydrogenation in water catalysed by rhodium phospine complexes bound to polyacrylic acid. Journal of Molecular Catalysis A: Chemical 139: 259.

Malmström T, Andersson C (2000) Rhodium catalysed enantioselective hydrogenation in water using pyrphos bound to poly-acrylic acid as ligand. Journal of Molecular Catalysis A: Chemical 157: 79-82.

Masamune S, Sato T, Kim BM, Wollman TA (1986) Organoboron compounds in organic synthesis. 4. asymmetric aldol reactions. J. Am. Chem. Soc. 108: 8279-8281.

Mayer SF, Kroutil W, Faber K (2001) Enzyme-initiated domino (cascade) reactions. Chem. Soc. Rev. 30: 332-339.

McAuliffe JC, Hindsgaul O (1997) Carbohydrate drugs - an ongoing challenge. Chemistry & Industry: 170-174.

McGill DJ, Dawes EA (1971) Glucose and fructose mechanism in *Zymomonas anaerobia*. Biochemical Journal 125: 1059-1068.

Meerwein H (1925) Annalen der Chemie: 221.

Mertens R, Greiner L, Müller MH, Ban Evd, Haaker H, Liese A (2002) Practical application of hydrogenase from *Pyrococcus furiosus* for generation and regeneration of nicotinamide cofactors. J. Mol. Cat.: Enz.: submitted.

Mioskowski C, Solladie G (1980) Asymmetrical synthesis of b-hydroxy acids by condensation of chiral a-sulfinylester enolate anions on carbonyl-compounds. Tetrahedron 36: 227-236.

Miyashita A, Yasuda A, Tanaka H, Toriumi K, Ito T, Souchi T, Noyori R (1980) Synthesis of 2,2'-bis(diphenylphosphino)-1,1'-binaphthyl (BINAP), an atropisomeric chiral bis(triaryl)phosphine, and its use in the rhodium(I)-catalyzed asymmetric hydrogenation of alpha-(acylamino)acrylic acids. J. Am. Chem. Soc. 102: 7932-7934.

Miyazaki M, Ogino K, Shibue M, Nakamura H, Maeda H (2002) A one-pot, two-step enzymatic synthesis of L-lactic acid from acetaldehyde. Chem. Lett.: 758-759.

Mochizuki N, Hiramatsu S, Sugai T, Ohta H, Morita H, Itokawa H (1995) Reductive conversion of carbonyl compounds by yeast .2. Improved conditions for the production and characterization of 1-arylpropane-1,2-diols and related compounds. Biosci. Biotechnol. Biochem. 59: 2282-2291.

Möllney M, Freyer S, Wiechert W, Weuster-Botz D (1993) Genetic algorithm for the optimization of processes (GALOP). edn version 2.2. Jülich, Germany: Institute of Biotechnology, Forschungszentrum Jülich GmbH.

Mori T, Fujita S, Okahata Y (1997) Transglycosylation in a two-phase aqueous-organic system with catalysis by a lipid-coated b-D-galactosidase. Carb. Res. 298: 65-73.

Moriyama H, Shimizu K (1996) On-line optimisation of culture temperature for ethanol fermentation using a genetic algorithm. J. Chem. Tech. Biotechnol. 66: 217-222.

Morozov SV, Karyakina EE, Zorin NA, Varfolomeyev SD, Cosnier S, Karyakin AA (2002) Direct and electrically wired bioelectrocatalysis by hydrogenase from *Thiocapsa roseopersiciana*.

Bioelectrochemistry 55: 169-171.

Moussou P, Archelas A, Baratti J, Furstoss R (1998) Microbiological transformations. 38. clues to the involvement of a general acid activation during hydrolyse of para-substituted styrene oxides by a soluble epoxide hydrolase from *Syncephalastrum recemosum*. J. Org. Chem. 63: 3532-3537.

Muniz K, Bolm C (2000) Configurational control in stereochemically pure ligands and metal complexes for asymmetric catalysis. Chem. Eur. J. 6: 2309-2316.

Mutschler E (1997) *Arzneimittelwirkung*. Stuttgart: Wissenschaftliche Verlagsgesellschaft mbH.

Nachtigall W (1991) Ein paar Millionen Jahre Entwicklungsvorsprung. In: Bionik - Patente der Natur. Edited by Witt R, Lieckfeld C-P: Pro Futura Verlag GmbH; 7-11.

Nagai H, Morimoto T, Achiwa K (1994) Facile enzymatic synthesis of optically active 2,5-hexandiol derivatives and its application to the preparation of optically pure cyclic sulfate for chiral ligands. Synlett 4: 289-290.

Nagasawa T, Shimizu H, Yamada H (1993) The superiority of the third-generation catalyst, *Rhodococcus rhodochrous* J1 nitrile hydratase, for industrial production of acrylamide. Appl. Microbiol. Biotechnol 40: 189-195.

Nagel U (1984) Asymmetrische Hydrierung von α-(Acetylamino)-zimtsäure mit einem neuen Rhodiumkomplex: Die Konzeption eines optimalen Liganden. Angew. Chem. 96: 425-426.

Nagel U, Kinzel E (1986) Enantioselektive katalytische Hydrierung von α-(Acetylamino)-zimtsäure mit einem Rhodium-Phosphankomplex in wässriger Lösung. Chem. Ber. 119: 1731-1733.

Nagel U, Kinzel E, Andrade J, Prescher G (1986) Synthese N-substituierter (*R,R*)-3,4-Bis(diphenylphosphino)-pyrrolidine und Anwendung ihrer Rhodiumkomplexe zur asymmetrischen Hydrierung von α-(Acylamino)-acrylsäurederivaten. Chem. Ber. 119: 3326-3343.

Nakamura K, Kondo S-i, Kawai Y, Hida K, Kitano K, Ohno A (1996) Enantio- and regioselective reduction of α-diketones by baker´s yeast. Tetrahedron Asymm. 7: 409-412.

Neuberg C, Ohle H (1921) Über ein Kohlenstoffketten knüpfendes Ferment (Carboligase). Biochem. Z. 127: 326-339.

Nicolet Y, Lemon BJ, Fontecilla-Camps JC, Peters JW (2000) A novel FeS cluster in Fe-only hydrogenases. TIBS 25: 138-143.

Nindakova LO, Shainyan BA (2001) Transformations of the chiral diphosphine rhodium catalyst [(1,5-COD)Rh(-)*R,R*-DIOP]$^+CF_3SO_3^-$ under conditions of hydrogenation. Russ. Chem. Bull., Int. Ed. 50: 1855-1859.

Noll T, Biselli M, Wandrey C (1996) Wirbelschichtreaktor und Biomasse-Monitor - ein leistungsfähiges Fermentationssystem für Säugerzellen. BIOSpektrum 1: 65-67.

Noll W (1968) Chemistry and Technology of Silicones. Orlando: Academic Press.

Noyori R (1994) Asymmetric Catalysis in Organic Synthesis. New York: John Wiley.

Noyori R, Hashigushi S (1996) Asymmetric synthesis. In: Applied Homogeneous Catalysis with Organometallic compounds. Edited by Cornils B, Herrmann WA: VCH; 575.

Nozaki H, Moriuti S, Takaya H, Noyori R (1966) Asymmetric induction in carbenoid reactions by means of a dissymmtric copper chelate. Tetrahedron Lett.: 5239-5244.

OECD (2001) Report on biotechnology for clean industrial processes - The application of biotechnology for industrial sustainability.

Oguni N, Omi T (1984) Enantioselective addition of diethylzinc to benzaldehyde catalyzed by a small amount of chiral 2-amino-1-alcohols. Tetrahedron Lett. 25: 2823-2824.

Ohta H, Ozaki K, Tsuchihashi GI (1986) Regio- and enantioselective reduction of α,γ-diketones by fermenting bakers´ yeast. Agric. Biol. Chem. 50: 2499-2502.

Ojima I (1989) The hydrosilylation reaction. In: The Chemistry of Organic Silicon Compounds. Edited by Patai S, Rappoport Z: John Wiley & Sons; 1479.

Ojima I (1993) Catalytic Asymmetric Synthesis. New York: VCH.

Okrasa K, Guibé-Jampel E, Therisod M (2000) Tandem peroxidase-glucose oxidase catalysed enantioselective sulfoxidation of thioanisoles. Journal of the Chemical Society, Perkin Transaction 1: 1077-1079.

Okura I, Kurabayashi K, Aono S (1987a) Regeneration of NADPH and ketone hydrogenation by hydrogen in the enzymatic system. Journal of Molecular Catalysis 42: 285-288.

Okura I, Kurabayashi K, Aono S (1987b) Regeneration of NADPH and hydrogenation of ketones to alcohols with the combination of hydrogenase, ferredoxin-NADP reductase, and alcohol

dehydrogenase. Bull. Chem. Soc. Jpn. 60: 3663-3666.

Osborn JA, Jardin FH, Young JF, Wilkinson G (1966) The preparation and properties of tris(triphenylphosphine)halogenorhodium(I) and some reaction thereof including catalytic homogeneous hydrogenation of olefins and acetylenes and their derivatives. J. Chem. Soc.: 1711-1732.

Otsuka K, Aono S, Okura I (1989) Regeneration of NADH and ketone hydrogenation by hydrogen with the combination of hydrogenase and alcohol dehydrogenase. Journal of Molecular Catalysis 51: 35-39.

Palmer MJ, Wills M (1999) Asymmetric transfer hydrogenation of C=O and C=N Bonds. Tetrahedron Asymm. 10: 2045-2061.

Pasteur L (1858) Mémoire sur la fermentation de l'acide tartrique. C. R. Acad. Sci. (Paris) 46: 615-618.

Patel RN (2000) Stereoselective Biocatalysis. New York: Marcel Dekker.

Patel RN (2001) Enzymatic Synthesis of Chiral Intermediates for Drug Development. Adv. Synth. Cat. 343: 527-546.

Payen B, Segui M, Monsan P, Schneider K, Friedrich CG, Schlegel HG (1983) Use of cytoplasmic hydrogenase from *Alcaligenes eutrophus* for NADH regeneration. Biotechnol. Lett. 5: 463-467.

Pedragosa-Moreau S, Archelas A, Furstoss R (1996) Microbiological transformations 32: Use of epoxide hydrolase mediated biohydrolysis as a way to enantiopure epoxides and vicinal diols: Application to substituted styrene oxide derivatives. Tetrahedron 52: 4593-4606.

Peschek GA (1979) Evidence for two distinct hydrogenases in *Anacystis nidulans*. Arch. Microbiol. 123: 81-92.

Peters J (1998a) Dehydrogenases - characteristics, design of reaction conditions, and applications. In: Biotechnology, edn Second. Edited by Rehm H-J, Reed G, Pühler A, Stadler P: Wiley-VCH; 391-474. [Kelly DR (Series Editor): Biotransformations I, vol 8a.

Peters J (1998b) Dehydrogenases - Characteristics, design of reaction conditions, and applications. In: Biotechnology. Edited by Rehm H-J, Reed G, Pühler A, Stadler P: Wiley-VCH; 393-474. vol 8a.

Pham T, Phillips RS, Ljungdahl LG (1989) Temperature-dependent enantiospecificity of secondary alcohol-dehydrogenase from thermoanaerobacter-ethanolicus. J. Am. Chem. Soc. 111: 1935-1936.

Pham T, Phillips RS (1990) J. Am. Chem. Soc. 112: 3629-3632.

Pichon M, Figadere B (1996) Synthesis of 2,5-disubstituted pyrrolidines. Tetrahedron Asymm. 7: 927-964.

Pohl M (1997) Protein design on pyruvate decarboxylase. Advances in Biochemical Enginering 58: 16-43.

Pohl M, K.Mesch, Iding H, G.Goetz, Kula MR (1997) US Patent, 197 36 104.8.

Pohl M, Siegert P, Mesch K, Bruhn H, Grötzinger J (1998) Active site mutants of pyruvate decarboxylase from *Zymomonas mobilis* - a site-directed mutagenesis study of L112, I472, I476 and N482. Eur. J. Bioch. 257: 538-546.

Pohnert G (2001) Diels-Alderases. Chembiochem 2: 873-875.

Ponndorf W (1926) Angew. Chem.: 138.

Pugin B, Landert H, Spindler F, Blaser U (2002) More than 100,000 turnovers with immobilized Ir-diphosphine catalysts in an enantioselective imine hydrogenation. Adv. Synth. Cat. 344: 974-979.

Pye PJ, Rossen K, Reamer RA, Tsou NN, Volante RP, Reider PJ (1997) A new planar chiral bisphosphine ligand for asymmetric catalysis: Highly Enantioselective hydrogenations under mild conditions. JACS 119: 6207-6208.

Ragnitz K, Syldatk C, Pietzsch M (2001) Optimization of the immobilization parameters and operational stability of immobilized hydantoinase and L-N-carbamoylase from *Arthrobacter aurescens* for the production of optically pure L- amino acids. Enzyme Microb. Technol. 28: 713-720.

Rai GP, Zong Q, Hager LP (2000) Isolation of directed evolution mutants of chloroperoxidase resistant to suicide inactivation by primary olefins. Isr. J. Chem. 40: 63-70.

Rai GP, Sakai S, Florez AM, Mogollon L, Hager LP (2001) Directed evolution of chloroperoxidase for improved epoxidation and chlorination catalysis. Adv. Synth. Cat. 343: 638-645.

Reetz MT, Wilensek S, Zha DX, Jaeger KEACIE, 40, 3589-3591 (2001) Directed evolution of an

enantioselective enzyme through combinatorial multiple-cassette mutagenesis. Angew. Chem. Int. Ed. Engl. 40: 3589-3591.

Rissom S, Schwarz-Linek U, Vogel M, Tishkov V, Kragl U (1997) Synthesis of chiral ε-lactones in a two-enzyme system of cyclohexanone mono-oxygenase and formate dehydrogenase with integrated bubble-free aeration. Tetrahedron Asymm. 8: 2523-2526.

Rissom S, Beliczey J, Giffels G, Kragl U, Wandrey C (1999) Asymmetric reduction of acetophenone in membrane reactors: comparison of oxazaborolidine and alcohol dehydrogenase catalysed processes. Tetrahedron Asymm. 0: 1-6.

Rodriguez S, Schroeder KT, Kayser MM, Stewart JD (2000) Asymmetric synthesis of beta-hydroxy esters and alpha-alkyl- beta-hydroxy esters by recombinant *Escherichia coli* expressing enzymes from baker's yeast. J. Org. Chem. 65: 2586-2587.

Ruppert R, Herrmann S, Steckhan E (1987) Efficient indirect electrochemical in-situ regeneration of NADH: Electrochemically driven enzymatic reduction of pyruvate catalyzed by D-LDH. Tetrahedron Lett. 28: 6583-6586.

Ruppert R, Herrmann S, Steckhan E (1988a) Very efficient reduction of $NAD(P)^+$ with formate catalysed by cationic rhodium complexes. J. Chem. Soc., Chem. Commun.: 1150-1151.

Ruppert R, Herrmann S, Steckhan E (1988b) Very efficient reduction of $NAD(P)^+$ with formate catalysed by cationic rhodium complexes. J. Chem. Soc., Chem. Commun.: 1150-1151.

Sadler JE, Rearick JI, Paulson JC, Hill RL (1979) Purification to homogeneity of a b-galactoside α2-3 sialyltransferase and partial purification of an α-*N*-galactosaminide α2-6 sialyltransferase from porcine submaxillary glands. J. Biol. Chem. 254: 4434-4443.

Sandee AJ, Petra DGI, Reek JNH, Kamer PCJ, Leeuwen PWNM (2001) Solid-phase synthesis of homogeneous ruthenium catalysts on silica for the continuous asymmetric transfer hydrogenation reaction. Chem. Eur.J. 7: 1202.

Saravanan P, Raina S, Sambamurthy T, Singh VK (1997) A practical synthesis of (2R,5R)-2,5-hexandiol. J. Org. Chem. 62: 2669-2670.

Sattler K (1995) Thermische Trennverfahren. Weinheim: VCH Verlagsgesellschaft mbH.

Schlegel HG, Schneider K (Ed) (1978): Göttingen: Goltze.

Schmid A, Dordick JS, Hauer B, Kiener A, Wubbolts M, Witholt B (2001a) Industrial biocatalysis today and tomorrow. Nature 409: 258-268.

Schmid A, Hofstetter K, Feiten HJ, Hollmann F, Witholt B (2001b) Integrated biocatalytic synthesis on gram scale: The highly enantio selective preparation of chiral oxiranes with styrene monooxygenase. Adv. Synth. Cat. 343: 732-737.

Schmid A, Hollmann F, Bühler B (2002a) Oxidations of alcohols. In: Enzyme Catalysis in Organic Synthesis, 2nd edition. Edited by Drauz K, Waldmann H: VCH-Wiley; 1108-1169. vol 3.

Schmid A, Hollmann F, Park JB, Buhler B (2002b) The use of enzymes in the chemical industry in Europe. Curr. Opin. Biotech. 13: 359-366.

Schneider K, Schlegel HG (1976) Purification and properties of soluble hydrogenase from *Alcaligenes eutrophus* H16. Biochim. Biophys. Acta 452: 66-80.

Schoevaart R, van Rantwijk F, Sheldon RA (2000) A four-step enzymatic cascade for the one-pot synthesis of non- natural carbohydrates from glycerol. J. Org. Chem. 65: 6940-6943.

Schoevaart R, van Rantwijk F, Sheldon RA (2001) Four-step enzymatic cascade for the one-pot synthesis of non- natural carbohydrates from glycerol. J. Org. Chem. 66: 351-351.

Schwab GM, Rudolph LM (1932) Naturwiss. 20: 362.

Schwientek T, Yeh JC, Levery SB, Keck B, Merkx G, van Kessel AG, Fukuda M, Clausen H (2000) Control of o-glycan branch formation - molecular cloning and characterization of a novel thymus-associated core 2 beta 1,6-n-acetylglucosaminyltransferase. J. Biol. Chem. 275: 11106-11113.

Seelbach K, Riebel R, Hummel W, Kula M-R, Tishkov VI, Egorov AM, Wandrey C, Kragl U (1996) A novel, efficient regenerating method of NADPH using a new formate dehydrogenase. Tetrahedron Lett. 37: 1377-1380.

Seelbach K (1997) Chloroperoxidase - Ein industrieller Katalysator ? Regio- und enantioselektive Oxidationen [PhD-thesis]. Bonn: Rheinische Friedrich-Wilhelms-Universität.

Seelbach K, Dreuzen MPJv, Rantwijk Fv, Sheldon RA, Kragl U (1997) Improvement of the total turnover number and space-time yield for chloroperoxidase catalyzed oxidation. Biotech. Bioeng.

55: 283-288.

Segel IH (1975) Enzyme kinetics. New York: John Wiley & Sons, Inc.

Selber K, Nellen F, Steffen B, Thömmes J, Kula M-R (2000) Investigation of mathematical methods for efficient optimisation of aqueous two-phase extraktion. Journal of Chromatography B 743: 21-30.

Selvaggi A, Tosi C, Barberini U, Franchi E, Rodriguez F, Pedroni P (1999) *In vitro* hydrogen photoproduction using *Pyrococcus furiosus* sulfhydrogenase and TiO_2. Journal of Photochemistry and Photobiology A: Chemistry 125: 107-112.

Shaked Z, Whitesides GM (1980) Enzyme-catalyzed organic-synthesis - NADH regeneration by using formate dehydrogenase. J. Am. Chem. Soc. 102: 7104-7105.

Sheldon RA (1993) Chirotechnology. New York: Marcel Dekker Inc.

Shorter J (1985) Die Hammett-Gleichung - und was daraus in fünfzig Jahren wurde. ChiuZ 19: 197-208.

Silva PJ, de Castro B, Hagen WR (1999) On the prosthetic groups of the NiFe sulfhydrogenase from *Pyrococcus furiosus*: topology, structure, and temperature-dependent redox-chemistry. Journal of Bioinorganic Chemistry 4: 284-291.

Silva PJ, van den Ban ECD, Wassink H, Haaker H, de Castro B, Robb FT, Hagen WR (2000) Enzymes of hydrogen metabolism in *Pyrococcus furiosus*. Eur. J. Biochem. 267: 6541-6551.

Smet K, Aerts S, Ceulemans E, Vankelecom I, Jacobs P (2001) Nanofiltration-coupled catalysis to combine the advantages of homogeneous and heterogeneous catalysis. Chem. Comm. 7: 597-598.

Smith ET, Odom LD, Awramko JA, M.Chiong, Blamey J (2001) Direct electrochemical characterization of hyperthermophilic *Thermococcus celer* metalloenzymes involved in hydrogen production from pyruvate. Journal of Biological and Inorganic Chemistry 6: 227-231.

Snapp KR, Heitzig CE, Ellis LG, Marth JD (2001) Differential requirements for the o-linked branching enzyme core 2 beta1-6-n-glucosaminyltransferase in biosynthesis of ligands for e-selectin and p-selectin. Blood 97: 3806-3811.

Solladie G, Huser N, Garcia-Ruano JL, Adrio J, Carreno MC, Tito A (1994) Asymmetric synthesis of both enantiomers of 2,5-hexane diol and 2,6-heptane diol induced by chiral sulfoxides. Tetrahedron Lett. 35: 5297-5300.

Speare DM, Olf P, Bugg TDH (2002) Hammett analysis of a C-C hydrolase-catalysed reaction using synthetic 6-aryl-2-hydroxy-6-ketohexa-2,4-dienoic acid substrates. Chem. Comm.: 2304-2305.

Stampfer W, Kosjek B, Moitzi C, Kroutil W, Faber K (2002) Biocatalytic asymmetric hydrogen transfer. Angew. Chem. 114: 1056-1059.

Steckhan E, Herrmann S, Ruppert R, Thömmes J, Wandrey C (1990) Kontinuierliche Erzeugung von NADH aus NAD^+ und Formiat mit einem molekulargewichtsvergrößerten Homogenkatalysator in einem Membranreaktor. Angew. Chem. 102: 445-447.

Steckhan E, Herrmann S, Ruppert R, Dietz E, Frede M, Spika E (1991) Analytical study of a series of substituted (2,2'-bipyridyl)(pentamethylcyclopentadienyl)rhodium and iridium complexes with regard to their effectiveness as redox catalysts for the indirect electrochemical and chemical-reduction of NAD(P)+. Organomet. 10: 1568-1577.

Steckhan E (1994) Electroenzymatic Synthesis. In: Electrochemistry V. Edited by; 83-111. Topics in Current Chemistry, vol 170.

Steckhan E, Arns T, Heineman WR, Hilt G, Hoormann D, Jörissen J, Kröner L, Lewall B, Pütter H (2001) Environmental protection and economization of resources by electroorganic and electroenzymatic syntheses. Chemosphere 43: 63-73.

Steinhauser H, Brüschke HEA (1994) Separation of light alcohols from anhydrous organic mixtures by pervaporation. In Synthetic Membranes in Science and Industry; Tübingen, Fed. Rep. of Germany: Dechema e.V.: 258-261.

Steuber J, Krebs W, Bott M, Dimroth P (1999) A membrane-bound $NAD(P)^+$-reducing hydrogenase provides reduced pyridine nucleotides during citrate fermentation by *Klebsiella pneumoniae*. J. Bacteriol. 181: 241-245.

Stewart JD (2000) Organic transformations catalyzed by engineered yeast cells and related systems. Curr. Opin. Biotech. 11: 363-368.

Stillger T, Bönitz M, Filho MV, Liese A (2002) Überwindung von thermodynamischen Limitierungen in substratgekoppelten Cofaktorregenerierungsverfahren. Chem.-Ing.-Tech. 74:

1035-1039.

Stinson SC (1999) Chiral triumphs. C&EN 22nd of November: 57.

Stoop RM, Bachmann S, Valentini M, Mezzetti A (2000) Ruthenium(II) complexes with chiral tetradentate P2N2 ligands catalyze the asymmetric epoxidation of olefins with H_2O_2. Organomet. 39: 4903.

Straathof A, Panke S, Schmidt A (2002) The production of fine chemicals by biotransformations. Curr. Opin. Biotech. 13: 538-556.

Stryer L (1990) Biochemie: Spektrum der Wissenschaft Verlagsgesellschaft.

Sun Y (1996) J. Am. Chem. Soc. 118: 1348.

Sun Y, Wang J, LeBlond C, Landau RN, Laquidara J, Sowa JR, Blackmond DG (1997) Kinetic influences on enantioselectivity in asymmetric catalytic hydrogenation. J. Mol. Cat.: Enz. 115: 495.

Suye S, Yokoyama S (1985) NADPH production from $NADP^+$ using malic enzyme of *Achromobacter parvulus* IFO-13182. Enzyme Microb. Technol. 7: 418-424.

Suzuki K, Fujimoto H, Ito Y, Sasaki T, Ajisaka K (1997) An efficient synthesis of a Galβ1-3GalNAc-serine derivative using β-galactosidase. Tetrahedron Lett. 38: 1211-1214.

Tabata K, Koizumi S, Endo T, Ozaki A (2002) Production of N-acetyl-D-neuraminic acid by coupling bacteria expressing N-acetyl-D-glucosamine 2-epimerase and N-acetyl-D- neuraminic acid synthetase. Enzyme Microb. Technol. 30: 327-333.

Tamminen A, Vuorilehto K, Ylasaari S (1996) Scale-up of an electrochemical cell for oxygen removal from water. J. Appl. Electrochem. 26: 113-117.

Tanaka A, Tosa T, Kobayashi T (1993) Industrial Application of Immobilized Biocatalysts. New York: Marcel Decker.

Taylor SJC, Holt KE, Brown RC, Keene PA, Taylor IN (2000) Choice of biocatalyst in the development of industrial biotransformations. In: Stereoselective Biocatalysis. Edited by Patel RN: Marcel Dekker, Inc.; 397-404.

Thomas SM, DiCosimo R, Nagarajan V (2002) Biocatalysis: applications and potentials for the chemical industry. Tibtech 20: 238-242.

Tishkov VI, Matorin AD, Rojkova AM, Fedorchuk VV, Savitsky PA, Dementieva LA, Lamzin VS, Mezentzev AV, Popov VO (1996) Site-directed mutagenesis of the formate dehydrogenase active centre: role of the His332-Gln313 pair in enzyme catalysis. FEBS Letters 390: 104-108.

Tishkov VI, Galkin AG, Fedorchuk VV, Savitsky PA, Rojkova AM, Gieren H, Kula MR (1999a) Pilot scale production and isolation of recombinant NAD(+)- and NADP(+)-specific formate dehydrogenases. Biotech. Bioeng. 64: 187-193.

Tishkov VI, Galkin AG, Fedorchuk VV, Savitsky PA, Rojkova AM, Gieren H, Kula M-R (1999b) Pilot scale production and isolation of recombinant NAD^+- und $NADP^+$-specific formate dehydrogenases. Biotech. Bioeng. 64: 187-193.

Treybal E (1963) Liquid Extraction edn 2nd edition. New York: McGraw-Hill.

Tsuchida T, Nishimoto Y, Kotani T, Iiizumi K (1993) Production of L-3,4-dihydroxyphenylalanine. US Patent, JP 5123177A.

Turner MK (1998) Perspectives in biotransformations. In: Biotransfromations I. Edited by Kelly DR: Wiley-VCH; 9ff. [Rehm H-J, Reed G (Series Editor): Biotechnology, vol Vol 8.

Uhlenbrock K (1994) Methoden zur reaktionstechnischen Optimierung enzymatischer Synthesen dargestellt am Beispiel der enantioselektiven Reduktion von p-Chloracetophenon im organisch-wässrigen Zwei-Phasen-System [Ph.D. thesis]. Germany: University of Bonn.

van de Velde F, Lourenco ND, Bakker M, van Rantwijk F, Sheldon RA (2000) Improved operational stability of peroxidases by coimmobilization with glucose oxidase. Biotech. Bioeng. 69: 286-291.

van de Velde F, van Rantwijk F, Sheldon RA (2001) Improving the catalytic performance of peroxidases in organic synthesis. Tibtech 19: 73-80.

van den Ban ECD (2001) Exploring the reductive capacity of *Pyrococcus furiosus* [Ph.D.]. Wageningen, The Netherlands: Wageningen Agricultural University.

van Deurzen MPJ, Seelbach K, van Rantwijk F, Kragl U, Sheldon RA (1997a) Chloroperoxidase: Use of a hydrogen peroxide-stat for controlling reactions and improving enzyme performance. Biocat. Biotransf. 15: 1-16.

van Deurzen MPJ, van Rantwijk F, Sheldon RA (1997b) Selective oxidations catalyzed by

peroxidases. Tetrahedron 53: 13183-13220.
Varki A (1993) Biological roles of oligosaccharides: all of the theories are correct. Glycobiology 3: 97-130.
Varki A, Cummings R, Esko J, Freeze H, Hart G, Marth J (1999) Essentials of Glycobiology. New York: Cold Spring Harbour Laboratory Press.
Verley A (1925) Bulletin de la Societe Chimique de France: 871.
Vos WED, Vankelecom IFJ, Jacobs PA (2000) Chiral catalyst immobilization and recycling. Weinheim: Wiley-VCH.
Vrtis JM, White AK, Metcalf WM, van der Donk WA (2002) Phosphite dehydrogenase: a versatile cofactor-regeneration enzyme. Angew. Chem. 114: 3391-3393.
Vuorilehto K, Tamminen A, Ylasaari S (1995) Electrochemical removal of dissolved-oxygen from water. J. Appl. Electrochem. 25: 973-977.
Wan K, Davis ME (1983) Ruthenium (II)-sulfonated BINAP: A novel water-soluble asymmetric hydrogenation catalyst. Tetrahedron Asymm. 4: 2461-2468.
Watanabe K, Koshiba T, Yasufuku Y, Miyazawa T, Ueji S (2001) Effects of substituent and temperature on enantioselectivity for lipase-catalyzed esterification of 2-(4-substituted phenoxy) propionic acids in organic solvents. Bioorg. Chem. 29: 65-76.
Watson JD, Crick FHC (1953) Molecular structure of nucleic acids. Nature 171: 737-738.
Wegman MA, van Langen LM, van Rantwijk F, Sheldon RA (2002) A two-step, one-pot enzymatic synthesis of cephalexin from D- phenylglycine nitrile. Biotech. Bioeng. 79: 356-361.
Weijers CAGM (1997) Enantioselective hydrolysis of aryl, alicyclic and aliphatic epoxides by *Rhodotorula glutinis*. Tetrahedron Asymm. 8: 639-647.
Wenz G (1994) Angew. Chem. 106: 851-870.
Westerhausen D, Herrmann S, Hummel W, Steckhan E (1992) Formate-driven, nonenzymatic NAD(P)H regeneration for the alcohol-dehydrogenase catalyzed stereoselective reduction of 4-phenyl-2-butanone. Angew. Chem.-Int. Edit. Engl. 31: 1529-1531.
Weuster-Botz D, Pramatarova V, Spassov G, Wandrey C (1995) Use of a genetic algorithm in the development of a synthetic growth-medium for *Arthrobacter simplex* with high hydrocortisone Δ(1)-dehydrogenase activity. J. Chem. Tech. Biotechnol. 64: 386-392.
Weuster-Botz D, Wandrey C (1995) Medium optimization by genetic algorithm for continuous production of formate dehydrogenase. Process Biochemistry 30: 563-571.
Whitesell JK, Felman SW (1977) Asymmetric induction. 2. enantioselective alkylation of cyclohexanone via a chiral enamine. J. Org. Chem. 42: 1663-1664.
Whitesell JK (1989) C2 symmetry and asymmetric induction. Chem. Rev. 89: 1581-1590.
Whitman WG (1923) The two-film theory of gas absorption. Chem. Metall. Eng.: 146-148.
Wichmann R, Wandrey C, Bückmann AF, Kula M-R (1981) Continuous enzymatic transformation in an enzyme membrane reactor with simultaneous NAD(H) regeneration. Biotech. Bioeng. 23: 2789-2802.
Wiese A, Wilms B, Syldatk C, Mattes R, Altenbuchner J (2001) Cloning, nucleotide sequence and expression of a hydantoinase and carbamoylase gene from *Arthrobacter aurescens* DSM 3745 in *Escherichia coli* and comparison with the corresponding genes from *Arthrobacter aurescens* DSM 3747. Appl. Microbiol. Biotechnol 55: 750-757.
Wilcocks R, Ward OP (1991) Factors affecting 2-hydroxypropiophenon formation by benzoylformate decarboxylase from *Pseudomonas putida*. Biotech. Bioeng. 39: 1058-1062.
Wilcocks R, Ward OP, Collins S, Dewdney NJ, Hong Y, Prosen E (1992) Acyloin formation by benzoylformate decarboxylase from *Pseudomonas putida*. Appl. Environ. Microbiol. 58: 1699-1704.
Wilkins PP, McEver RP, Cummings RD (1996) Structures of the o-glycans on p-selectin glycoprotein ligand-1 from hl-60 cells. J. Biol. Chem. 271: 18732-18742.
Wilson SR, Pasternak A (1990) Preparation of a new class of C2-symmetric chiral phosphines: The first asymmetric staudinger reaction. Synlett: 199-200.
Wolberg M, Hummel W, Wandrey C, Müller M (2000) Highly regio- and enantioselective reduction of 3,5-dioxocarboxylates. Angew. Chem. 112: 4476-4478.
Wöltinger J (2001) Begleitbrief zur Übersendung des polymervergrößerten Katalysators. Hanau, 7. Januar 2001.

Wöltinger J, Bommarius AS, Drautz K, Wandrey C (2001a) The chemzyme membrane reactor in the fine chemical industry. Org. Proc. Res. Dev. 5: 241-248.

Wöltinger J, Drauz K, Bommarius AS (2001b) The membrane reactor in the fine chemicals industry. Appl. Cat. A 221: 171-185.

Wong C-H, Daniels L, Orme-Johnson WH, Whitesides GM (1981) Enzyme-catalyzed organic synthesis: NAD(P)H regeneration using dihydrogen and the hydrogenase from *Methanobacterium thermoautothrophicum*. JACS 103: 6227-6228.

Wong C-H, Whitesides GM (1981) Enzyme-catalyzed organic synthesis: NAD(P)H cofactor regeneration by using glucose-6-phosphate and the glucose-6-phosphate dehydrogenase from *Leuconostoc mesenteroides*. JACS 103: 4890-4899.

Wong C-H, Whitesides GM (1982) Enzyme-catalyzed organic synthesis: NAD(P)H cofactor regeneration using ethanol/alcohol dehydrogenase/aldehyde dehydrogenase and methanol/alcohol dehydrogenase/aldehyde dehydrogenase/formate dehydrogenase. J. Org. Chem. 47: 2816-2818.

Wong C-H, Whitesides GM (1994) Enzymes in Synthetic Organic Chemistry, vol 12. Edited by Baldwin JE, Magnus PD. Oxford: Elsevier Science Ltd.

Wong C-H, Halcomb RL, Ichikawa Y, Kajimoto T (1995a) Enzyme in der organischen Synthese: das Problem der molekularen Erkennung von Kohlenhydraten (Teil 1). Angew. Chem. 107: 453-474.

Wong C-H, Halcomb RL, Ichikawa Y, Kajimoto T (1995b) Enzyme in der organischen Synthese: das Problem der molekularen Erkennung von Kohlenhydraten (Teil 2). Angew. Chem. 107: 569-593.

Wong WK, Chik TW, Hui KN, Williams I, Feng X, Mak TCW, Che CM (1996) Preparation of chiral diiminodiphosphine and diaminodiphosphine ligands and their Cu-I and Ag-I complexes - X-ray crystal-structures of (Cu(1*S*,2*S*-cyclohexyl-P_2N_2))(PF_6) and (Ag(1*R*,2*R*-cyclohexyl-$P_2N_2H_4$))(BF_4). Polyhedron 15: 4447-4460.

Woodward J, Cordray KA, Edmonston RJ, Blanco-Rivera M, Mattingly SM, Evans BR (2000a) Enzymatic hydrogen production: conversion of renewable resources for energy production. Energy & Fuels 14: 197-201.

Woodward J, Orr M, Cordray KA, Greenbaum E (2000b) Enzymatic production of biohydrogen. Nature 405: 1014-1015.

Wu JT, Wu LH, Knight JA (1986a) Stability of NADPH: Effects of various factors on the kinetics of degradation. Clin. Chem. 32: 314-319.

Wu JT, Wu LH, Knight JA (1986b) Stability of NADPH: effect of various factors on the kinetics of degradation. Clinical Chemistry 32: 314-319.

Wynberg H (1986) Asymmetric catalysis by alkaloids. Topics Stereochem. 16: 87-129.

Yamada H, Ryuno K, Nagasawa T, Enomoto K, I. Watanabe ABC, 50, 2859-2865. (1986) Optimum culture conditions for production by *Pseudomonas chlororaphis*. Agric. Biol. Chem. 50: 2859-2865.

Yamada H, Kobayashi M (1996) Nitrile hydratase and its application to industrial production of acrylamide. Biosci. Biotechnol. Biochem. 60: 1391-1400.

Yamada H (1998) Screening of novel enzymes for the production of useful compounds. In: New Frontiers in Screening for Microbial Biocatalysis. Edited by Kieslich K, Beek CPvd, Bont JAMd, Tweel WJJvd: Elsevier; 13-17. Studies in Organic Chemistry, vol 53.

Yamakawa M, Ito H, Noyori R (2000) The metal-ligand bifunctional catalysis: A theoretical study on the ruthenium (II)-catalyzed hydrogen transfer between alcohols and carbonyl compounds. J. Am. Chem. Soc. 122: 1466.

Yamazaki T, Welch JT, Plummer JS, Gimi RH (1991) The enantioselective fluoroacetamide acetal claisen rearrangements of N-fluoroacetyl-trans-(2R,5R)-2,5-dimethylpyrrolidine. Tetrahedron Lett. 32: 4267-4270.

Yasohara Y, Kizaki N, Hasegawa J, Wada M, Kataoka M, Shimizu S (2001) Stereoselective reduction of alkyl 3-oxobutanoate by carbonyl reductase from *Candida magnoliae*. Tetrahedron-Asymmetry 12: 1713-1718.

Zaks A (2001) Industrial biocatalysis. Current Opinion in Chemical Biology 5: 130-136.

Zassinovich G, Mestroni G, Gladiali S (1992) Asymmetric hydrogen transfer reactions promoted by homogeneous transition metal catalysts. Chem. Rev. 92: 1051-1069.

Zelinski T, Liese A, Wandrey C, Kula M-R (1999) Asymmetric reductions in aqueous media: Enzymatic synthesis in cyclodextrin containing media. Tetrahedron Asymm. 10: 1681-1687.

Zervosen A, Elling L (1996) A novel three-enzyme reaction cycle for the synthesis of N-acetyllactosamine with in situ regeneration of uridine 5'- diphosphate glucose and uridine 5'-diphosphate galactose. J. Am. Chem. Soc. 118: 1836-1840.

Zhang H, Xue F, Mak TCW, Chan KS (1996) Enantioselectivity increases with reactivity: Electronically controlled asymmetric addition of diethylzine to aromatic aldehydes catalysed by a chiral pyridylphenol. J. Org. Chem. 61: 8002-8003.

8 Publications & Patents of Prof. Dr. Andreas Liese

8.1 in Journals

1. A. Liese, M. Karutz, J. Kamphuis, C. Wandrey, U. Kragl
Enzymatic resolution of 1-phenyl-1,2-ethanediol by enantioselective oxidation: Overcoming product inhibition by continuous extraction
Biotechnology and Bioengineering 51 (1996) 544-550

2. A. Liese, T. Zelinski, M.-R. Kula, H. Kierkels, M. Karutz, U. Kragl, C. Wandrey
A novel reactor concept for the enzymatic reduction of poorly soluble ketones
Journal Molecular Catalysis B, Enzymatic 4 (1998) 91-99

3. T. Zelinski, A. Liese, C. Wandrey, M.-R. Kula
Asymmetric reduction in aqueous media: Enzymatic synthesis in cyclodextrin containing buffers Tetrahedron Asymmetry 10 (9) (1999) 1681-1687

4. A. Liese, M. Villela Filho
Production of fine chemicals using biocatalysis
Current Opinion in Biotechnology 10 (6) (1999) 595-603

5. H. Iding, P. Siegert, T. Dünnwald, M. Müller, L. Greiner, A. Liese, J. Grötzinger, A. Demir, M. Pohl
Benzoylformate decarboxylase from Pseudomonas putida as stable catalyst for the synthesis of chiral 2-hydroxy ketones
Chemistry – a European Journal 6 (8) (2000) 1483-1495

6. G. Dudziak, N. Bézay, T. Schwientek, H. Clausen, H. Kunz, A. Liese
Cyclodextrin- assisted glycan chain extension on a protected glycosyl amino acid
Tetrahedron 56 (32) (2000) 5865-5869

7. C. Wandrey, A. Liese, D. Kihumbu
Industrial biocatalysis: Past, present and future
Organic Process Research & Development 4 (2000) 286-290

8. J.-S. Shin, B.-G. Kim, A. Liese, C. Wandrey
Kinetic resolution of chiral amines with w-transaminase using an enzyme-membrane reactor Biotechnology & Bioengineering 73 (3) (2001) 179-187

9. N. Brinkmann, M. Malissard, M. Ramuz, U. Römer, T. Schumacher, E. G. Berger, L. Elling, C. Wandrey, A. Liese
Chemo-enzymatic synthesis of the Galili epitope Galα(1→3)Galβ(1→4)GlcNAc on a homogeneously soluble PEG polymer by a multi-enzyme system
Bioorganic & Medicinal Chemistry Letters 11 (2001) 2503-2506

10. N. Bézay, G. Dudziak, A. Liese, H. Kunz
Chemoenzymatisch-chemische Synthese eines (2-3)-Sialyl-T-Threonin-Bausteins und dessen Einsatz in der Synthese der N-terminalen Sequenz von Leukämie-assoziierten

Leikosialin (CD34)
Angewandte Chemie 113 (12) (2001) 2350-2352
Angewandte Chemie Int. Ed. 40, (2001) 2292-2295

11. S. Laue, L. Greiner, J. Wöltinger, A. Liese
Continuous application of chemzymes in a membrane reactor: Asymmetric transfer hydrogenation of acetophenone
Advanced Synthesis & Catalysis 343 (6-7) (2001) 711-720

12. C. Hoh, G. Dudziak, A. Liese
Optimization of enzymatic synthesis of O-glycan core 2 structure by use of a genetic algorithm
Bioorganic & Medicinal Chemistry Letters 12 (7) (2002) 1031-1034

13. A. Liese, U. Kragl, H. Kierkels, B. Schulze
Membrane reactor development for the kinetic resolution of ethyl 2-hydroxy-4-phenylbutyrate
Enzyme Microbial Technology 30 (5) (2002) 673 – 681

14. J. Haberland, A. Kriegesmann, E. Wolfram, W. Hummel, A. Liese
Diastereoselective synthesis of optically active (2R,5R)-hexanediol
Applied Microbiology & Biotechnology 58 (2002) 595-599

15. D. Kihumbu, T. Stillger, W. Hummel, A. Liese
Enzymatic Synthesis of all Stereoisomers of 1-Phenylpropane-1,2-diol
Tetrahedron Asymmetry 13 (2002) 1069-1072

16. T. Stillger, M. Bönitz, M. Villela Filho, A. Liese
Überwindung von thermodynamischen Limitierungen in substratgekoppelten Cofaktorregenerierungsverfahren
Chemie Ingenieur Technik 74(7) (2002) 1035-1039

17. J. Haberland, W. Hummel, T. Dausmann, A. Liese
New continuous production process for enantiopure (2R,5R)-hexanediol
Organic Process Research & Development 6 (2002) 458-462
(online publication DOI http://dx.doi.org/10.1021/op020023t)

18. A. Buchholz, L. Greiner, C. Hoh, A. Liese
Genetic algorithms as tool for capillary electrophoresis method development
Journal of Capillary Electrophoresis and Microchip Technology 7(3&4) (2002) 51-60

19. I. Chin-Joe, J. Haberland, A. Straathof, J. Jongejan, A. Liese, J. Heijnen
Reduction of ethyl 3-oxobutanoate using non-growing baker's yeast in a continuously operated reactor with cell retention
Enzyme Microbial Technology 31 (2002) 665-672

20. D. Vasic-Racki, J. Bongs, U. Schörken, G. A. Sprenger, A. Liese
Modeling of reaction kinetics for reactor selection in the case of L-erythrulose synthesis
Bioprocess and Biosystems Engineering 25 (5) (2003) 285-290

21. I. Schröder, E. Steckhan, A. Liese
In situ NAD(P)$^+$ regeneration using 2,2'-azinobis(3-ethylbenzothiazolin-6-sulfonate) as an electron transfer mediator
Journal of Electroanalytical Chemistry 541 (2003) 109-115

22. D. Vasic-Racki, U. Kragl, A. Liese
Benefits of enzyme kinetics modelling
Chemical and Biochemical Engineering Quarterly 17 (1) (2003) 7-18

23. H. Visser, M. Villela Filho, A. Liese, C. Weijers, J. Verdoes
Construction and characterization of a genetically engineered Escherichia coli strain for the epoxide hydrolase-catalyzed kinetic resolution of epoxides
Biocatalysis and Biotransformations 21 (2003) 33-40

24. L. Greiner, D. Müller, E. van den Ban, J. Wöltinger, C. Wandrey, A. Liese
Membrane aerated hydrogenation: Enzymatic and chemical homogeneous catalysis
Advanced Synthesis and Catalysis 345 (2003) 679-683

25. M. Villela Filho, T. Stillger, M. Müller, A. Liese, C. Wandrey
Is the polarity a convenient criterion to guide the choice of solvents for biphasic enzymatic reactions?
Angewandte Chemie 115(26) (2003) 3101-3104
Angewandte Chemie Int. Ed. 42 (26) (2003) 2993-2996

26. R. Mertens, L. Greiner, E. C. D. van den Ban, H. Haaker, A. Liese
Practical applications of hydrogenase I from Pyrococcus furiosus for NADPH generation and regeneration
Journal Molecular Catalysis B, Enzymatic 24-25 (2003) 39-52

27. P. S. Dragovich, T. J. Prins, R. Zhou, T. O. Johnson, Y. Hua, H. T. Luu, S. K. Sakata, E. L. Brown, F. C. Maldonado, T. Tuntland, C. A. Lee, S. A. Fuhrman, L. S. Zalman, A. K. Patick, D. A. Matthews, E. Y. Wu, M. Guo, B. C. Borer, N. K. Nayyar, T. Moran, L. Chen, P. A. Rejto, P. W. Rose, M. C. Guzman, E. Z. Dovalsantos, S. Lee, K. McGee, M. Mohajeri, A. Liese, J. Tao, M. B. Kosa, B. Liu, M. R. Batugo, J.-P. R. Gleeson, Z. P. Wu, J. Liu, J. W. Meador, R. A. Ferre
Structure-based design, synthesis, and biological evaluation of irreversible human rhinovirus 3C protease inhibitors. 8. Pharmacological optimization of orally bioavailable 2-pyridone-containing peptidomimetics
Journal of Medicinal Chemistry 46(21) (2003) 4572-4585

28. L. Greiner, I. Schröder, D. H. Müller and A. Liese
Utilization of adsorption effects for the continuous reduction of NADP$^+$ with molecular hydrogen by Pyrococcus furiosus hydrogenase
Green Chemistry 5(6) (2003) 697 - 700

29. D. Degenring, I. Schröder, A. Liese, L. Greiner
Resolution of 1,2-diols by enzyme catalyzed oxidation with anodic mediated cofactor regeneration in the extractive membrane reactor - Gaining insight by adaptive simulation
Organic Process Research & Development (accepted)

30. A. Rentmeister, C. Hoh, S. Weidner, G. Dräger, L. Elling, A. Liese, C. Wandrey
Kinetic examination and simulation of GDP-β-L-fucose synthetase reaction using NADPH and NADH
Biocatalysis and Biotransformations (accepted)

31. W. Braun, B. Calmuschi, J. Haberland, W. Hummel, A. Liese, T. Nickel, O. Stelzer, A. Salzer
Optically active phospholanes as substituents on ferrocene and chromium-arene complexes
European Journal of Inorganic Chemistry (accepted)

8.2 Book chapters

32. U. Kragl, A. Liese
Biotransformations, engineering aspects
in: The Encyclopedia of Bioprocess Technology: Fermentation, Biocatalysis & Bioseparation, eds. M. C. Flickinger and S. W. Drew, John Wiley & Sons, New York, (1999) 454-464

33. A. Liese
Replacing chemical steps by biotransformations: Industrial applications and processes using biocatalysis
in Enzyme Catalysis in Organic Synthesis, 2nd edition, (K. Drauz, H. Waldmann, eds.), Wiley-VCH (2002) 1419-1460

34. A. Liese, S. Lütz
Relevanz der Elektrochemie in oxidativen Biotransformationen
GDCh Monographie der GDCh-Fachgruppe Angewandte Elektrochemie: Elektronentransfer in Chemie und Biochemie (J. Russow, H.J. Schäfer) 23 (2002) 305-308

35. A. Liese
53 Keywords in Catalysis from A to Z (Cornils, Hermann, Schlögl, Wong, eds.) Wiley-VCH (2003)

36. N. Rao, A. Liese
Stereoselective synthesis with the help of recombinant enzymes
in Molecular Biology in Medicinal Chemistry (Dingermann, Folkers, Steinhilber, eds.; Series: Methods and Principles in Medicinal Chemistry, series editors: K. Mannhold, H. Kubinyi, G. Folkers), Wiley-VCH, (2003) 125-152

37. B. Lingen, A. Liese, Michael Müller
Enantioselective synthesis of hydroxy ketones via benzaldehyde lyase- and benzoylformate decarboxylase-catalyzed C-C bond formation
in Thiamine: Catalytic Mechanisms and Role in Normal and Disease States (M. S. Patel and. F. Jordan, eds.), Marcel Dekker, New York (in press)

8.3 Book

38. A. Liese, K. Seelbach, C. Wandrey
Industrial Biotransformation
Wiley-VCH, 2000, 423 S.

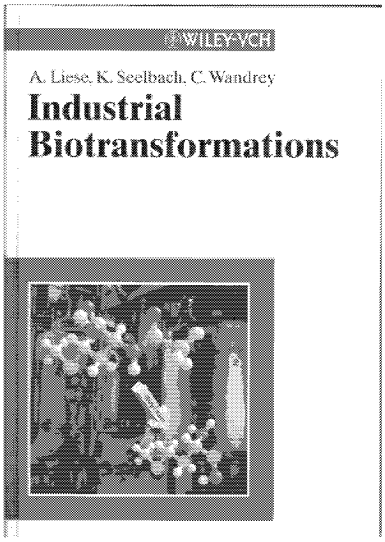

8.4 Patents

1. J. Beliczey, U. Kragl, A. Liese, C. Wandrey, H. Coenen, K. Hamacher und T. Tierling
Enzymatic synthesis of 3-fluoroneuraminic acid (5-acetamido-3,5-didesoxy-3-fluoro-D-glycero-D-galacto-nonulopyranosonic acid) and other 3,5-didesoxy-3-fluorononulo-pyranosonic acid derivatives
US 6,355,453 B1 (12.03.2002, patent application: US 09/156322, 18.09.1998)

8.5 Patent applications

2. J. Beliczey, U. Kragl, A. Liese, C. Wandrey, H. Coenen, K. Hamacher und T. Tierling
Verfahren zur Herstellung von potentiell in der in vivo-Pharmakokinetik verwendbaren organischen Fluorverbindungen sowie 3-Desoxy-3-Fluoroctulopyranosonsäuren und 3-Desoxy-3-Fluornonulopyranosonsäuren
DE 198 42 133.8-43 (15.09.1998)

3. T. Dünnwald, L. Greiner, H. Iding, A. Liese, M. Müller, M. Pohl
Stereoselektive Synthese chiraler 2-Hydroxyketone mittels Benzoylformiatdecarboxylase
DE 199 18 935.8 (26.04.1999)
Stereoselective synthesis of 2-hydroxyketones
EP 00108709.7-2110 (22.04.2000)

4. J. Wöltinger, O. Burkhardt, A. Bommarius, A. Karau, J.-L. Philippe, K. Drauz, J. Allgaier, A. Liese, C. Wandrey
Polymervergößerte Katalysatoren
DE 199 10 691.6-41 (11.03.1999)
Polymer enlarged catalysts
WO 053305 A1 (14.09.2000)

5. W. Hummel, A. Liese, C. Wandrey
Verfahren zur Reduktion von Ketogruppen enthaltenden Verbindungen
DE 199 32 040.3 (09.07.1999)
Process for reducing keto-group containing compounds
EP 00113127.51-2110 (29.06.2000)

6. S. Lütz, E. Steckhan, A. Liese, C. Wandrey
Verfahren zur enzymatischen Oxidation von Substraten mit H_2O_2
DE 100 54 082.1 (31.10.2000)

7. T. Stillger, M. Villela, A. Liese, C. Wandrey
Verfahren und Vorrichtung zur enzymatischen Co-Faktor-Regenerierung
DE 100 60 602.4 (05.12.2000)

8. A. Bommarius, K. Drauz, J. Wöltinger, S. Laue, A. Liese, C. Wandrey
Verwendung von molekulargewichtsvergrößerten Katalysatoren in einem Verfahren zur asymmetrischen kontinuierlichen Hydrierung, neue molekulargewichtsvergrößerte Liganden und Katalysatoren
DE 100 02 975.2 (24.01.2000)

9. E. van den Ban, H. Haaker, L. Greiner, R. Mertens, A. Liese
Verfahren zur enzymatischen Reduktion von Substraten mit molekularem Wasserstoff
DE 101 39 958.8 (21.08.2001)
Enzymatic reduction with molecular hydrogen
PCT Int. Appl. (2003), WO 2003018824 A2 20030306

10. C. Wandrey, M. de Oliviera Villela Filho, A. Liese, J. de Bont, J. Verdoes, C. Weijers, H. Visser, C. Dreisbach
Process for the stereoselective preparation of functionalized vicinal diols
EP 01 120 796.6 (11.09.2001) und US 10/238,308 (09.09.2002)

11. A. Bommarius, H.-P. Krimmer, D. Reichert, J. Almena, A. Karau, J. Wöltinger, K. Drauz, A. Liese, L. Greiner, C. Wandrey
Volumenbegasung
DE 101 63 168.5 (21.12.2001)
Volume gassing suitable for hydrogen addition to organic compounds for hydrogenation
PCT Int. Appl. (2003), WO 2003053886 A1 20030703

12. M. de Oliviera Villela Filho, W. Hummel, C. Wandrey, A. Liese
Verfahren zu Herstellung von Alkoholen aus Substraten mittels Oxidoreduktasen, Zweiphasensystem umfassend eine wässrige Phase und eine organische Phase sowie Vorrichtung zur Durchführung des Verfahrens
DE 102 08 007.0 (26.02.2002)

Schriften des Forschungszentrums Jülich
Reihe Lebenswissenschaften / Life Sciences

1. **Toxizitätsprüfungen in Zellkulturen für eine Vorhersage der akuten Toxizität (LD50) zur Einsparung von Tierversuchen**
   von W. Halle (1998), 92 Seiten
   ISBN: 3-89336-221-5

2. **Die Rolle der Reaktionstechnik in der mikrobiellen Verfahrensentwicklung**
   von D. Weuster-Botz (1999), II, 320 Seiten
   ISBN: 3-89336-245-2

3. **Cell Culture Models as Alternatives to Animal Experimentation for the Testing of Neuroprotective Compounds in Stroke Research**
   Practical Handbook of Methods
   edited by A. J. Carter, H. Kettenmann (1999), 144 pages
   ISBN: 3-89336-250-9

4. **Action and Visuo-Spatial Attention**
   Neurobiological Bases and Disorders
   Book of Abstracts
   collected by P. H. Weiss (2000), XIV, 56 pages
   ISBN: 3-89336-272-X

5. **Genomweite Genexpressionsanalysen mit DNA-Chips zur Charakterisierung des Glucose-Überflussmetabolismus von *Escherichia coli***
   von T. Polen (2003), 100 Seiten
   ISBN: 3-89336-337-8

6. **Auslegung des Detektorsystems für einen hochauflösenden Positronen-Emissions-Tomographen mit hoher Sensitivität**
   von U. Heinrichs (2003), IV, 238 Seiten
   ISBN: 3-89336-340-8

7. **Biological Principles Applied to Technical Asymmetric Catalysis**
   von A. Liese (2003), VI, 206 pages
   ISBN: 3-89336-344-0

Andreas Liese is currently professor for biotechnology at the University of Münster. This book is summarizing the research of his group at the Research Centre Jülich (Institute of Biotechnology 2, head Prof. Christian Wandrey) from 1998 to 2003, leading to the post-doctoral lecture qualification.

The production of enantiopure compounds is of increasing importance to the chemical and biotechnological industries. Bioorganic transformations are predestined to meet this demand due to their inherent regio- and stereoselective nature. Indeed, a growing amount of enantiopure chemicals for pharmaceutical purposes are being produced bio-catalytically today, in contrast to the production of racemic bulk commodities in the past. In this sense, biosynthesis needs to be understood as "chemistry by nature". The biological principles optimized over thousands of years experience a new renaissance when applied to technical asymmetric catalysis. Nevertheless, one key tool or prerequisite for their application is the appropriate technology, namely reaction engineering. The objective of this book is to understand selected biological principles as well as processes in chemical terms, to transfer, apply them to and combine them with the traditional concepts of chemical, i.e., homogeneous catalysis. Simultaneously, the aim is to design and to develop novel reactors, i.e., engineered systems based on these biological principles. Currently, in technical asymmetric synthesis different biological principles are already being applied without the scientific community at large being aware of it. In those examples namely, where additionally reaction engineering has been integrated, very efficient production processes were designed. This gives rise to high expectations for the future of a sustainable, technical asymmetric catalysis.

Forschungszentrum Jülich
in der Helmholtz-Gemeinschaft

Band / Volume 7
ISBN 3-89336-344-0

Lebenswissenschaften
Life Sciences